U.S.NRC
United States Nuclear Regulatory Commission
Protecting People and the Environment

NUREG/CR-6983
BNL-NUREG-81548-2008

Seismic Analysis of Large-Scale Piping Systems for the JNES-NUPEC Ultimate Strength Piping Test Program

Office of Nuclear Regulatory Research

AVAILABILITY OF REFERENCE MATERIALS IN NRC PUBLICATIONS

NRC Reference Material

As of November 1999, you may electronically access NUREG-series publications and other NRC records at NRC's Public Electronic Reading Room at http://www.nrc.gov/reading-rm.html. Publicly released records include, to name a few, NUREG-series publications; *Federal Register* notices; applicant, licensee, and vendor documents and correspondence; NRC correspondence and internal memoranda; bulletins and information notices; inspection and investigative reports; licensee event reports; and Commission papers and their attachments.

NRC publications in the NUREG series, NRC regulations, and *Title 10, Energy*, in the Code of *Federal Regulations* may also be purchased from one of these two sources.

1. The Superintendent of Documents
   U.S. Government Printing Office
   Mail Stop SSOP
   Washington, DC 20402–0001
   Internet: bookstore.gpo.gov
   Telephone: 202-512-1800
   Fax: 202-512-2250
2. The National Technical Information Service
   Springfield, VA 22161–0002
   www.ntis.gov
   1–800–553–6847 or, locally, 703–605–6000

A single copy of each NRC draft report for comment is available free, to the extent of supply, upon written request as follows:
Address: Office of the Chief Information Officer, Reproduction and Distribution
Services Section
U.S. Nuclear Regulatory Commission
Washington, DC 20555-0001
E-mail: DISTRIBUTION@nrc.gov
Facsimile: 301–415–2289

Some publications in the NUREG series that are posted at NRC's Web site address http://www.nrc.gov/reading-rm/doc-collections/nuregs are updated periodically and may differ from the last printed version. Although references to material found on a Web site bear the date the material was accessed, the material available on the date cited may subsequently be removed from the site.

Non-NRC Reference Material

Documents available from public and special technical libraries include all open literature items, such as books, journal articles, and transactions, *Federal Register* notices, Federal and State legislation, and congressional reports. Such documents as theses, dissertations, foreign reports and translations, and non-NRC conference proceedings may be purchased from their sponsoring organization.

Copies of industry codes and standards used in a substantive manner in the NRC regulatory process are maintained at—

The NRC Technical Library
Two White Flint North
11545 Rockville Pike
Rockville, MD 20852–2738

These standards are available in the library for reference use by the public. Codes and standards are usually copyrighted and may be purchased from the originating organization or, if they are American National Standards, from—

American National Standards Institute
11 West 42nd Street
New York, NY 10036–8002
212–642–4900
www.ansi.org

Legally binding regulatory requirements are stated only in laws; NRC regulations; licenses, including technical specifications; or orders, not in NUREG-series publications. The views expressed in contractor-prepared publications in this series are not necessarily those of the NRC.

The NUREG series comprises (1) technical and administrative reports and books prepared by the staff (NUREG–XXXX) or agency contractors (NUREG/CR–XXXX), (2) proceedings of conferences (NUREG/CP–XXXX), (3) reports resulting from international agreements (NUREG/IA–XXXX), (4) brochures (NUREG/BR–XXXX), and (5) compilations of legal decisions and orders of the Commission and Atomic and Safety Licensing Boards and of Directors' decisions under Section 2.206 of NRC's regulations (NUREG–0750).

U.S.NRC
United States Nuclear Regulatory Commission
Protecting People and the Environment

NUREG/CR-6983
BNL-NUREG-81548-2008

Seismic Analysis of Large-Scale Piping Systems for the JNES-NUPEC Ultimate Strength Piping Test Program

Manuscript Completed: August 2008
Date Published: November 2008

Prepared by
G. DeGrassi, J. Nie, and C. Hofmayer

Brookhaven National Laboratory
Upton, NY 11973-5000

S. Ali, NRC Project Manager

NRC Job Code N6076

Office of Nuclear Regulatory Research

ABSTRACT

The Japan Nuclear Energy Safety Organization/Nuclear Power Engineering Corporation (JNES/NUPEC) conducted a multi-year test program for the Ministry of Economy, Trade and Industry (METI) of Japan to investigate the behavior of typical Nuclear Power Plant (NPP) piping systems under large seismic loads. The objectives of this program were to develop a better understanding of the elasto-plastic response and ultimate strength of nuclear piping systems, to ascertain the seismic safety margins in current piping design codes, and to assess new code allowable stress rules. The test program consisted of a series of static and dynamic material tests, piping component tests, simplified piping system tests, and large-scale piping tests. As part of collaborative efforts between the United States and Japan on seismic issues, the U.S. Nuclear Regulatory Commission (NRC) and Brookhaven National Laboratory (BNL) participated in this program by performing both pre-test and post-test analysis for selected tests, and by evaluation of program results. A summary of the BNL analysis of the simplified piping system tests was documented in an earlier NUREG/CR report. This report describes the BNL post-test analyses of the large-scale piping system tests and discusses the insights gained from this program.

FOREWORD

This report documents the collaborative efforts between the U.S. Nuclear Regulatory Commission (NRC), the Japan Nuclear Energy Safety Organization (JNES), and the Nuclear Power Engineering Corporation of Japan (NUPEC) under the NRC-JNES agreement in the area of seismic engineering research. Under contract to the NRC, Brookhaven National Laboratory (BNL) participated in this program and performed this study. This piping test program is one of a series of large-scale seismic testing programs of nuclear power plant (NPP) structures, systems and components conducted by JNES/NUPEC. The research conducted and information exchanged under this collaborative agreement have allowed the NRC to obtain valuable seismic data from large-scale test programs that are not available anywhere else in the world. In addition, this program has enhanced interactions with various Japanese organizations to promote the exchange of information and awareness of ongoing seismic research in Japan.

The NUPEC Ultimate Strength Piping Test Program was a multi-year program to investigate the behavior of NPP piping systems under large seismic loads. The objectives were to develop a better understanding of the elasto-plastic response and ultimate strength of nuclear piping systems, ascertain the seismic safety margins in current piping design codes, and assess new code-allowable stress rules. The program included static and dynamic loading tests of piping material specimens and piping components, and seismic shaking table tests of piping systems. The seismic shaking tests included small "simplified" piping system test specimen configurations and large-scale representative piping system configurations. In both series of seismic tests, the specimens were shaken to levels well above typical design earthquake excitation levels. A summary description of these tests is included in this report.

The NRC's primary contribution to this collaborative effort was the analysis of selected piping system tests. In an earlier phase of this collaborative program, BNL performed analyses of selected piping component and simplified piping system seismic tests and the results were documented in NUREG/CR-6889. This report presents the results of the final phase of this program in which BNL analyzed the large-scale piping systems. The analyses included (1) linear analyses and stress evaluations in accordance with the piping design rules of the American Society of Mechanical Engineers (ASME) Boiler and Pressure Vessel Code, and (2) nonlinear analyses to predict the response of representative large-scale piping systems under beyond-design-basis levels of earthquake motion. The results of the linear analyses provided comparative information on the minimum safety margins in various types of piping components provided by different versions of the ASME Code including the latest NRC-endorsed version (1993) and the most recent version (2006) which is undergoing NRC review. The nonlinear analyses focused on evaluating the capability of current theoretical methods and computer programs to predict the response of piping systems under large earthquake loads. These analyses further developed and improved analysis methods and modeling techniques that were used in the earlier simplified piping system nonlinear seismic analyses. The results of these analyses demonstrated the difficulty of accurately predicting the piping response when it is subjected to large earthquake loads, and the importance of validating the analytical model against test data.

The JNES/NUPEC tests have provided valuable test data on the seismic response of piping systems subjected to strong earthquake motions. The linear code evaluation analyses have provided valuable information on seismic safety margins that can be helpful in resolving the staff's technical concerns in their assessment of new seismic piping design rules in the latest version of the ASME Code including acceptable damping values. From a regulatory standpoint, it is important for reviewers to understand the limitations, sensitivities, and uncertainties of nonlinear analysis methods and the importance of validating these methods against test data. The analyses conducted under this program have provided valuable insights that will assist the staff in their review of licensee submittals involving nonlinear analysis methods.

CONTENTS

Figures

Tables

EXECUTIVE SUMMARY

This report presents the results of BNL collaboration efforts on the JNES/NUPEC Ultimate Strength Piping Test Program. JNES/NUPEC conducted a multi-year test program to investigate the behavior of typical NPP piping systems under large seismic loads. JNES/NUPEC's objectives were to develop a better understanding of the elasto-plastic response and ultimate strength of nuclear piping systems, to ascertain the seismic safety margins in current piping design codes, and to assess new code allowable stress rules. The test program included monotonic and cyclic loading tests of piping material specimens, static and dynamic tests of piping components such as elbows and tees, seismic shaking table tests of two simple piping systems, and seismic shaking table tests of a representative large-scale piping system.

NRC and BNL participated in this JNES/NUPEC program under a collaboration agreement between the United States and Japan on seismic issues. As part of the collaboration, BNL performed pre-test and post-test analyses for selected tests. JNES/NUPEC presented their test results to NRC and BNL and provided selected test data in electronic format. Periodic technical meetings were held in Japan and the U.S. during the course of the program to discuss and exchange ideas on the test program plans, to review and evaluate the test results, and to review and evaluate both pre-test and post-test analyses. A detailed summary of the earlier JNES/NUPEC material, component, and simplified piping tests and of the previous BNL analysis of these tests was documented in an earlier NUREG/CR report [DeGrassi and Hofmayer 2005].

This report provides a summary of the JNES/NUPEC tests, describes the BNL large-scale piping post-test analyses, and discusses the insights gained from this program. A major objective of the JNES/NUPEC test program was to perform a seismic proving test of a representative NPP large-scale piping system. In order to gain a better understanding of the behavior of piping under severe seismic loads, JNES/NUPEC first carried out a series of material and piping component tests and shaking table tests of small (simplified) piping systems. The material specimen tensile tests provided stress-strain curves and basic material strength properties including yield and ultimate stresses, percent elongation and ultimate strain. Strain-controlled cycling tests were also performed which provided cyclic stress-strain curves and stress-strain hysteresis curves for incremental cycling amplitudes. The piping component tests included static and dynamic cycling tests of pressurized elbows, tees, nozzles and reducers. The tests were carried out at high strain levels and illustrated the accumulation of ratcheting strain. The specimens were cycled until a through-wall crack occurred.

The simplified piping system tests were designed to excite the systems to seismic levels well above the typical design earthquake levels in order to induce elasto-plastic response in the system's components. The test systems were simple two-dimensional (Model A) and three-dimensional (Model B) geometric configurations of 65 mm (2 ½ inch) nominal diameter pipe. The Model A pipe routing configuration was in the horizontal plane and was excited in the horizontal direction. The Model B routing was in the horizontal and vertical planes and was subjected to horizontal, vertical, and simultaneous horizontal and vertical seismic motions. The piping systems were pressurized and instrumented with accelerometers, displacement sensors and strain gages at critical locations. A number of tests were carried out to investigate different loadings and design variations. There were no failures reported during the application of any single time history. In the final tests, JNES/NUPEC applied high seismic input motions repeatedly to both specimens in an attempt to induce failure. In these tests, an elbow crack occurred in the Model A configuration after five high seismic level tests. For Model B, a nozzle weld developed a crack during the eighteenth test. In both cases, the failures were attributed to fatigue ratcheting.

In the final phase of the test program, JNES/NUPEC carried out a series of shaking table tests on a representative large-scale piping system. The test specimen was a 200 mm (8 inch) nominal diameter Schedule 40 carbon steel pipe. It included straight pipe, nine elbows, a tee, and a 1000 kg (2200 lb) added mass representing a valve. The system was pressurized and supported by nozzles, an anchor, three two-directional supports, a horizontal support, a vertical support, and a spring hanger. The three-dimensional routing of the piping was representative of nuclear power plant piping systems. The system was instrumented with accelerometers, displacement sensors, and strain gages at critical locations.

Two series of tests were performed: a design method confirmation test and an ultimate strength test. For the design method confirmation test, the first input motion was selected to induce a maximum stress equal to the Japanese Code primary stress limit of $3S_m$ for the Japanese high level S_2 design earthquake. Additional design confirmation tests were then performed using the same test specimen with the seismic input incrementally increased up to a maximum elastically-calculated stress of $13.5S_m$ in the system. The tests were conducted at room temperature and simultaneous horizontal and vertical seismic input motions were applied in all test runs. No evidence of pipe failure was observed.

The ultimate strength test used a similar but modified piping test specimen. An additional mass was added and a support was removed. The intent of these modifications was to induce failure in the system. The pipe was internally pressurized and the tests were performed at room temperature. Horizontal seismic input motion corresponding to a maximum elastically-calculated stress level of $24S_m$ was applied. The test was repeated until failure occurred. During the fifth test run, a through-wall crack developed in an elbow. An examination confirmed that the failure was the result of fatigue ratcheting.

In accordance with the collaboration agreement, BNL performed finite element analyses for selected piping system seismic tests. The BNL analyses had two major objectives. First, linear analyses were performed in accordance with ASME Code requirements. Since the ASME seismic evaluation requirements have been undergoing significant changes in recent years, a comparative study was carried out in which the piping systems were analyzed and evaluated according to three different Code versions. They include the latest NRC-endorsed version (1993 Addenda), the 1994 Addenda which incorporated an alternative higher seismic stress allowable which was not endorsed by NRC, and the most recent 2004 Edition which reinstated the original (1993) stress allowable but introduced an alternative method for calculating seismic stresses in certain piping components. This alternative method is still included in the latest ASME Code Edition (2006) but has not been endorsed by NRC. The analyses also included variations in modal damping ratios consistent with the Code versions. Analyses conducted in accordance with the 1994 and 2004 Code versions used the specified 5 percent damping. Analyses based on the 1993 Code version used 4 percent damping as recommended in the latest 2007 Regulatory Guide 1.61 Revision 1. Additional 1993 Code analyses used damping values that are also acceptable to NRC including ASME Code Case N-411 damping, and the earlier 1973 Regulatory Guide 1.61 Revision 0 damping of 2 percent.

The Code evaluation analyses were carried out for two selected design method confirmation tests and for the ultimate strength test. Based on JNES/NUPEC analyses, design stresses at the critical elbow for all selected load cases exceeded Code allowables. The BNL analyses identified the degree to which the calculated stresses exceeded the ASME Code allowable stresses. The ratios of calculated to allowable stress define the minimum margins of safety provided by different versions of the ASME Code rules. The BNL study provides comparisons of these ratios calculated in accordance with the different rules and damping values, which provide a measure of the relative safety margins between different Code versions. For the ultimate stress test, which actually resulted in an elbow failure, the analyses showed that the 1994 and the 2004 Code analyses with 5 percent damping provided essentially identical margins of 2.63. The NRC-endorsed 1993 Code analyses using the NRC recommended damping value of 4 percent from Regulatory Guide 1.61 Revision 1 provided about 70 percent higher margins (4.50). The 1993 Code analyses using the NRC-accepted damping values from Code Case N-411 provided about 50 percent

higher margins (3.94) than the 2004 Code analyses. Analyses using the Regulatory Guide 1.61 Revision 0 damping value of 2 percent provided the largest (140 percent higher) margins (6.35). Since a failure actually occurred at the highest stressed elbow in the ultimate strength test, these margins may be interpreted as failure margins based on stress level for this specific test. However, it should be noted that since the number of cycles in these tests far exceeded the normal number of SSE design cycles and the failure was characterized as a fatigue failure, some additional margin may be available. On the other hand, since the dominant seismic input frequency for the ultimate strength test was on-resonance, it is possible that a different seismic input may result in a smaller margin. The results of these studies and of possible further evaluation of the large-scale piping test data could be useful in resolving some of the staff's technical concerns over the 2004 ASME Code alternative seismic piping design rules including damping values.

The second major objective of the BNL analyses was to perform nonlinear analyses to investigate and evaluate the adequacy of state-of-the-art methods for predicting the elasto-plastic response of piping systems subjected to large earthquake loads. BNL used the ANSYS computer program for performing these analyses. ANSYS is a computer program widely used by the nuclear industry that has been enhanced in recent years to include a number of improvements in its nonlinear analysis capability. The JNES/NUPEC Ultimate Strength Piping Test Program provided substantial test data for benchmarking elasto-plastic analysis methods and computer codes. The BNL nonlinear analyses for the large-scale piping tests built upon the nonlinear analysis methods applied to the simplified piping system tests reported by DeGrassi and Hofmayer [2005] and attempted to further improve and refine those earlier methods for application to the large-scale piping analyses. This included improvements in defining the material models, input motion characterization, and finite element mesh density. Numerous complex nonlinear transient analyses were carried out. Two finite element models were created for both the design method confirmation tests and the ultimate strength tests. The first was a piping system model which used plastic pipe elements and a multi-linear material model to obtain the displacement and acceleration responses for the entire piping system. The second model was an elbow model that used a finite strain shell element and the Chaboche nonlinear material model to obtain the strain response. The displacement responses at two nodes around one critical elbow generated from the piping system model were used as the input displacement boundary conditions for the elbow model.

The analyses showed that the piping system model can accurately predict the displacement and acceleration responses for low to moderate input motions but less accurately for high input motions. For the design method confirmation tests, it was noted that the plasticity accumulation in the piping system model only affected the performance of the piping system model during the early part of the input motion and did not change the overall response for the entire time histories. The displacement and acceleration responses appear to be restrained for large input motions which may imply that the multi-linear material model resulted in shakedown behavior. The elbow model predicted relatively accurate strain ratcheting histories compared to test data. However, it was noted that the level of accuracy for the analysis to test strain comparisons was not as good as for the piping system displacement and acceleration response. The comparison of the maximum strain ranges appeared to be more consistent among the four selected elements and generally better than comparisons using the entire strain ratcheting histories.

Although improvements in the analytical predictions with the updated material and finite element models were observed, large variations in the test comparisons, particularly for strain and strain ratcheting were still noted. The nonlinear dynamic characteristics of a large piping system are difficult to predict with high accuracy even when state-of-the-art models and finite element codes are used. In regulatory activities related to piping systems in nuclear power plants, reviewers should be aware of such difficulties and uncertainties in any piping system seismic analysis submittals involving elasto-plastic analysis.

Continued investigation of the subject may lead to a better understanding of the analytical methods and even quantification of the uncertainties in these methods and the supporting test data. For potential further studies of these test results, some additional modeling and analysis improvements can be explored. These improvements may include (1) refinement of the piping system model with smaller element sizes, (2) refinement of the elbow model locally at the strain range location, (3) characterization of the strain gradient along the hoop direction, (4) a transient analysis of the elbow model to take into account the inertia and damping effect, (5) a combined model with pipe elements for straight pipe segments and shell elements for the elbows and nozzles, (6) investigation of methods to better consider the plasticity accumulation over a series of consecutive tests, and (7) examination of the fatigue ratcheting failure mechanism. Items 4 through 7 require the use of high performance computers.

ACKNOWLEDGMENTS

The research program described in this report was sponsored by the Office of Nuclear Regulatory Research of the U.S. Nuclear Regulatory Commission. The authors would like to express their gratitude to Dr. Syed Ali, NRC Project Manager, for the technical and administrative support he provided in performing this study.

This research program was performed as part of the Implementing Agreement between the U.S. Nuclear Regulatory Commission and the Japan Nuclear Energy Safety Organization (JNES) in the Area of Seismic Engineering Research. This agreement is an item of the Implementing Arrangement between the United States Nuclear Regulatory Commission and the Nuclear and Industrial Safety Agency (NISA) of Japan for Cooperation in the Field of Nuclear Regulatory Matters and Nuclear Safety Research and Development.

Prior to the establishment of JNES, the Nuclear Power Engineering Corporation (NUPEC) of Japan performed the Ultimate Strength Piping Test Program discussed in this report. All of the test results and information about the test models included in this report were provided by JNES/NUPEC and are greatly appreciated. The authors especially thank Dr. Kenichi Suzuki of JNES/NUPEC for his support and technical guidance throughout this collaborative study. The authors also wish to acknowledge the helpfulness and cooperation provided by Mr. Hiroshi Abe, Mr. Yuichi Uchiyama, and Mr. Masakatsu Inagaki of JNES/NUPEC, and Mr. Takaaki Sakakida and Tadashi Iijima of Hitachi, Ltd.

The authors also thank Dr. Jim Xu of BNL for his assistance in generating the response spectra used in the linear analysis and for performing the initial linear analysis and code evaluation.

Giuliano DeGrassi, who led the work for BNL on the ultimate strength piping project, died on July 30, 2008 as final editing for the publication of this report was nearing completion. Giuliano is well known and respected by NRC and JNES/NUPEC staff, as well as other international collaborators, for his expertise in mechanical engineering, particularly the analysis and design of nuclear power plant piping systems and components. His tireless efforts and contributions to the many projects performed as part of the U.S. and Japan collaboration on seismic issues, as well as many other BNL and NRC projects, will be remembered. He was a wonderful colleague and extraordinary friend to many at BNL. Above all, his kind and caring personality will be missed by everyone who knew him.

1 INTRODUCTION

Prior to the establishment of the Japan Nuclear Energy Safety Organization (JNES), the Nuclear Power Engineering Corporation (NUPEC) of Japan conducted a multi-year Ultimate Strength Piping Test Program for the Ministry of Economy, Trade and Industry (METI) of Japan to investigate the behavior of typical Nuclear Power Plant (NPP) piping systems under large seismic loads. This project was taken over and completed by JNES upon its establishment. The objectives of this program were to develop a better understanding of the elasto-plastic response and ultimate strength of nuclear piping systems, to ascertain the seismic safety margins in current piping design codes, and to assess new code allowable stress rules. The test program consisted of a series of static and dynamic material tests, piping component tests, simplified piping system tests, and large-scale piping tests. The test program consisted of four phases: (1) monotonic and cyclic loading tests of piping material specimens; (2) static and dynamic tests of piping components such as elbows and tees; (3) seismic shaking table tests of two simple piping systems; and (4) seismic shaking table tests of a representative large-scale piping system.

As part of collaborative efforts between the United States and Japan on seismic issues, the U.S. Nuclear Regulatory Commission (NRC) and Brookhaven National Laboratory (BNL) participated in this program. The collaboration program included a series of periodic technical meetings held in Japan and the U.S. to discuss and exchange ideas on the test program plans, to review and evaluate the test results, and to review and evaluate both pre-test and post-test analyses. In accordance with the collaboration agreement, JNES/NUPEC provided their test results to NRC and BNL in the form of presentations and also provided selected test data for test runs to be analyzed by BNL in electronic format. NRC agreed to have BNL perform analyses for selected tests and provide the results in a series of presentations and reports. An earlier NUREG/CR report [DeGrassi and Hofmayer 2005] presented the results of the BNL analyses performed for the piping component tests and the simplified piping system tests. That report also included detailed descriptions of the material tests, piping component tests, and simplified piping tests that preceded the large-scale piping test. This report presents the results of the BNL analyses performed for the large-scale piping system tests and is the final product of the efforts under the Ultimate Strength Piping Test Program.

The purpose of this report is to present a summary of the JNES/NUPEC large-scale piping test program, to describe the BNL linear and nonlinear analyses of the large-scale piping system tests, and to discuss the insights gained from the program. Section 2 of this report provides a description and summary results of the JNES/NUPEC large-scale test program including background descriptions of the material tests, piping component tests, and simplified piping system tests. Section 3 presents the BNL linear seismic piping analyses and ASME Code evaluations for selected large-scale piping system tests. These analyses identify the highest stressed components and the degree to which the maximum stresses exceed Code allowables. By performing the evaluations in accordance with different versions of the Code and with different modal damping ratios, the minimum margins to failure associated with the NRC endorsed Code version (1993 Addenda) are calculated and compared with the margins based on the 1994 ASME Code Addenda and the 2004 Edition.

The results of the BNL nonlinear analyses are presented in Section 4. The objective of these analyses was to perform nonlinear analyses to investigate and evaluate the adequacy of currently available methods for predicting the elasto-plastic response of piping systems subjected to large earthquake loads. Similar analyses and investigations had been conducted previously for the simplified piping system tests by DeGrassi and Hofmayer [2005]. Continuing that work, for the large-scale piping system tests, additional analytical studies were carried out to include improvements in the material models, input motion characterization, and many parametric studies for the complex nonlinear transient analyses. Due to the large size of the model, the analyses required two models: a plastic piping element model for performing

dynamic time history analysis, and a shell element model for determining strains and strain ratcheting in the critical elbow. The piping element model computed displacements, and the displacements at the ends of the elbow were applied statically to the elbow model. Section 4 describes the various analytical studies, shows the comparisons of analysis results to test data, and discusses and assesses the findings from these studies

A summary of conclusions including regulatory insights and lessons learned from the program, and recommendations for further research are presented in Section 5.0.

2 DESCRIPTION OF JNES/NUPEC TEST PROGRAM

2.1 Introduction

A major goal of the JNES/NUPEC test program was the performance of a seismic proving test of a representative large-scale piping system. In order to gain a better understanding of the piping behavior prior to performing the proving test, JNES/NUPEC conducted a series of material and piping component static and dynamic tests, and simplified piping system seismic tests. An earlier NUREG/CR report [DeGrassi and Hofmayer 2005] provided detailed descriptions of the material, component, and simplified piping tests. This chapter briefly summarizes those tests and provides a detailed description of the large-scale piping system tests.

2.2 Material Tests

JNES/NUPEC carried out a series of static monotonic loading and cyclic loading tests to develop stress-strain curves and properties for typical piping materials. In the monotonic loading tests, the specimens were tensile tested to failure. The results of the tests provided the stress-strain curves and basic material properties including yield strength, ultimate strength, percent elongation, percent area reduction, and ultimate strain. A typical stress-strain curve for STS410 carbon steel is shown in Figure 2-1. In the cyclic loading tests, the specimens were subjected to strain-controlled incremental cycling in consecutive blocks of twenty increasing amplitude cycles followed by twenty decreasing amplitude cycles. These tests provided stress-strain hysteresis curves and also provided cyclic stress-strain curves for the materials for strains up to 2.5%. A typical series of hysteresis curves for STS410 carbon steel are shown in Figure 2-2. A typical cyclic stress-strain curve is shown in Figure 2-3. JNES/NUPEC also carried out a series of low-cycle strain-controlled ratcheting fatigue tests for typical piping materials. Test results provided data on strain versus number of cycles for different strain ranges and mean strain accumulation rates. They demonstrated that higher mean strain accumulation rates result in shorter fatigue lives for all materials and temperatures.

2.3 Piping Component Tests

In the second phase of the program, JNES/NUPEC conducted static and dynamic tests on typical piping components that included elbows, tees, nozzles and reducers. A total of sixteen static tests were performed. A typical test setup for a static elbow test is shown in Figure 2-4. In the monotonic loading tests, the specimens were unpressurized and loaded to failure to determine the lower bound collapse moment. In the cyclic loading tests, the test specimens were pressurized to induce an internal pressure stress equal to S_m, and then subjected to quasi-static sinusoidal displacements until a fatigue crack developed. The specimens were cycled until through-wall cracks were detected. JNES/NUPEC reported the monotonic test results as plots of load versus deflection and strain versus deflection up to the collapse load. The cyclic test results were reported as plots of load-deflection hysteresis curves, strain distributions at critical component sections, and maximum strain versus number of cycles. The strain versus cycle plots illustrated the accumulation of ratcheting strain during the tests. A typical plot of strain versus number of cycles up to failure for the SE-4 test is shown in Figure 2-5.

The component dynamic tests were performed on a seismic shaking table. The test specimens were subjected to either sinusoidal or seismic wave acceleration input motions. A large mass on rollers was attached to one end of the test specimen. Test specimen variations included pipe component type, material, and diameter. All tests were conducted at room temperature. All specimens were pressurized to induce a stress level of either S_m or 0.5 S_m. The specimens were tested until though-wall cracking was observed. The test results were reported as plots of load-deflection hysteresis curves, displacement time histories, and strain time histories. The strain versus time plots illustrated the accumulation of ratcheting strain during the tests.

2.4 Simplified Piping System Tests

In the third phase of the program, JNES/NUPEC conducted a series of simplified piping system shaking table tests to investigate the elasto-plastic response of small systems with typical piping components under large seismic excitations. These tests included two-dimensional test model configurations (Model A) and three-dimensional configurations (Model B). The pipe was 65 mm (2-½ inch) Schedule 40 carbon steel grade JIS STS410. In the two-dimensional configuration, the pipe routing was in the horizontal plane and was subjected to single-direction horizontal seismic input motion. A typical Model A simplified piping system test setup is shown in Figure 2-6. The system was pressurized to 19.8 MPa (2870 psi) to induce a pressure stress equal to S_m. Concentrated masses were clamped to the pipe to provide the desired dynamic characteristics for the system. Pipe routing for the three-dimensional configuration (Model B) was identical to the Model A routing in the horizontal plane with the addition of a branch line in the vertical plane as shown in Figure 2-7. The branch line was connected to the horizontal run pipe with a tee, and consisted of a riser pipe, a long radius elbow, and a horizontal straight pipe that terminated at a nozzle. An additional concentrated mass was attached to the horizontal portion of the branch line. Variable spring hangers were used to provide gravity support to the system without constraining vertical motion. The system was pressurized to 19.8 MPa (2870 psi). Both systems were instrumented with accelerometers, displacement sensors, and strain gages at critical locations.

The basic seismic input excitations for the tests were selected to represent typical horizontal and vertical building floor response spectra for Japanese PWR and BWR plants. However, the time scales were adjusted to provide near resonant responses and the amplitudes of the seismic waves were modified to obtain the desired large elasto-plastic responses. The tests were performed at a medium and at a high excitation level. JNES/NUPEC conducted a number of tests of both Model A and Model B specimens to investigate different loading and design variations. The basic two-dimensional test (A-1) subjected the pipe to a single horizontal direction medium level seismic load. In test A-2, a large level seismic load was applied. The three-dimensional test (Model B) load cases subjected the test specimens to horizontal, vertical and simultaneous horizontal and vertical motions. Test B-1 subjected the pipe to a single horizontal direction medium level seismic load. Test B-2 subjected the pipe to a vertical direction medium level seismic load. In test B-3, simultaneous horizontal and vertical medium level seismic motions were applied.

The piping systems were monitored during each test to measure accelerations, displacements, and strains at selected locations. The results illustrated the accumulation of permanent deformations and strains that occurred during the tests. There were no failures reported during the application of a single seismic time history. However, JNES/NUPEC repeated selected high input level tests to induce failure and reported that cracking at the elbow A location was observed after seven tests of the high level seismic time history. Cracking at the nozzle occurred after 18 applications of the high level seismic time history. For both tests, the failures were attributed to fatigue ratcheting.

2.5 Large-Scale Piping System Tests

In the final phase of the test program, JNES/NUPEC performed a series of seismic shaking table tests on a representative large-scale piping system. The tests were performed using the large high performance shaking table at the Tadotsu Engineering Laboratory. The test specimen was a 200 mm (8 inch) nominal diameter) Schedule 40 carbon steel (STS410) pipe. Two series of tests were performed using two different test specimens. The first was a Design Method Confirmation (DM) Test and the second was an Ultimate Strength (US) Test. The three-dimensional routing of the Design Method Confirmation Test specimen represented typical configuration characteristics of safety-related Japanese nuclear power plant piping systems. The piping system included straight pipe, nine elbows, a tee, and a 1000 kg (2200 lb) added mass representing a valve as illustrated in Figure 2-8. The system was supported by nozzles, an anchor, three two-directional supports, a horizontal support, a vertical support and a spring hanger.

Photographs of the DM Test Piping and its components are shown in Figure 2-9 through Figure 2-14. The system was instrumented with accelerometers, displacement sensors, and strain gages at critical locations as shown in Figure 2-15 through Figure 2-18. The Ultimate Strength Test piping specimen had an identical piping configuration with the same piping components. Since this test was designed to stress the pipe to failure, it was modified by the addition of another 1000 kg (2200 lb) mass and the removal of a lateral support as illustrated in Figure 2-19. As shown, one of the two-directional supports was replaced by a vertical support. Photographs of the US Test Piping and its components are shown in Figure 2-20 through Figure 2-22. This system was also instrumented with accelerometers, displacement sensors, and strain gages at critical locations as shown in Figure 2-23 through Figure 2-25

A series of test load cases were carried out for each piping test specimen. A summary of the test cases is presented in Table 2-1. The design method confirmation tests included preliminary tests (DM1), allowable stress tests (DM2), and elasto-plastic response tests (DM4). Preliminary tests included horizontal and vertical low-level sine sweep tests (DM1-1) to determine the frequencies and modal damping values as summarized in Table 2-2, and seismic tests (DM1-2) in which seismic input motions were applied separately in the horizontal and vertical directions. The seismic input motion was selected based on the Japanese "S_2" seismic wave for a PWR. For each test, the seismic wave was adjusted to achieve the desired maximum stress limits. The input motion for the DM2-1 test was selected to induce a maximum stress equal to the Japanese Code primary stress limit of $3S_m$ (JEAG 4601-1984 Edition). For the DM2-2 test, the input motion was to induce a maximum stress level equal to 1.5 times the Code limit or $4.5S_m$. Seismic table motion was applied simultaneously in the horizontal and vertical directions. In this series of tests, the dominant input motion frequency was not close to the fundamental piping system frequency (off-resonance). The DM4 series of elasto-plastic response tests applied higher input motions to achieve plasticity with stress levels from 2 to 4.5 times the primary stress limit ($6S_m$, $10.5S_m$, and $13.5S_m$). In order to achieve these high levels, the seismic waves were adjusted so that the dominant input motion frequency was close to the fundamental piping system frequency (on-resonance). In all of these tests, the piping system was internally pressurized to induce a hoop stress equal to the design stress intensity S_m. The tests were conducted at room temperature and no evidence of pipe failure was observed.

JNES/NUPEC provided the results of the Design Method Confirmation tests shown in Table 2-1 as digitized acceleration, displacement, support load, and strain time histories. Frequencies and damping ratios at high levels of seismic acceleration were also calculated by JNES/NUPEC and are shown in Table 2-4. Representative time history results are shown in Figure 2-26 to Figure 2-28. Horizontal and vertical seismic acceleration input motions for the DM4-2(2) test are shown in Figure 2-26. Maximum piping response displacement time history is shown in Figure 2-27. The maximum strains were measured at the flanks of piping elbow 2. Hoop strain time history at this elbow for the DM4-2(2) tests is shown in Figure 2-28

The Ultimate Strength Test was designed to fail the pipe. As indicated in Table 2-1, this test series included preliminary low-level sine sweep tests (US1) to determine the frequencies and modal damping values as shown in Table 2-3, and ultimate strength seismic tests (US2). The seismic input motion was designed to induce a maximum stress level equal to 8 times the Code limit or $24S_m$. In order to achieve this high stress level, the seismic waves were adjusted so that the dominant input motion frequency was close to the fundamental piping system frequency (on-resonance). In these tests, the seismic table motion was applied only in the horizontal direction. The piping system was internally pressurized to a design stress intensity of S_m and the tests were conducted at room temperature. The seismic input motion was repeated until failure occurred. During the fifth test run, a longitudinal through-wall crack developed in elbow 2. A photograph of the failure is shown in Figure 2-29. A close-up of the longitudinal crack in the elbow is shown in Figure 2-30. An examination confirmed that the failure was the result of fatigue ratcheting.

JNES/NUPEC provided the results of the Ultimate Strength tests shown in Table 2-1 as digitized acceleration, displacement, support load and strain time histories. Representative results are shown in Figure 2-31 to Figure 2-33. Horizontal seismic acceleration input motion for the US2 test is shown in Figure 2-31. Maximum piping response displacement time history is shown in Figure 2-32. As expected, the maximum strains were measured at the flanks of piping elbow 2. Hoop strain time history at this elbow for the US2 test is shown in Figure 2-33.

Table 2-1 JNES/NUPEC Large-Scale Piping System Test Load Cases

Test Case			Excitation Wave	Excitation Direction	Design Stress Level	Dominant Frequency
Design Method Confirmation Test	Preliminary Test	DM1-1	Sweep	Horizontal	(Elastic)	—
			Sweep	Vertical	(Elastic)	—
		DM1-2	Seismic	Horizontal	(=DM2-1,2)	Off-resonance
			Seismic	Vertical	(=DM2-1,2)	
	Allowable Stress Test	DM2-1	Seismic	H + V	3Sm (=S2 limit)	Off-resonance
		DM2-2	Seismic	H + V	4.5Sm	
	Elasto-Plastic Response Test	DM4-1	Seismic	H + V	6Sm	On-resonance
		DM4-2(1)	Seismic	H + V	10.5Sm	
		DM 4-2(2)	Seismic	H + V	13.5Sm	
Ultimate Strength Test	Preliminary Test	US1	Sweep	Horizontal	(Elastic)	—
			Sweep	Vertical	(Elastic)	—
	Ultimate Strength Test	US2	Seismic	Horizontal	24Sm	On-resonance

Table 2-2 DM Test Frequencies and Damping Ratios from Low Level Sine Sweep Tests

Mode	Frequency (Hz)	Damping Ratio (%)	Direction
1st	6.3	2.1	Horizontal
2nd	8.1	4.8	Vertical

Table 2-3 US Test Frequencies and Damping Ratios from Low Level Sine Sweep Tests

Mode	Frequency (Hz)	Damping Ratio (%)	Direction
1st	3.8	0.9	Horizontal
2nd	6.4	1.2	Vertical

Table 2-4 DM and US Test Frequencies and Damping Ratios from Seismic Tests

Test Case	Resonant Frequency (Hz)	Damping Ratio (%)	Maximum Design Stress
DM2-1	6.3	2.1	$3S_m$
DM2-2	6.2	2.3	$4.5S_m$
DM4-1	6	2.4	$6S_m$
DM4-2(1)	6	2.9	$10.5S_m$
DM4-2(2)	5.9	3.4	$13.5S_m$
US2	3.6	4.5	$24S_m$

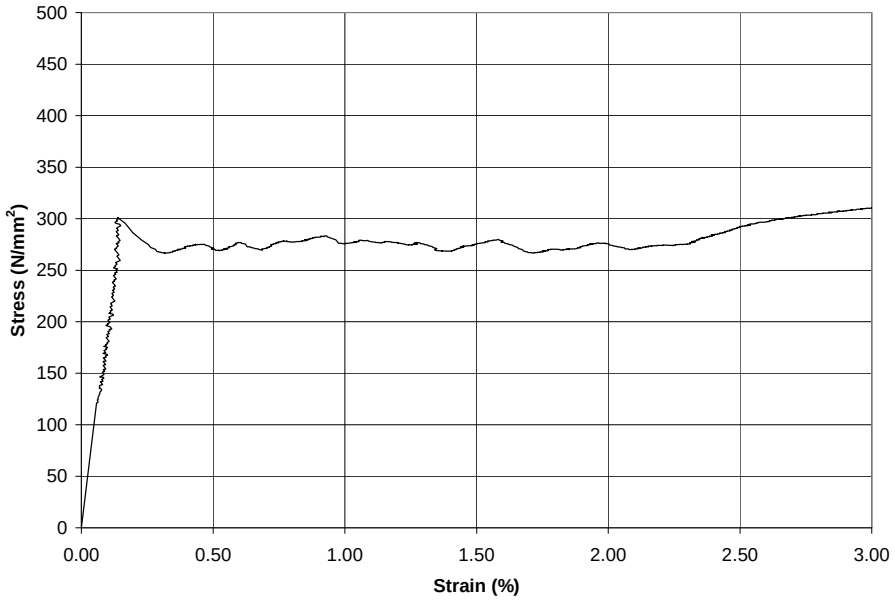

Figure 2-1 Monotonic Loading Stress-Strain Curve for STS410 Carbon Steel
(1 N/mm^2 = 145 psi)

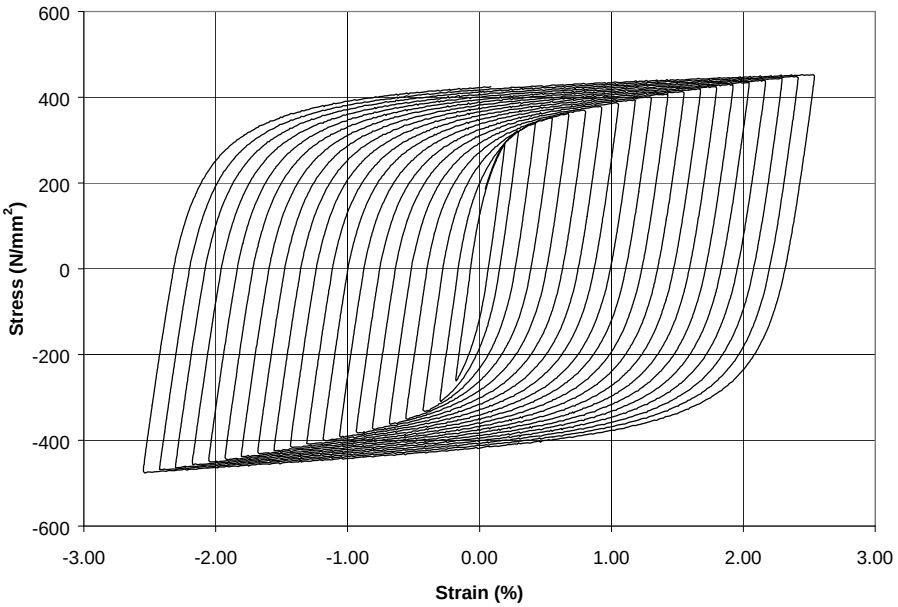

Figure 2-2 Uniaxial Cycling Test Hysteresis Curves for STS410 Carbon Steel
(1 N/mm^2 = 145 psi)

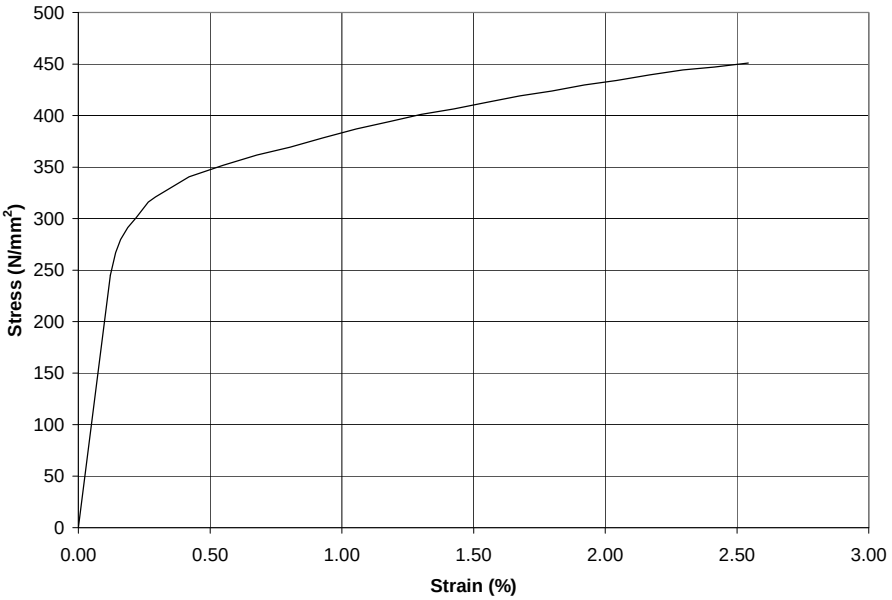

Figure 2-3 Cyclic Stress-Strain Curve for STS410 Carbon Steel

(1 N/mm^2 = 145 psi)

Dimension shown in mm;
1 mm = 0.03937 in

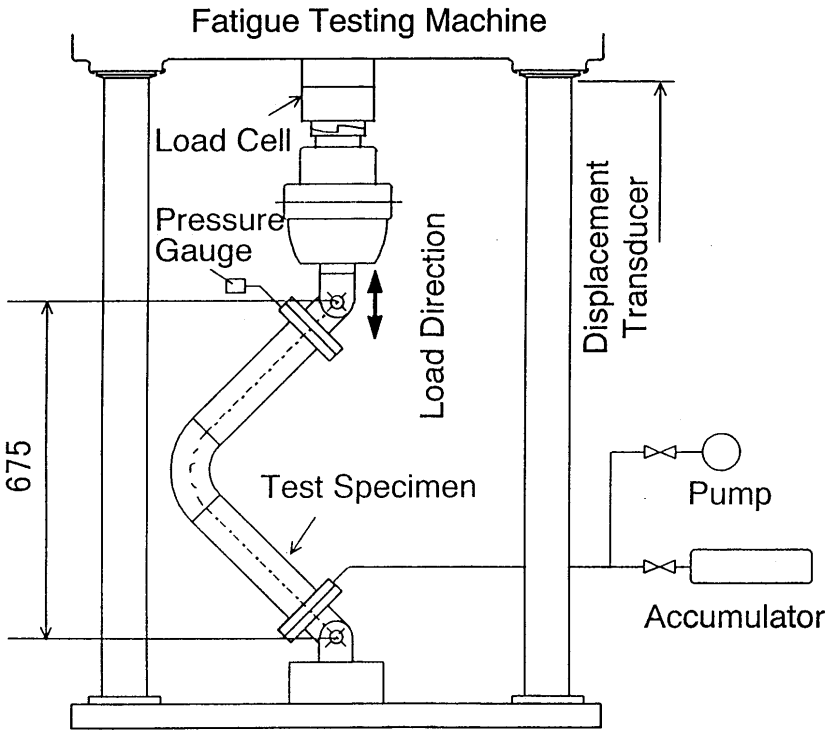

Figure 2-4 Static Elbow Cycling Test Setup

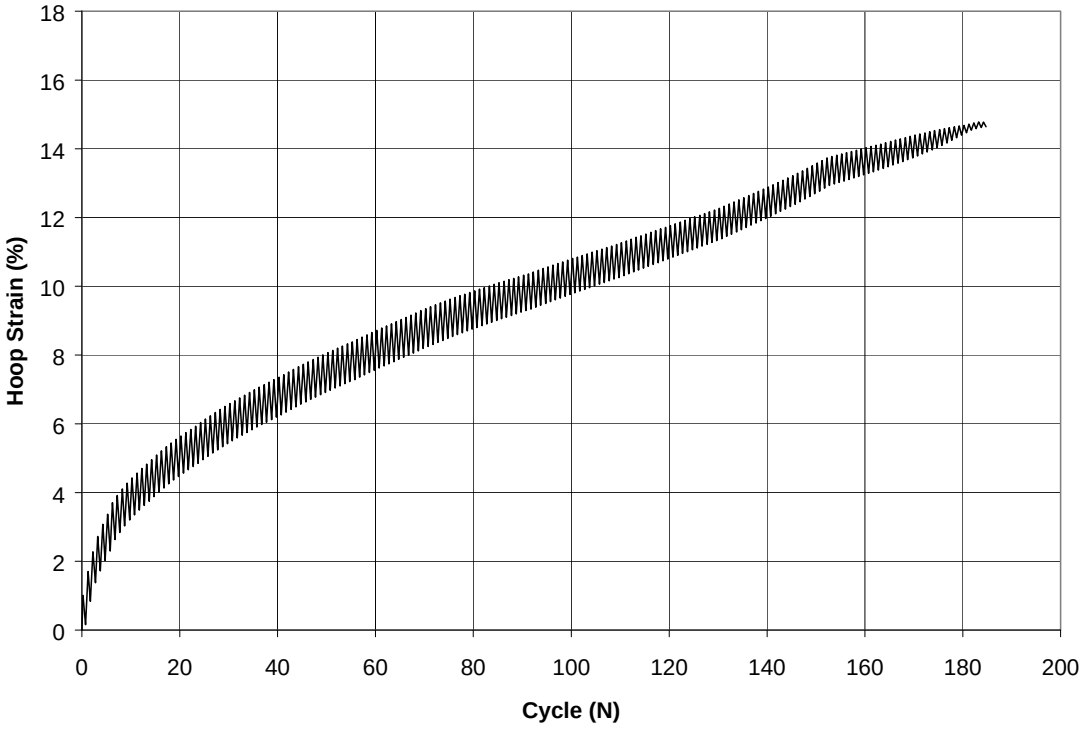

Figure 2-5 Elbow Static Cycling Test SE-4 Hoop Strain vs. Cycle at Elbow Flank

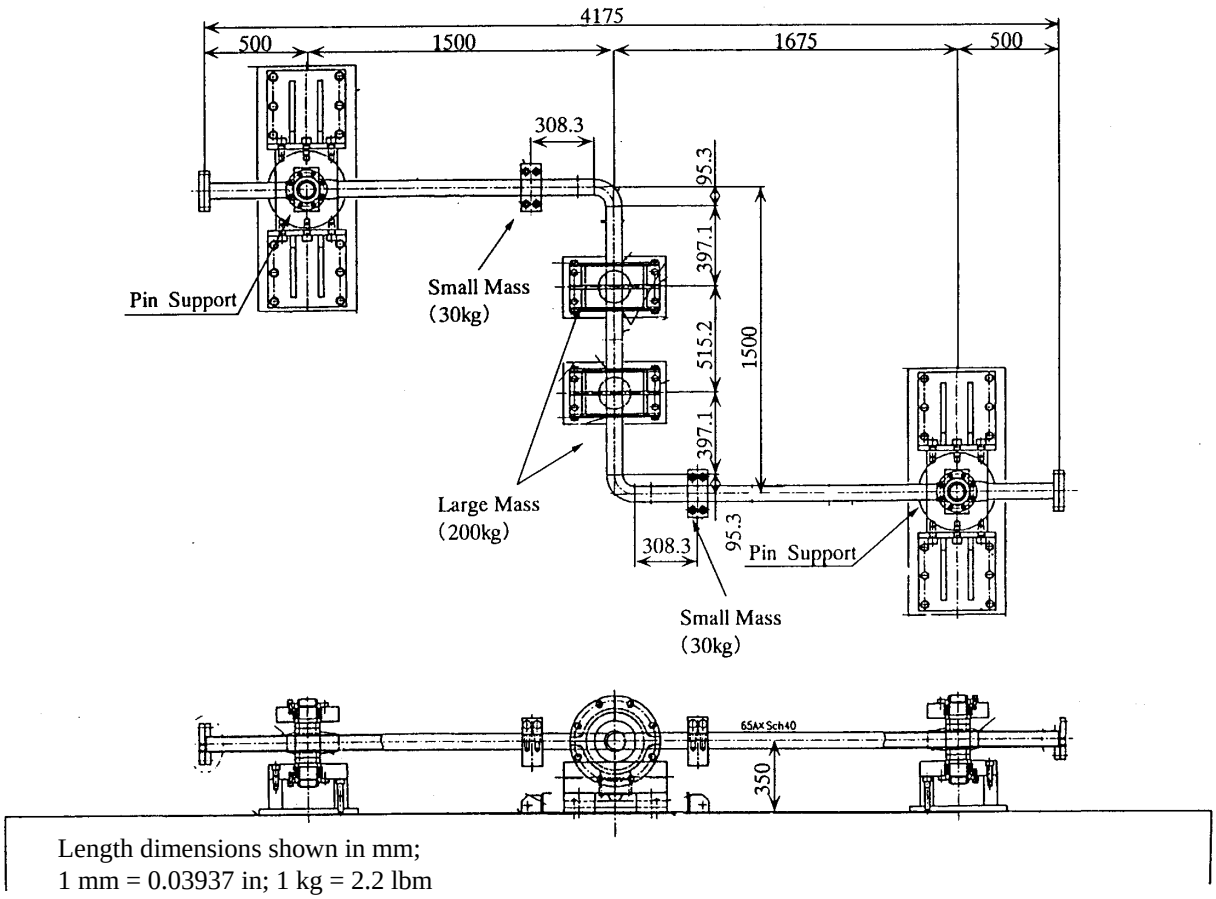

Figure 2-6 Model A Simplified Piping System Test Setup

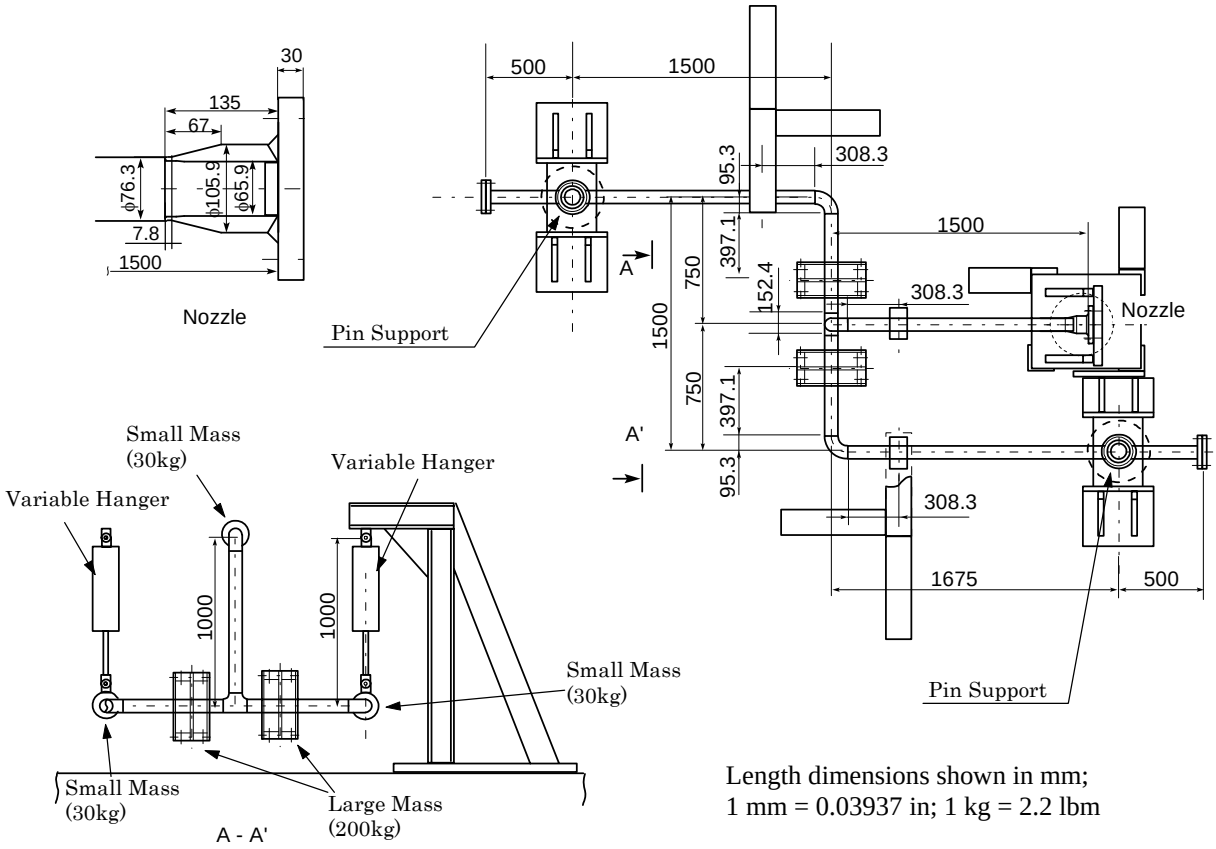

Figure 2-7 Model B Simplified Piping System Test Setup

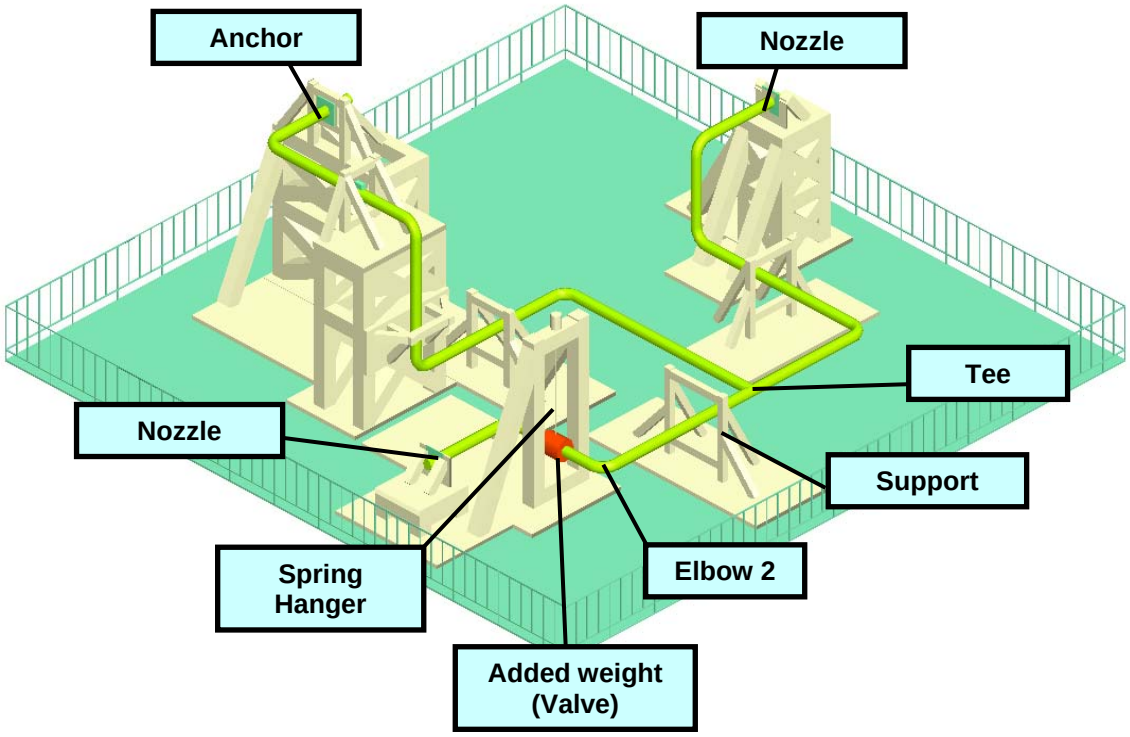

Figure 2-8 Design Method Confirmation Test Setup

Figure 2-9 Overview of Design Method Confirmation Test Piping System

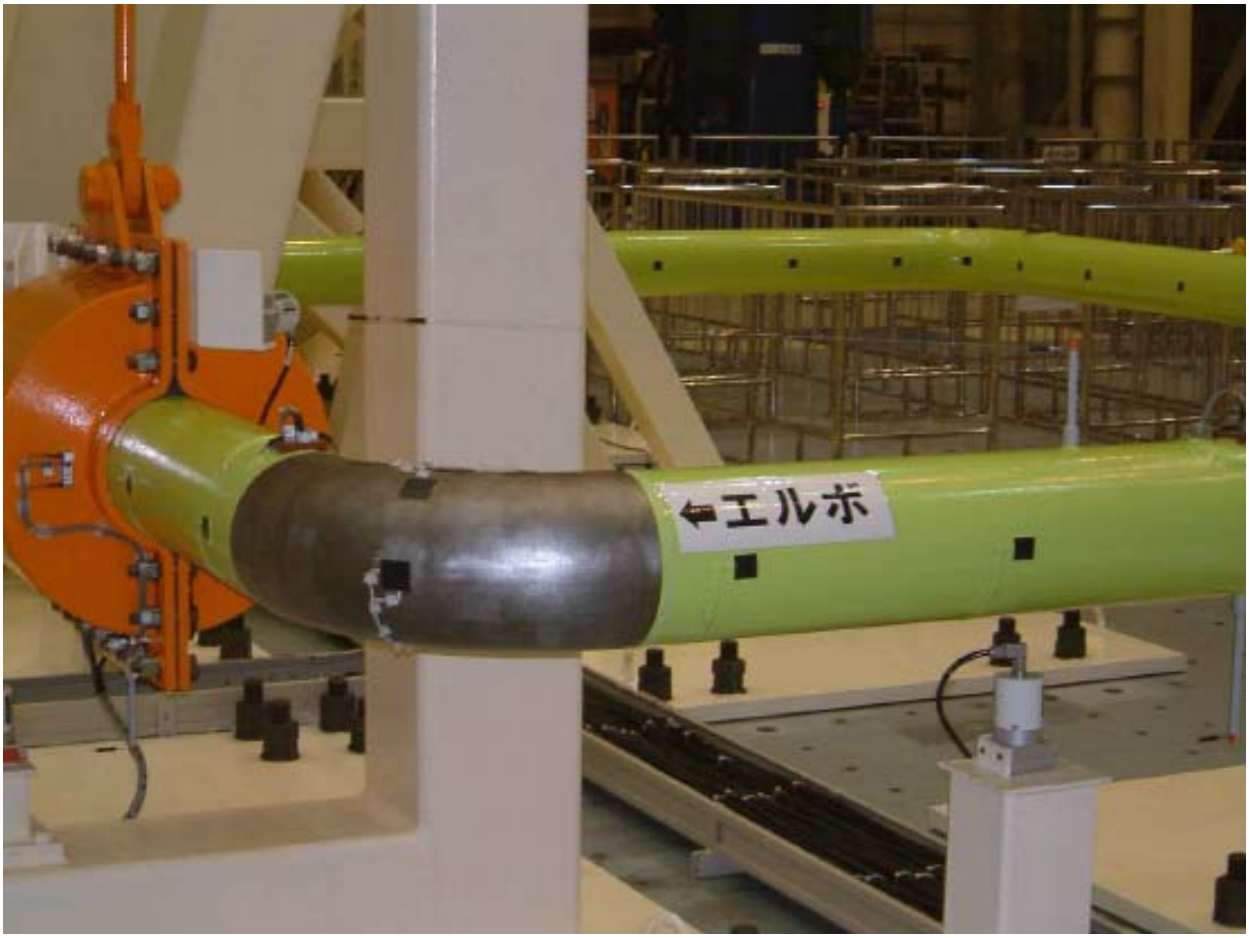

Figure 2-10 DM Test Critical Elbow 2 and Added Mass

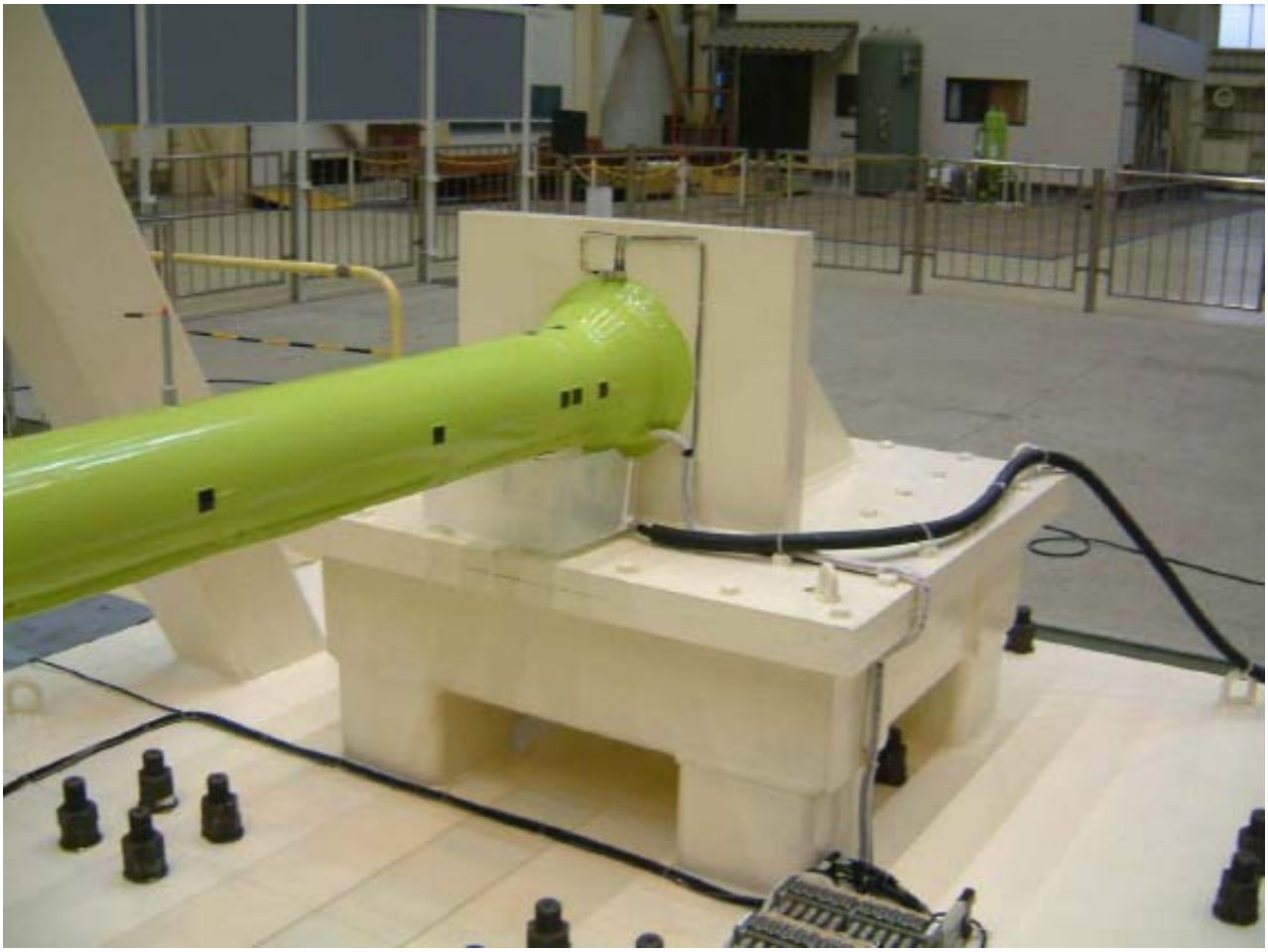

Figure 2-11 DM Test Nozzle

Figure 2-12 DM Test Anchor

Figure 2-13 DM Test Spring Hanger

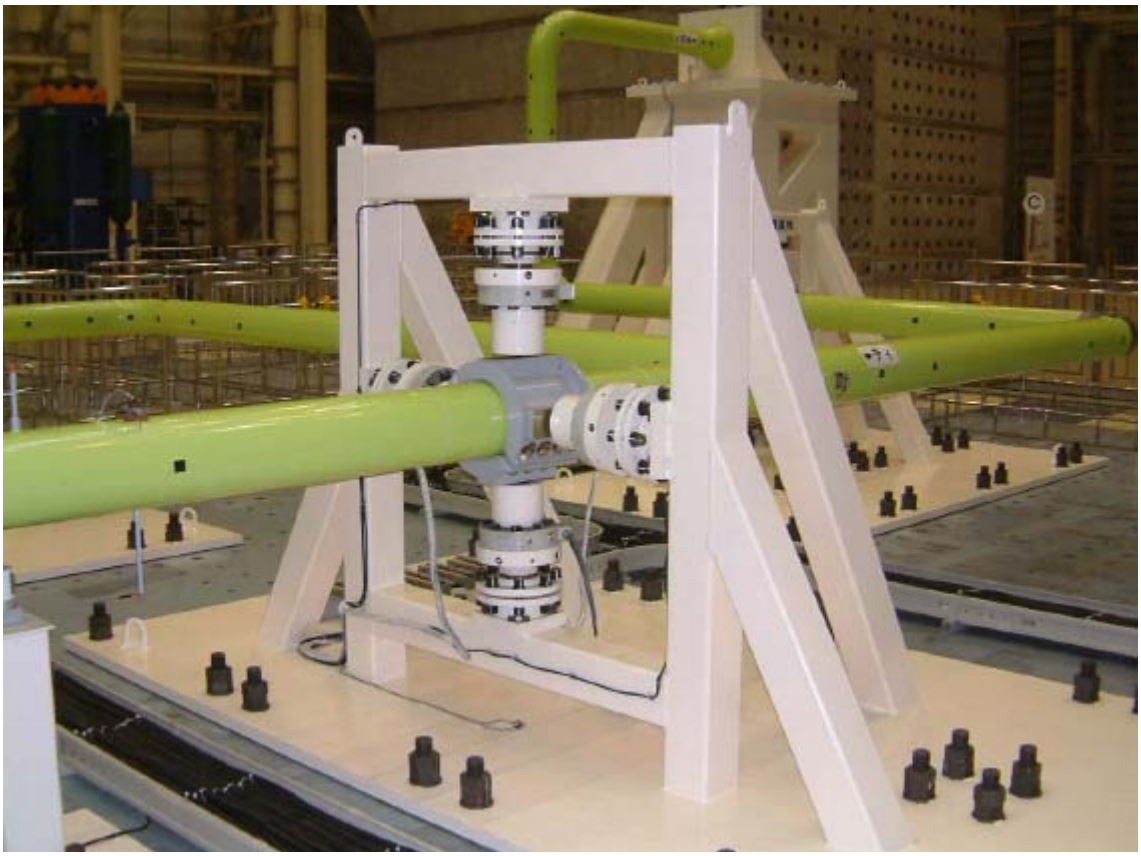

Figure 2-14 DM Test Typical Two-Directional Support

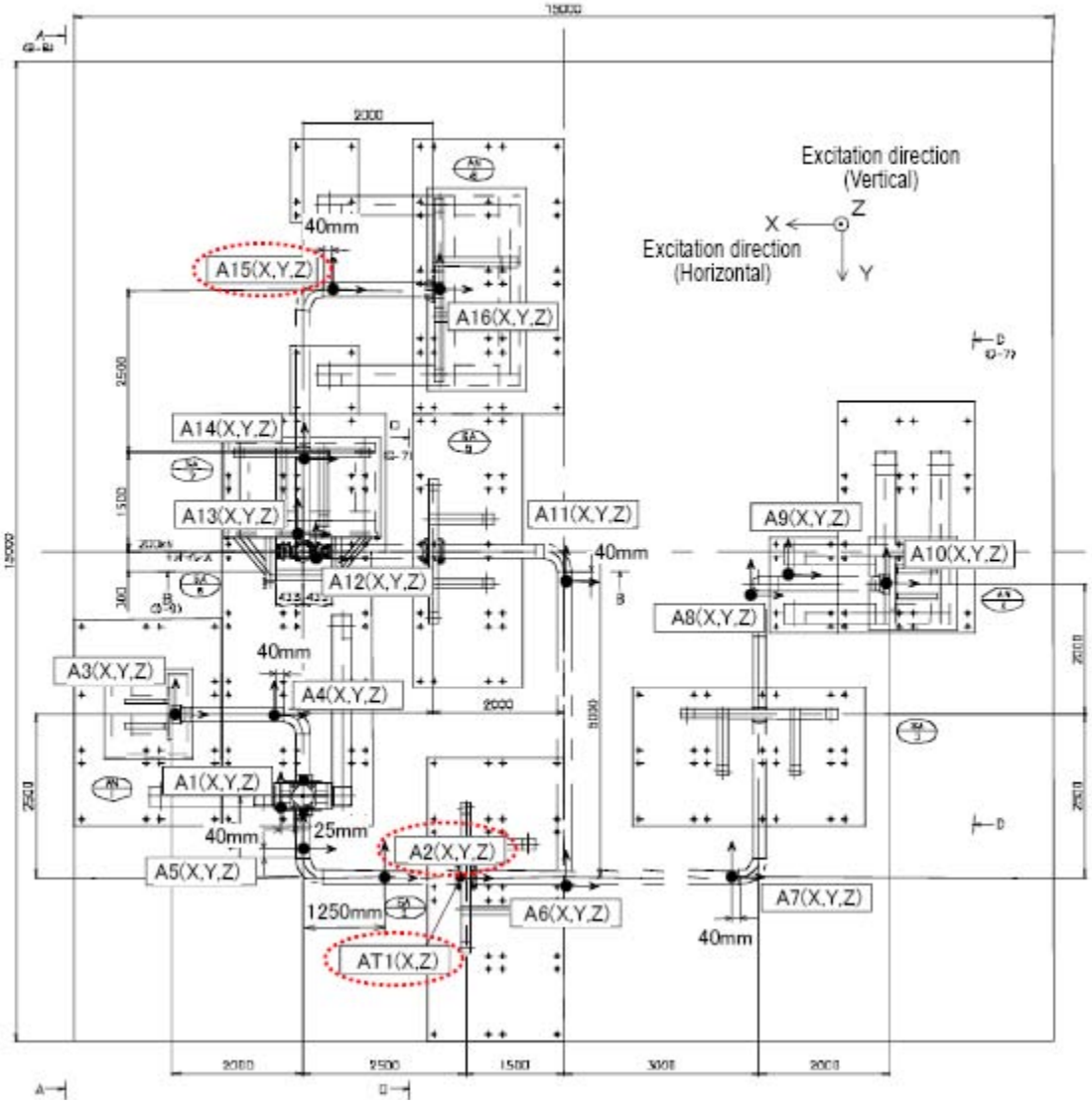

Figure 2-15 DM Test Accelerometer Locations

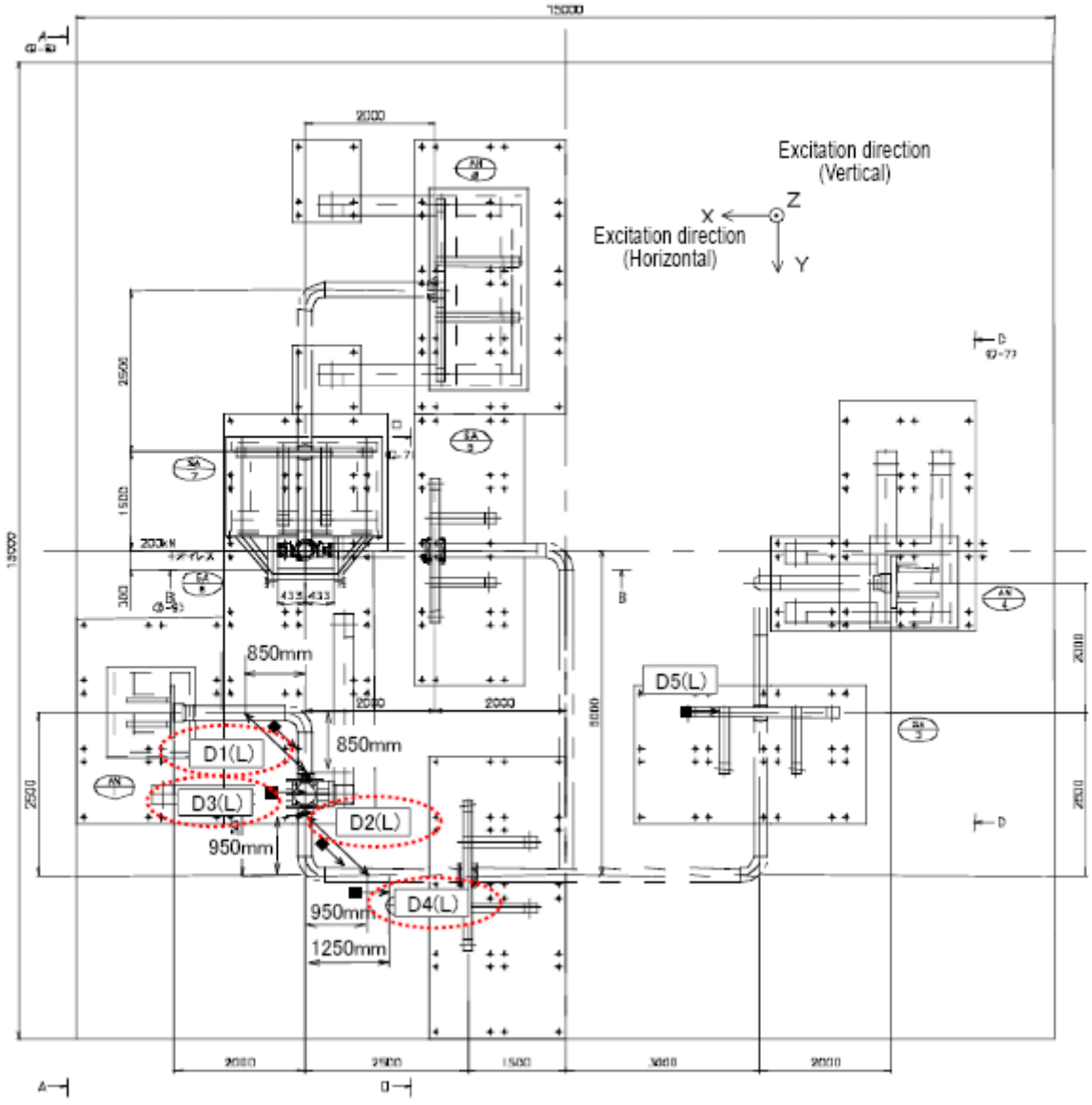

Figure 2-16 DM Test Displacement Gage Locations

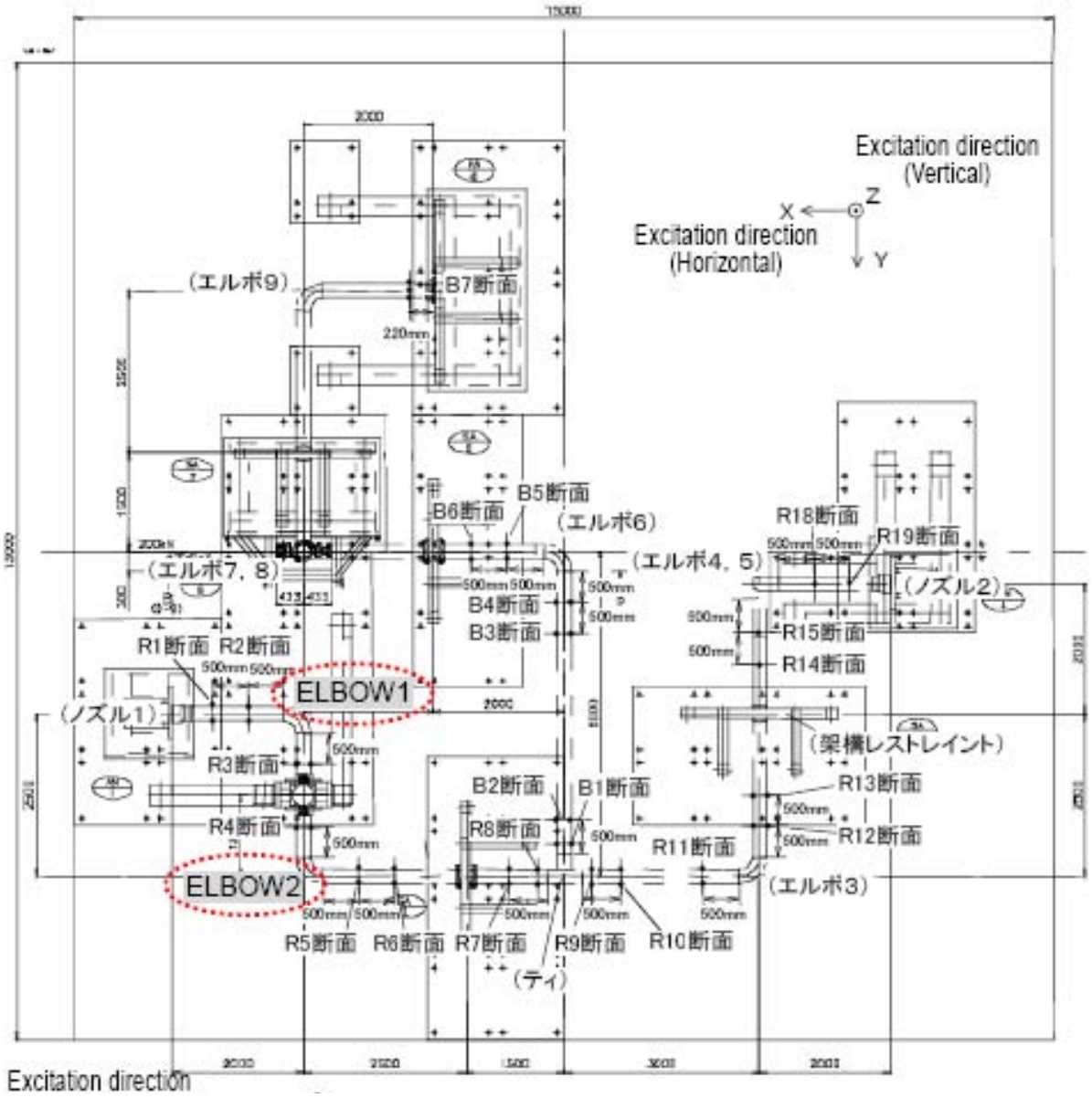

Figure 2-17 DM Test Strain Gage Locations

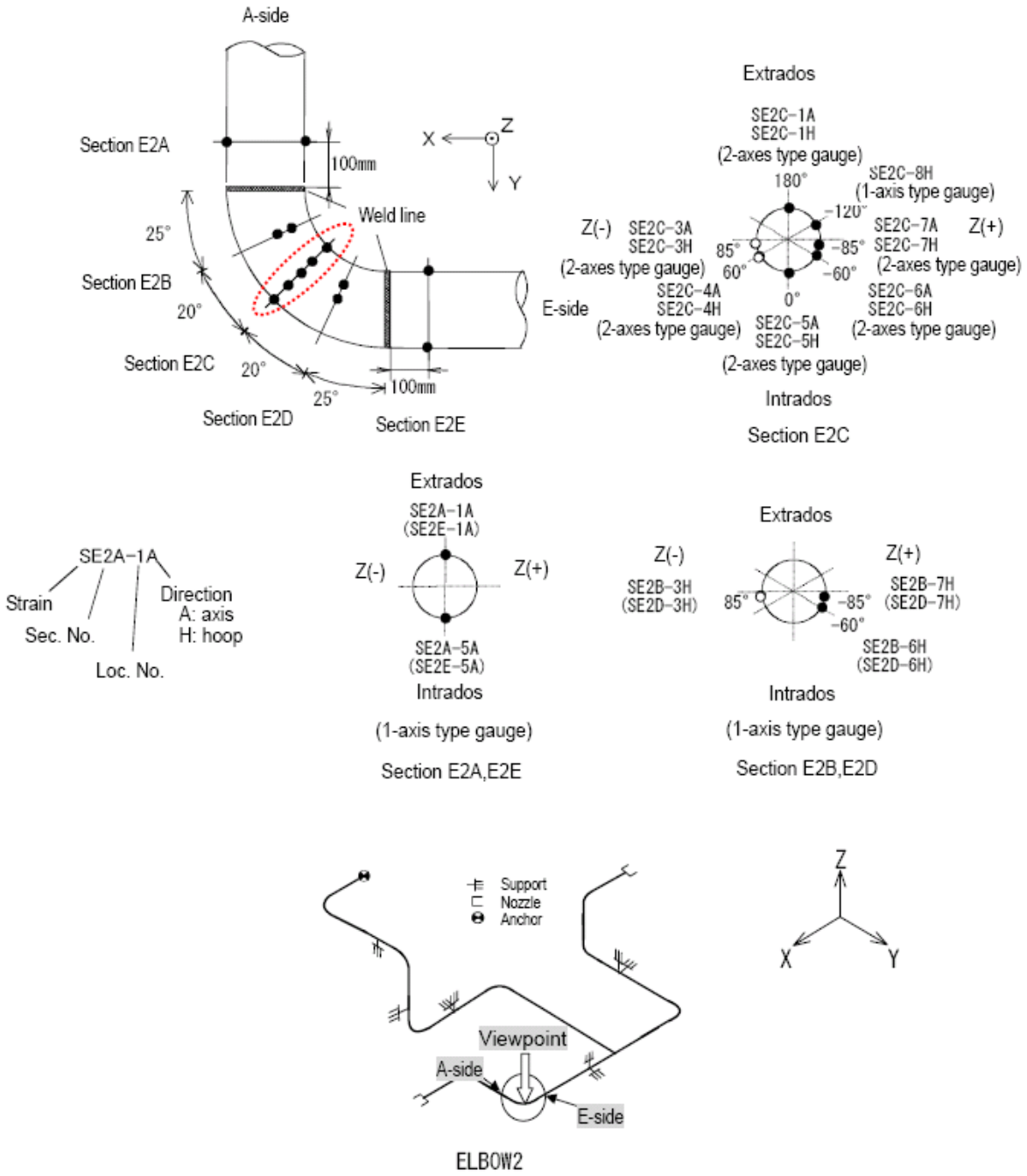

Figure 2-18 Strain Gage Locations at Elbow 2 (DM Test and US Test)

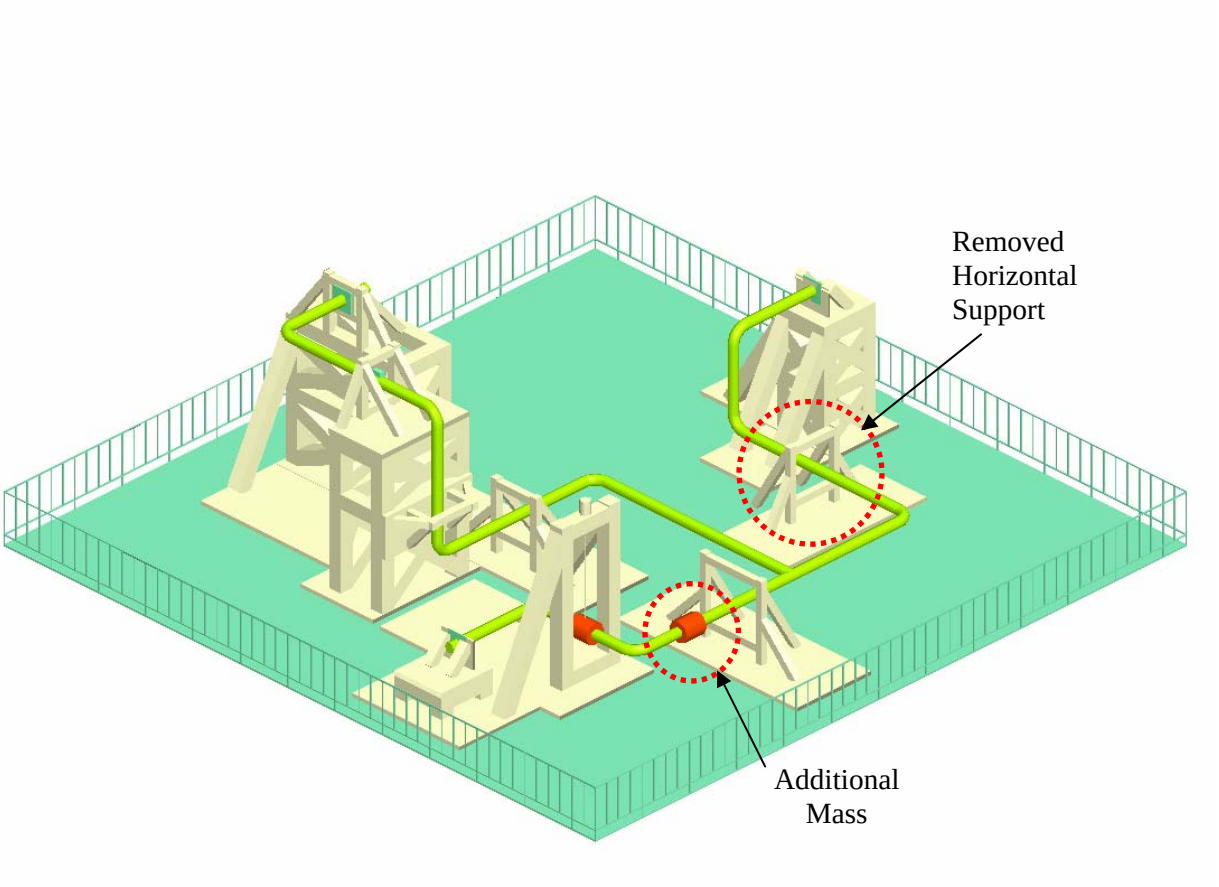

Figure 2-19 US Test Piping System Setup showing differences from DM Test Setup

Figure 2-20 Overview of Ultimate Strength Test Piping System

Figure 2-21 US Test Elbow 2 and Added Masses

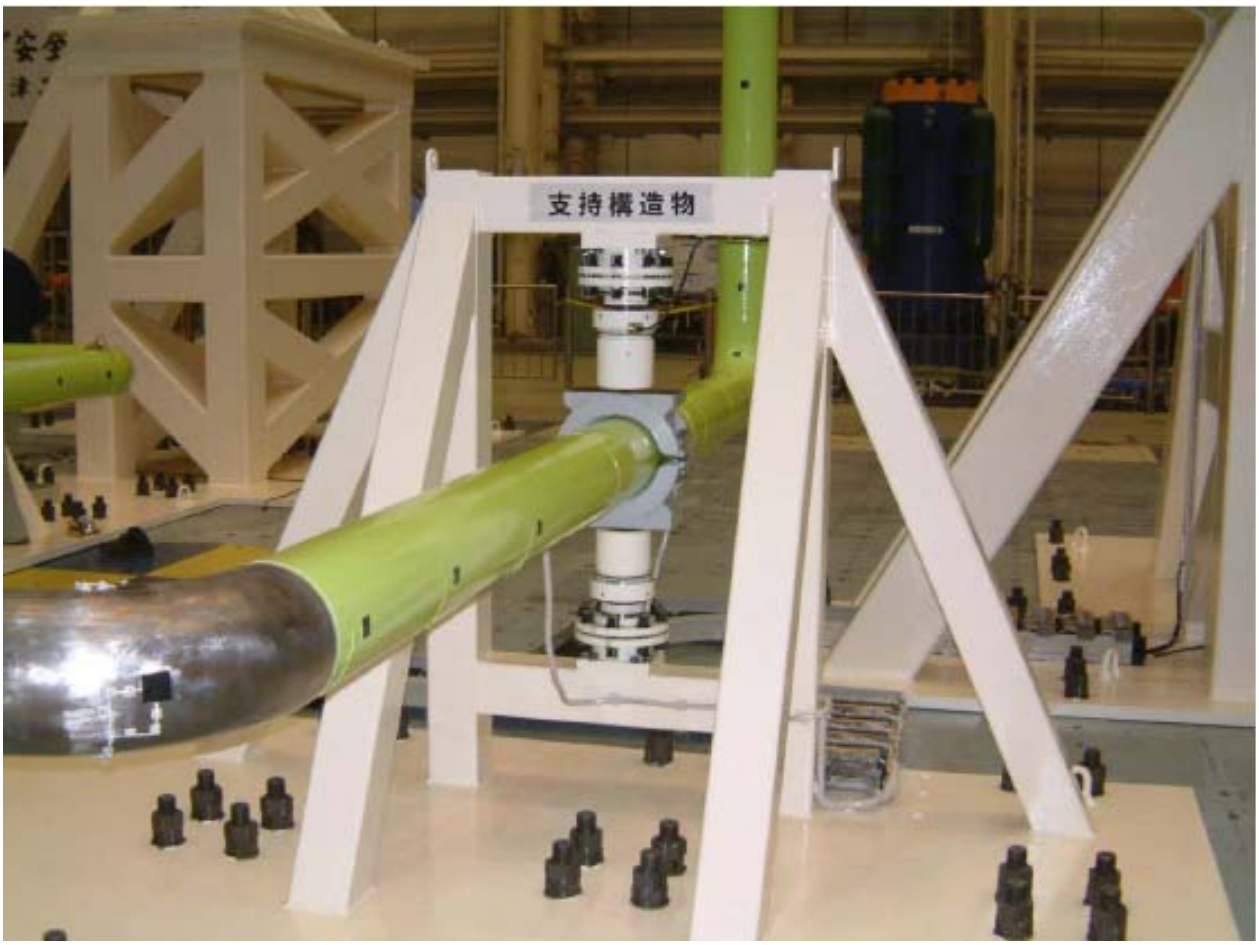

Figure 2-22 US Test One-Directional Vertical Support

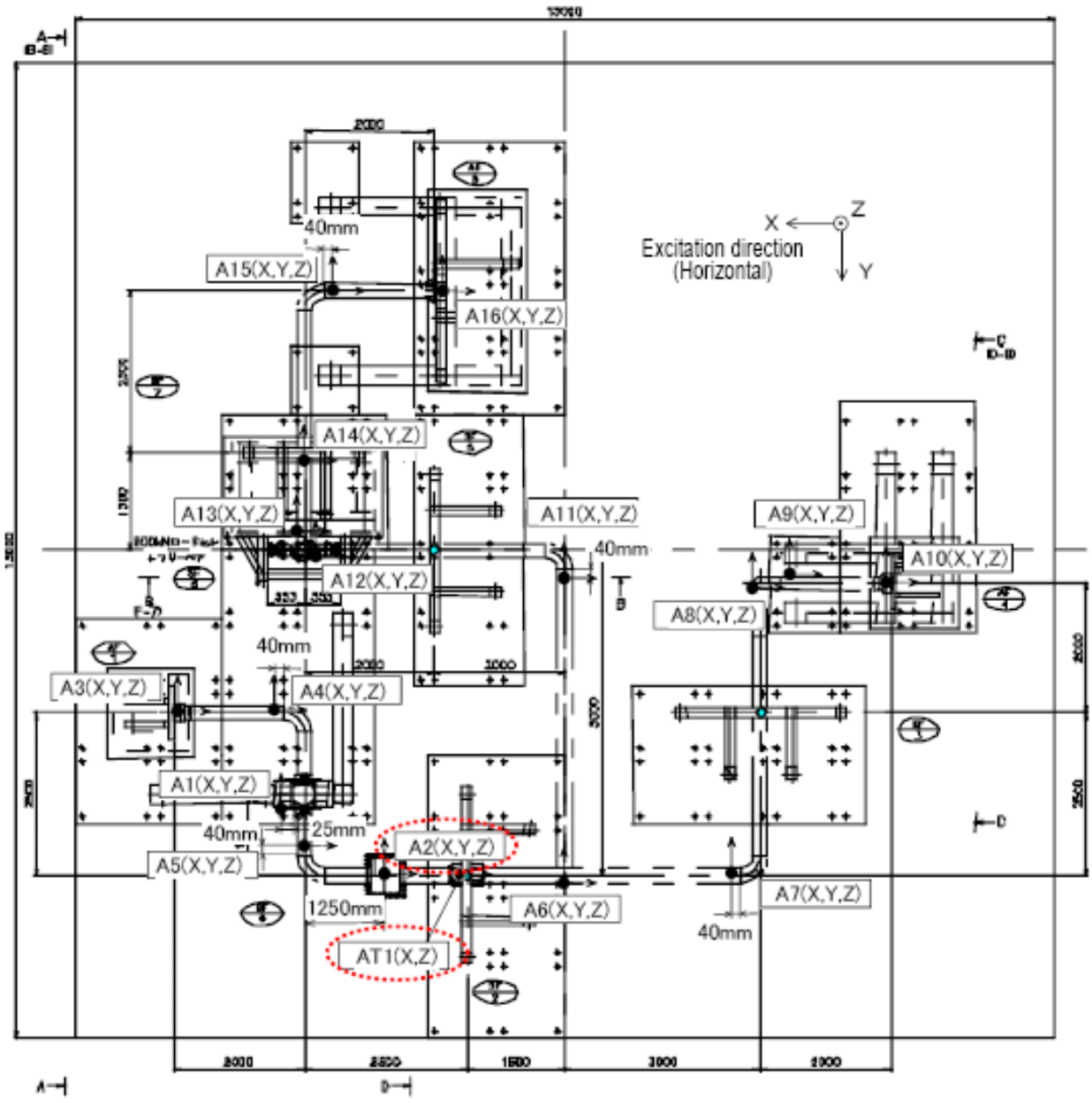

Figure 2-23 US Test Accelerometer Locations

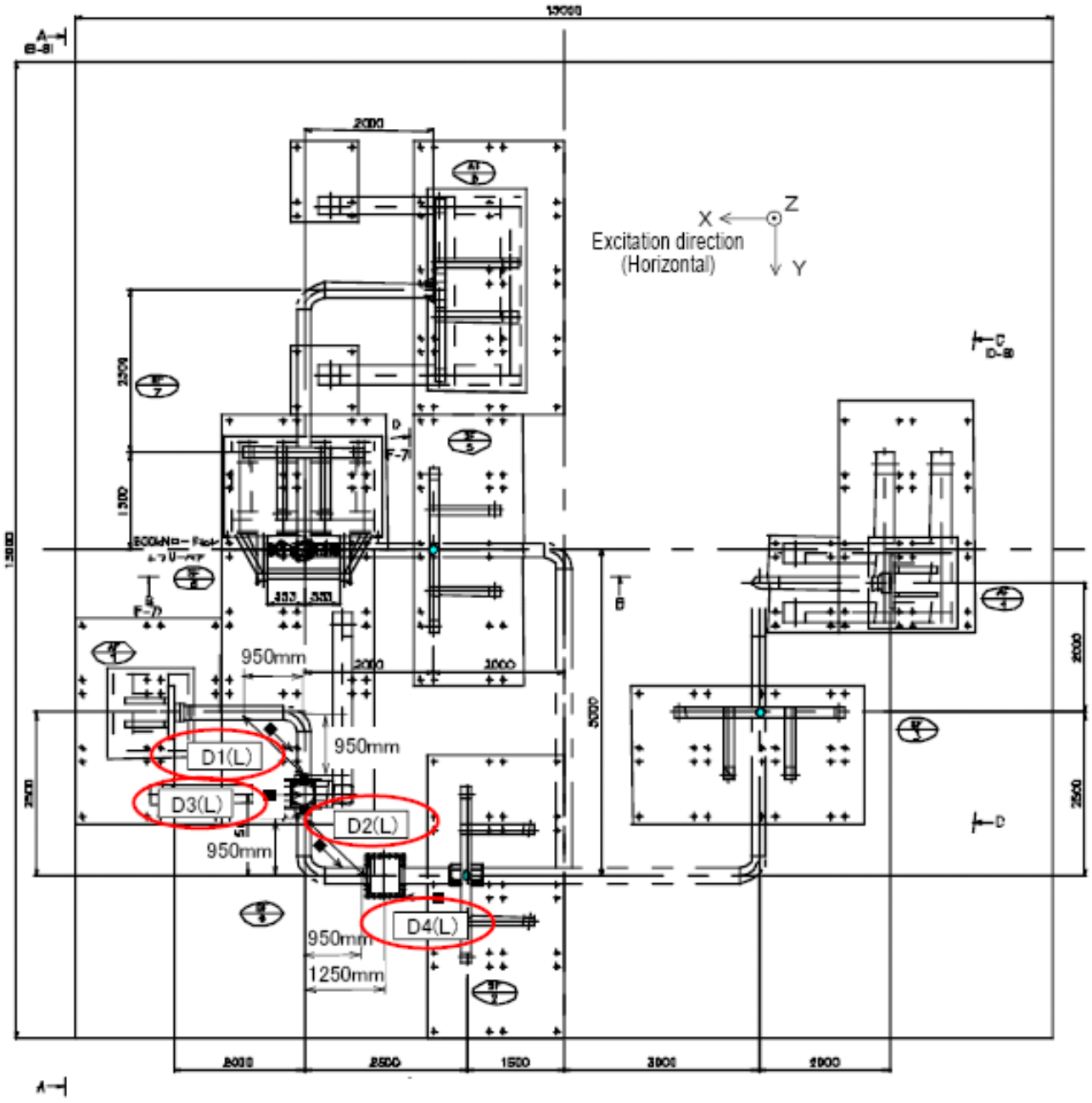

Figure 2-24 US Test Displacement Gage Locations

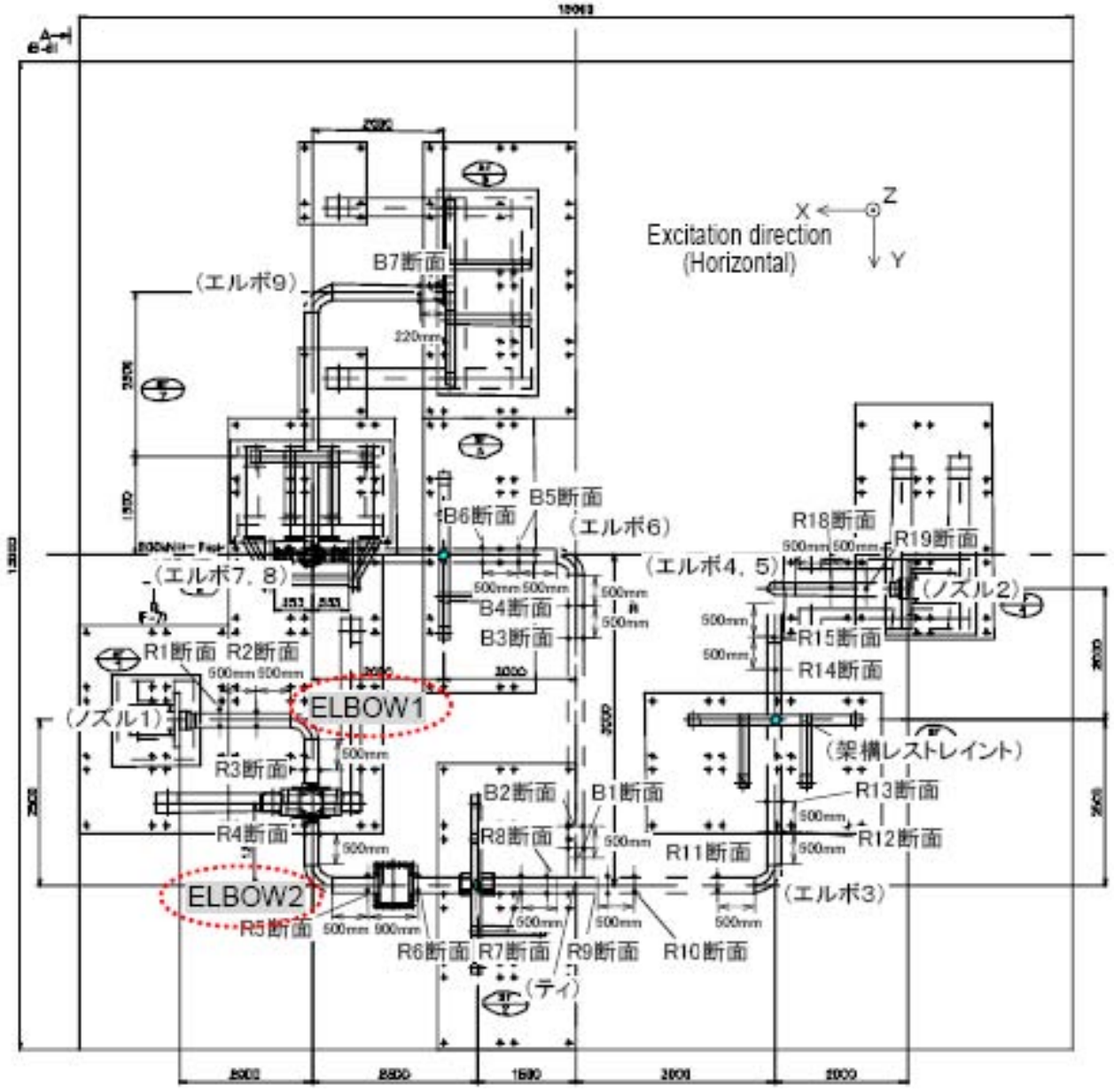

Figure 2-25 US Test Strain Gage Locations

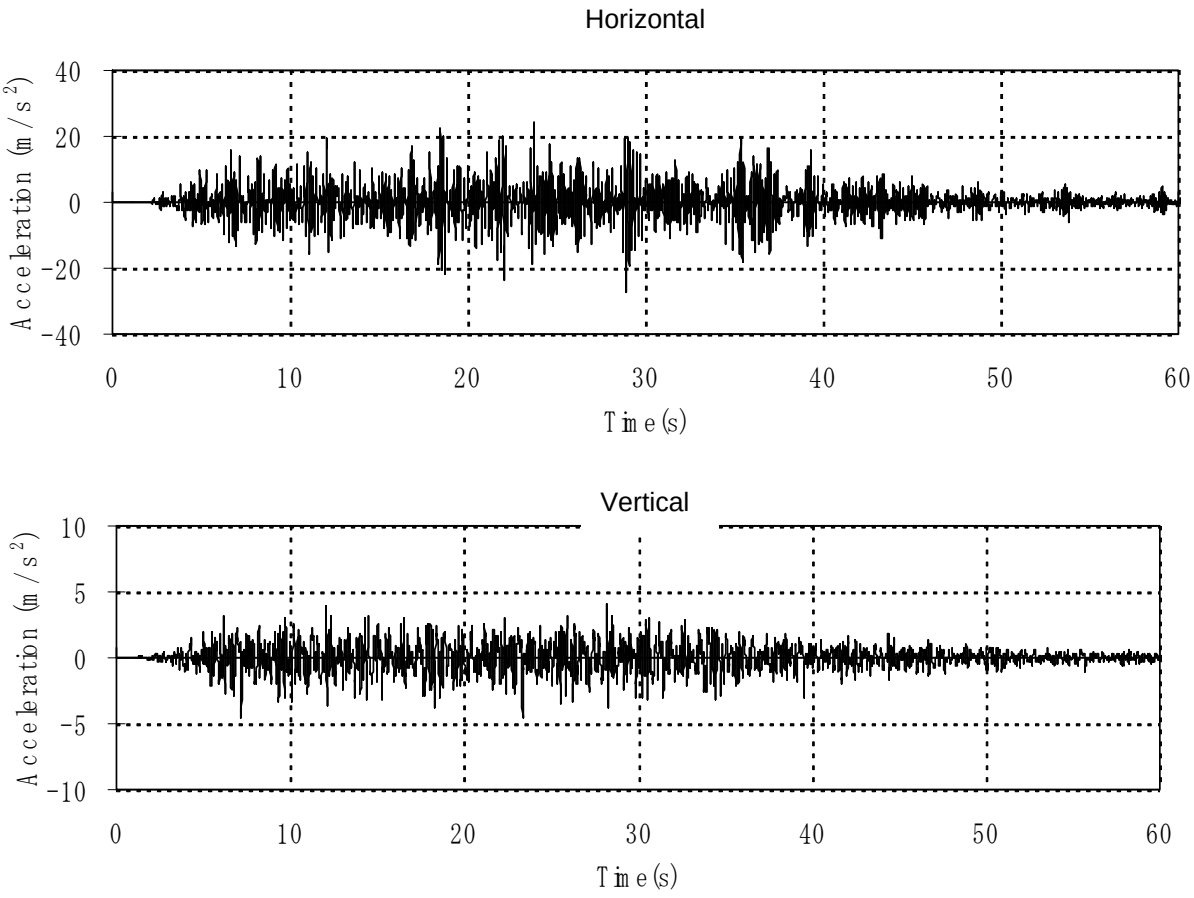

Figure 2-26 DM4-2(2) Test Table Motion Acceleration Time Histories

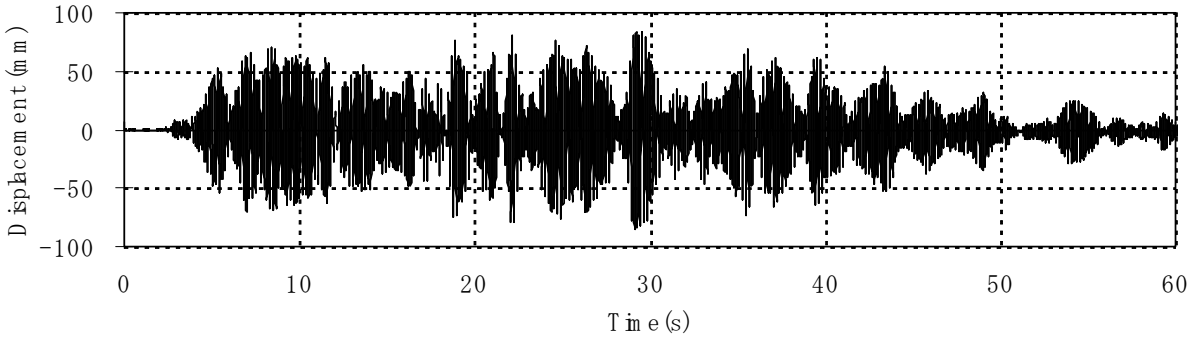

Figure 2-27 DM4-2(2) Test Pipe Displacement Time History (Horizontal)

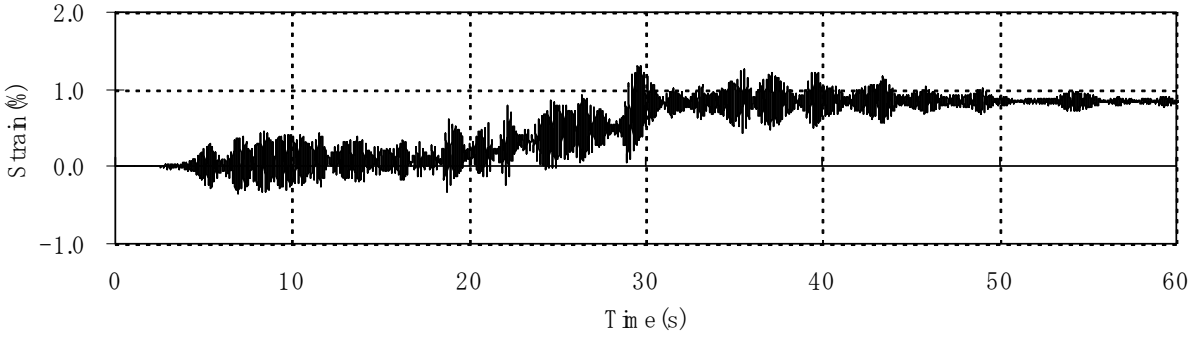

Figure 2-28 DM4-2(2) Test Elbow 2 Hoop Strain Time History

Figure 2-29 Ultimate Strength Test piping Failure at Elbow 2

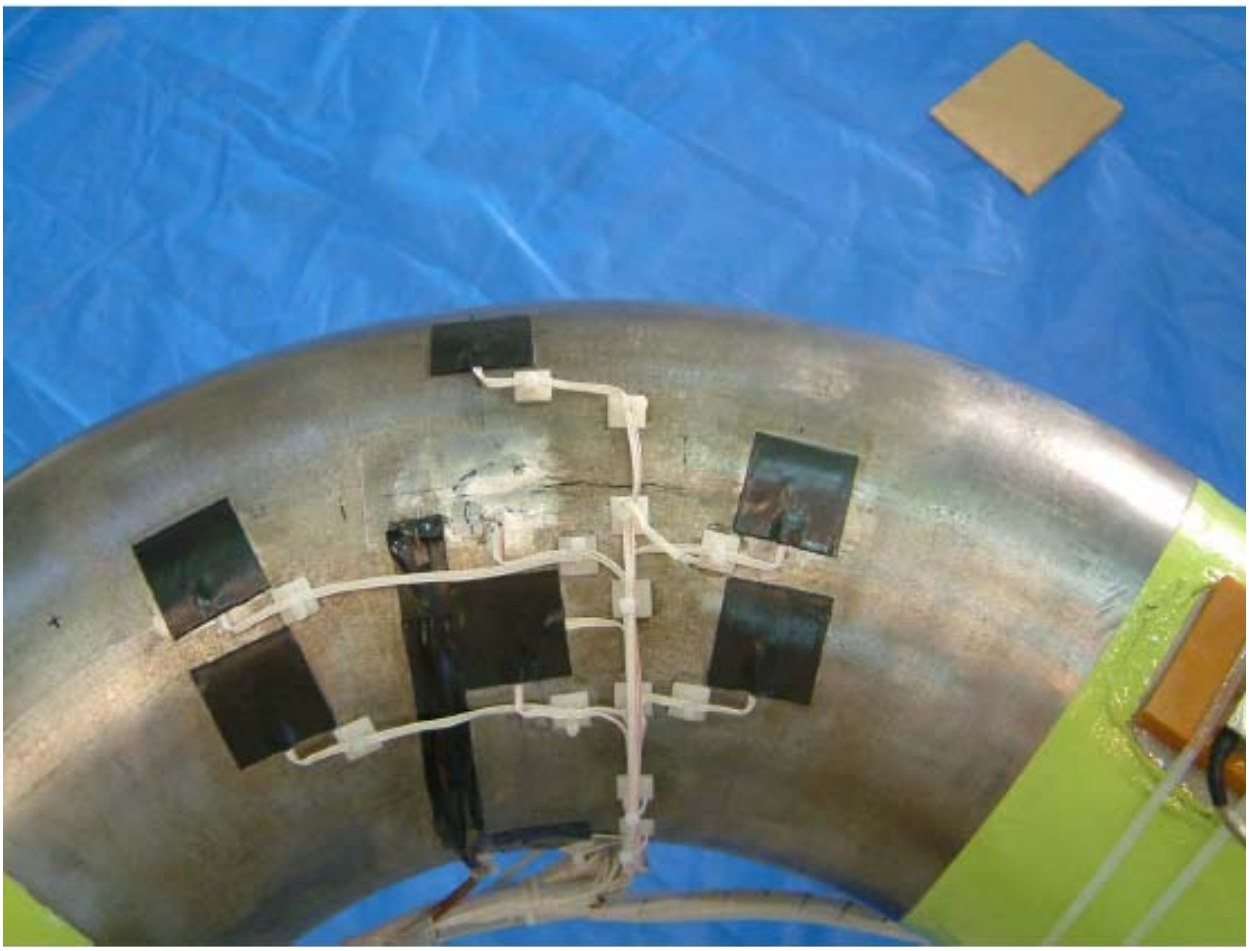

Figure 2-30 US Test Elbow 2 Fatigue Crack

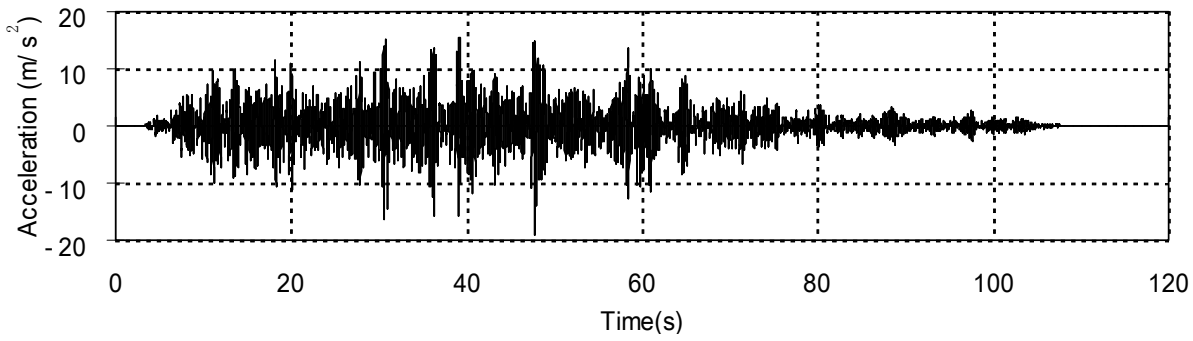

Figure 2-31 US2 Test Table Motion Acceleration Time History (Horizontal)

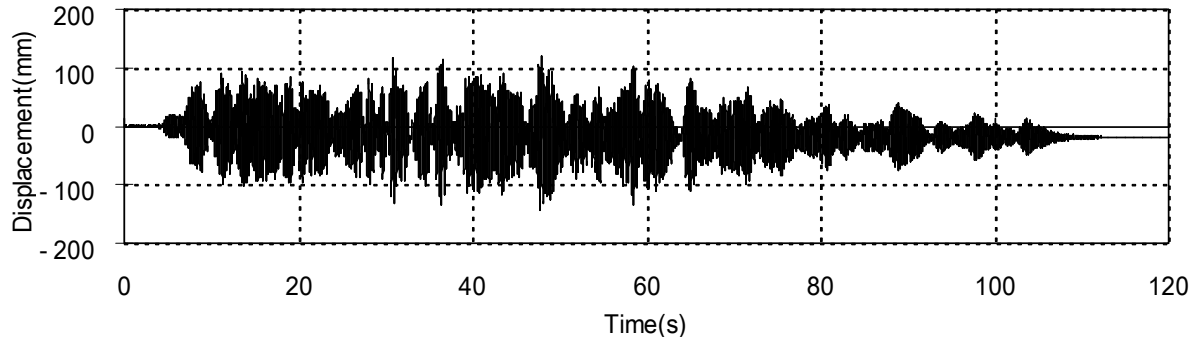

Figure 2-32 US2 Pipe Displacement Time History (Horizontal)

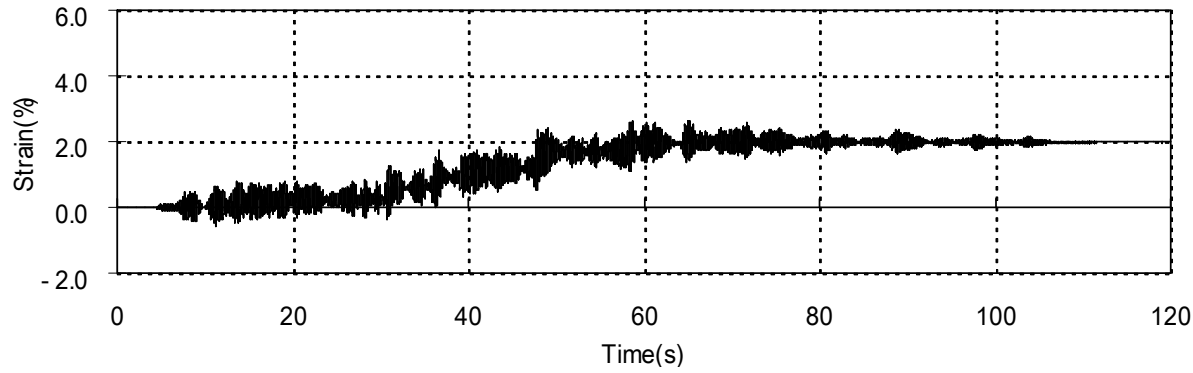

Figure 2-33 US2 Test Elbow 2 Hoop Strain Time History

3 BNL LINEAR ANALYSES AND CODE EVALUATIONS

3.1 Introduction

One of the primary objectives of the BNL collaboration effort was to assess the safety margins in piping systems designed in accordance with ASME Code requirements. Since the early 1990's, ASME Code piping subcommittees and working groups have worked to update piping seismic design requirements to more accurately reflect the probable failure mode of nuclear power plant piping systems under large seismic excitations. A number of test programs have demonstrated that piping systems subjected to earthquakes or other reversing dynamic loads will more likely fail due to fatigue ratcheting versus a collapse type failure as ASME Code Level D stress limits are intended to protect against. In the 1994 Addenda, the ASME Code rules for seismic design of piping underwent a major revision which provided a series of alternative rules for Service Level D limits that include reversing dynamic loads. However, the NRC staff had a number of concerns regarding the technical basis for the alternative limits and did not endorse this Code version. As a result of efforts to resolve the staff's concerns, the Code Committee proposed new rules in 2001. The new rules were approved with some additional changes and were incorporated into the 2004 Edition of the ASME Code. The latest rules, however, did not satisfy all of the staff's technical concerns and have not been endorsed by NRC.

As part of the collaboration effort, BNL conducted a series of linear elastic seismic analyses and ASME Code seismic evaluations for the JNES/NUPEC piping system tests. The primary objective of these studies was to provide additional data on safety margins based on the JNES/NUPEC seismic test program which can be used by the NRC staff in future assessments of ASME Code alternative piping seismic stress limits. Since the piping system tests were designed to load the piping systems to stress levels beyond Code allowables, the analyses were intended to determine and compare the minimum factors of safety to failure in critical piping components in piping systems designed in accordance with different versions of the Code. Similar analyses had been performed for the simplified piping tests with results reported in a NUREG/CR report by DeGrassi and Hofmayer [2005]. The analyses and Code evaluations and minimum safety margins for selected large-scale piping tests are presented below. As in previous analyses, it is important to emphasize that the safety margins reported below are minimum safety margins since not all tests resulted in pipe failure.

3.2 ASME Code Criteria

The latest version of the ASME Code Piping Design Criteria endorsed by NRC is the 1992 Edition including the 1993 Addenda. The piping design rules are defined in Section III, Division 1, Subsections NB, NC, and ND for Class 1, 2 and 3 components, respectively. Stress limits for piping subjected to seismic and other Level D loads are given in paragraphs NB/NC/ND-3656. For Class 1 piping, the Code stress equation for Level D primary stresses is as follows:

$$B_1 \frac{PD_0}{2t} + B_2 \frac{D_0}{2I} M_i \le 3.0 S_m \qquad (3\text{-}1)$$

where:

P = pressure
D_0 = outside diameter
t = wall thickness
B_1, B_2 = primary stress indices
I = moment of inertia
M_i = resultant moment
S_m = allowable stress intensity

The resultant moment term in the above equation includes deadweight, seismic and other Level D moments. The revised 1994 Addenda to the Code provided an alternate stress limit which was 50% higher than the old limit which could be applied when certain additional conditions were met. The new equation was:

$$B_1 \frac{PD_0}{2t} + B_2 \frac{D_0}{2I} M_E \leq 4.5 S_m \qquad (3\text{-}2)$$

The resultant moment term, M_E, in the above equation includes deadweight, seismic inertia and other "reversing" Level D moments. Additional conditions for application of this equation included the following:

(1) The analysis must be based on the linear elastic response spectrum method with 5% damping and 15% peak broadening.
(2) The ratio of outside pipe diameter to wall thickness shall not exceed 50.
(3) Stress due to weight moments is limited to 0.5 S_m.
(4) Stress due to seismic anchor motion moments is limited to 6 S_m.
(5) Stress due to seismic anchor motion longitudinal forces is limited to S_m.
(6) Maximum pressure during the SSE must not exceed the design pressure.

In 2001, the following changes were proposed to the alternate Level D primary stress limit equation:

$$B_1 \frac{PD_0}{2t} + B_2' \frac{D_0}{2I} M_E \leq 3.0 S_m \qquad (3\text{-}3)$$

where:

$B_2' = B_2$ for all piping components except:

$B_2' = ¾\ B_2$ for elbows, bends, and tees
$B_2' = 1.33$ for girth butt welds between items which do not have nominally identical thicknesses.

When this equation is used, the same additional conditions must be met, except that the ratio of outside pipe diameter to wall thickness shall not exceed 40. This equation reinstated the original 3.0 S_m stress limit but modified the stress indices for critical components. Compared to the 1993 Code, for straight pipes, the equation is identical to equation (3-1). For elbows, bends and tees, the change is approximately equivalent to using a stress limit of 4.0 S_m in equation (3-1). For girth butt welds between items which do not have nominally identical wall thicknesses as may be the case at equipment nozzles, the change is approximately equal to a stress limit of 2.25 S_m in equation (3-1).

Equation (3-3) and the new B_2' stress indices for seismic loads listed above were acceptable to the NRC staff and would have been formally endorsed. However, ASME comments submitted March 22, 2004, on the proposed 10 CFR 50.55a rulemaking (Federal Register Volume 69, Number 4, January 7, 2004) indicated that these B_2' stress indices were a typographical error that will be corrected by an errata. According to the ASME position, the criteria should be $B_2' = 2/3\ B_2$ for elbows, bends, and tees. Subsequently, the following alternate Code stress equation for seismic and other "reversing" stresses was published in the 2004 Edition of the ASME Code as follows:

$$B_1 \frac{PD_0}{2t} + B_2' \frac{D_0}{2I} M_E \leq 3.0 S_m \quad (3\text{-}4)$$

where:

$B_2' = B_2$ for all piping components except:

$B_2' = 2/3\ B_2$ for elbows, bends, and tees
$B_2' = 1.33$ for girth butt welds between items which do not have nominally identical thicknesses.

As in Equations (3-2) and (3-3) above, the resultant moment term, M_E, includes deadweight, seismic inertia and other "reversing" Level D moments. Additional conditions for application of this equation are the same as those for Equation (3-3):

(1) The analysis must be based on the linear elastic response spectrum method with 5% damping and 15% peak broadening.
(2) The ratio of outside pipe diameter to wall thickness shall not exceed 40.
(3) Stress due to weight moments is limited to 0.5 S_m.
(4) Stress due to seismic anchor motion moments is limited to 6 S_m.
(5) Stress due to seismic anchor motion longitudinal forces is limited to S_m.
(6) Maximum pressure during the SSE must not exceed the design pressure.

Compared to the 1993 Code, for straight pipes, this equation is identical to equation (3-1). For elbows, bends and tees, the change is approximately equivalent to using a stress limit of 4.5 S_m in equation (3-1). For girth butt welds between items that do not have nominally identical thicknesses, the change is approximately equivalent to a stress limit of 2.25 S_m in equation (3-1). Although this alternate stress criterion has been published in the 2004 Edition of the ASME Code, to date, it has not been endorsed by the NRC.

3.3 Linear Analysis and Code Evaluation of Large-Scale Piping Systems

3.3.1 Selection of Load Cases

As indicated in Table 2-1, JNES/NUPEC conducted a series of Design Method Confirmation Tests and Ultimate Strength Tests. The two Design Method Allowable Stress Tests (DM2 series) were intended to induce maximum piping stresses up to the S_2 design earthquake stress limit of $3S_m$, and up to 1.5 times the stress limit ($4.5S_m$). At these stress levels, the piping system response is essentially elastic. The dominant frequency of the input motion was not close to the fundamental frequency of the piping system (off-resonance). The three Design Method Elasto-Plastic Response Tests (DM4 series) were intended to induce plasticity in the system with maximum elastically-calculated stress levels of $6S_m$, $10.5S_m$ and $13.5S_m$. In order to achieve these high stress levels, the input motions were adjusted so that the dominant frequency was close to the fundamental frequency of the piping system (on-resonance). The Ultimate Strength Tests (US2 series) were designed to induce higher plastic response with a maximum elastically-calculated stress level of $24S_m$. In order to achieve this stress level, the piping system was modified by the addition of a large mass and the removal of a lateral restraint. In addition, the dominant frequency was close to the fundamental frequency of the piping system (on-resonance). The tests were repeated five times at the same level of input motion resulting in fatigue failure of the highest stressed elbow. For the purpose of this Code margin evaluation, the three load cases with the highest stress within each test series were selected for analysis. They are identified as DM2-2, DM4-2(2), and US2.

3.3.2 Finite Element Models and Analyses

The selected large-scale piping systems were analyzed and evaluated using ASME Code seismic criteria by applying linear analysis methods and assumptions in accordance with nuclear industry practice. The ANSYS [2007] general purpose finite element analysis program was used to develop the models and analyze the selected load cases. The Design Method Confirmation (DM) test specimen was modeled using ANSYS three-dimensional linear elastic straight pipe (PIPE16) and curved pipe (PIPE18) elements as shown in Figure 3-1. MASS21 elements were used to represent the 1000 kg added mass attached to the pipe. The mass of the water in the pipes was included in the pipe elements. The internal pressure of 10.7 MPa was applied to all pipe elements. The spring hanger was represented by a constant vertical force balancing the gravity load. Boundary conditions included full translational and rotational restraints at the nozzles and anchor, and horizontal and vertical translational restraints at the supports.

The Ultimate Strength (US) test specimen was modeled in a similar manner using the same types of elements and including the water mass and internal pressure. The spring hanger was represented by a constant vertical force balancing the gravity load. Support, anchor and nozzle restraints were represented in the same manner. The configuration of the piping system was identical to the DM test specimen. The only differences were the addition of a second 1000 kg mass, the removal of a lateral support, and the addition of masses representing pipe bands around the pipe at the support locations. The US Test Linear ANSYS model is shown in Figure 3-2

Linear response spectrum analyses were performed in accordance with industry practice and regulatory guidelines for piping design with only two exceptions: (1) since the input motions were measured with no uncertainty and the objective was to identify minimum margins to failure, unbroadened instead of broadened response spectra were applied in the analyses; and (2) since actual piping component dimensions had been provided by JNES/NUPEC, two sets of analyses were performed using both design dimensions and as-built dimensions. In reviewing the as-built measurements, it was noted that the elbows were approximately 25% thicker than the design dimensions for 200A Schedule 40 pipe. This difference had a significant effect on the piping system frequencies and the system responses, and was therefore believed to be an important consideration in the evaluation of stress margins.

The response spectra for each load case were generated from their respective table motion acceleration time history records using the P-CARES program [Nie, et al 2007]. The horizontal and vertical response spectra for the large-scale piping DM load cases are shown in Figure 3-3 through Figure 3-6. The horizontal response spectra for the US test shown in Figure 3-7. The spectra were generated for 2 percent, 4 percent and 5 percent modal damping values. These damping values cover the range of NRC-accepted and ASME-proposed values for nuclear power plant piping systems that have been applied in the past three decades or proposed in more recent years. Two percent damping was specified in NRC Regulatory Guide 1.61 [1973] for safe shutdown earthquakes (SSE) for piping systems with pipe diameter equal to or less than 12 inches (300 mm). This damping value had been applied in piping system seismic design analyses for most operating nuclear plants. ASME Code Case N-411 [1986] allowed frequency dependent damping as an alternative for all earthquakes and all pipe sizes. The damping values are 5 percent for modes with frequencies less than 10 Hz and 2 percent for modes with frequencies greater than 20 Hz. For frequencies between 10 Hz and 20 Hz, the damping values are linearly interpolated between 2 and 5 percent. The staff accepted N-411 damping with certain limitations specified in Regulatory Guide 1.84 and used it primarily to review operating reactor issues. This Code case expired in 2000, but was incorporated into ASME Code Section III Appendix N. In 2007, NRC issued Revision 1 to Regulatory Guide 1.61 [2007] which specified 4 percent damping for SSE for all pipe sizes and analysis methods. It also allowed the use of N-411 frequency dependent damping as an alternative for piping systems analyzed by the uniform support motion response spectrum method and subject to the restrictions that had been specified in RG 1.84. The ASME Code 1994 Addenda significantly revised the piping seismic stress

limits and specified that stresses shall be computed by linear response spectrum analyses with 5 percent modal damping. The 2004 Edition of the ASME Code modified the alternative piping seismic stress limits and specified that the stresses shall be computed by linear response spectrum analyses with damping values as specified in Appendix N (5 percent modal damping). As discussed in Section 3.2 above, the NRC has not endorsed the 1994 or later ASME Code Addenda.

Linear analyses were carried out for pressure, deadweight and seismic loading for the DM2-2, DM4-2(2), and US2 load cases. For each load case, multiple analyses were performed to calculate stresses in accordance with the three different ASME Code versions (1993, 1994 and 2004) for Service Level D loading. For the NRC-endorsed 1993 Addenda, the seismic response spectrum analyses were repeated for 2 percent, 4 percent, and frequency dependent (N-411) damping. For the 1994 Addenda and 2004 Edition, the response spectrum analyses used 5 percent damping. The highest stresses in the critical components (elbows, tee, and nozzles) were determined in accordance with the different equations, stress indices and stress allowables of each code version. The component with the largest ratio of stress to allowable stress was identified as the critical component. The results for each load case are presented below.

3.3.3 Analysis and Code Evaluation Results

The results for each load case are summarized in Table 3-1 through Table 3-6. The tables provide the maximum calculated stress in the highest stressed elbow, the highest stressed nozzle, and the tee. The first three rows of the tables give the results of the analyses performed in accordance with the NRC-endorsed 1993 ASME Code Addenda for the three damping values acceptable to NRC. The last two rows give the results of the analyses performed in accordance with the 1994 Addenda and the 2004 Edition which have not been endorsed by the staff. The tables provide the highest stress in each component and the stress margin (maximum stress divided by Code allowable) for the highest stressed component. As discussed in Section 3.2, the Service Level D stress allowable is $3S_m$ except for the 1994 Addenda analyses which used an allowable of $4.5S_m$. The value of S_m provided by JNES/NUPEC is 137 MPa. The tables present the results of analyses using both piping design dimensions and as-built dimensions.

In order to properly interpret the results of these analyses, it should be understood that the "margins" presented in Tables 3-1 through 3-6 represent the ratios of the highest stress in a piping system (calculated in accordance with the specific code version rules which include the stress equation, stress indices, and damping) divided by the allowable stress (defined by the specific code version). None of the piping systems failed during a single seismic load application. The ultimate strength test US2 resulted in a fatigue failure after five applications of high level earthquake motion. Therefore these should not be interpreted as margins to failure. Instead they should be considered minimum margins to failure or minimum Code stress margins.

3.3.3.1 DM2-2 Test

Maximum Code stresses and stress margins for the DM2-2 test are presented in Table 3-1 for the analyses that used pipe design dimensions and in Table 3-2 for analyses that used as-built dimensions. For all cases, the critical location is the elbow. It is noted that for the design dimension case analyzed in accordance with the 1993 Code and R.G. 1.61 Rev 0 (2%) damping, the stress margin is consistent with the JNES/NUPEC goal of achieving 1.5 times the S_2 earthquake allowable of 3Sm. Due to the relatively low excitation level, the stresses and stress margins are low and are therefore not useful indicators of margins to failure. A comparison of stress margins between the design and as-built dimension cases show that as-built system stresses are much lower. This is attributed to the shift in piping frequency and the thicker elbow dimensions. A comparison of stresses between the different Code Editions show that the NRC-endorsed 1993 Code edition provides higher margins than the 1994 or 2004 ASME Code. As expected, the 1993 Edition with 2% damping gives the highest margins followed by the 4% damping and

the N-411 damping cases. It should be noted that due to the low frequencies of the significant modes, N-411 damping is essentially 5%. The 1994 and 2004 Code provided essentially identical stress margins.

3.3.3.2 DM4-2(2) Test

Maximum Code stresses and stress margins for the DM4-2(2) test are presented in Table 3-3 for the analyses that used pipe design dimensions and in Table 3-4 for analyses that used as-built dimensions. As in the DM2-2 test, for all cases, the critical location is the elbow. It is noted that for the design dimension case analyzed in accordance with the 1993 Code and R.G. 1.61 Rev 0 (2%) damping, the maximum stress level is approximately $12S_m$ which is slight lower than the JNES/NUPEC goal 0f $13.5S_m$. Due to the higher excitation level, larger stresses and stress margins are observed. However, these should not be interpreted as margins to failure since the piping system maintained its pressure integrity. A comparison of stress margins between the design and as-built dimension cases show that as-built system stresses are much lower. This is attributed to the shift in piping frequency and the thicker elbow dimensions. A comparison of stresses between the different Code Editions show the same trend observed in the previous test analyses with the NRC-endorsed 1993 Code edition providing higher margins than the 1994 or 2004 ASME Code. As expected, the 1993 Edition with 2% damping gives the highest margins followed by the 4% damping and the N-411 damping cases. It should be noted that due to the low frequencies of the significant modes, N-411 damping is essentially 5%. The 1994 and 2004 Code again provided essentially identical stress margins.

3.3.3.3 US2-1 Test

Maximum Code stresses and stress margins for the US2-1 test are presented in Table 3-5 for the analyses that used pipe design dimensions and in Table 3-6 for analyses that used as-built dimensions. As in the other load cases, the critical location is the elbow. It is noted that for the design dimension case analyzed in accordance with the 1993 Code and R.G. 1.61 Rev 0 (2%) damping, the maximum stress level is approximately $24S_m$ which is consistent with the JNES/NUPEC goal of $24S_m$. This test was designed to fail the pipe and, as expected, provided the highest stresses and stress margins. Since the elbow developed a crack after five tests, the margins may be interpreted as failure margins based on stress level. However, it should be noted that the number of stress cycles in the tests far exceeded the normal earthquake design cycles, so in reality some additional margin would be available.

For the design dimension cases, the 1993 Code analysis with 2 percent damping shows the highest stress margin of 7.98. With 4 percent and N-411 damping, the margins are 5.24 and 4.67, respectively. The 1994 and 2004 Code analyses with 5% damping show identical margins of 3.11. For the as-built dimension cases, the margins are lower due to the shift in frequency and the thicker elbows. The 1993 Code analysis with 2 percent damping shows a stress margin of 6.35. The analyses using 4 percent and N-411 damping show margins of 4.50 and 3.94, respectively. The 1994 and 2004 Code analyses with 5% damping show identical margins of 2.63.

3.4 Summary of Results

The linear analyses and Code evaluations of the two JNES/NUPEC Design Method Confirmation tests and of the Ultimate Strength test provided comparative data on stress margins calculated in accordance with the current NRC-endorsed 1993 ASME Code version with three different damping values and with the current alternative design rules provided in 1994 and the 2004 ASME Code versions. All analyses showed that the highest stress occurred at an elbow. In all cases, the 1994 and the 2004 Code analyses provided essentially identical margins. The 1993 Code analyses using the highest NRC-accepted damping values from Code Case N-411 provided about 50 percent higher margins than the 1994 or 2004 Code analyses. Using the latest Regulatory Guide 1.61 Revision 1 recommended damping value of 4 percent, the 1993 Code analyses margins were generally about 70 percent higher. Analyses using

Regulatory Guide 1.61 Revision 0 damping value of 2 percent provided margins that were generally at least 100 percent higher.

The Ultimate Strength test was designed to produce a maximum elastically-calculated elbow stress of $24S_m$ and induce pipe failure. This occurred after five applications of the high-level earthquake input excitation. The Code analyses of this load case provided the highest stress margins. Analyses of the piping system using design dimensions based on 1993 Code provided margins of 7.98 for 2 percent damping, 5.24 for 4 percent damping, and 4.67 for N-411 damping. Analyses based on the 1994 and 2004 Code with 5 percent damping provided margins of 3.11. Since the measured elbow thickness from the test specimen were approximately 25% thicker than the design dimensions, the analyses were repeated using as-built dimensions. Due to the shift in piping system frequency and the higher wall thickness, the stresses and stress margins were lower. The 1993 Code analyses provided margins of 6.35 for two percent damping, 4.50 for 4 percent damping, and 3.94 for N-411 damping. Analyses based on the 1994 and 2004 Code with 5 percent damping provided margins of 2.63. Since a failure occurred at the highest stressed elbow, these margins may be interpreted as failure margins based on stress level for this specific test. However, since the number of cycles in these tests far exceeded the normal number of SSE cycles, some additional margin may be available. On the other hand, as discussed in Section 2.5, the seismic waves for the ultimate strength test were adjusted so that the dominant input motion frequency was close to the fundamental piping system frequency (on-resonance). Therefore, it is possible that a different seismic input may result in a smaller margin.

Further discussion on the impact of 4 percent and 5 percent damping ratios on piping system responses is included in Appendix A.

Table 3-1 DM2-2 Test Maximum Code Stresses and Margins (Design Dimensions)

Code Edition	Damping	Maximum Stress (MPa)			Critical Location	Stress/Allowable (Margin)
		Elbow	Tee	Nozzle		
1993	R.G. 1.61 Rev 0	630	331	269	Elbow	1.53
1993	RG 1.61 Rev 1	507	283	231	Elbow	1.23
1993	N-411	470	268	219	Elbow	1.14
1994	5%	470	268	219	Elbow	0.76
2004	5%	313	203	219	Elbow	0.76

1 MPa = 145 psi

Table 3-2 DM2-2 Test Maximum Code Stresses and Margins (As-Built Dimensions)

Code Edition	Damping	Maximum Stress (MPa)			Critical Location	Stress/Allowable (Margin)
		Elbow	Tee	Nozzle		
1993	R.G. 1.61 Rev 0	246	210	176	Elbow	0.60
1993	RG 1.61 Rev 1	235	203	171	Elbow	0.57
1993	N-411	231	201	169	Elbow	0.56
1994	5%	231	201	169	Elbow	0.38
2004	5%	169	158	169	Elbow	0.41

1 MPa = 145 psi

Table 3-3 DM4-2(2) Test Maximum Code Stresses and Margins (Design Dimensions)

Code Edition	Damping	Maximum Stress (MPa)			Critical Location	Stress/Allowable (Margin)
		Elbow	Tee	Nozzle		
1993	R.G. 1.61 Rev 0	1625	737	585	Elbow	3.95
1993	RG 1.61 Rev 1	1076	519	412	Elbow	2.62
1993	N-411	810	462	366	Elbow	1.97
1994	5%	810	462	366	Elbow	1.31
2004	5%	623	333	366	Elbow	1.52

1 MPa = 145 psi

Table 3-4 DM4-2(2) Test Maximum Code Stresses and Margins (As-Built Dimensions)

Code Edition	Damping	Maximum Stress (MPa)			Critical Location	Stress/Allowable (Margin)
		Elbow	Tee	Nozzle		
1993	R.G. 1.61 Rev 0	1154	670	566	Elbow	2.81
1993	RG 1.61 Rev 1	834	615	429	Elbow	2.03
1993	N-411	729	454	383	Elbow	1.77
1994	5%	729	454	383	Elbow	1.18
2004	5%	486	327	383	Elbow	1.18

1 MPa = 145 psi

Table 3-5 US2-1 Test Maximum Code Stresses and Margins (Design Dimensions)

Code Edition	Damping	Maximum Stress (MPa)			Critical Location	Stress/Allowable (Margin)
		Elbow	Tee	Nozzle		
1993	R.G. 1.61 Rev 0	3282	2225	302	Elbow	7.98
1993	RG 1.61 Rev 1	2155	1487	223	Elbow	5.24
1993	N-411	1918	1332	207	Elbow	4.67
1994	5%	1918	1332	207	Elbow	3.11
2004	5%	1279	916	207	Elbow	3.11

1 MPa = 145 psi

Table 3-6 US2-1 Test Maximum Code Stresses and Margins (As-Built Dimensions)

Code Edition	Damping	Maximum Stress (MPa)			Critical Location	Stress/Allowable (Margin)
		Elbow	Tee	Nozzle		
1993	R.G. 1.61 Rev 0	2611	2040	278	Elbow	6.35
1993	RG 1.61 Rev 1	1849	1467	219	Elbow	4.50
1993	N-411	1619	1293	201	Elbow	3.94
1994	5%	1619	1293	201	Elbow	2.63
2004	5%	1080	890	201	Elbow	2.63

1 MPa = 145 psi

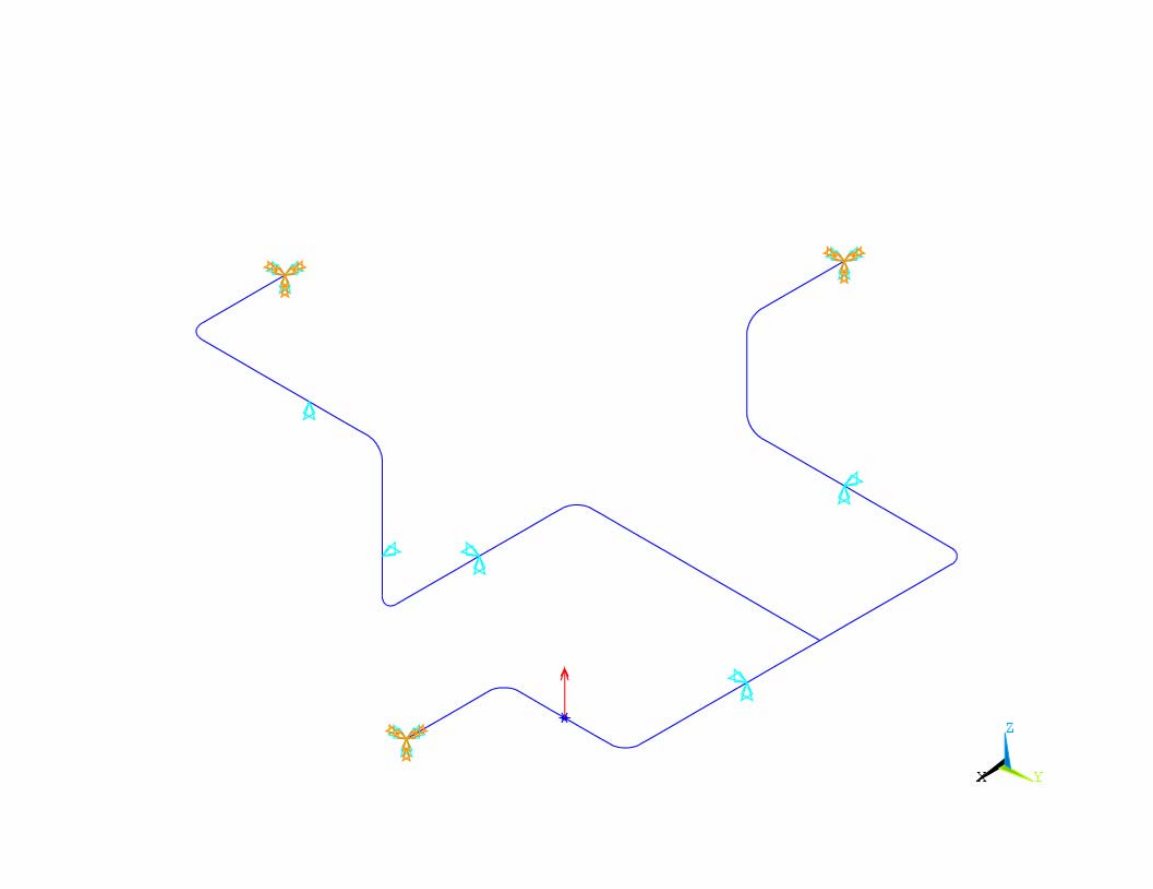

Figure 3-1 Design Method Confirmation Test Linear ANSYS Model

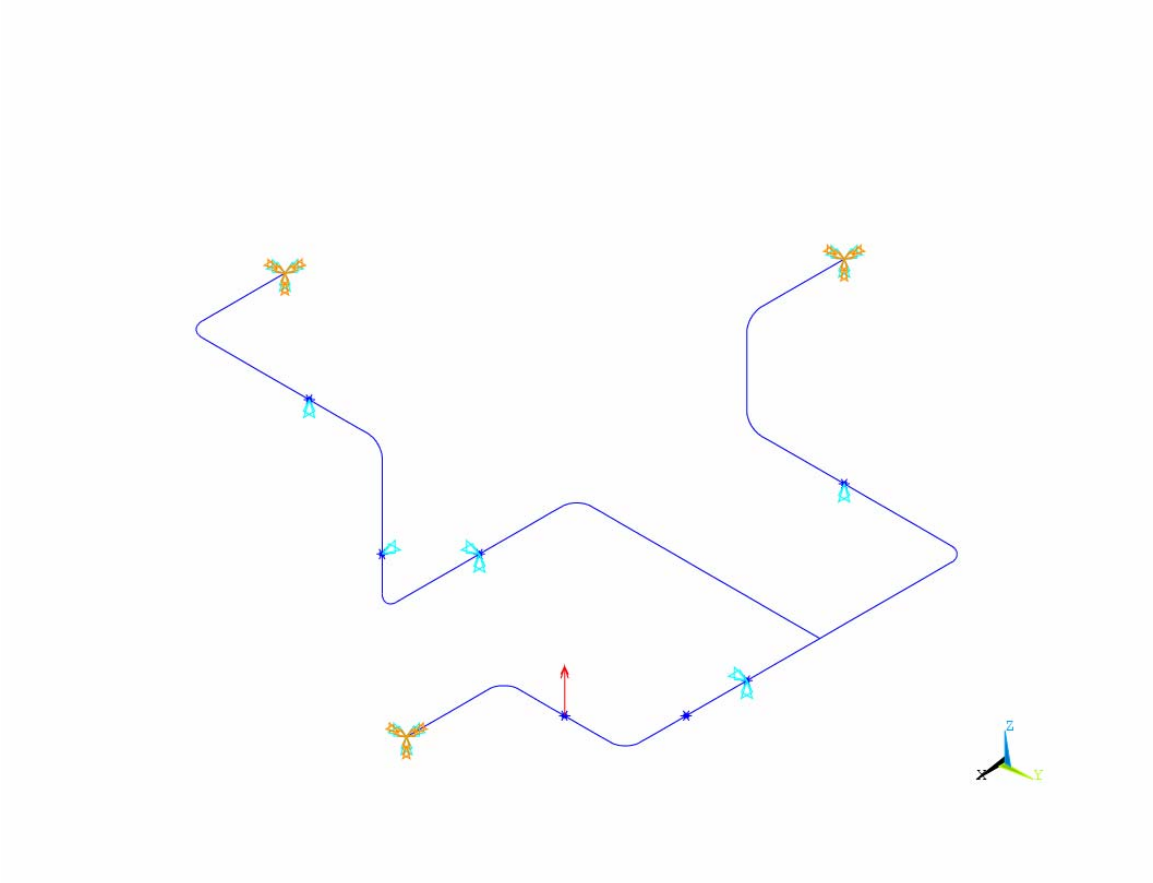

Figure 3-2 Ultimate Strength Test Linear ANSYS Model

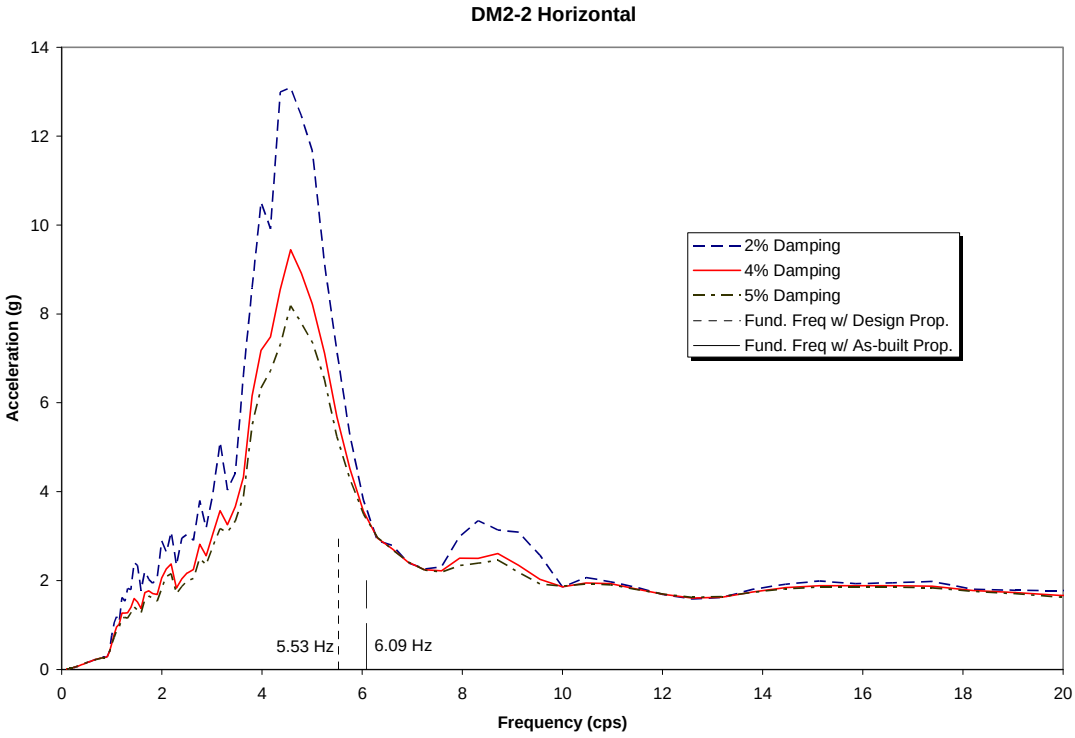

Figure 3-3 DM2-2 Horizontal Response Spectra (2%, 4%, and 5% Damping)

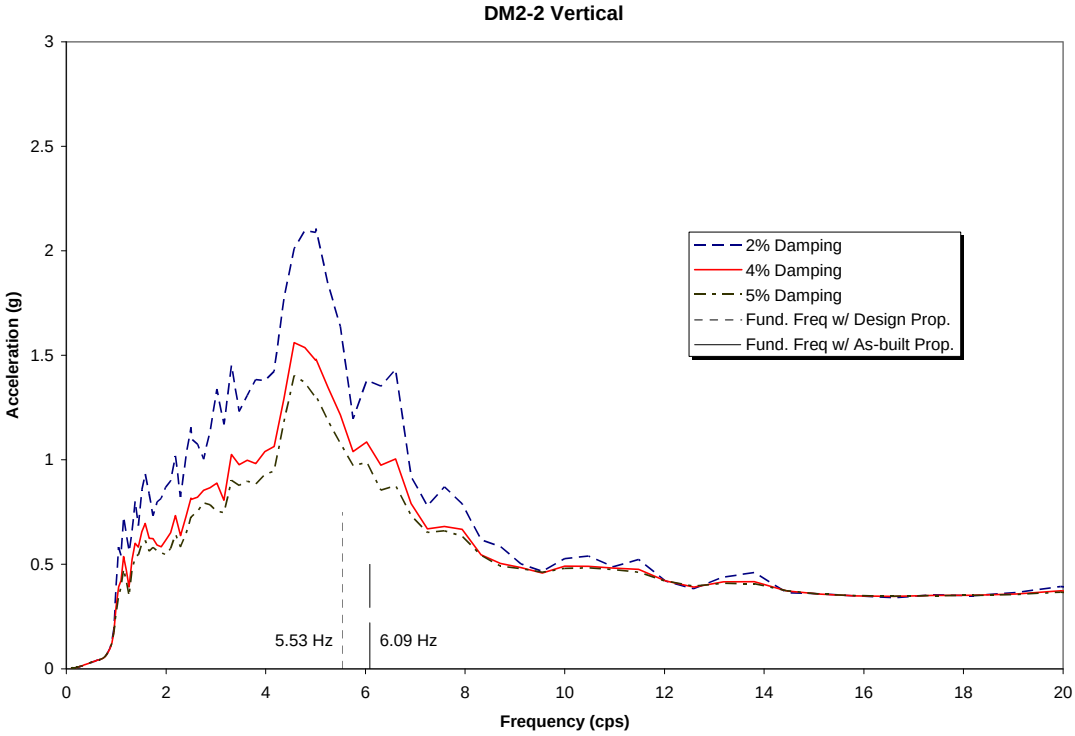

Figure 3-4 DM2-2 Vertical Response Spectra (2%, 4%, and 5% Damping)

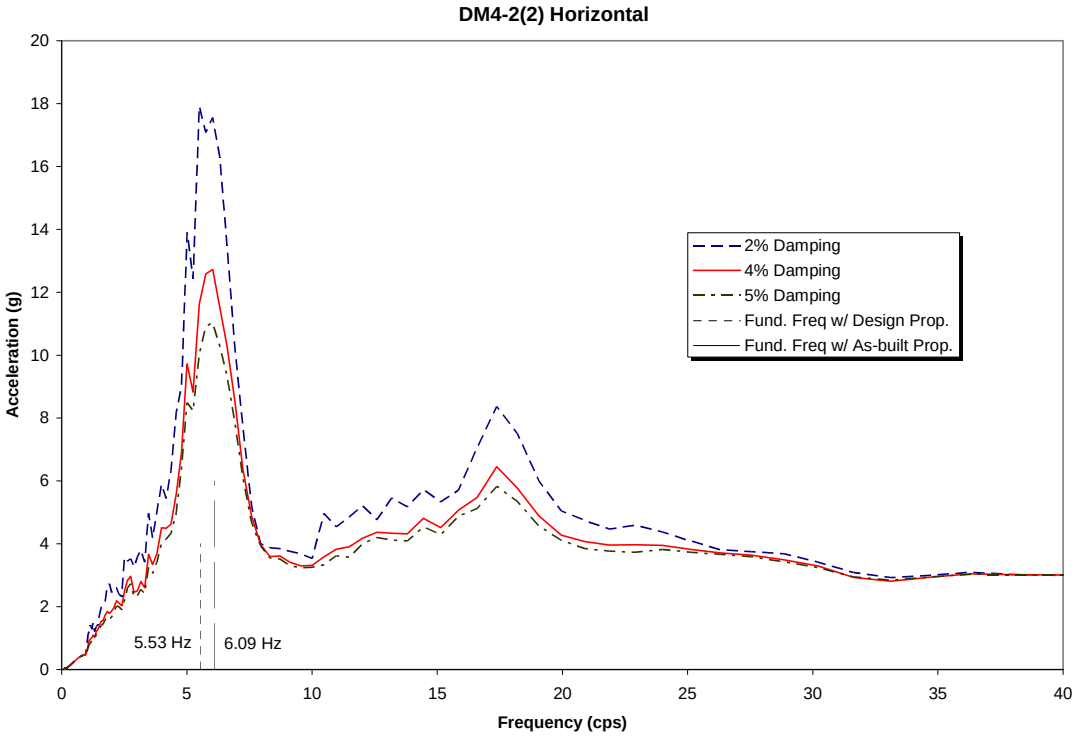

Figure 3-5 DM4-2(2) Horizontal Response Spectra (2%, 4%, and 5% Damping)

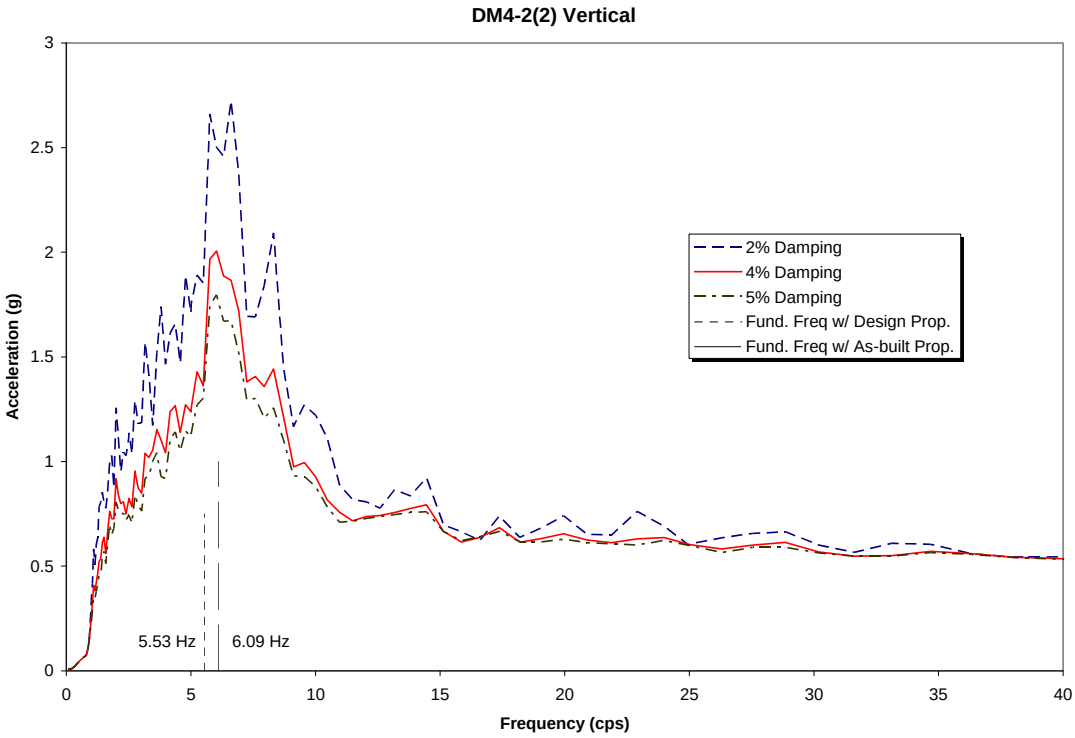

Figure 3-6 DM4-2(2) Vertical Response Spectra (2%, 4%, and 5% Damping)

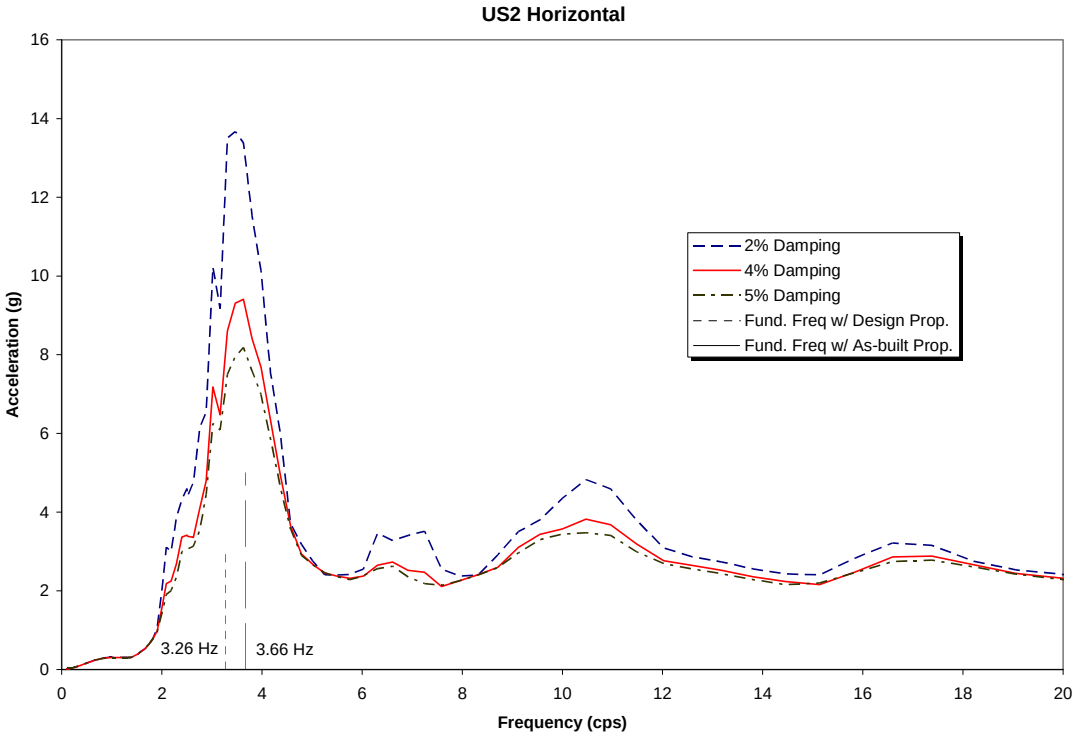

Figure 3-7 US2 Horizontal Response Spectra (2%, 4%, and 5% Damping)

4 BNL NONLINEAR ANALYSIS FOR LARGE SCALE PIPE TESTS

4.1 Introduction

This section describes the BNL nonlinear analyses of the large-scale pipe tests that were performed by JNES/NUPEC. The tests included a series of design method confirmations tests and a series of ultimate strength tests. The analyses were performed using the ANSYS ver. 11 finite element (FE) code. Similar to the JNES/NUPEC studies using the ABAQUS FE code, each of the BNL nonlinear analyses for the large scale pipe tests consists of two phases: (1) a transient analysis of the whole piping system using plastic pipe elements is performed to obtain the overall responses; (2) a static analysis of one of the elbows using plastic shell elements is carried out with displacement boundary conditions extracted from the piping system analysis in phase (1) to obtain the ratcheting strain responses.

As described in Section 2, the JNES/NUPEC design confirmation tests and the ultimate tests were carried out with several input motions of different magnitudes and frequency characteristics. Therefore, for each set of tests, the input motions will be examined first, followed by a description of the ANSYS modeling and analysis. The analytical results will be compared and assessed last.

4.2 Analysis for the Design Method Confirmation Test

4.2.1 Shaking Table Input Motions

The specimen for the design method confirmation test was subjected to a series of shaking table excitations ranging from elastic preliminary tests, to allowable stress tests, and to elasto-plastic response tests. As shown in Table 2-1, the elastic preliminary tests started with two sweep tests in the horizontal and the vertical directions respectively to determine the modal frequencies, and also included another four elastic tests with one-directional input motions in either horizontal or vertical directions. These four one-directional input motions were taken from the allowable stress tests (to be introduced next), and will not be considered in the ANSYS analyses for this report. The input motions to the piping system are taken as the acceleration time histories recorded at the top of the shaking table.

Two allowable stress tests, namely DM2-1 and DM2-2, were conducted by JNES/NUPEC with simultaneous horizontal (X direction) and vertical (Z direction) excitations, the dominant frequencies of which were off resonant. The DM2-1 test was intended to reach a design stress level of $3S_m$, while the DM2-2 test was to achieve a maximum stress level of $4.5S_m$. Figure 4-1 and Figure 4-2 show the acceleration time histories and their 5% damping response spectra for tests DM2-1 and DM2-2, respectively. The peak ground accelerations (PGA) of the horizontal and vertical input motions are 0.936 g and 0.201 g respectively for DM2-1, and 1.581 g and 0.298 g respectively for DM2-2. The dominant frequency is about 4.5 Hz for both directions of DM2-1 and DM2-2, which is off from the measured piping system fundamental frequencies of 6.3 Hz and 6.2 Hz for these two tests. The durations of the input motions for these two tests are 90 seconds, and the time increments are 0.005 seconds.

The elasto-plastic response tests by JNES/NUPEC included three consecutive runs that are designated as DM4-1, DM4-2(1) and DM4-2(2). Their acceleration time histories and their 5% damping response spectra are shown in Figure 4-3 through Figure 4-5. Consisting of both horizontal (X direction) and vertical (Z direction) components, these three tests were reported to attain maximum stress levels of $6S_m$, $10.5S_m$, and $13.5S_m$, respectively. The PGAs for these three tests are 1.293 g, 1.925 g, and 2.791 g respectively in the horizontal direction, and 0.221 g, 0.361

g, and 0.471 g respectively in the vertical direction. For the motions used in these three tests, including both horizontal and vertical components, the dominant frequency is about 6 Hz, as shown by the corresponding response spectra plots (Figure 4-3 through Figure 4-5). The resonant frequencies measured in these three tests are 6 Hz, 6 Hz, and 5.9 Hz, respectively, confirming that the input motions were specified to have their dominant frequency at the resonance. It should be noted that the resonant frequencies are slightly smaller than those measured in the elastic tests. The durations of the input motions for these three tests are 82 seconds, and the time increments are 0.005 seconds.

All input motions, recorded at the shaking table top, were found to include large drifting displacements, which may numerically reduce the accuracy of the calculated responses. Therefore, the input motions are adjusted using a Lagrange-multiplier based correction algorithm [Borsoi, L. and Ricard, A. 1985], also termed in this report *baseline-corrected* or *baseline correction* whichever form applies. Figure 4-6 shows the acceleration history, its Fourier transform, the velocity history, and the displacement history of the original record (in red dotted lines) and the baseline-corrected record (in blue solid lines) for the horizontal input motion of DM4-1. The displacement of the original record appears to reach about 65 m in a monotonic fashion at the end of the time history, which is unrealistic and will probably shadow the displacement responses that are in the magnitudes of millimeters. A similar drifting pattern can be observed in the original velocity time history, although it oscillates along its drifting path. After adjusted by baseline correction, the displacement and the velocity oscillate around zero, with the displacement variation nearly invisible in Figure 4-6. It is noticeable in the plot of the acceleration time history that the original record (in red) is basically overlapped by the corrected record (in blue), indicating that the modification to the acceleration time history is small. This observation is also shown in the Fourier spectra plot, in which only the low frequency content is affected and the frequency content that excites the piping system the most is almost identically preserved by the baseline correction.

The slight change in the acceleration time history during the baseline correction can be better noticed in Figure 4-7, in which the two time history records are plotted side by side. The 5% damping response spectra of the original and the baseline-corrected acceleration time histories are identical to the extent shown by Figure 4-7. More importantly, the change in the input motions due to baseline correction has virtually no effect in the analytical responses. In a preliminary analysis of the piping system using DM4-1 input motions, the displacement responses due to the original and the baseline-corrected input motions are nearly identical (see Figure 4-8 for an example of displacement time history comparison). It should be noted that this preliminary analysis only serves as a sensitivity study of the baseline correction and its results do not necessarily match those in the result sections because subsequent modifications of the material and the finite element models were made.

In addition, the removal of the residual displacement in the input motions for the analysis should not significantly affect the result comparison because the displacement measurements in the experiment were taken as relative values with the top of the shaking table as the reference. Therefore, all input motions used in the BNL analyses reported in the following are baseline-corrected.

4.2.2 ANSYS Material Models

Three kinematic hardening rules available in ANSYS have been studied in the piping analysis in the previous report [DeGrassi and Hofmayer 2005]. In the analysis for the design confirmation method tests and also the ultimate strength tests, only the multi-linear kinematic hardening model and the Chaboche nonlinear kinematic hardening model [Chaboche 1986] are used in the final

analyses, because the bi-linear model cannot describe the stress-strain relationship accurately enough for the strain range these two sets of tests have shown. Both the multi-linear material model and the Chaboche material model have been revised to represent the material test data more accurately.

Both hardening models are based on the Von Mises yield criterion and the associated flow rule. The multi-linear hardening rule does not permit the change of plastic modulus due to the presence of a mean stress, and consequently cannot predict strain ratcheting for a stress controlled loading and unloading test. On the other hand, the Chaboche nonlinear hardening rule allows strain ratcheting because its plastic modulus consists of several exponential functions of the plastic strain. A more detailed discussion of the general plasticity theory and the three plastic hardening rules can be found in the previous report [DeGrassi and Hofmayer, 2005]. This report only describes the development of the multi-linear kinematic hardening model and the Chaboche nonlinear kinematic hardening model for the purpose of this study.

4.2.2.1 Multi-linear Kinematic Hardening Model

The multi-linear kinematic material model is utilized in the first analysis phase that consists of a transient analysis of the whole piping system using the straight and curved plastic pipe elements provided by the ANSYS FE program. The ANSYS pipe elements do no accept the Chaboche nonlinear kinematic hardening rule. Instead of using the cyclic test data as described in the previous report, the multi-linear model for the large scale piping tests is developed using the monotonic tensile test data, which was described in Section 2. As shown in Figure 4-9, the engineering stress-strain curve obtained from the material test was first transformed to a true stress-strain curve as required in large strain analysis. The difference between the engineering and the true stress-strain curves is negligible for small strains; therefore, the true stress-strain curve is valid for both the small deformation analysis and the large deformation analysis. As shown in Figure 4-10, the multi-linear kinematic material model is developed by fitting straight-line segments over four strain ranges on the true stress-strain curve for a strain range below 5%. The line segment designed Sig_e represents the elastic domain, and the Sig_1 to Sig_3 segments represent the multi-linear plastic domain. The ANSYS multi-linear model is then created by finding the Young's modulus and the intersections of the nearby line segments. Using the line segment equations shown in Figure 4-10, the Young's Modulus is found to be 1.8866e5 MPa, and the intersection points are (0.146 %, 275.942 MPa), (2.184 %, 280.140 MPa), (2.701 %, 312.550 MPa), and (5.000 %, 379.340 MPa). The model defined by this set of parameters is termed as the *mono* multi-linear kinematic hardening material model.

A minor modification in the mono multi-linear kinematic material model is needed for the (elastic) allowable stress tests DM2-1 and DM2-2. Preliminary analyses for these two tests have shown that the predicted acceleration and displacements using the unmodified mono multi-linear model can be more than 30 % larger than those from the tests, while those for the three elasto-plastic tests showed an extremely good match to tests. It appeared that the scale of the excitation has a nontrivial impact on the performance of the material model in predicting the response of the piping system. One of the possible reasons is that the constraints at various locations in the piping system can change their restraining properties as the scale of the excitation increases, perhaps because of local yielding of the piping at these locations at higher excitations. The local yielding of the piping system at the constraint locations makes the constraints more like simple translational ones. However, modeling of these constraints of varying restraining properties requires the use of semi-rigid connections, which demands more effort and introduces another possibility of modeling inaccuracy.

A simple approach has been taken in this study to cope with this problem. For the (elastic) allowable stress tests DM2-1 and DM2-2, a Young's modulus of 2.03e5 MPa, which was obtained from the cyclic test and was reported in the previous NUREG/CR report, is used instead of the 1.8866e5 MPa as determined by the Monotonic tensile test. This slightly higher Young's modulus incurs a change of the first intersection point in the mono multi-linear material model to (0.136 %, 275.920 MPa), which represents just a minor decrease (of 0.022 MPa) in the yield stress. The resultant multi-linear kinematic model is hereafter referred to as the *hybrid* multi-linear kinematic hardening model.

4.2.2.2 Chaboche Nonlinear Kinematic Hardening Model

The Chaboche kinematic hardening model is used for the elbow model that consists of nonlinear shell elements in order to capture the strain ratcheting effect in the tests. The Chaboche hardening rule is a superposition of several "decomposed" Armstrong-Frederick hardening rules [Chaboche 1986]. A three decomposed-rule model as commonly adopted in the literature [Bari, et al 2000, DeGrassi and Hofmayer 2005] is used in this study. Chaboche proposed that the three rules, designated by the backstresses as α_1, α_2, α_3, simulate three portions of a plastic stress-strain curve respectively: the initial high plastic modulus at the onset of yielding, the transient nonlinear portion of the plastic stress-strain curve, and the linear part of this curve for high strain values, as shown on the "Test" curve in Figure 4-12. With a key parameter $\gamma_3 = 0$, the third rule α_3 is a linear rule and can result in a complete shakedown of ratcheting. Therefore, a small positive γ_3 was recommended by Chaboche [1986] to improve the ratcheting capability of the 3-rule model with no significant change imposed on the hysteresis loop. More recently, Bari, et al [2000] suggested that instead of using a monotonic stress-strain curve, a uniaxial strain-controlled stable hysteresis curve should be used to develop the parameters for the three rules except for γ_3, which can be determined later by fitting the test data of a uniaxial ratcheting experiment. This approach was utilized by DeGrassi and Hofmayer [2005] with exception for γ_3, which was determined using the results of a strain-controlled cyclic test of an elbow component.

It has been observed in the previous literature that the simulated forward loading curve by the so-developed Chaboche nonlinear kinematic material model does not agree particularly well with the test in the transient region. To obtain a more accurate model, the implementation of the Chaboche model in this study follows a more rigorous approach to develop the parameters (except for γ_3). For the convenience of discussion, the equations for the Chaboche model are summarized as,

$$\sigma_x = \sigma_y + \alpha_1 + \alpha_2 + \alpha_3, \tag{4-1}$$

$$\alpha_i = \frac{C_i}{\gamma_i}\left[1 - 2\exp\left\{-\gamma_i\left(\varepsilon_p - \varepsilon_{pl}\right)\right\}\right], \text{ for } i = 1 \text{ or } 2, \tag{4-2}$$

$$\alpha_3 = C_3\varepsilon_p, \tag{4-3}$$

where σ_x is the total axial stress, σ_y the yield stress, ε_p the plastic axial strain, ε_{pl} the plastic strain limit of the stable hysteresis loop (negative), C_i and γ_i the parameters for the three "decomposed" Armstrong-Frederick hardening rules α_i (backstresses). The Chaboche model requires the determination of elastic modulus, yield stress, and C_i and γ_i, in which the elastic modulus and the yield stress were identified in developing the multi-linear hardening models.

From the JNES/NUPEC strain-controlled uniaxial cyclic test of an STS410 steel specimen, the same forward loading curve as used by DeGrassi and Hofmayer [2005] was identified for the

development of the parameters (except for γ_3) for the Chaboche model in this study. The curve from the test was presented in terms of engineering stress-strain and was first converted into a true stress-strain curve for consistency with the multi-linear kinematic hardening material models and for compatibility with large deformation analysis option utilized in this study. The elastic strain was then removed from the total stress-strain curve by subtracting the elastic strain (stress / Young's modulus). As shown in Figure 4-11, the initial values of C_1 and C_3 are determined by fitting the elastic portion and the very end of the linear portion of the forward loading curve. The initial values of C_2, γ_1, and γ_2 were taken from the previous report [DeGrassi and Hofmayer 2005]. Utilizing the initial values of C_1, C_2, γ_1, and γ_2, a least-square minimization of the difference between the test and the developed forward loading curve (Eq. 4-1) can yield an optimal set of values for these parameters. C_3 does not participate in this least-square minimization in order to maintain the linear portion of the plastic stress-strain curve. The excellent match between the test curve and the Chaboche curve with the optimal parameters can be clearly seen in Figure 4-12. Also demonstrated in Figure 4-12, the change of the parameters during the minimization process does not change the original intention of the three rules proposed by Chaboche [1986]; the three rules α_1, α_2, and α_3 still represent the initial high plastic modulus portion, the transient nonlinear portion, and the linear portion of the plastic stress-strain curve, respectively.

Using the same approach as the one in the previous report, the parameter γ_3 was determined by performing a parametric study of γ_3 using the strain-controlled cyclic test (SE-4) of an elbow component [DeGrassi and Hofmayer 2005]. By varying γ_3 while maintaining other parameters, a series of trial-and-error runs of an ANSYS shell model (see Figure 4-13) developed for the SE-4 test were carried out, and a value of γ_3 was then found to achieve the best prediction of the strain ratcheting behavior of the elbow component. Figure 4-14 shows a comparison of the final hoop and axial strain ratcheting behaviors between the test and the analysis, with γ_3 =2.2.

In summary, the revised Chaboche nonlinear kinematic hardening material model used in the analyses is defined by the follow parameters: σ_y=275.92 MPa, E =203000 MPa, C_1 =65191.29 MPa, C_2 =14909.91 MPa, C_3 =1653.90 MPa, γ_1 =1044.83, γ_2 =177.06, and γ_3 =2.2.

4.2.3 Finite Element Models and Analyses

DeGrassi and Hofmayer have shown that the curved plastic pipe element in ANSYS is not adequate to simulate the elbow strain ratcheting behavior [2005]. Therefore, a shell representation of the elbow is necessary to predict its strain ratcheting behavior. In line with the analysis strategy as indicated in the beginning of this report, two FE models were developed to obtain the analytical responses. One model uses simple pipe elements (beams) to represent the whole piping system, while the other uses nonlinear shell elements to represent one of the nine elbows in the test. This modeling strategy is necessitated primarily by the high computational demand of a nonlinear transient analysis of the whole piping system. Such an analysis can be computationally very expensive if the piping system is modeled entirely with shell elements. Even a hybrid model involving pipe elements (beam elements) for straight pipe segments and shell elements for elbows has been shown to be prohibitive for a nonlinear transient analysis. In deed, even a nonlinear transient analysis of a shell model of a single elbow was found to be an intolerably lengthy calculation in a preliminary study.

Some analysis options are shared by all models and analyses. Together with the true stress-strain curves, the large deformation option in ANSYS is set for both the piping system model and the elbow model, since responses due to both small and large input motions should be predicted well with this option. Automatic time stepping in ANSYS is used for all analyses with the upper bound equal to the time step of the input motions (0.005 sec) and with the lower bound so small

so as not to prevent ANSYS from finding an efficient and converged solution. Occasionally, the solution stabilization option has also been turned on to overcome convergence problems for large input motions. All outputs of interest are requested at exactly every 0.005 sec by utilizing appropriate output specification arrays, in order to make the analytical results easy to be compared with the test results.

This subsection describes the relevant modeling and analyses for the piping system model and the elbow model.

4.2.3.1 Piping System Model Using Pipe Elements

Figure 4-15 shows the ANSYS FE model of the piping system, overlaid with various major dimensions and symbols for boundary conditions. The entire piping system for the large-scale design method confirmation test is modeled with pipe elements, with the straight pipe segments discretized by PIPE20 elements that are mostly 500 mm long and with elbows discretized by four PIPE60 elements. In ANSYS, PIPE20 is a plastic straight pipe element while PIPE60 is a plastic curved (elbow) thin-walled pipe element. Both element types can handle large plastic deformation, and have tension-compression, bending, and torsion capabilities. These pipe elements do not allow the use of the Chaboche nonlinear kinematic hardening material model, and therefore the multi-linear kinematic hardening models described previously are used in the piping system analysis. The averaged as-built diameter and the averaged as-built thickness of the piping system are used for the FE model, with values of 219.2 mm and 10.38 mm, respectively. The mass of the water is considered in the analyses indirectly by increasing the mass density of the pipe material, with a resultant mass density of 12,388 kg/m^3. The added weight of 1000 kg in the specimen was represented by a MASS21 element at node 35.

The piping system for the design method confirmation test was subjected to an internal pressure of 10.7 MPa. Gravity load is considered in the transient analyses. The spring hanger is represented by a concentrated vertical force at node 35, which was determined as the reaction force to gravity assuming a vertical translational support at this location. At the beginning of the analysis, the two nozzles and one anchor are fixed for the six translational/rotational degrees of freedom and various translational restraints in the test are modeled by unidirectional displacement boundary conditions, as shown in Figure 4-15. Some of these restraints and the fixed boundary conditions are replaced by the acceleration time history in the transient analyses.

The Rayleigh damping model is used for the transient analyses. The frequencies of the first two modes from the sine sweep tests, 6.3 Hz and 8.1 Hz, and the corresponding measured damping ratios, 2.1% and 4.8% respectively, were used to calculate the ALPHAD (mass term) and BETAD (stiffness) parameters for the Rayleigh damping model in ANSYS. However, these measured frequencies and damping ratios resulted in a negative ALPHAD; therefore, only the BETAD parameter was considered in analyses for the design method confirmation tests. The stiffness only damping parameter BETAD was calculated to be 1.061E-3 using the fundamental frequency and the corresponding measured damping ratio. JNES/NUPEC had also provided the fundamental frequencies and damping ratios for all tests, showing that frequency generally decreases while damping ratio increases as the piping system experiences the increasing levels of input excitations. These damping ratios were not used for the analyses because they are believed to include the energy dissipation effect from the hysteresis loops, which have already been directly taken into account by the multi-linear kinematic material models. In fact, a preliminary run of DM4-1 using the larger damping ratio measured in the test showed that the analytical responses became smaller than the test results and the result comparison became worse.

With the internal pressure and gravity load applied, modal analyses of this piping model can provide an indication of the accuracy of this model. Using the hybrid multi-linear kinematic hardening material model, the frequencies of the first two modes were found to be 6.09 Hz and 7.60 Hz, representing relative differences of -3.3% and -6.2% from the sine sweep tests, respectively. Using the mono multi-linear kinematic hardening material model, the frequencies of the first two modes were determined to be 5.88 Hz and 7.33 Hz, which represent -6.6% and -9.5% off the values from the sine sweep tests, respectively. However, these frequencies are considered to be acceptably accurate, especially when the hybrid multi-linear model is used for the lower excitation tests (DM2-1 and DM2-2) and the mono multi-linear model is used for the higher excitation tests (DM4-1, DM4-2(1), and DM4-2(2)), in which the fundamental frequencies were reported to be 5.9~6.0 Hz [JNES 2003].

Responses to be compared between the analysis and the test are taken at or around Elbow 2, as indicated in Figure 4-15. Some of the nodes around this location were relocated slightly from the regular 500 mm discretization, in order to make the comparisons at the same locations as the instrumentation. Four responses are selected in this study for comparison, as described in the following.

- D2: a relative displacement measurement between nodes 30 and 34. This response is designated in this report as "D2TEST" or "D2," indicating the test result or analytical result, respectively.
- D4X: a displacement measurement in the test in the X direction at node 29, relative to the shaking table top (reference node 1 in the FE model). This response is designated in this report as "D4TEST" or "DX29-1," indicating the test results or analytical result, respectively.
- A2X: an absolute acceleration measurement in the X direction at node 29. This response is designated in this report as "A2TEST" or "ACC29," indicating the test result or analytical result, respectively.
- S85: strain measurements at a location on the exterior surface of elbow 2, which are designated in the test by strain gauge SE2C-7A (axial) and SE2C-7H (hoop). The strain responses will be taken from the analysis of the elbow model (to be described in the next subsection). The comparison will be made based on the strain ratcheting time history and the maximum strain range (typically determined in conjunction with fatigue analysis).

In addition to these responses that will be compared to the test results, the relative displacements and rotations between node 30 and node 34 are saved from the analyses of the system model and will be used as inputs to the elbow shell model.

4.2.3.2 Analysis of the Piping System and Result Assessment

Except for the two (elastic) allowable stress tests DM2-1 and DM2-2, the three elasto-plastic tests have significant accumulation of plasticity, which may change the dynamic properties for the subsequent tests. Therefore, attempts have been made in investigating the plasticity accumulation effect through the ANSYS restart option that can preserve the deformed model to the analysis of next test. More specifically, the analyses of DM4-2(1) and DM4-2(2) were performed using two approaches: (1) analyses using the initial undeformed piping system model and (2) analyses using the deformed piping system model.

The results of the transient analyses of the five tests are compared to test results provided by JNES/NUPEC. For acceleration responses, the comparisons are made with time histories and response spectra with a damping ratio of 5%; while for displacement responses, the comparisons

are made with time histories and Fourier spectra. Figure 4-16 through Figure 4-36 show plots for these comparisons. The time history plots are arranged with the test results shown at the top and the analytical results shown at the bottom, while the other plots show the test results and the analytical results overlapped. In these figures, red dots indicate the maxima while blue dots indicate the minima. A summary of these comparisons are provided as follows.

DM2-1:

Comparisons for the DM2-1 test regarding the displacement D2, D4, and acceleration A2 are provided in Figure 4-16 through Figure 4-18. The overall shapes and the peak responses of the time histories agree excellently between the test and the analysis, with a maximum peak difference of about 12% (over-predicted by the analysis). Since the input motions are the smallest among the five tests, the responses are relatively small and therefore the relative error may have been over shadowed by other uncertainties in the test and the analysis. The Fourier spectra comparisons show this point better. The Fourier spectra of the test displacements show a flat region for frequencies above 10 Hz, suggesting that white noise was recorded in the test. The white noise can also be identified as the small but non-trivial responses in the tails of the time histories from the test. The dominant responses, which are in the vicinity of 4~6 Hz, and the nearby responses between 1~10 Hz compare especially well between the test and analysis. The displacement magnitudes at very low frequencies are between the peak responses at around 4~6 Hz and the high frequency responses (white noise recorded in the test). The slight differences of the displacement responses at the low frequencies reflect the difference in the residual displacements and the overall shapes, and may be due to the baseline correction of the input motions. As discussed previously, the baseline correction affects mainly the low frequency range. The low frequency content represents the gross shape or the slight skew of a time history and usually does not determine the major dynamic characteristics of a system. The response spectra of the acceleration A2 for the test and analysis match very well, with the test results having a slightly wider resonant region extending to the high frequency. The peaks are at a frequency of about 5 Hz, which is between the input dominant frequency of 4.5 Hz and the piping system's fundamental frequency of 6.09 Hz (6.3 Hz from test). The relative difference between the maximum spectra responses is only about 0.3%, comparing to the relative difference of about 9% between the PGA's (a borrowed term, meaning peak ground acceleration).

DM2-2:

Comparisons for the DM2-2 test regarding the displacement D2, D4, and acceleration A2 are provided in Figure 4-19 through Figure 4-21. The overall shapes and the peak responses of the time histories agree excellently between the test and the analysis, with a maximum peak difference of about 10% (over-predicted by the analysis). Similarly to DM2-1, the Fourier spectra of the test displacements show a flat region for frequencies above 10 Hz, suggesting that white noise was recorded in the test, as can also be identified as the small but non-trivial responses in the tails of the time histories from the test. The dominant responses, which are in the vicinity of 4~6 Hz, and nearby responses between 1~10 Hz compare especially well between the test and analysis. Both the test and the analysis show a clear discontinuity around 1 Hz in the Fourier spectra. The displacement magnitudes at very low frequencies are between the peak responses at around 4~6 Hz and the high frequency responses (white noise recorded in the test). The slight differences of the displacement responses at the low frequencies reflect the difference in the residual displacements and the overall shapes, and may be due to the baseline correction of the input motions. In the frequency range of 0.1 to 1 Hz, the difference in D2 may indicate some plasticity in the elbow, which the analysis may not capture accurately. The response spectra of the acceleration A2 for the test and analysis match very well, with the test results having a

slightly wider resonant region towards the high frequency. The peaks are at a frequency of about 5 Hz, which is between the input dominant frequency of 4.5 Hz and the fundament frequency of the pipe system of 6.09 Hz (6.2 Hz from test). The relative differences of both the maximum spectra responses and the PGA's are only about 2%.

DM4-1:

Comparisons for the DM4-1 test regarding the displacement D2, D4, and acceleration A2 are provided in Figure 4-22 through Figure 4-24. The overall shapes and the peak responses of the time histories agree excellently between the test and the analysis, with a maximum peak difference of about 10% (over-predicted by the analysis). The analytical time histories appear to be slightly less damped than the test. The Fourier spectra of the test displacements show a flat region for frequencies above 20 Hz, suggesting white noise was recorded in the test. Unlike the white noise for tests DM2-1 and DM2-2, the white noise for this test cannot be easily identified in the time histories because the white noise is about five magnitudes smaller than the peak response. The dominant responses, which are at a frequency of slightly less than 6 Hz, and most responses for frequencies below 10 Hz compare especially well between the test and analysis. Both the test and the analysis show discontinuities at around 1 Hz and 10 Hz in the Fourier spectra. There is not a significant difference in the general trend of the displacement responses at the low frequencies. The slight differences of the displacement responses at the low frequencies reflect the difference in the residual displacements and the overall shapes, and may be due to the baseline correction of the input motions. As discussed previously the baseline correction affects mainly the low frequency range. The response spectra of the acceleration A2 for the test and analysis match very well. The spectral response peaks are at a frequency of slightly less than 6 Hz, which is the same as the input dominant frequency and the fundamental frequency of the pipe system (6.0 Hz from test DM4-1). The relative difference between the maximum spectra responses is only about 12% (over-predicted by the analysis), comparing to the relative difference of about 1% between the PGA's.

DM4-2(1) (Restart):

This analysis considered the plasticity developed during DM4-1. Comparisons for the DM4-2(1) with restart regarding the displacement D2, D4, and acceleration A2 are provided in Figure 4-25 through Figure 4-27. The overall shapes and the peak responses of the time histories agree excellently between the test and the analysis, with a maximum peak difference of about 5%. The analytical time histories appear to be slightly less damped than the test. The Fourier spectra of the test displacements show a flat region for frequencies above 20 Hz, suggesting white noise was recorded in the test. Unlike for tests DM2-1 and DM2-2, the white noise cannot be easily identified in the time histories because the white noise is about 4~5 magnitudes smaller than the peak response. The dominant responses, which are at a frequency of slightly less than 6 Hz, and most responses for frequencies between 0.3~20 Hz compare especially well between the test and analysis. Both the test and the analysis show discontinuities at around 1 Hz and 10 Hz in the Fourier spectra. The differences of the displacement responses at the low frequencies reflect the difference in the residual displacements and the overall shapes, and may be due to the baseline correction of the input motions. The response spectra of the acceleration A2 for the test and analysis match very well. The spectral response peaks are at a frequency of slightly less than 6 Hz, which is the same as the input dominant frequency and close to the fundamental frequency of the pipe system (6.0 Hz from test DM4-2(1)). The relative difference of the maximum spectra responses is only about 9% (over-predicted by the analysis), comparing to the relative difference of about 2% of the PGA's.

DM4-2(2) (Restart):

This analysis considered the plasticity developed during DM4-1 and DM4-2(1). Comparisons for the DM4-2(2) with restart regarding the displacement D2, D4, and acceleration A2 are provided in Figure 4-28 through Figure 4-30. The overall shapes and the peak responses of the time histories agree generally well between the test and the analysis, with a maximum peak difference of about 6%. All response peaks in the time histories are under-predicted by the analysis. The analytical time histories appear to be slightly less damped than the test. In addition, the analytical time histories show some tendency that the responses are encapsulated within constant limits, which may imply that the mono multi-linear kinematic hardening model may result in strain shakedown for this level of input motions. The Fourier spectra of the test displacements show a flat region for frequencies above 20 Hz, suggesting white noise was recorded in the test. Unlike for tests DM2-1 and DM2-2, the white noise cannot be easily identified in the time histories because the white noise is about 4~5 magnitudes smaller than the peak response. The dominant responses, which are at a frequency of slightly less than 6 Hz, and most responses for frequencies between 1~20 Hz compare especially well between the test and analysis. Both the test and the analysis show discontinuities at around 1 Hz and 10 Hz in the Fourier spectra. The differences of the displacement responses at the low frequencies reflect the difference in the residual displacements and the overall shapes, and may be due to the baseline correction of the input motions. The response spectra of the acceleration A2 for the test and analysis match very well. The spectral response peaks are at a frequency of slightly less than 6 Hz, which is the same as the input dominant frequency and close to the fundamental frequency of the pipe system (5.9 Hz from test DM4-2(2)). The relative difference of the maximum spectra responses is only about 5% (over-predicted by the analysis), comparing to the relative difference of about 6% of the PGA's (under-predicted by the analysis).

DM4-2(1) (Without Restart):

This analysis did not consider any plasticity developed previously. Comparisons for the DM4-2(1) without restart regarding the displacement D2, D4, and acceleration A2 are provided in Figure 4-31 through Figure 4-33. Compared to DM4-2(1) with restart, no significant difference can be found for the various comparisons for this analysis, meaning that the previous plasticity accumulation does not have a significant impact on the displacement and the acceleration responses considered in the analysis.

DM4-2(2) (Without Restart):

This analysis did not consider any plasticity developed previously. Comparisons for the DM4-2(2) without restart regarding the displacement D2, D4, and acceleration A2 are provided in Figure 4-34 through Figure 4-36. Compared to DM4-2(2) with restart, no significant difference can be found for the various comparisons for this analysis, meaning that the previous plasticity accumulation does not have a significant impact on the displacement and the acceleration responses considered in the analysis.

In summary, the comparisons of the piping system analyses of the design method confirmation tests demonstrated that displacement and acceleration time history responses were predicted with high accuracy, mostly within a maximum relative error of 10%. The analyses tend to over-predict the responses for low level input motions while somewhat under-predict the responses for high level input motions. The analyses are capable to capture closely the dominant frequency content, in view of the Fourier spectra and response spectra. Major features in the Fourier spectra,

such as the peaks and discontinuities, were accurately predicted by the analyses. The comparisons of the response spectra are especially accurate.

4.2.3.3 Elbow Model Using Shell Elements

In the refined analyses for the strain ratcheting effect, Elbow 2 is taken as the part of the piping specimen between nodes 30 and 34 in the piping system model, as shown in Figure 4-15. Each branch of Elbow 2 has a centerline length of 950 mm and the radius of the elbow centerline is 304.8 mm. The diameter of the pipe is 219.2 mm and its wall thickness is 10.38 mm, the same as-built values as used in the piping system model.

As shown in Figure 4-37, Elbow 2 is modeled entirely with the ANSYS plastic SHELL181 elements, including the straight pipe segments and the elbow. The elbow model has a total of 1152 shell elements, with 36 elements circumferentially for both straight and curved segments, 7 elements axially for the straight pipe segments, and 18 elements axially for the elbow. The elements for the straight pipe segments have varied axial lengths so that the sizes of the elements are close around the junctions of the straight segments and the curve segment. The ANSYS shell element SHELL181 is a 4-node finite strain shell element that is suitable for large rotation and large strain nonlinear simulation of thin to moderately thick shell structures [ANSYS 2007]. For nonlinear analysis, this element can take into account the change of shell thickness. Unlike the reduced integration scheme, the full integration scheme used in this study for the shell elements makes them to have non-constant strain. Because significant plasticity was found in a preliminary analysis to accumulate in the straight pipe segments at regions close to the elbow, the element type SHELL181, being computationally expensive, was chosen for the entire model rather than the computationally inexpensive elastic element type. For the same reason, the model cannot be made shorter so as to include the elbow itself only; otherwise, the boundary conditions on the short model would be too complicated to approximate with a reasonably good and simple model.

The boundary condition at each end of this elbow model is modeled with a *surface-based constraint*, which couples the motion of the edge nodes to a single pilot node at the centerline (either node 30 or node 34). The ANSYS surface-based constraint can be specified as either *force-distributed constraint* or *rigid surface constraint*, both of which were investigated in this study. Different from the one used by DeGrassi and Hofmayer [2005] that utilized rigid pipe elements, the surface-based constraint approach is conceptually simpler and has the advantage that allows the deformation of the pipe at the ends using the force-distributed constraint option [ANSYS 2007]. The deformable boundary condition appeared to be very attractive initially because it allowed the appropriate simulation of the pipe end deformation due to the internal pressure, compared to the rigid pipe element method which cannot. Preliminary analyses using the force-distributed constraints did clearly show this deformable capability. Nevertheless, these analyses also showed that the predicted ratcheting strains were much lower than the test results at the end of the time histories. This finding lead to the final use of the more traditional rigid surface constraint option in this study. The differential displacement time histories obtained from the piping system model are applied at the pilot node 30 while the pilot node 34 is restrained from motion for all six degrees of freedom. The gravity and the internal pressure are applied in the elbow model. As stated before, the analyses of the elbow shell model are static nonlinear analyses; therefore, the damping and the local inertial effects are not included.

The Chaboche nonlinear kinematic hardening material model is used in the elbow shell model, since it is compatible with the SHELL181 elements. As stated previously, this material model is not allowed for the PIPE20 and PIPE60 element types used in the piping system model.

The only responses obtained from this elbow shell model are the hoop and axial strain time histories at locations where the strain gauges SE2C-7A (axial) and SE2C-7H (hoop) are in the tests. This location is close to the top (+Z direction) on the exterior surface of the elbow at the symmetry plane (with a 45° intersection line in the XY plane). The analyses showed great variations in the strain predictions around this location; consequently, the four elements close to this location will be presented in the comparisons to the test results. It should be noted that the location of the gauges SE2C-7A and SE2C-7H were believed to have the highest hoop strain in the elbow. In comparison of the strains from analyses and those from the test, it should also be noted that although the thickness and diameter of the elbow have been assumed to be the (constant) average as-built values in the shell model, these values do vary circumferentially (and axially). At the section where strain gauges SE2C-7A and SE2C-7H are located, the measured diameter was larger in the intrados-extrados direction than in the flank direction; while the measured pipe thickness is generally at its maximum at the intrados, at its minimum at the extrados, and in between at the flanks. The variation of the thickness at this section can be as much as 17.5% compared to the average thickness of 10.38 mm; while the variation of the diameter is negligible. The variations in the pipe diameter and thickness in the test certainly affect the accuracy of the assessment of the predicted strains in the analyses. Figure 4-38 shows the strain gauge location and the surrounding four selected elements 145, 154, 639, and 648 in the elbow model. The position of the strain gauges SE2C-7A and SE2C-7H in the test were located between elements 154 and 648.

4.2.3.4 Input Motions for the Elbow Model

The input motions to the elbow shell model were generated in the piping system analyses, including six differential displacement/rotation time histories between node 30 and node 34. These input motions are designated as DX, DY, and DZ for displacements and as RX, RY, and RZ for rotations. These input motions are plotted in Figure 4-39 through Figure 4-45 for tests DM2-1, DM2-2, DM4-1, DM4-2(1) (restart), DM4-2(2) (restart), DM4-2(1) (fresh start), and DM4-2(2) (fresh start), arranged in line with the analyses of the piping system model. An examination of these input motions can provide insights on how Elbow 2 has behaved in the piping system model using the multi-linear kinematic hardening material models. There are no test results available for comparison of these input motions, and therefore observations regarding the input motions for the elbow model will be qualitative.

These input motions demonstrate that the most significant vibrational input motions are the displacements DX and the rotations RZ. This is expected because the shaking table vibrated mainly in the X direction, together with small Z directional motions. The magnitudes of these input motions to the shell model increase as the shaking table excitation increases. As shown in Figure 4-39 and Figure 4-40, the input motion plots for DM2-1 and DM2-2 confirm that the elbow model behaves elastically for these tests because the time histories oscillate around zero and have no residual displacements. The input motions for DM4-1 shown in Figure 4-41 show some permanent residual displacements, implying plastic deformation has started to develop in Elbow 2 in this test.

In line with the two approaches that either consider or neglect the previous plasticity buildup for tests DM4-2(1) and DM4-2(2) in the piping system analyses, two sets of input motions for the elbow shell model were generated. Figure 4-42 and Figure 4-43 show the input motion plots for these two tests that consider the plasticity states from the previous analyses (using the ANSYS restart option in the piping system analyses), clearly showing that residual deformations have been assumed from the previous analyses. Although the input motions DY, DZ, RX, RY do not oscillate as much as DX and RZ, kinks of significant magnitude can be clearly seen in these time

histories, with some even reversed in sign. It is obvious that Elbow 2 has undergone substantial plastic deformations in the analyses. The rotational plastic deformations RX and RY can even reach magnitudes comparable to the most significant and mostly oscillating rotational deformation RZ.

Figure 4-44 and Figure 4-45 show the input motions to the elbow model without consideration of the plasticity accumulation from the previous analyses (fresh start). The input motions for DM4-2(1) (fresh start) are very similar to those for DM4-2(1) (restart), because the plasticity accumulation before this test is minimal. For DM4-2(2), except for the residual deformations inherited from the previous analysis, deformations DX and RZ do not exhibit significant difference between the restart analysis and the fresh start analysis, partly because the oscillating nature of the time histories obscure subtle differences. For the other four displacements/rotations, DY, DZ, RX, and RY, the differences between the two analytical approaches can be significant, particularly in the first 20 to 25 seconds. However, after the beginning period of time when the fresh start analysis predicted much lower responses, the deformations DY, DZ, RX, and RY from the fresh start analysis show a great deal of similarity to those from the restart analysis. This observation implies that the fresh start option may be able to capture the overall strain ratcheting behavior at the end of the analysis.

4.2.3.5 Analysis of the Elbow Model and Result Assessment

Since tests DM2-1 and DM2-2 have been expected to behave elastically, no elbow analyses for these two tests were performed. Although plasticity accumulation had been considered by using the ANSYS restart option in the piping system analyses, a similar approach for the elbow model had not shown any sign of plasticity. Therefore, analytical strain results for DM4-2(1) (restart) and DM4-2(2) (restart) are not available for comparison. However, since the input motions for the DM4-2(1) (fresh start) and DM4-2(2) (fresh start), after about 20 to 25 seconds in the time histories, show characteristics similar to those obtained using the restart option, they will be used to generate the strain ratcheting data for comparison to the test results. In summary, the strain comparison will be made in the following for analyses DM4-1, DM4-2(1) (fresh start), and DM4-2(2) (fresh start).

Because the full integration scheme for a shell element results in a non-constant strain field over the element, the strain comparison is based on the average of the strain ratcheting time histories at the four nodes of the subject element. Each strain comparison plot consists of four subplots: two for the test axial and hoop total strain (elastic + plastic) time histories at the top, and two for those for the ANSYS analyses at the bottom. The axial strain plots are on the left, while the hoop strain plots are on the right.

DM4-1:

Figure 4-46 through Figure 4-49 show the comparison of strain time histories for DM4-1 for elements 145, 154, 639, and 648, respectively. The best match between the analytical result and the test occurs at element 145, with the closest peak values for both the axial and hoop strains. The strain ratcheting phenomena are predicted relatively accurately. Although the first plateau in the analytical hoop strain time history is lower than half of that from the test, the final hoop (plastic) strain from the analysis, less the initial elastic strain, is extremely close to that from the test. The axial strain ratcheting is under-predicted. However, since the magnitude of the axial strain is much smaller than the hoop strain, the comparison in the axial direction may not be as important as in the hoop direction. The comparison for element 639 is slightly less accurate than for element 145. The comparisons for elements 154 and 648, which are located closer to the strain gauges than the other two elements, are unexpectedly less accurate than for the other two

elements. The final hoop (plastic) strains from the analysis for elements 154 and 648 are only about 1/6 of that from the test.

DM4-2(1) (Fresh Start):

Figure 4-50 through Figure 4-53 show the strain comparison for DM4-2(1) (fresh start) for elements 145, 154, 639, and 648, respectively. The comparisons for this analysis show an opposite phenomena to the one for DM4-1. The comparisons for elements 154 and 648, which are closer to the strain gauges than the other two elements, are much better than for the other elements that are about 10° away from the strain gauge location. The best match between the analytical result and the test occur at element 648, with the analytical final hoop (plastic) strain less the initial elastic strain being close to the test. The first plateau in the analytical hoop strain time history is higher than that from the test. The analytical axial strain ratcheting history, though with smaller oscillations, is predicted very accurately. The hoop strain for element 639 slightly over-predicted the test, while the axial strain for this element predicted well. The hoop strains for elements 145 and 639 over-predicted the test by a factor of about four. One similarity that this analysis shares with the DM4-1 analysis is that the calculated hoop strain is higher for elements away from the strain gauge location.

DM4-2(2) (Fresh Start):

Figure 4-54 through Figure 4-57 show the strain comparison for DM4-2(2) (fresh start) for elements 145, 154, 639, and 648, respectively. The strain comparisons for all four elements have shown to over-predict the test results. The final hoop (plastic) strains predicted in elements 154 and 648 are about twice as large as the test, and in the other two elements 145 and 639 are about 5 times larger than the test. As discovered previously, the first 20 to 25 seconds of the input motions for this analysis do not match the test because the plasticity accumulation effect is not considered, which implies that this analysis may cover the plasticity development for previous tests and for this test itself. Just for the sake of argument, if a residual plastic strain of 0.7% for DM4-2(1) and the initial elastic strain for the internal pressure were taken out from the hoop strain history, the resultant final hoop strain would be about 0.9% at the strain gauge location, which becomes just about 10% higher than the test. The shape of the strain ratcheting history from the test shows a virtually zero-ratcheting zone of 20 seconds at the beginning, which suggests that the plastic deformation accumulated in the previous tests can accommodate this part of the input motions without further significant plasticity development. In contrast, since the analysis starts with an intact piping system, the initial plasticity accumulation is very fast and the strain history shows a short plateau of about 0.9% between 10~20 Hz that imitates the initial flat region for the test strain history. The axial strains are not significant in magnitude, and their comparisons are not crucial. Similar to previous analyses, it is also found true for this analysis that the calculated hoop strain is higher for elements away from the strain gauge location.

In summary, the strain comparison using the strain ratcheting time histories can be relatively accurate if the strain in the analysis is taken from some element in the vicinity of the strain gauge instead of the exact location of the strain gauge. The strain prediction by the analysis appears to be location sensitive or excitation sensitive. In addition, the plasticity accumulation has been found important for accurate prediction of the entire strain ratcheting history, which may require further investigation of the ANSYS software. Examination of the strain gradient in the hoop direction may provide more insights. However, such an examination requires further effort beyond the present study.

As discussed previously, the thickness of the elbow at the section where the strain gauges are located varies by as much as 17.5% in the test specimen, compared to the uniform thickness used in the analysis. The variation in the pipe thickness in the test specimen may be a factor affecting the accuracy of the comparison, in addition to the limitations of the analytical models that are currently the most sophisticated.

The same (average) strain ratcheting time histories are also utilized to determine the maximum strain ranges for these analyses. As the tests showed that the pipe system specimen failed by fatigue ratcheting, the maximum strain range becomes a reasonable measure in assessing the analytical methods. In fatigue analysis of a non-sinusoidal loading, the maximum strain range can be determined by various cycle counting algorithms, which determine the ranges and cycles in the application of Miner's rule for fatigue life prediction. The rainflow cycle-counting algorithm developed by Matsuiski and Endo [1968] is the most popular one and has quite a number of variations in the literature for various application scenarios. Implemented for this study are two versions of the rainflow cycle-counting algorithms provided in the ASTM standard E 1049-85, named *rainflow counting* and *simplified rainflow counting for repeating histories*. The latter version was developed by Downing and Socie [1982].

In the rainflow counting method, ranges that remain as uncounted at the end of the peak-valley sequence are regularly treated as half-cycle ranges. For the purpose of this study, since the strain ratcheting is prominent, these remaining ranges can be better perceived as strain ratcheting effect than as cyclic strain ranges for fatigue analysis. However, the highly nonlinear nature of the test and the analyses does not warrant any clear cut in distinguishing all the ranges and cycles. Therefore, two maximum strain ranges are created in the rainflow method: one considering all ranges and the other excluding the consideration of the uncounted ranges, which are in this report attributed by "all ranges" and "regular ranges," respectively. Figure 4-58 shows a sequence of ranges obtained using the rainflow counting method, indicating the regular ranges and the remaining uncounted ranges.

The simplified rainflow counting method for repeating histories assumes that the subject strain time history is repeated to constitute a longer history. It requires the strain history to be rearranged such that it starts with its maximum peak or minimum valley. This requirement results in only full cycles. Figure 4-59 shows a sequence of ranges obtained using the simplified rainflow counting method. The assumption of repeating histories does not appear to be an appropriate one for the strain ratcheting time history; however, the results using this method are presented in this report to evaluate the similarity and the difference between the methods.

The program implementing the rainflow counting method (with all ranges or regular ranges) and the simplified rainflow counting method was verified using the corresponding examples provided in the ASTM standard E 1049-85, before its application to the test data and the analytical results for the four elements.

Table 4-1 shows the maximum hoop strain ranges for tests DM4-1, DM4-2(1), DM4-2(2), and US2-1 (to be assessed later in this report), using the two rainflow counting methods implemented for this study and the reported JNES values [JNES, 2003]. It should be noted that the JNES values were obtained by using its in-house version of a rainflow counting method. The JNES values are listed in the table for references. As shown in this table, different algorithms may produce different maximum strain ranges for the test data and for the analytical data. In general, the rainflow method considering just the regular ranges produces very consistent maximum strain ranges among the four elements, compared to the rainflow method considering all ranges and the simplified rainflow method. Using the rainflow method with regular ranges, the ANSYS results

are somewhat smaller than but in an acceptable range to those for tests DM4-1, DM4-2(1), and DM4-2(2). The comparison of the maximum strain range appears to be better than the strain ratcheting time history; all four elements predict generally the same level of maximum strain range but vastly different strain ratcheting time history. The rainflow method with regular ranges produces maximum strain ranges in a similar magnitude to JNES's results for the DM tests.

4.3 Analysis for the Ultimate Strength Test

4.3.1 Shaking Table Input Motions

The specimen for the ultimate strength test was subjected to elastic preliminary tests (US1) and elasto-plastic response tests (US2). As shown in Table 2-1, the elastic preliminary tests included two sine sweep tests in the horizontal and the vertical directions respectively to determine the modal frequencies. Since the excitation levels are very small in these two tests, only the elasto-plastic response tests will be used for the analyses. The input motions to the piping system are taken as the acceleration time histories recorded at the shaking table top.

The US2 tests only include input motions in the horizontal (X) direction. A number of reruns using essentially the same input motion were carried out by JNES/NUPEC to test the piping system until a fatigue crack developed in Elbow 2, which is shown in Figure 4-61. The input motion was specified to be capable of achieving a maximum stress level of $24S_m$. The time history of this input motion and its 5% damping response spectrum are shown in Figure 4-60, in which the PGA is shown as 1.943 g. The dominant frequency of the input motion is determined to be about 3.6 Hz, which is the same as the fundamental frequency of the piping system for US2-1 (the first run) and is slightly smaller than the fundamental frequency of 3.8 Hz for the US1 sweep tests. The duration of the US2-1 input motion is 120 seconds, and the time increment is 0.005 seconds.

The US2-1 input motion was baseline-corrected for the ANSYS analysis, for the same reason as that for the input motions for the DM tests.

4.3.2 ANSYS Material Models

Because the DM and US specimens were made of the same material, the mono multi-linear kinematic hardening model and the Chaboche nonlinear kinematic hardening model developed previously for the DM tests are used for the transient piping system analysis and the static elbow analysis of the US2 tests, respectively.

4.3.3 Finite Element Models and Analyses

4.3.3.1 Differences of Piping System FE Modeling from DM Models

The overall configuration of the US test is similar to that of the DM test; therefore, the FE models for the US test were developed based on those models for the DM test. The same ANSYS element types PIPE20, PIPE60, and MASS21 are used. Compared to the piping system model for the DM test, the FE model for the US test, as shown in Figure 4-61, does not have the restraint in the X direction at node 13. In addition, this model includes another 1000 kg concentrated mass at node 29 and other small masses at the constraint locations. The as-built diameter and thickness of this specimen were determined to be 219.1 mm and 10.16 mm (average values), respectively.

The internal pressure for the piping system is 10.7 MPa, the same as for the DM tests, and the gravity load is considered. A new concentrated force at node 35 was determined to simulate the spring hanger. Using the first two modal frequencies 3.8 Hz and 6.4 Hz from the test and the

corresponding damping ratios 0.9% and 1.2%, the ALPHAD and BETAD for the Rayleigh damping model were calculated to be 0.138 and 5.113×10^{-4}, respectively.

A parametric study of the frequency characteristics of this model was performed to further investigate the effect of the element types and material models on the modal frequencies, and the results are summarized in the following:

Material Types	Element Types	Young's Modulus (MPa)	1st Mode Freq. (Hz)	2nd Mode Freq. (Hz)
Linear Model	PIPE 16 & 18	2.0300×10^{5}	3.74	6.42
Hybrid Model	PIPE 20 & 60	2.0300×10^{5}	3.72	6.35
Mono Model	PIPE 20 & 60	1.8866×10^{5}	3.59	6.12
Sweep Test			3.8	6.4
US2-1 Test			3.6	N/A

It can be seen from the above table that the linear model (using linear element types and material models) and the hybrid multi-linear kinematic hardening model predict frequencies closest to the sweep test results, while the mono multi-linear kinematic hardening model predicts the fundamental frequency very close the US2-1 test. Utilizing the same reasoning as for the analyses of the DM tests, the mono multi-linear kinematic hardening model will be used for the US2-1 analysis, because the input motion for this test is very large.

The same responses as used in the comparisons for the DM test will be used for the US test.

4.3.3.2 Analysis of Piping System and Result Assessment

JNES/NUPEC provided BNL five sets of analytical results, designated as US2-1, US2-2, US2-3, US2-4, and US2-5. However, only the analysis of US2-1 will be presented in this report because (1) the application of the ANSYS restart option to the elbow shell model has not been successful and (2) the model is not intended to predict fatigue ratcheting that caused the test specimen to fail. For acceleration responses, the comparisons are made with time histories and 5% damping response spectra; while for displacement responses, the comparisons are made with time histories and Fourier spectra. Figure 4-62 through Figure 4-64 show plots for these comparisons for the US2-1 test. The time history plots are arranged with the test results shown at the top and the analytical results shown at the bottom, while the other plots show the test results and the analytical results overlapped. Red dots indicate the maxima while blue dots indicate the minima.

The overall shapes of the displacement and the acceleration time histories D2, D4, and A2 from the analysis show some degree of agreement with the test results. The analysis under-predicted the peak responses of the time histories by about 23%. The analytical time histories appear to be less damped than the test. In addition, the analytical time histories show a strong indication that the responses are trimmed from the peaks; this is particularly obvious for the acceleration time history. The analysis cannot predict the large residual displacements at the end of the analysis. It appears that the mono multi-linear kinematic hardening model may result in strain shakedown prematurely for this level of input motion. The Fourier spectra of the test displacements show a flat region for frequencies above 20 Hz, suggesting white noise was recorded in the test. The white noise cannot be easily identified in the time histories because it is about 4 to 5 magnitudes smaller than the peak response. The dominant responses, which are at about 3.6 Hz, and most responses for frequencies between 2 to 10 Hz compare well between the test and analysis. The test results show a discontinuity at about 2 Hz, which however was not predicted correctly by the analysis. The differences of the displacement responses at the low frequencies reflect the

difference in the residual displacements and the overall shapes; these differences may be due to the limitation of the material model as well as the baseline correction to the input motions. The differences in the displacement Fourier spectra between 1 Hz and 2Hz and the strong cyclic behavior of the analytical results between 10 Hz and 40 Hz may have contributed to the shape and peak differences in the time histories. The analytical peak spectral response of the acceleration A2 is lower than the test result by about 10% and the analytical PGA is lower than the test result by about 8%. Nevertheless, the spectral responses from the test and the analysis agree fairly well for the dominant frequency range around 3.6 Hz, which is the same as the resonance frequency of the input motion and the fundamental frequency of the piping system. The analytical response spectra shows a bump around 10 Hz, but the test does not.

In summary, although some comparisons of the analytical results for the US2-1 test are reasonably good, most of the comparisons are not as accurate as those for the DM tests. It should be noted that the comparisons for the DM4-2(2) test had already been shown to be less accurate (mostly under-predicted) than those for the other DM tests that are subjected to lower level input motions. The reason for the less accurate comparisons may be that the mono multi-linear kinematic hardening model reaches shakedown for large input motions (large piping responses).

4.3.3.3 Difference of Elbow FE Modeling from DM Models

Because the differences in the piping system configuration between the US tests and the DM tests are located outside of the Elbow 2 boundaries, the elbow shell model for the US tests is almost identical to that for the DM tests. The only exceptions are the pipe diameter and the wall thickness, which are 219.1 mm and 10.16 mm (average as-built values), respectively. Therefore, Figure 4-37, showing the overall mesh of the elbow model, is valid for both the DM tests and the US tests.

Figure 4-65 shows the strain gauge location and the four selected elements 145, 154, 315, and 324 in the elbow model for strain comparisons. The position of the strain gauges SE2C-7A and SE2C-7H in the test were located between elements 154 and 324.

4.3.3.4 Input Motions for the Elbow Model

Figure 4-66 shows the input motions for the elbow model for US2-1. These motions were generated from the piping system analysis described above. These input motions are designated as DX, DY, and DZ for displacements and as RX, RY, and RZ for rotations. There are no test results available for comparison of these input motions, and therefore observations regarding the input motions for the elbow model will be qualitative.

As expected, the most significant vibrational input motions are displacement DX and rotation RZ, because the shaking table excitation is only in the X direction for this test. DZ, RX and RY oscillate in an apparently lower frequency than that of DX, DY, and RZ, indicating substantial plasticity development rather than excited vibration. The rotational plastic deformations RX and RY can reach magnitudes comparable to the major oscillating rotational deformation RZ. Figure 4-66 clearly shows that more severe plasticity in Elbow2 was caused in US2-1 than the DM tests.

4.3.3.5 Analysis of the Elbow Model and Result Assessment

Several attempts have been made in this study to obtain a complete execution of the analysis of the elbow model (120 seconds) in ANSYS. However, the analysis could only reach as far as about 77 seconds before ANSYS prematurely terminated with an output operation failure. However, as shown in Figure 4-60, the significant part of the shaking table input motion has

already passed at a time of 77 seconds, therefore the analysis was considered sufficiently long for the strain comparison.

Figure 4-67 through Figure 4-70 show the strain comparison for the analysis of the US2-1 test for elements 145, 154, 315, and 324, respectively. As shown in these figures, the strain gauge in the hoop direction failed prematurely in the test, and therefore comparison in this direction is not feasible. The magnitudes of the axial strains are very small, and consequently the comparison in the axial direction may not be important. The hoop strain reached 2.5% in the test before the strain gauge failed; while the hoop strain reaches about 3.5% for the two elements (154 and 324) which are closer to the strain gauge location. The hoop strain reaches about 8.5% for the other two elements (145 and 315). The analytical strain time histories appear to level off at or before 77 seconds. The gradient of the hoop strain at this location is similar to that of the DM tests, in the sense that the calculated hoop strain is higher as an element is located farther away from the strain gauge location.

The maximum strain ranges for US2-1 are shown in Table 4-1. Since the hoop strain gauge was failed prematurely in US2-1, the maximum strain ranges from JNES are from US2-2 to US2-5. Using the rainflow method with regular ranges, the ANSYS results are close to or slightly larger than that for US2-1 (using incomplete strain time history), but are smaller than the JNES values for the tests US2-2 to US2-5. However, the ANSYS results are considered in an acceptable range to those from the tests, especially considering that different rainflow counting algorithms may yield very different results.

4.4 Summary of FE Nonlinear Analysis for Large Scale Pipe Tests

Continuing the work by DeGrassi and Hofmayer [2005], BNL performed additional analytical effort on the correlation study of the large-scale pipe tests conducted by JNES/NUPEC. This study included improvements on material models, input motion characterization, and many complex nonlinear transient analyses for the large-scale pipe tests.

Recognizing that the bilinear kinematic hardening material model cannot describe accurately the monotonic tensile test curve, a multi-linear model was developed for the strain range of interest. This model is based on the true stress-strain curve that was converted from the engineering stress-strain curve provided by JNES/NUPEC. The material test used the pipe material STS410 steel. This (mono) multi-linear model was then slightly corrected using a Young's modulus from the cyclic test to create a hybrid multi-linear model to be used for low excitation tests. Based on the true stress-strain curve from the strain-controlled cyclic test performed by JNES/NUPEC, the Chaboche nonlinear kinematic material model was also updated using a least-square minimization technique so that the forward loading curve using the new Chaboche model is nearly identical to the test curve.

Two FE models have been created for both the design method confirmation tests and the ultimate strength tests. One is a piping system model which used plastic pipe elements and the multi-linear material model to obtain the displacement and acceleration responses for the entire piping system, and the other is an elbow model which used finite strain shell elements and the Chaboche nonlinear material model to obtain the strain responses. The displacement responses at two nodes around the elbow were generated from the piping system model and were used as the input displacement boundary condition for the elbow model. The analyses have shown that the piping system model can accurately predict the responses for low to moderate input motions and less accurately for high input motions. For the design method confirmation tests, considering the plasticity accumulation in the piping system model affects the performance of the piping system model only during the beginning part of the input motions but does not change the overall

response for the entire time histories, partly because of the increasing level of shaking table excitation. The displacement and acceleration responses appear to be restrained for large input motions, implying the multi-linear material model resulted in shakedown type behavior. The elbow model can predict relatively accurate strain ratcheting history if the comparison is based on a small region around the strain gauge location rather than the exact location. However, the level of accuracy for the strain comparison was found not as high as that for the piping system responses. The comparison of the maximum strain ranges appear to be more consistent among the four selected elements and generally better than comparisons using the entire strain ratcheting histories.

Although improvements in the analytical predictions with the updated material and FE models were observed, large variations in the test comparisons, particularly for strain and strain ratcheting were still noted. The nonlinear dynamic characteristics of the large-scale piping system are difficult to predict with high accuracy even when state-of-the-art models and FE codes are used. In regulatory activities related to piping systems in nuclear power plants, reviewers should be aware of such difficulties and uncertainties in any piping system seismic analysis submittals involving elasto-plastic analysis. Furthermore, continued investigation of the subject may lead to a better understanding of the analytical methods and even quantification of the uncertainties in these methods and the supporting test data.

For potential further studies of these test results, some additional modeling and analysis improvements can be explored. These improvements may include: (1) refinement of the piping system model with smaller element sizes, (2) refinement of the elbow model locally at the strain range location, (3) characterization of the strain gradient along the hoop direction, (4) a transient analysis of the elbow model to take into account the inertia and damping effect, (5) a combined model with pipe elements for straight pipe segments and shell elements for the elbows and nozzles, (6) investigation of methods to better consider the plasticity accumulation over a series of consecutive tests, and (7) examination of the fatigue ratcheting failure mechanism. Items 4 through 7 require the use of high performance computers.

Table 4-1 Maximum Hoop Strain Ranges for Tests DM4-1, DM4-2(1), DM4-2(2), and US2-1

Tests	Strain History	Rainflow Method Regular Ranges	Rainflow Method All Ranges	Simplified Rainflow Method	JNES [2003]
DM4-1	Test Data	0.866	0.866	0.866	0.74
	Ele. 145	0.588	1.625	0.588	
	Ele. 154	0.520	0.711	0.520	
	Ele. 639	0.569	1.521	0.569	
	Ele. 648	0.507	0.665	0.507	
DM4-2(1)	Test Data	0.787	0.787	0.787	0.84
	Ele. 145	0.721	3.500	3.500	
	Ele. 154	0.568	1.235	1.235	
	Ele. 639	0.694	3.291	3.291	
	Ele. 648	0.562	1.130	0.562	
DM4-2(2)	Test Data	0.920	0.920	0.944	1.03
	Ele. 145	0.829	0.829	0.829	
	Ele. 154	0.707	0.707	0.707	
	Ele. 639	0.802	0.802	0.802	
	Ele. 648	0.713	0.713	0.713	
US2-1	Test Data	0.895	2.508	0.895	1.85-3.31*
	Ele. 145	1.157	8.710	8.710	
	Ele. 154	0.891	2.142	0.891	
	Ele. 315	1.105	8.391	8.391	
	Ele. 324	0.903	3.663	3.663	

* Value range is from RUN 2 to RUN 5 for reference; the strain gauges prematurely failed in RUN 1 of the US2 test.

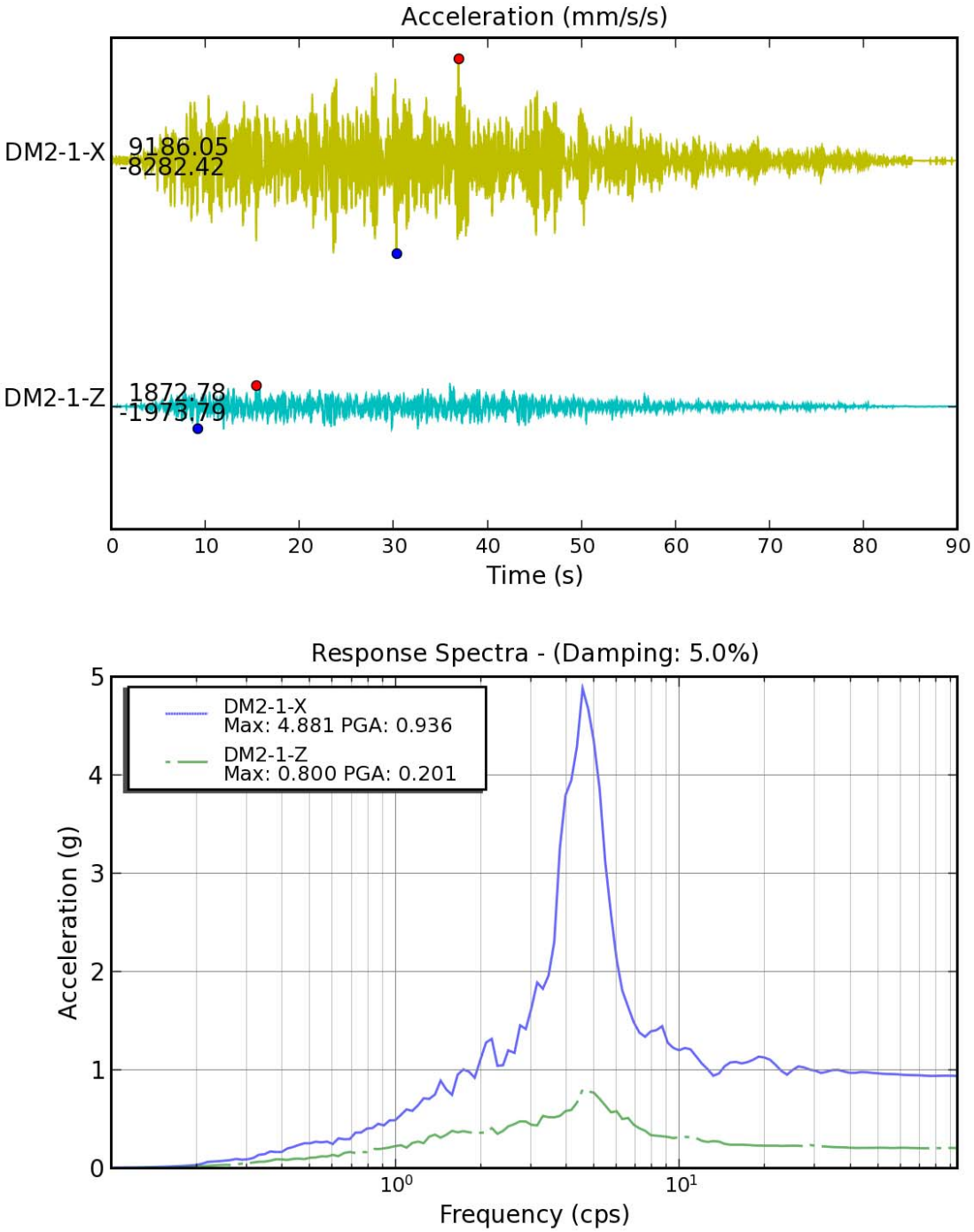

Figure 4-1 Horizontal and Vertical Input Motions and Their 5% Response Spectra For DM2-1

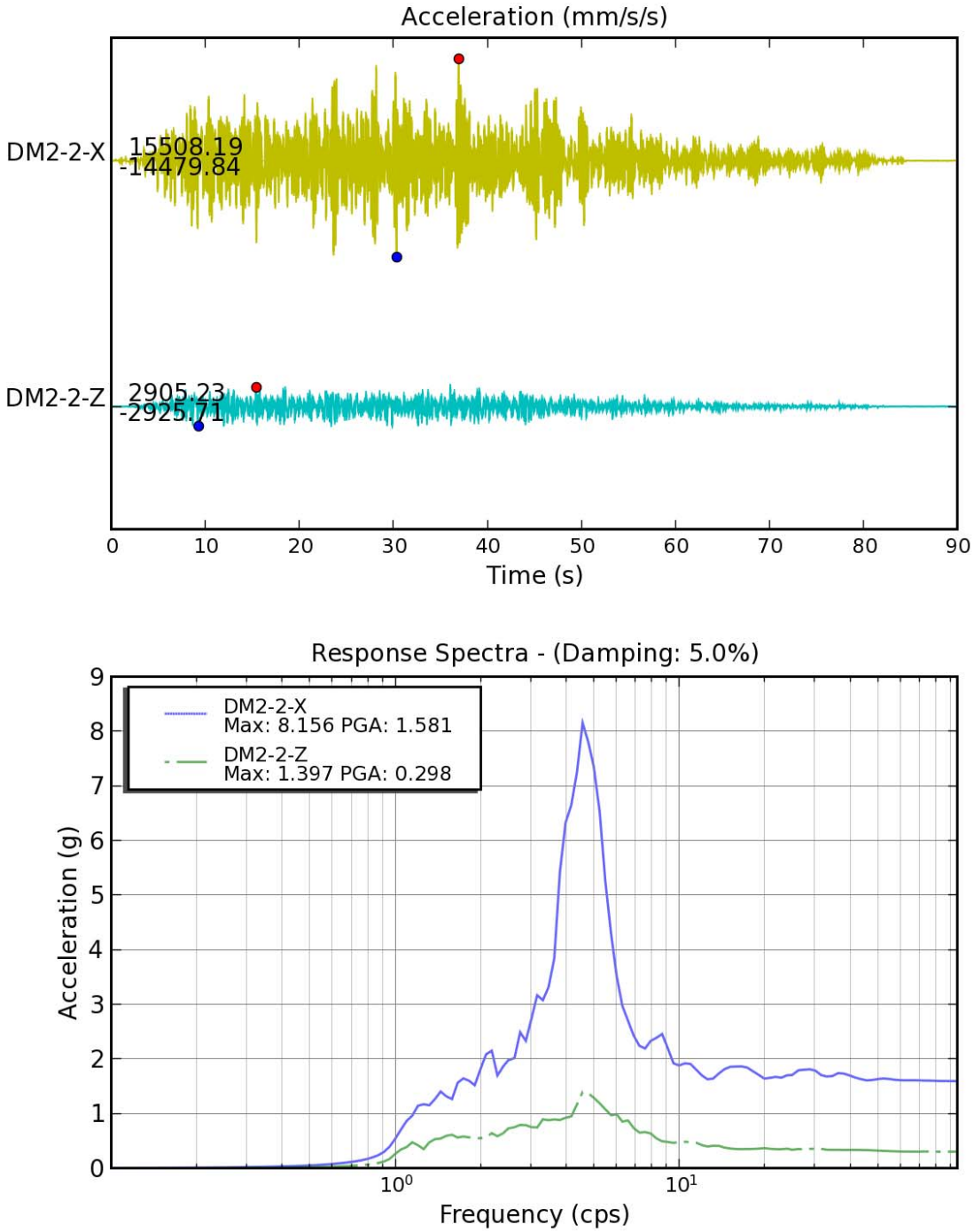

Figure 4-2 Horizontal and Vertical Input Motions and Their 5% Response Spectra For DM2-2

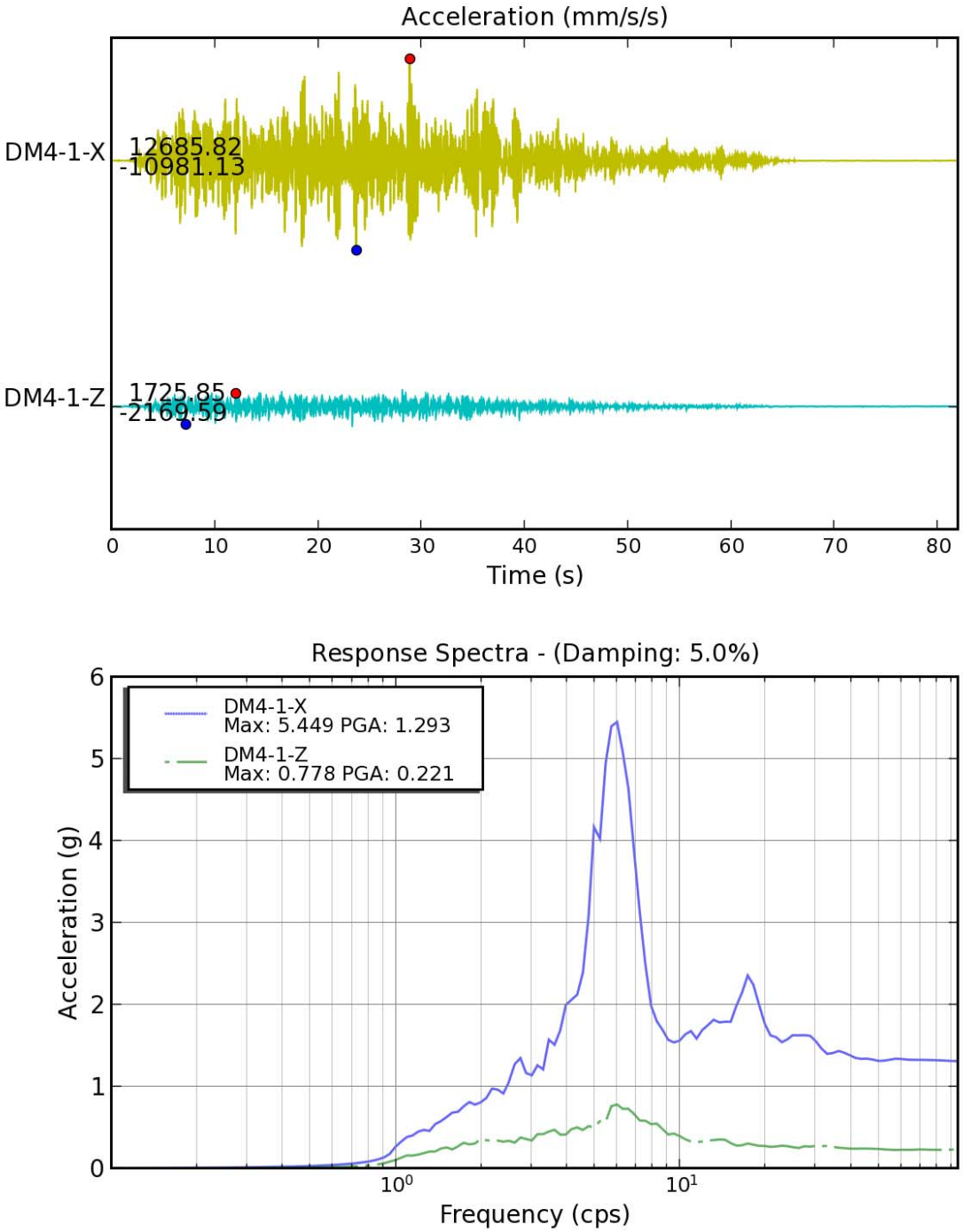

Figure 4-3 Horizontal and Vertical Input Motions and Their 5% Response Spectra For DM4-1

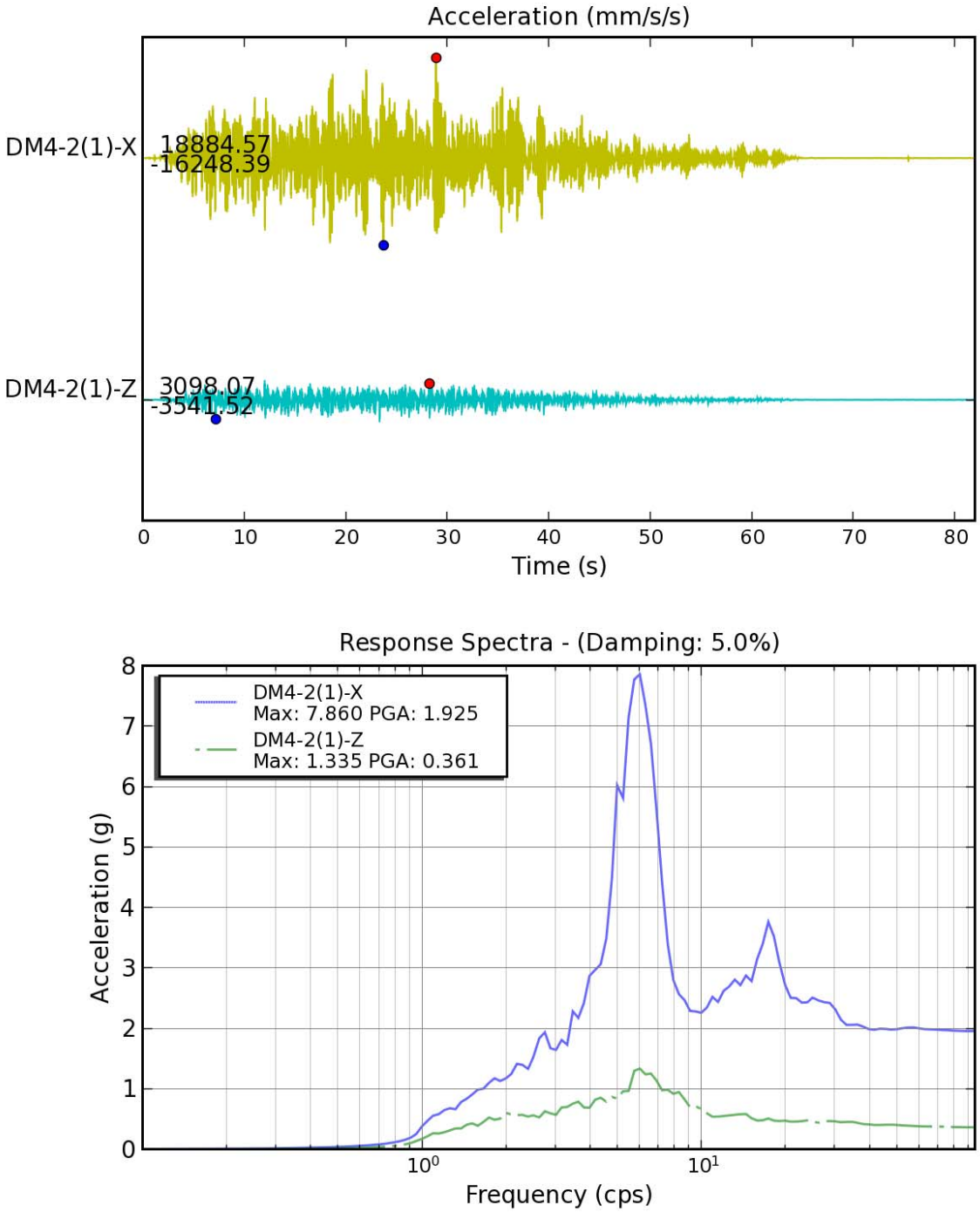

Figure 4-4 Horizontal and Vertical Input Motions and Their 5% Response Spectra For DM4-2(1)

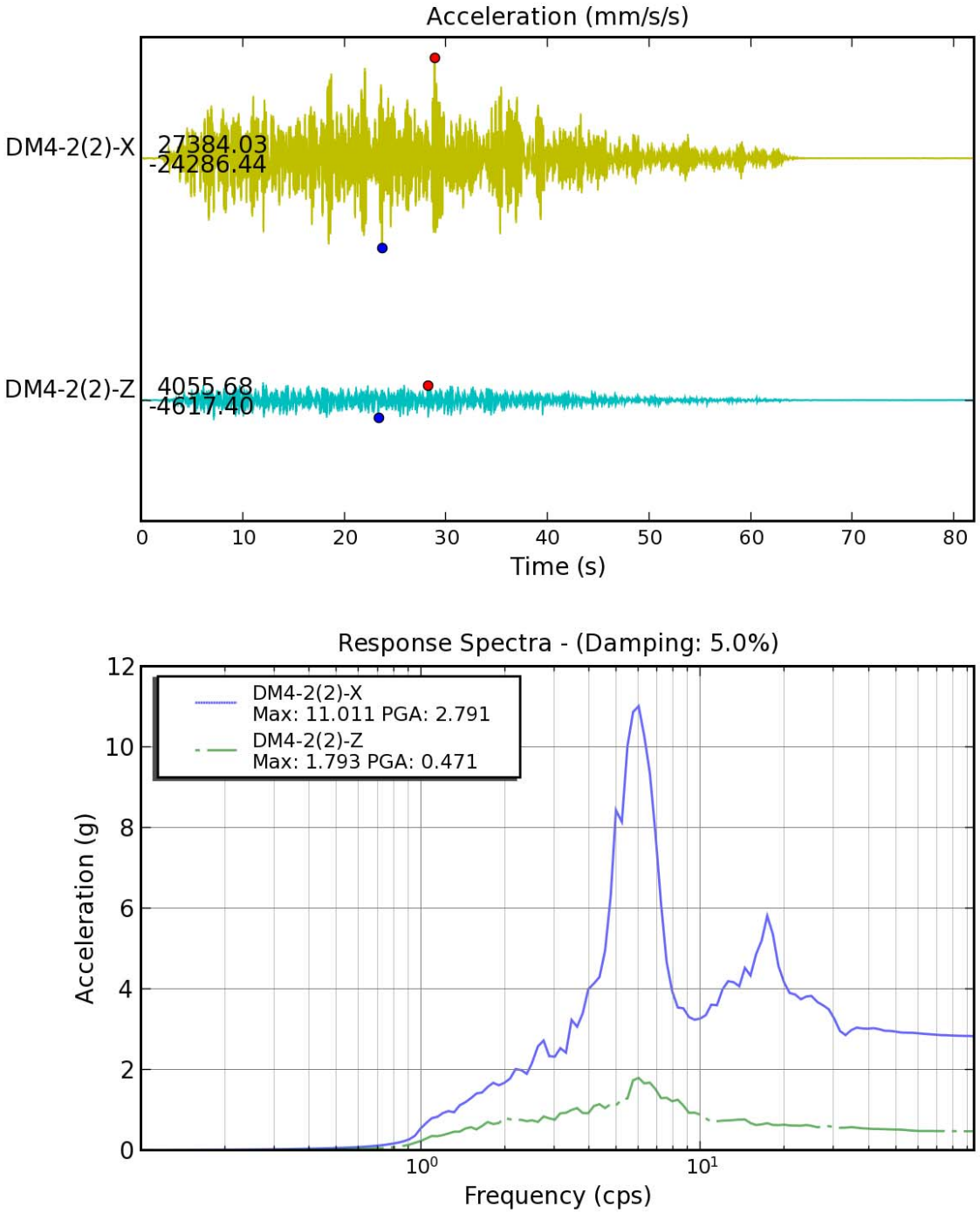

Figure 4-5 Horizontal and Vertical Input Motions and Their 5% Response Spectra For DM4-2(2)

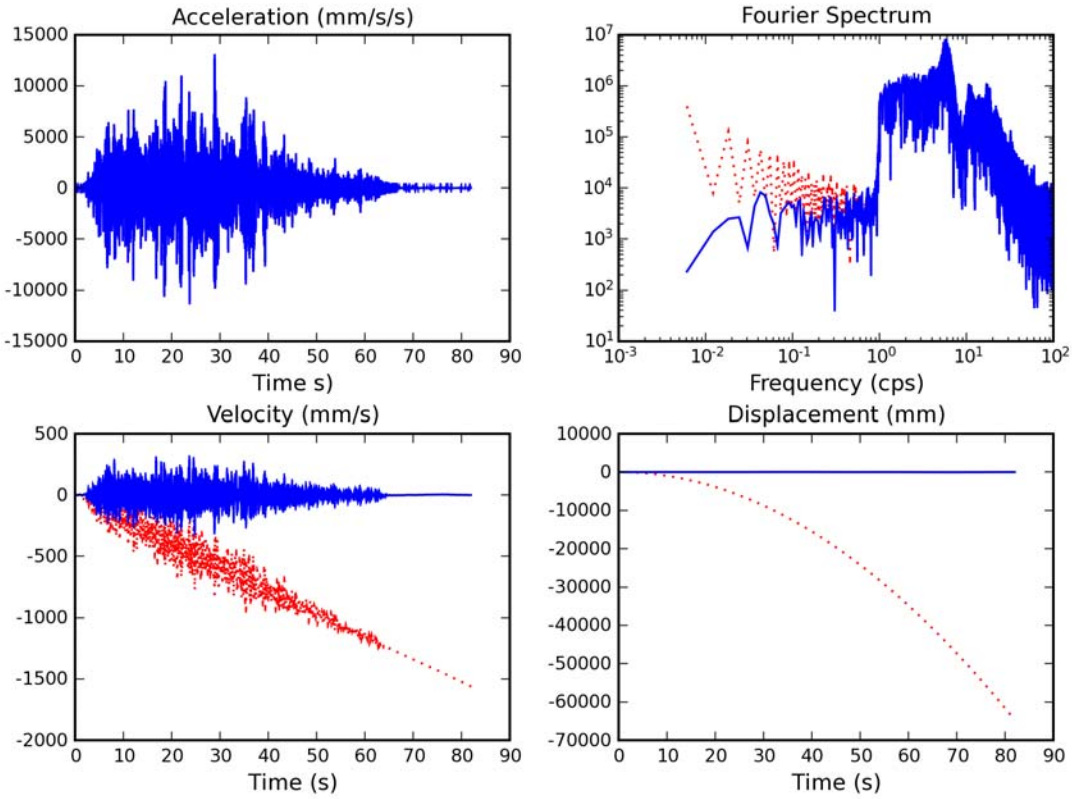

Figure 4-6 Baseline Correction of the Horizontal Input Motion for DM4-1

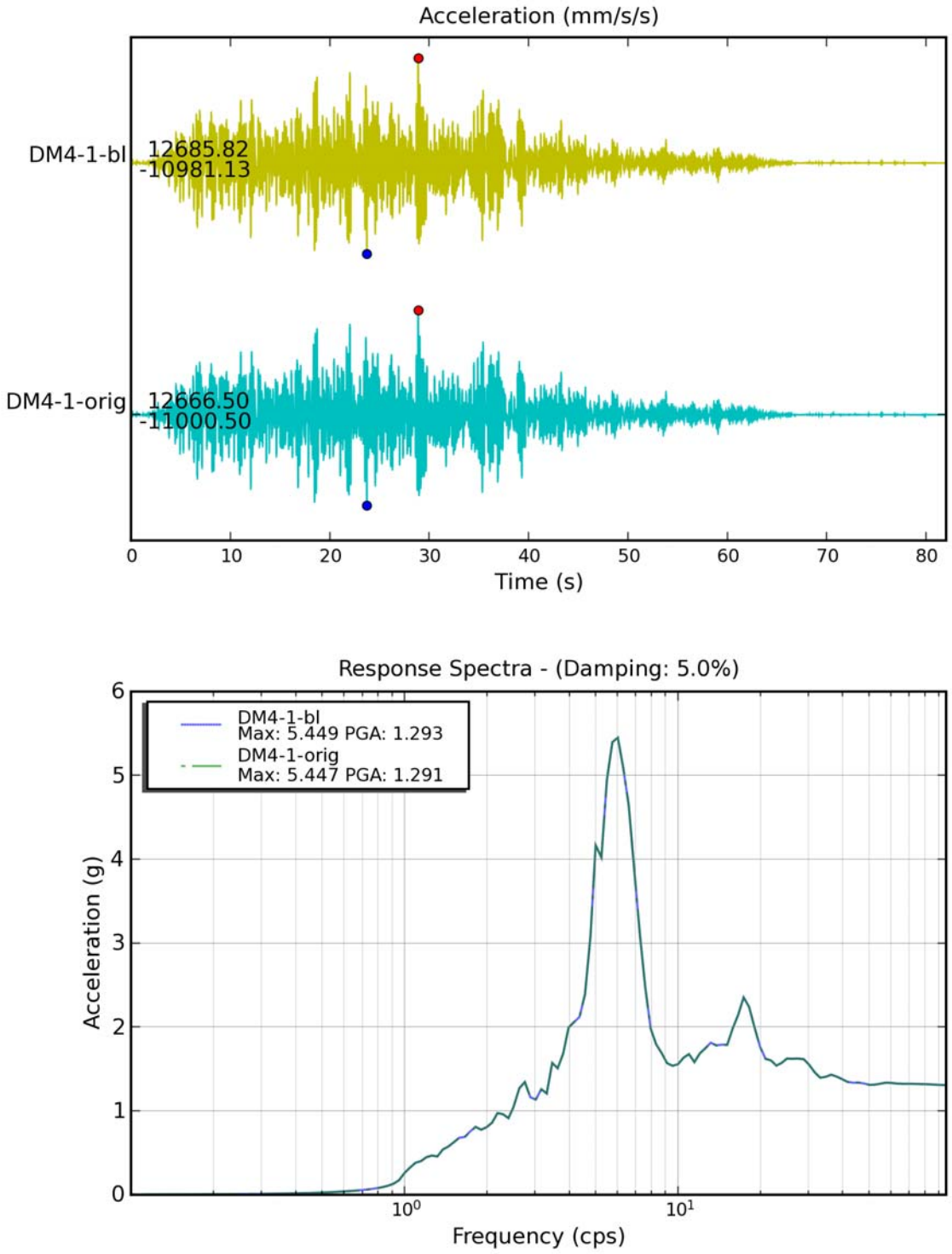

Figure 4-7 Comparison of Baseline-corrected and Original Horizontal Input Motions for DM4-1

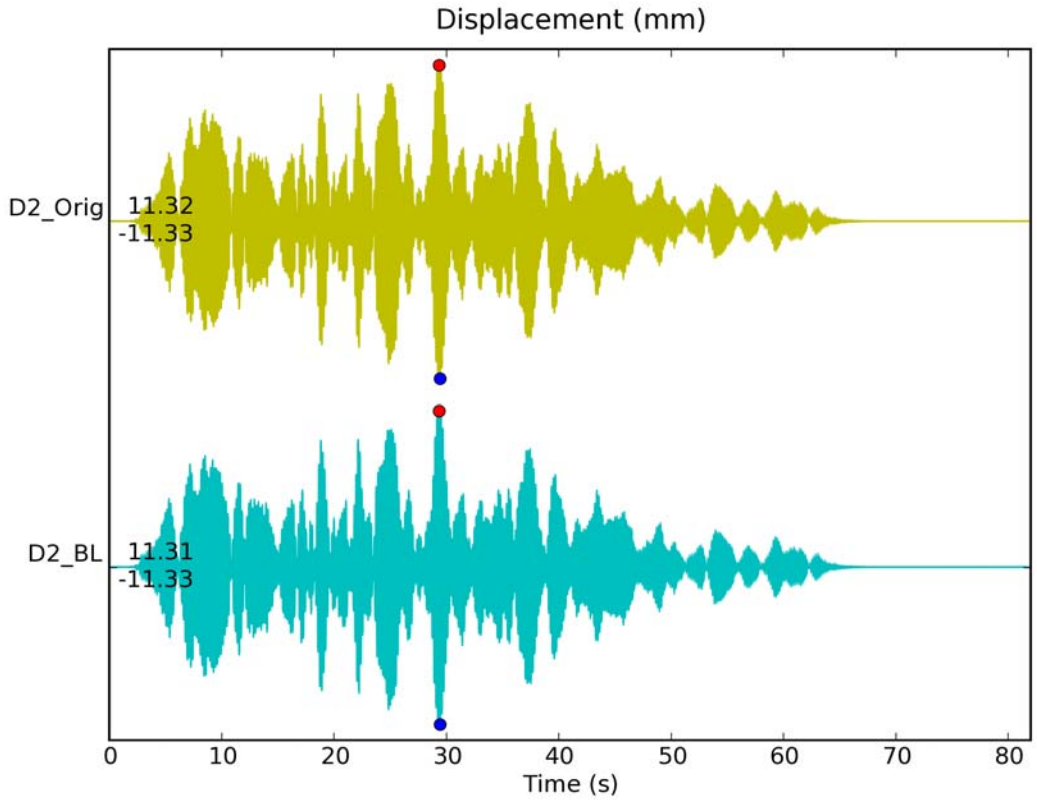

Figure 4-8 Illustrative Response Comparison for Baseline-corrected and Original Input Motions for DM4-1

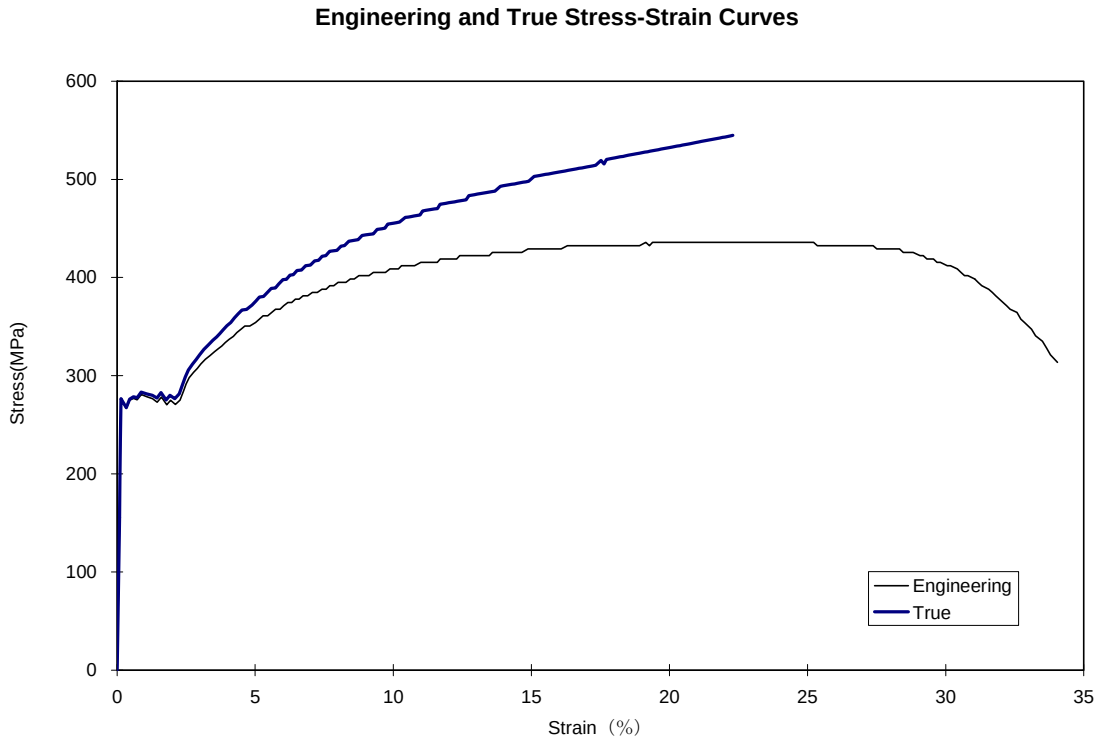

Figure 4-9 Engineering and True Stress-Strain Relation for the Monotonic Tensile Test

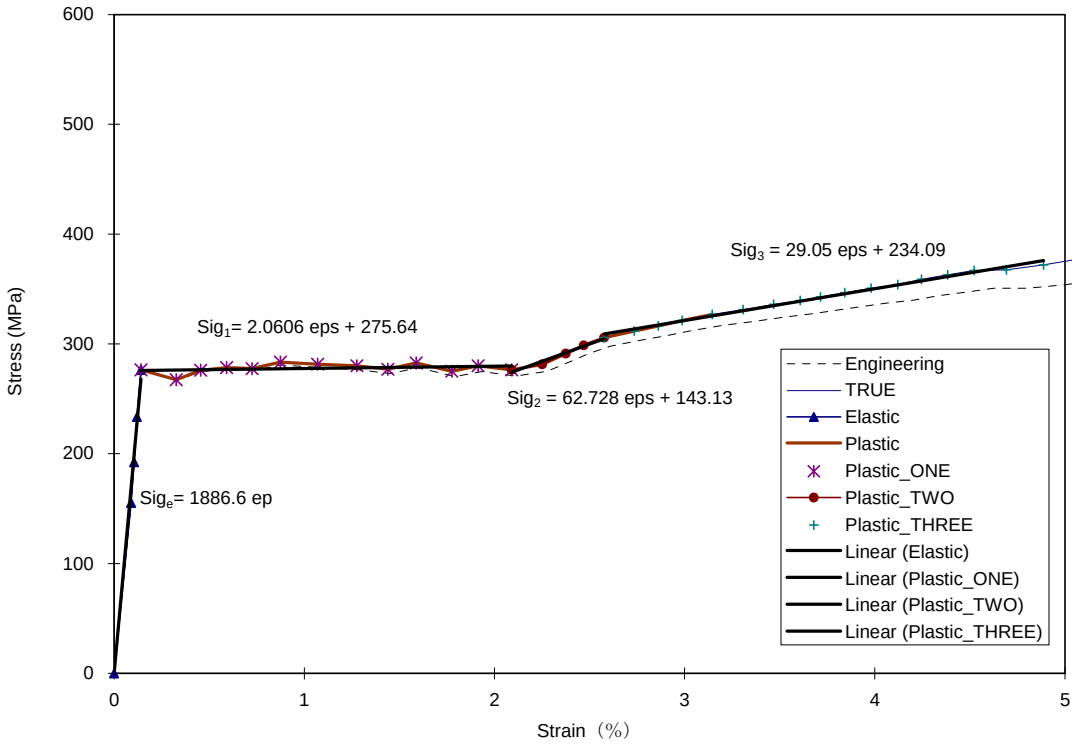

Figure 4-10 Multi-linear Material Model by Fitting the Monotonic Tensile Test

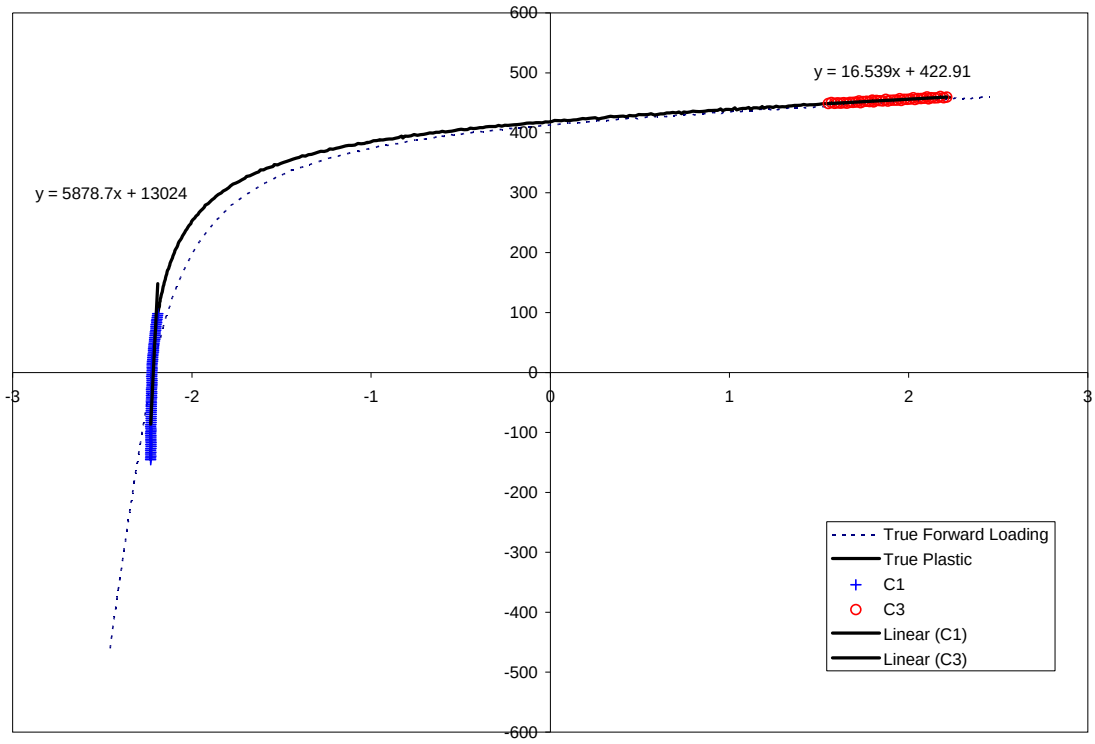

Figure 4-11 Forward Loading Curve Processing and Development of Initial C_1 and C_3

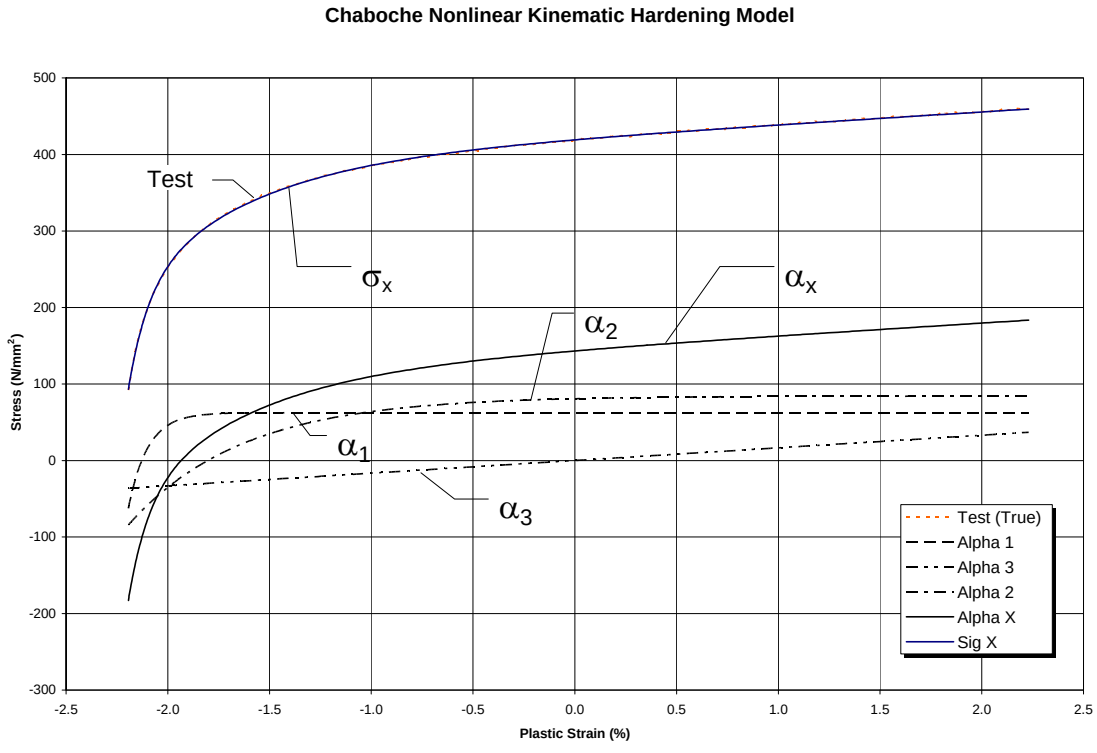

Figure 4-12 Chaboche Nonlinear Kinematic Hardening Model (except for γ_3)

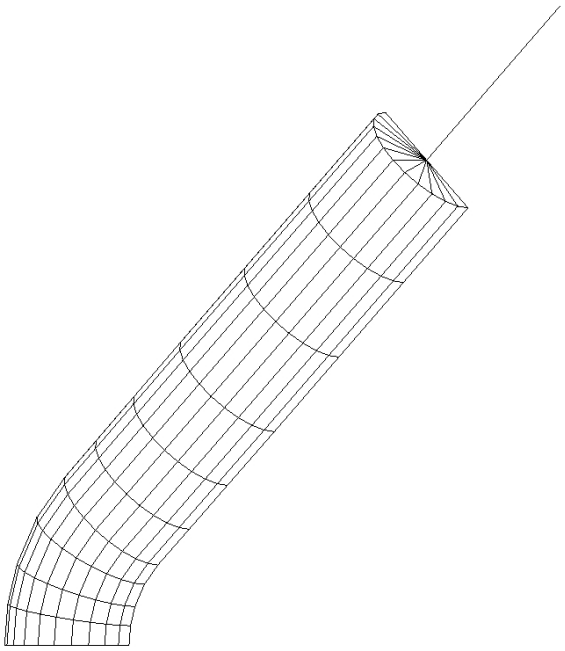

Figure 4-13 SE-4 Test ANSYS Shell Element Model [DeGrassi and Hofmayer 2005]

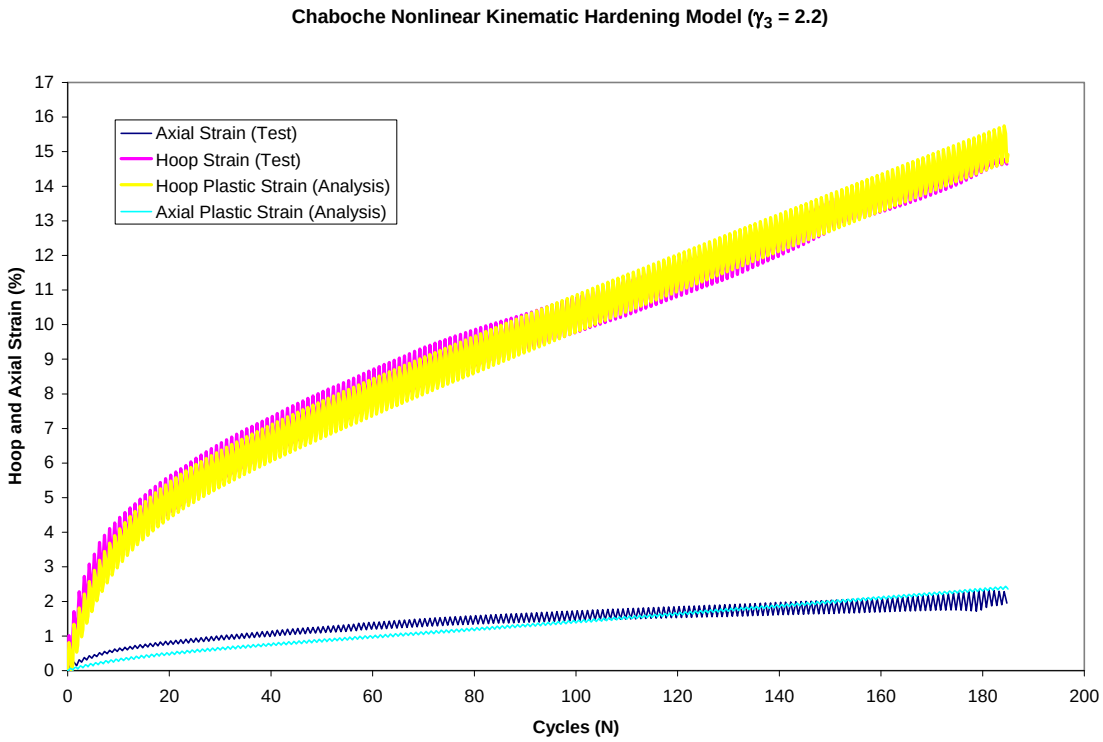

Figure 4-14 Chaboche Nonlinear Kinematic Hardening Model (for γ_3)

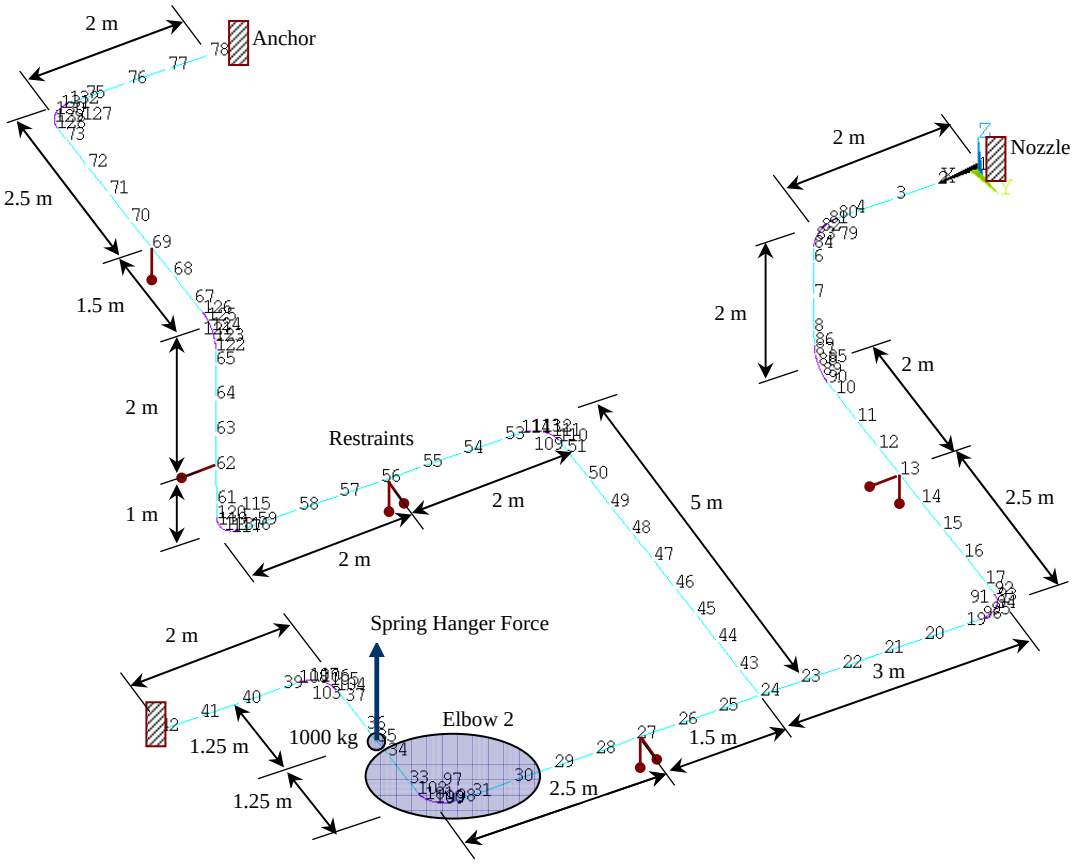

Figure 4-15 Piping System FE Model using Pipe Elements for Design Method Confirmation Test

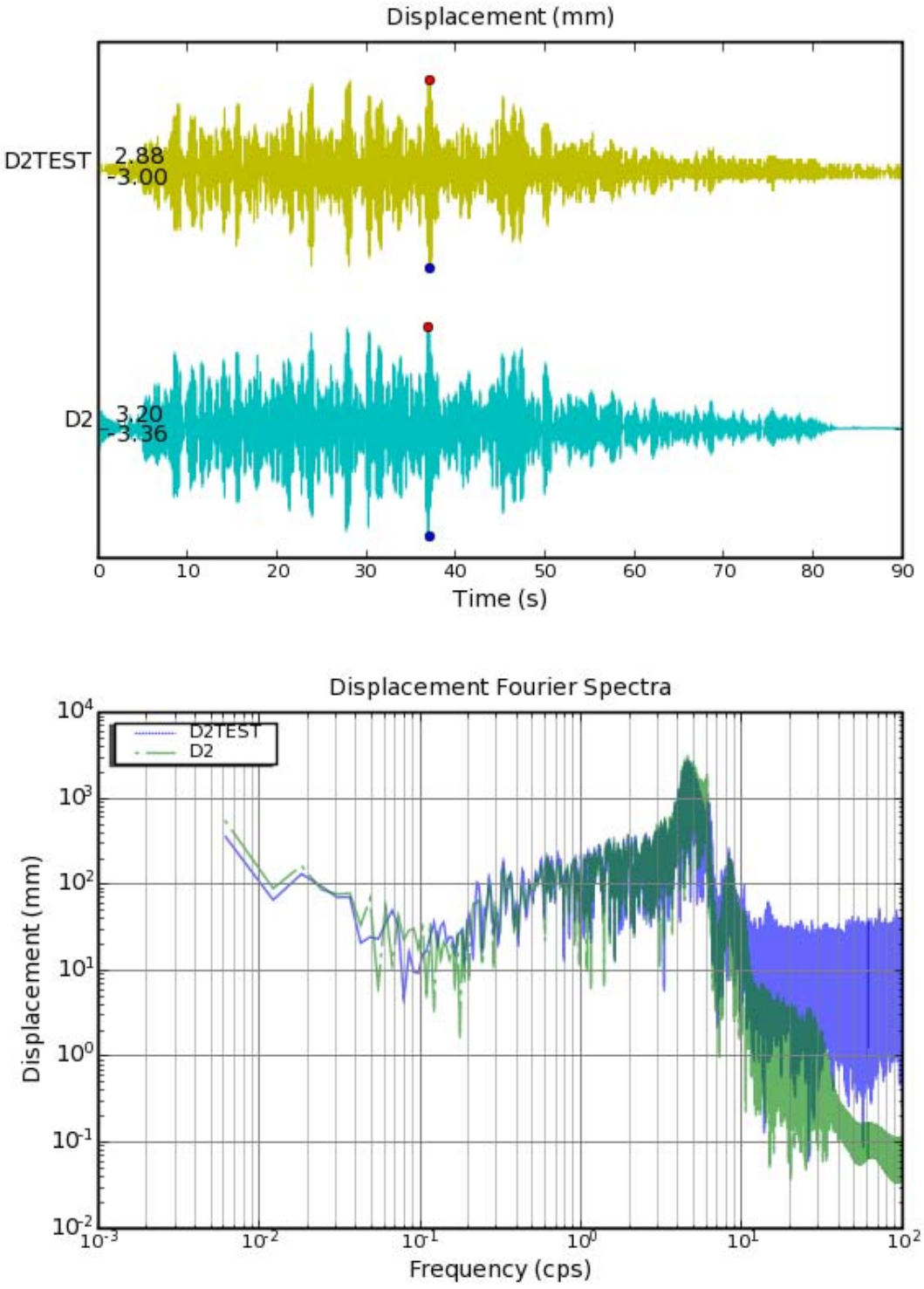

Figure 4-16 Displacement D2 Comparison for DM2-1

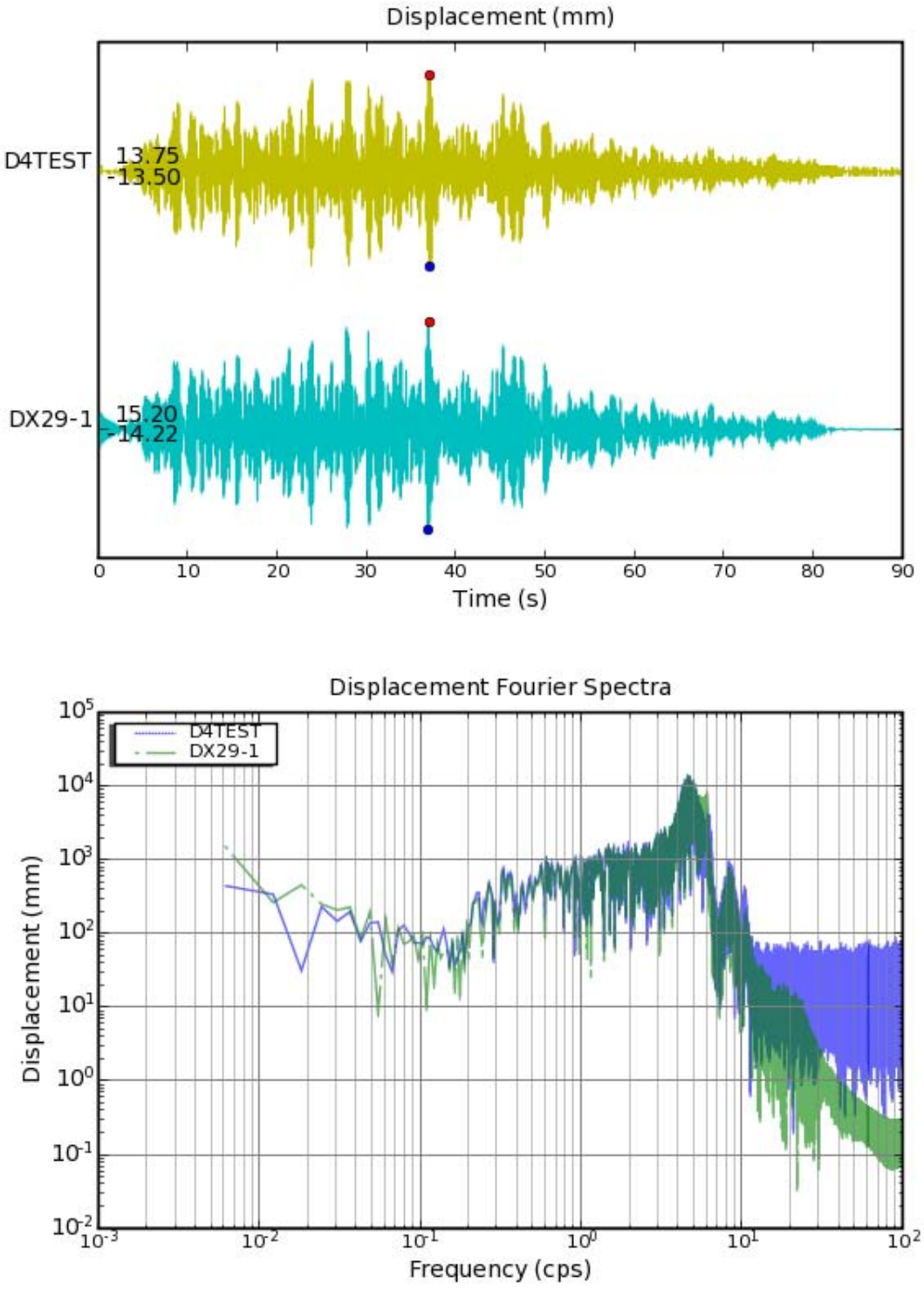

Figure 4-17 Displacement D4 Comparison for DM2-1

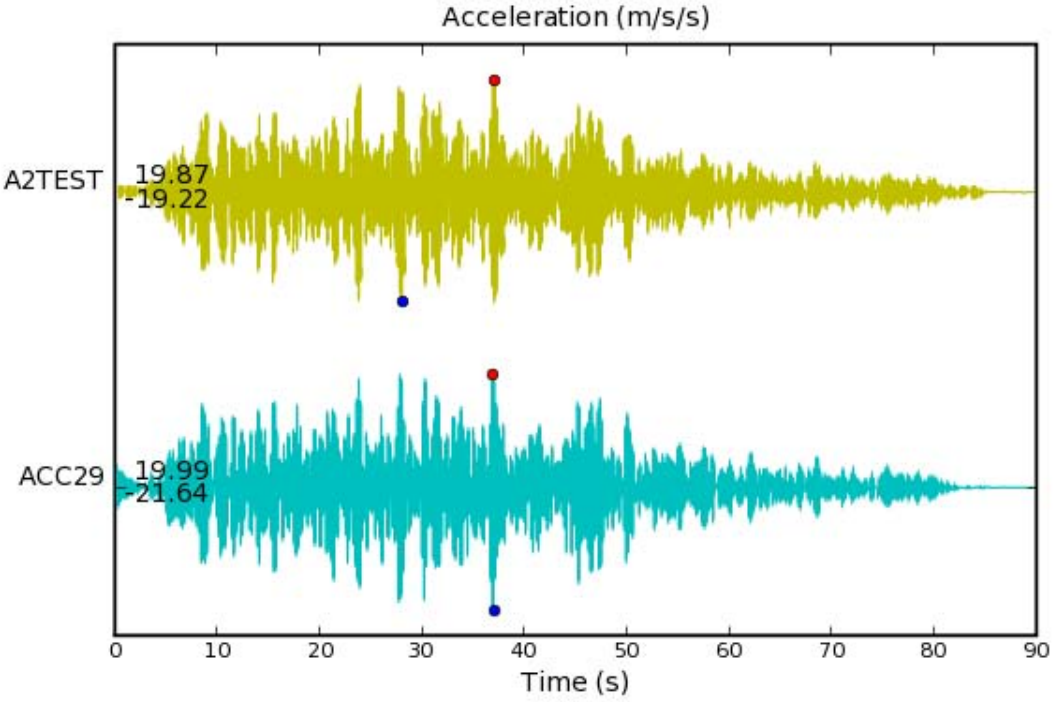

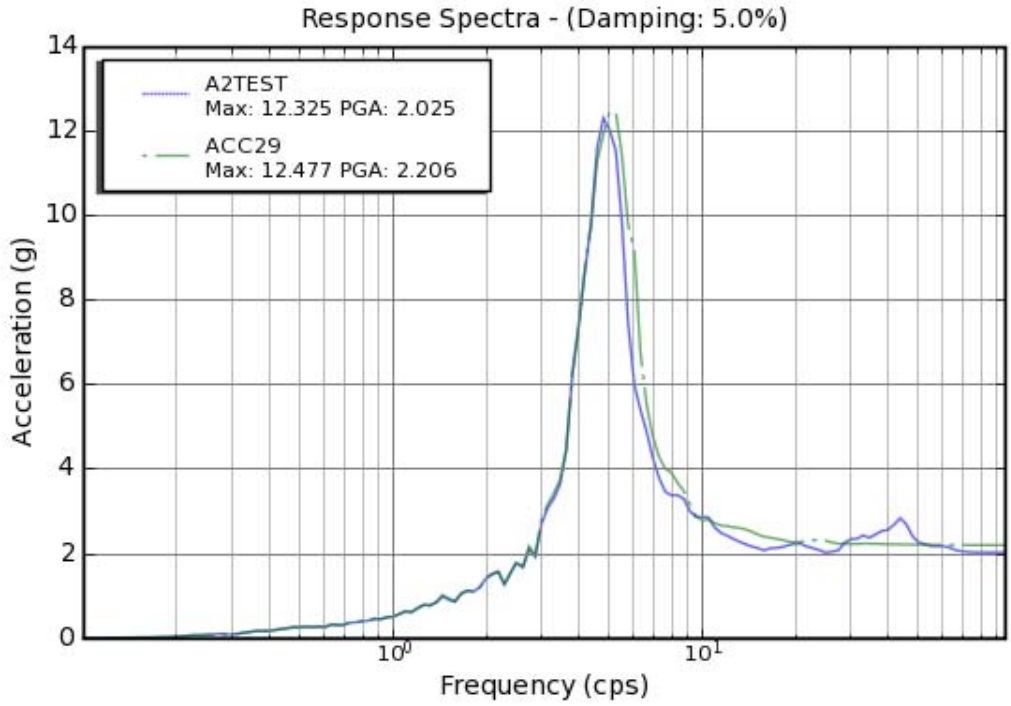

Figure 4-18 Acceleration A2 Comparison for DM2-1

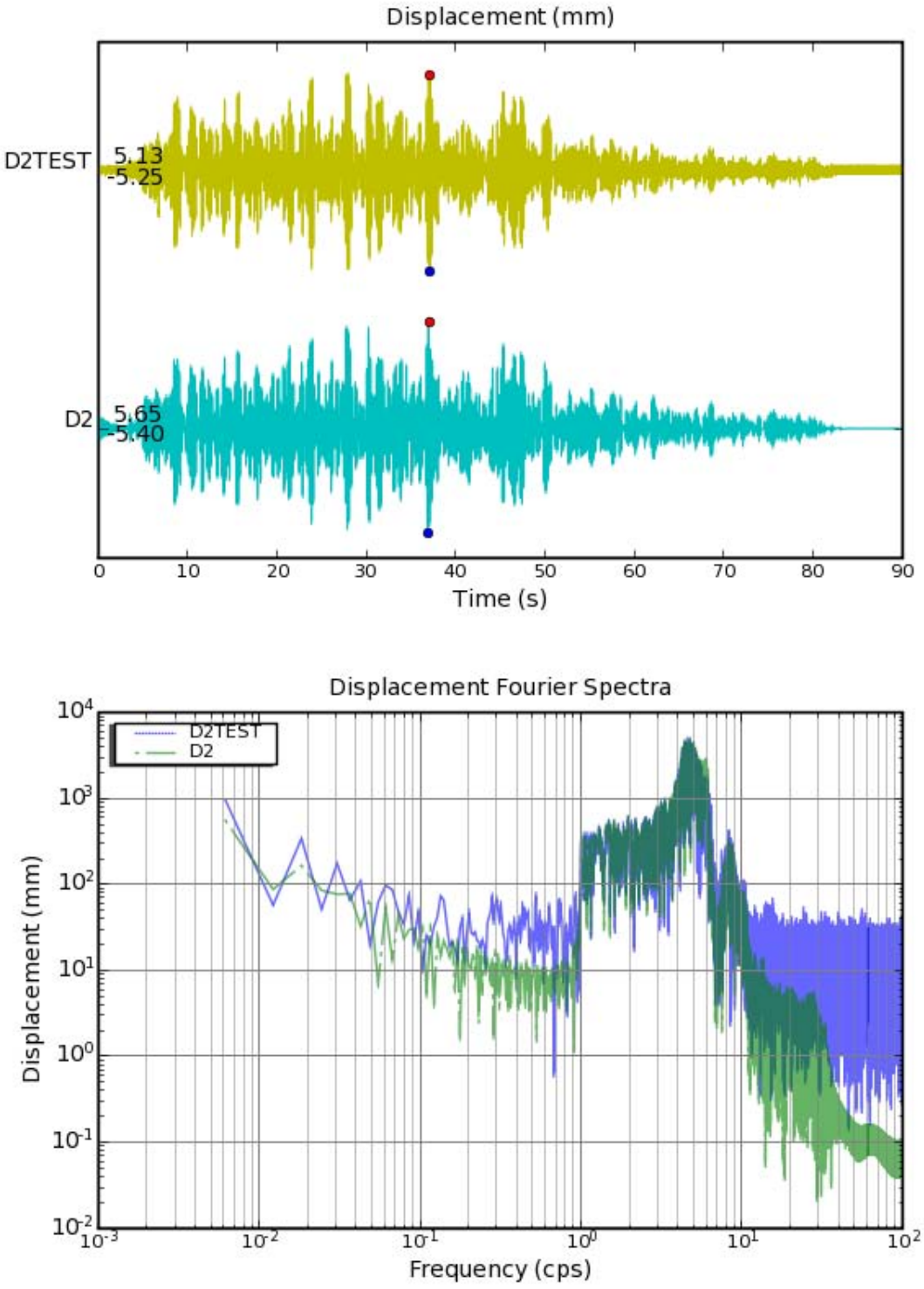

Figure 4-19 Displacement D2 Comparison for DM2-2

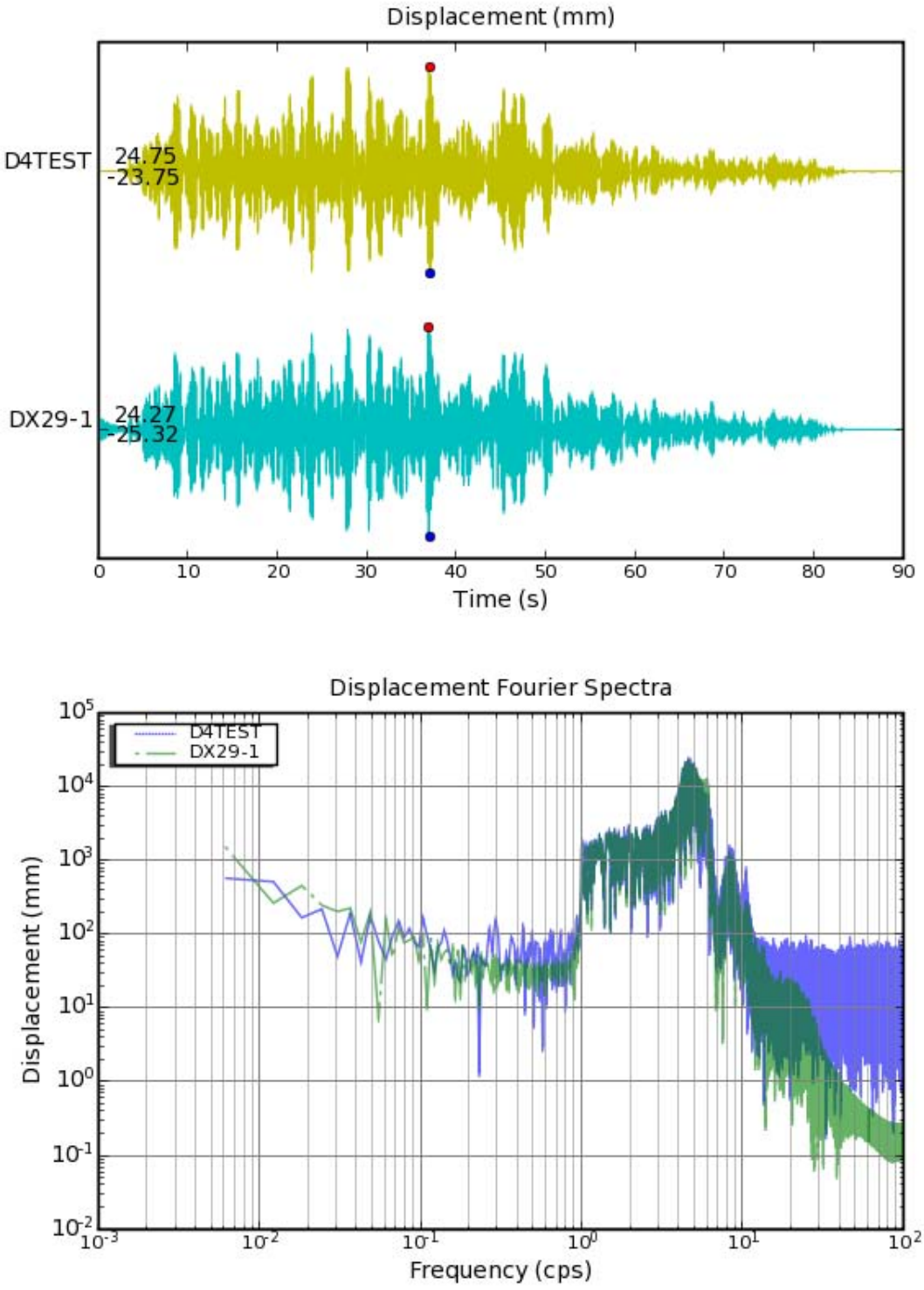

Figure 4-20 Displacement D4 Comparison for DM2-2

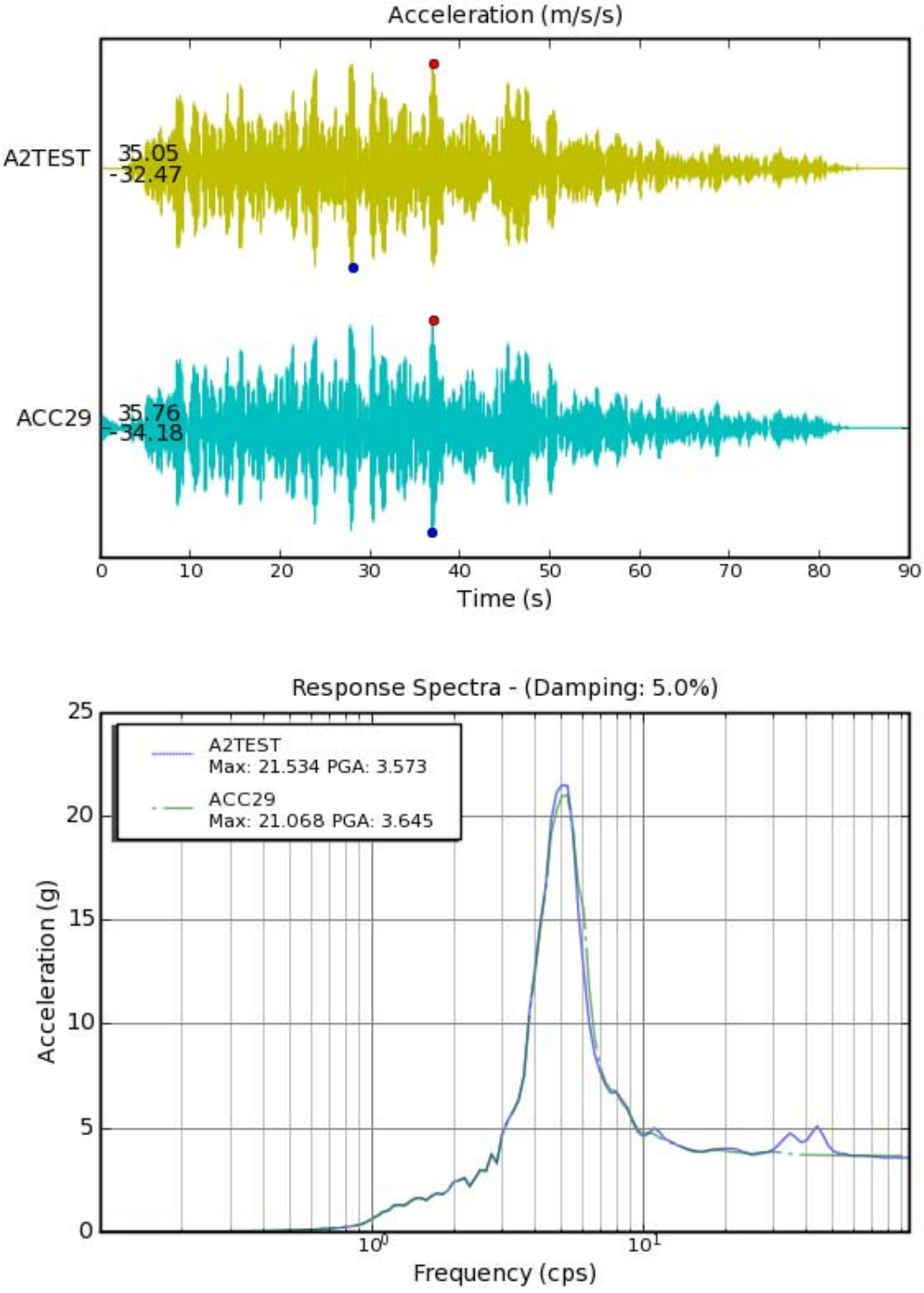

Figure 4-21 Acceleration A2 Comparison for DM2-2

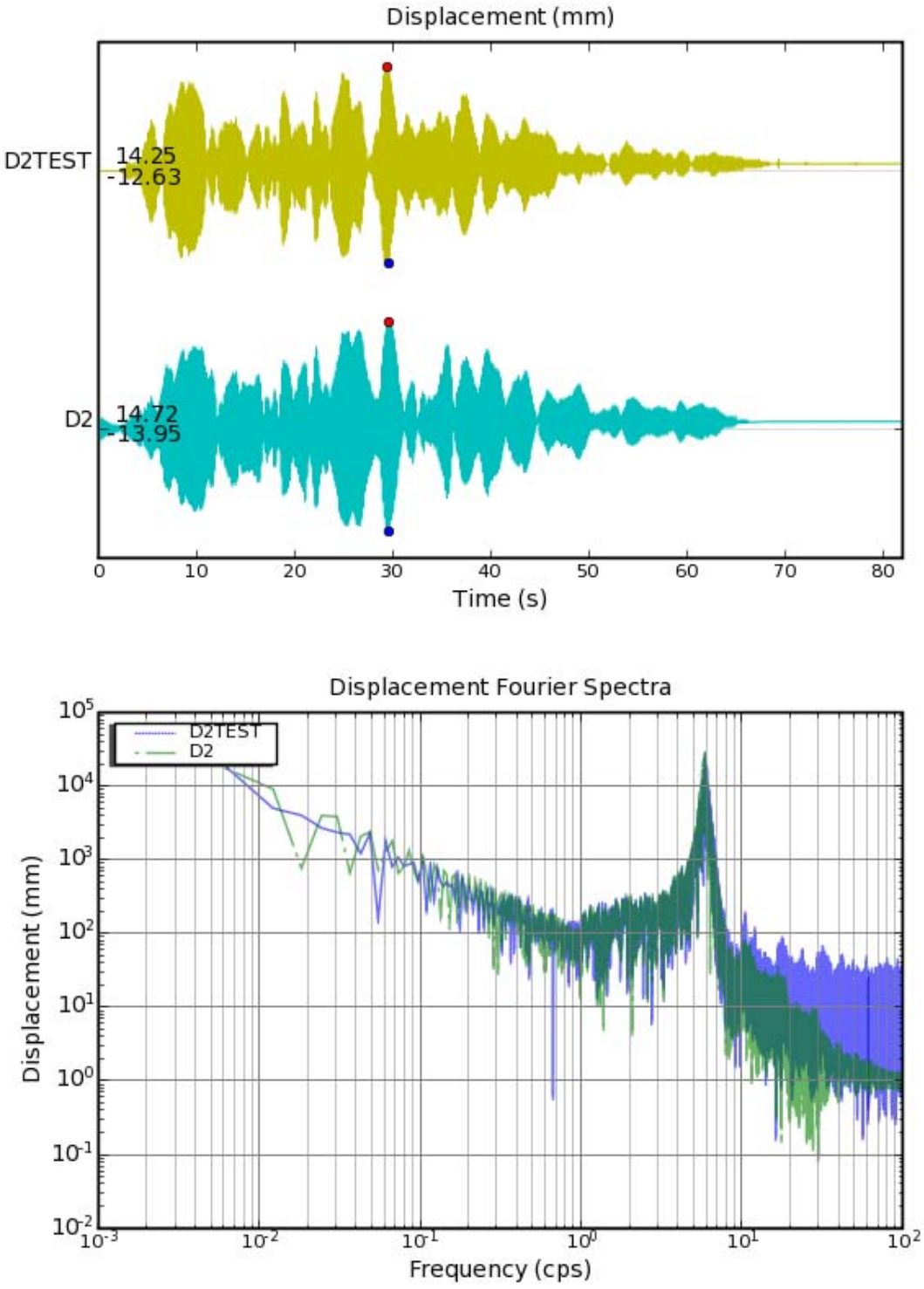

Figure 4-22 Displacement D2 Comparison for DM4-1

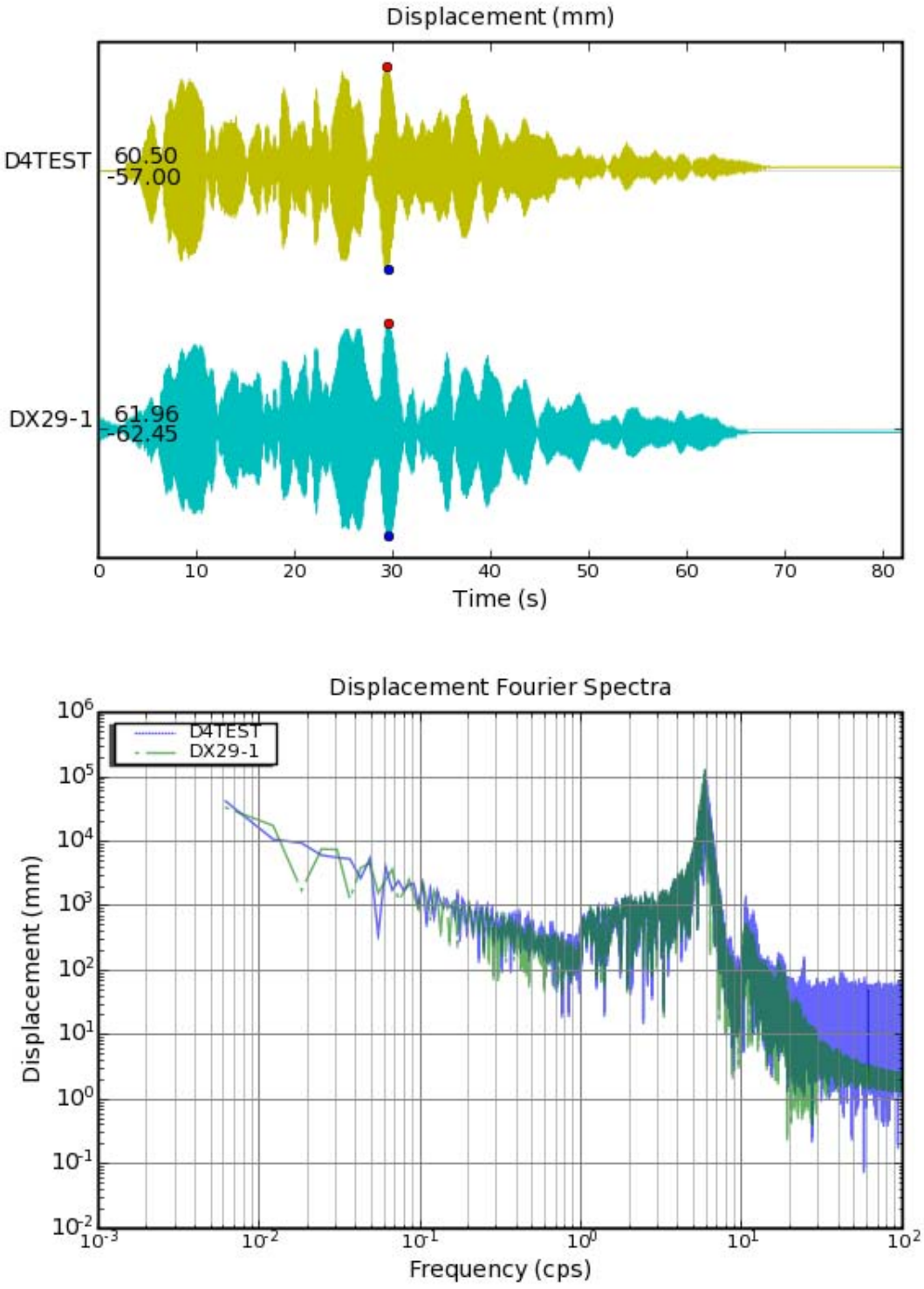

Figure 4-23 Displacement D4 Comparison for DM4-1

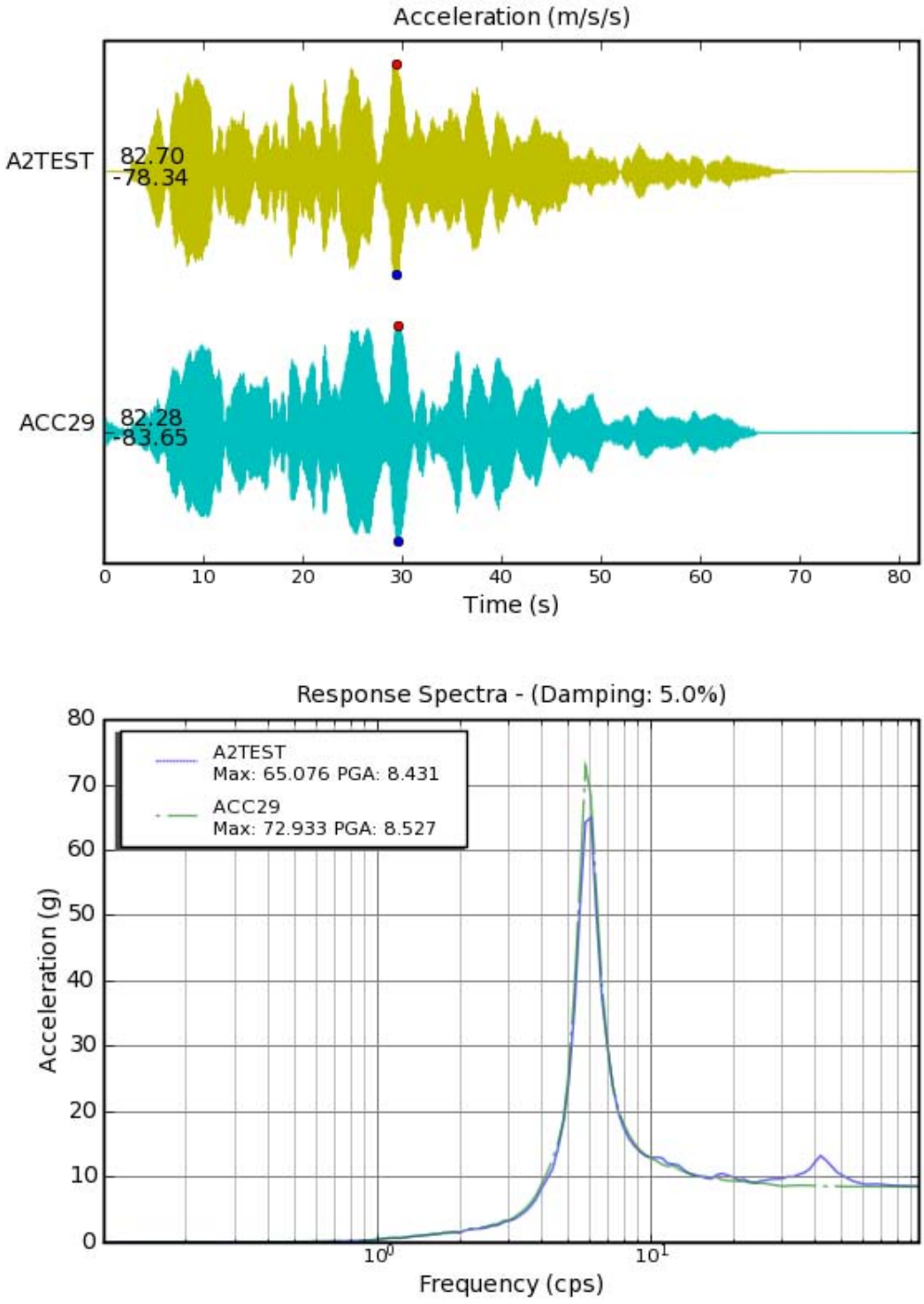

Figure 4-24 Acceleration A2 Comparison for DM4-1

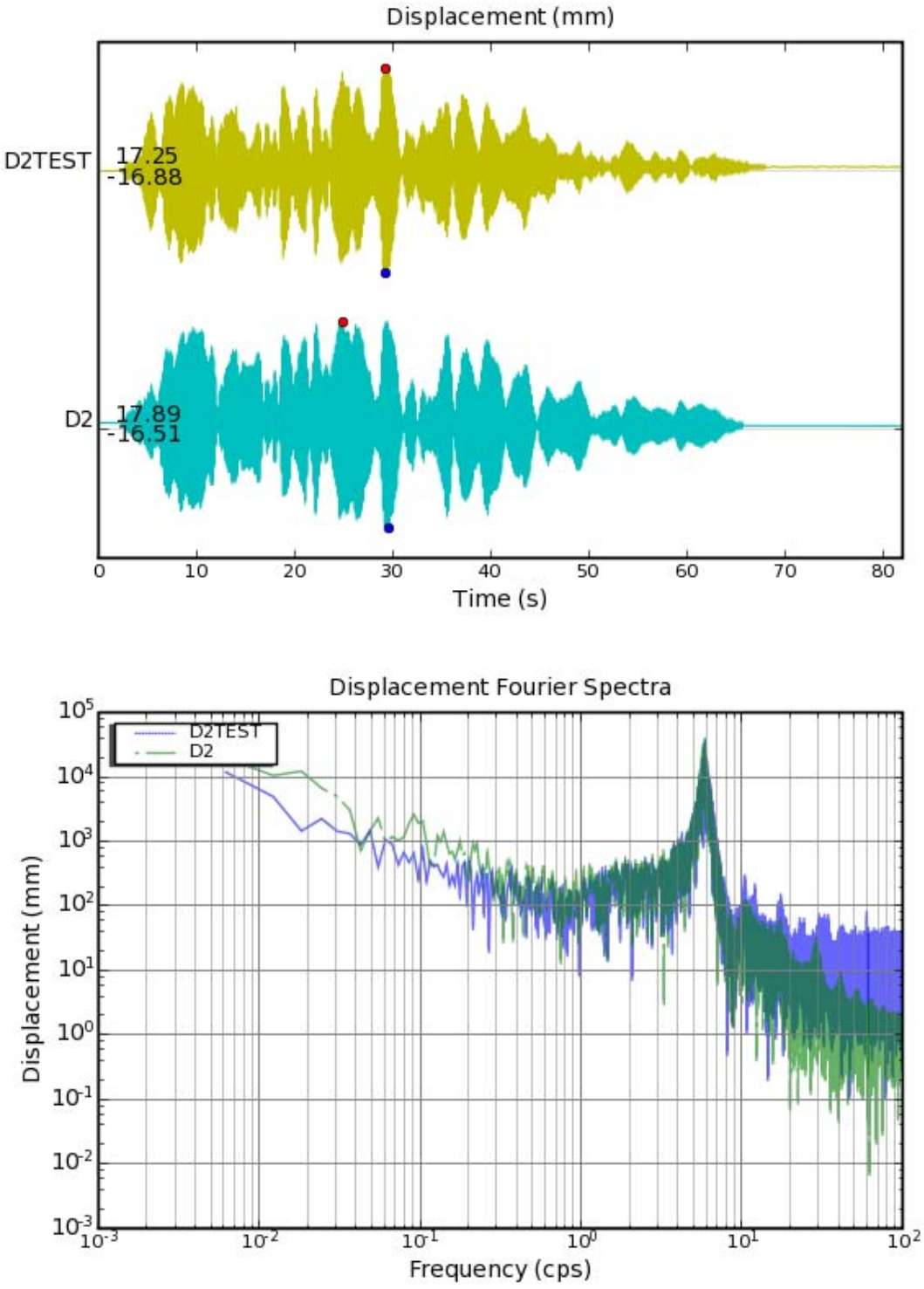

Figure 4-25 Displacement D2 Comparison for DM4-2(1) (Restart)

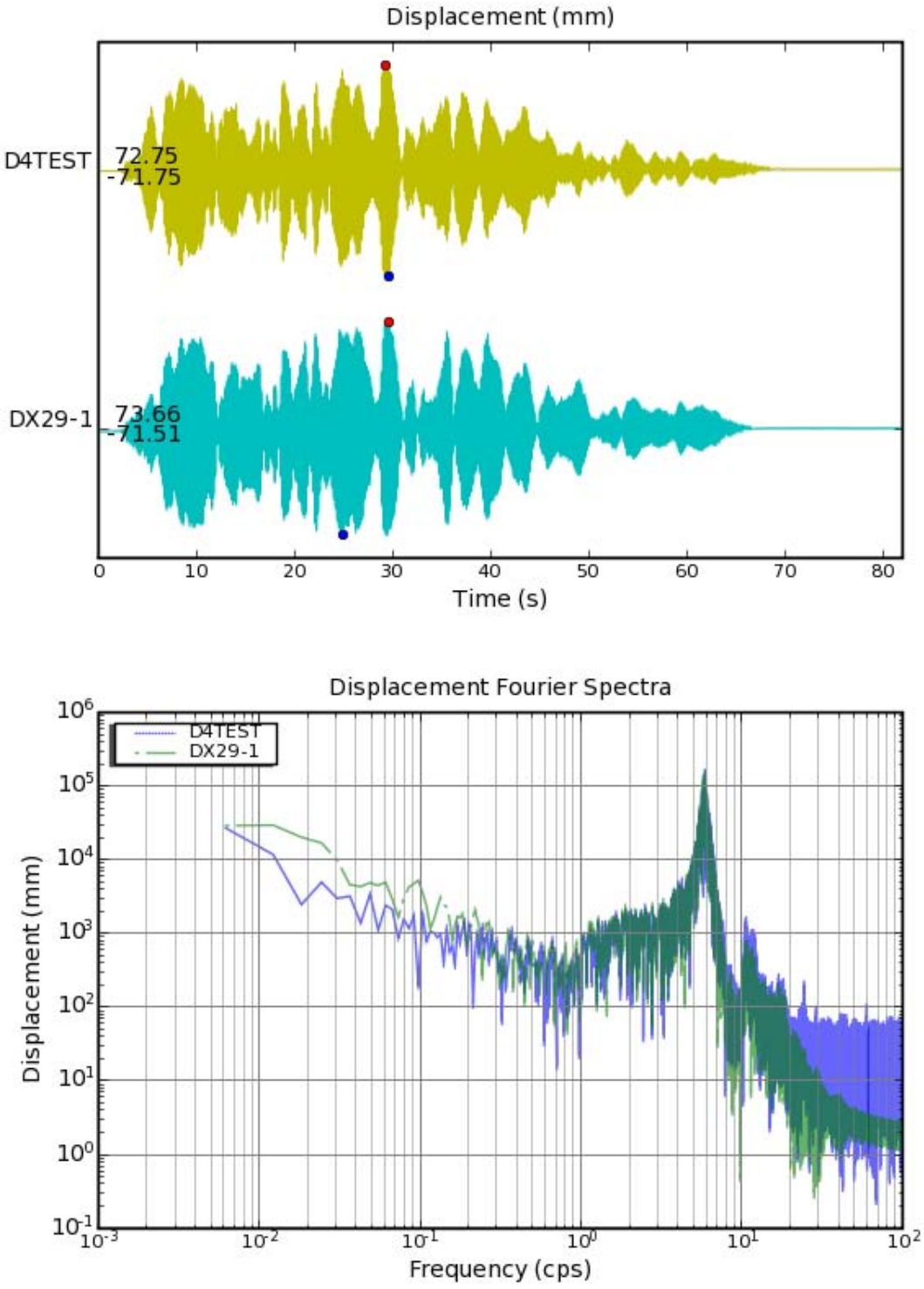

Figure 4-26 Displacement D4 Comparison for DM4-2(1) (Restart)

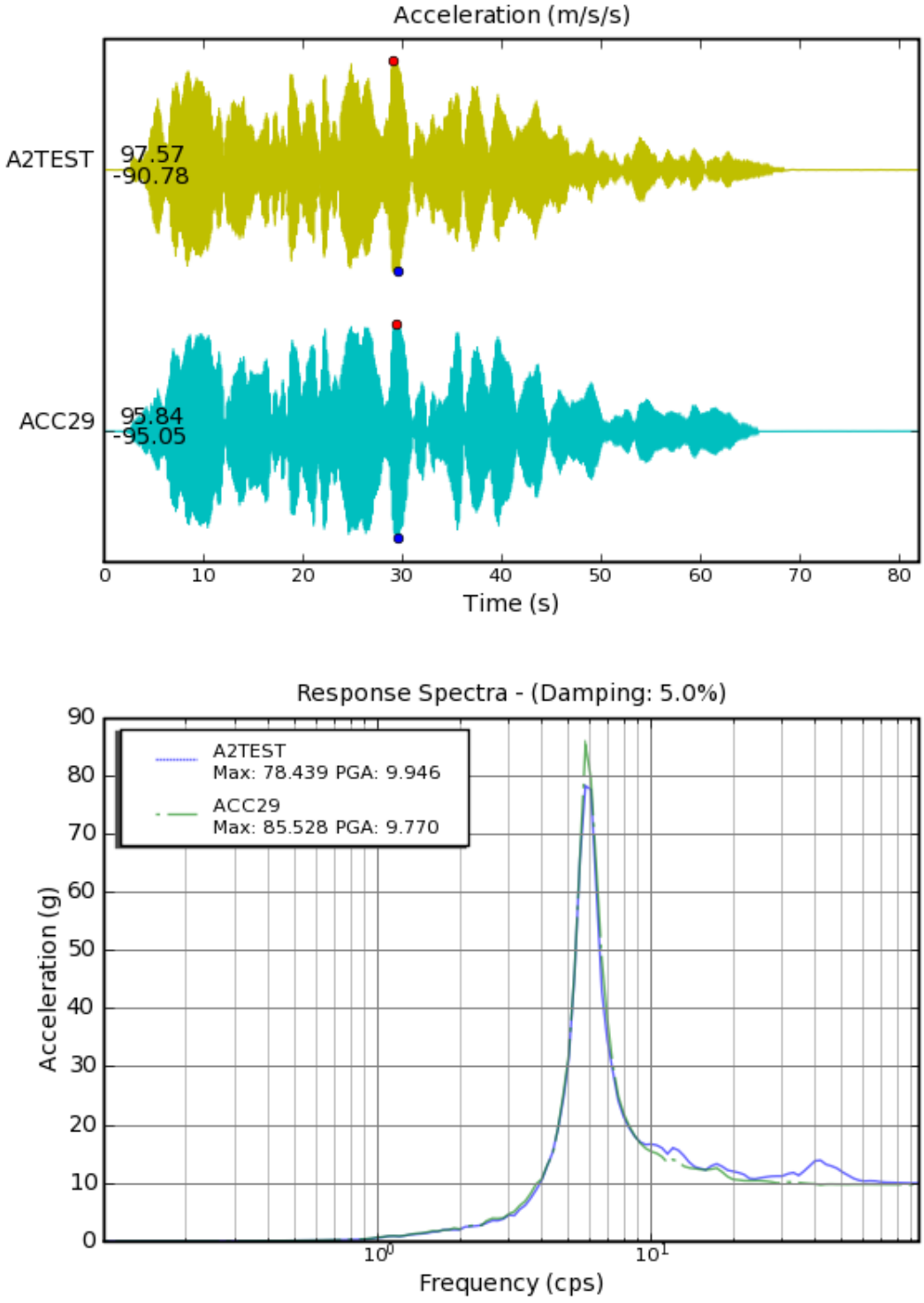

Figure 4-27 Acceleration A2 Comparison for DM4-2(1) (Restart)

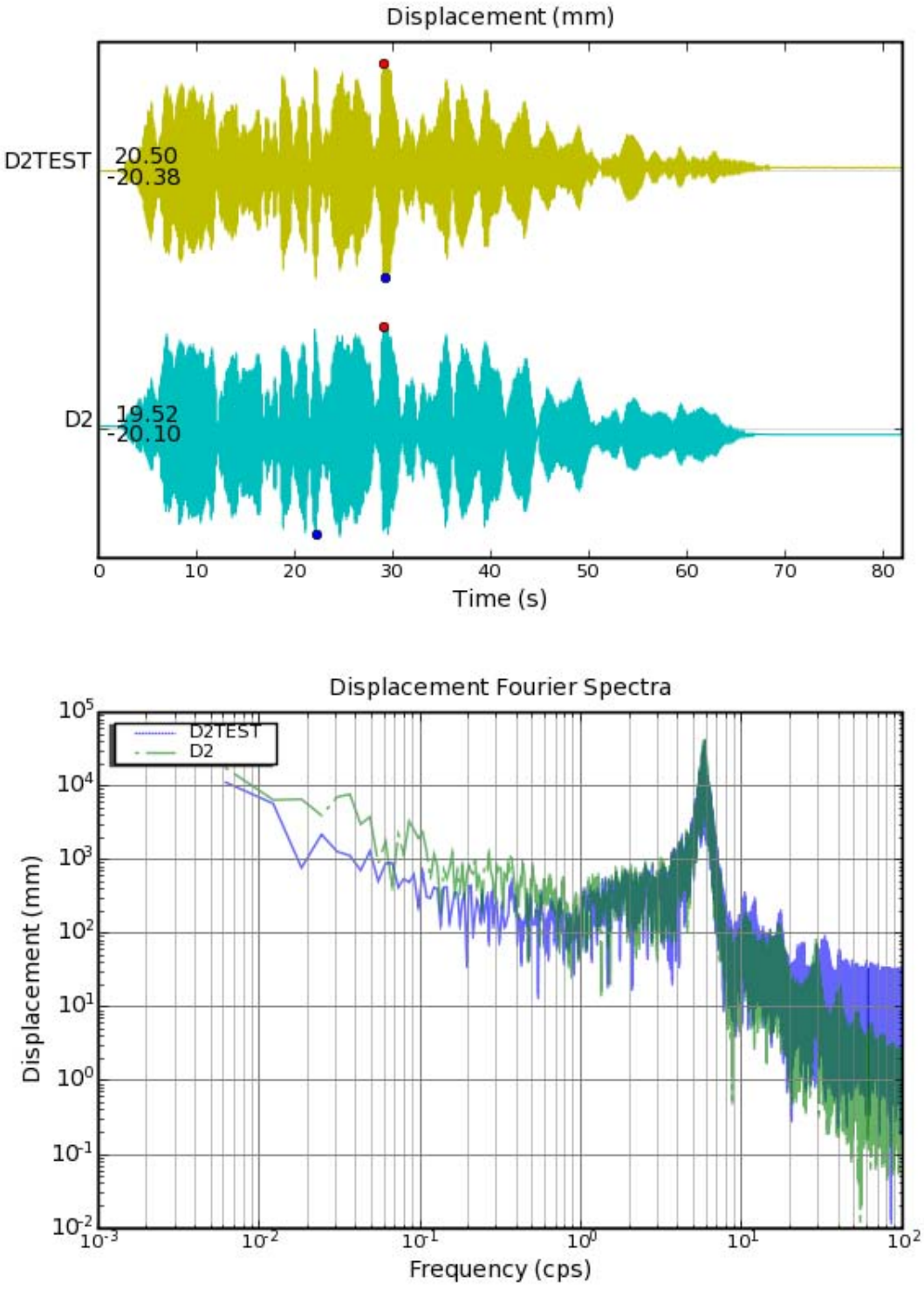

Figure 4-28 Displacement D2 Comparison for DM4-2(2) (Restart)

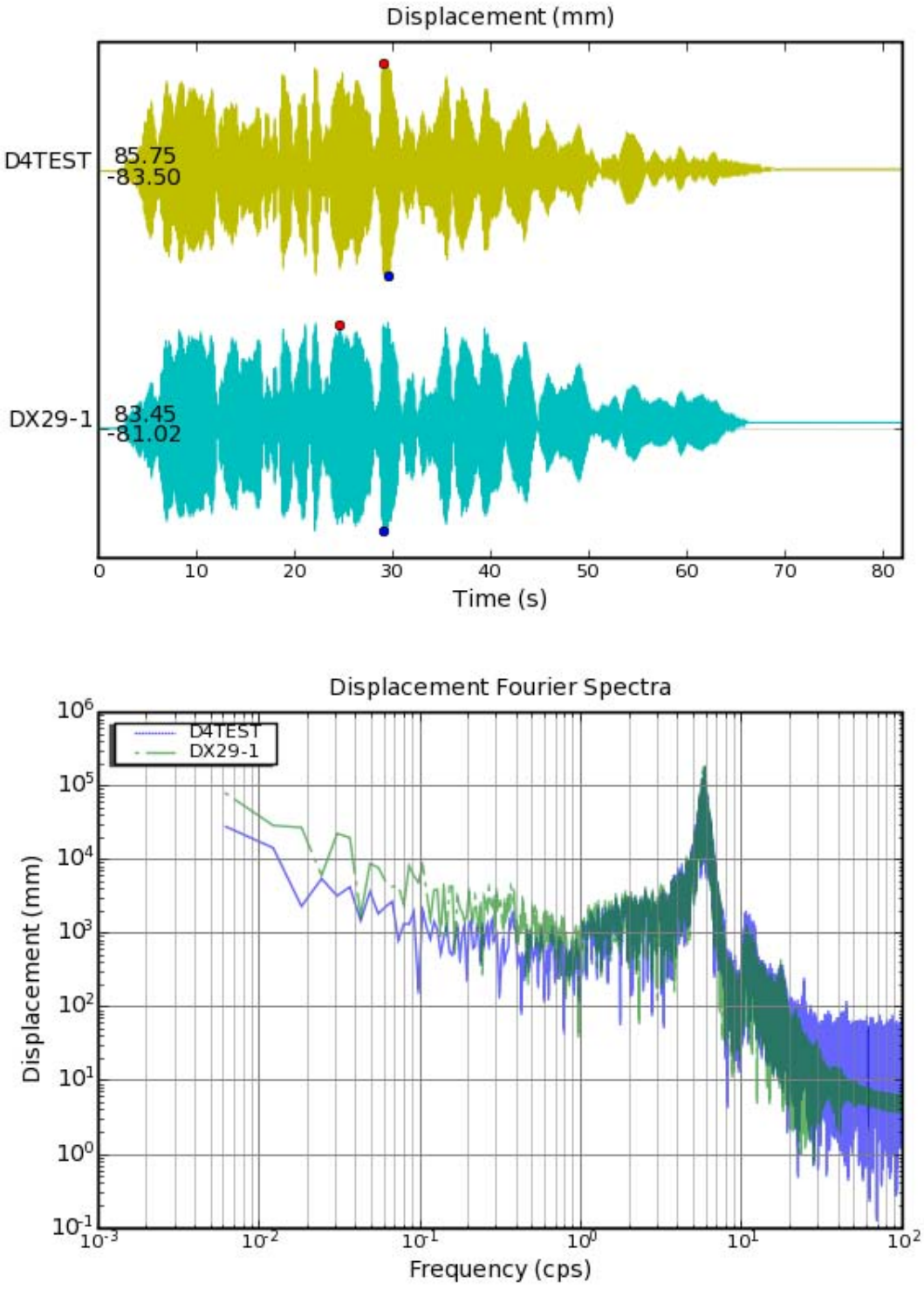

Figure 4-29 Displacement D4 Comparison for DM4-2(2) (Restart)

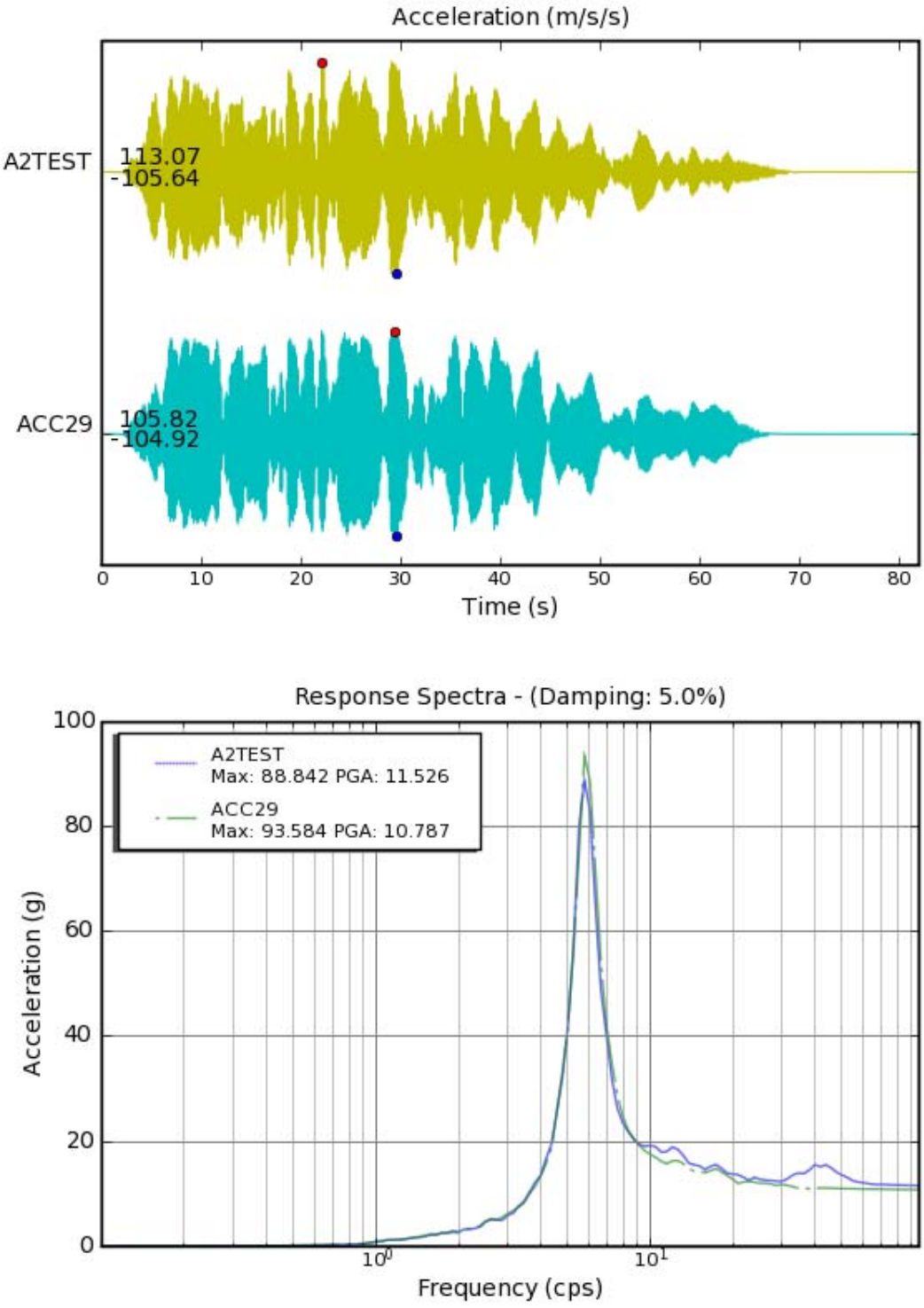

Figure 4-30 Acceleration A2 Comparison for DM4-2(2) (Restart)

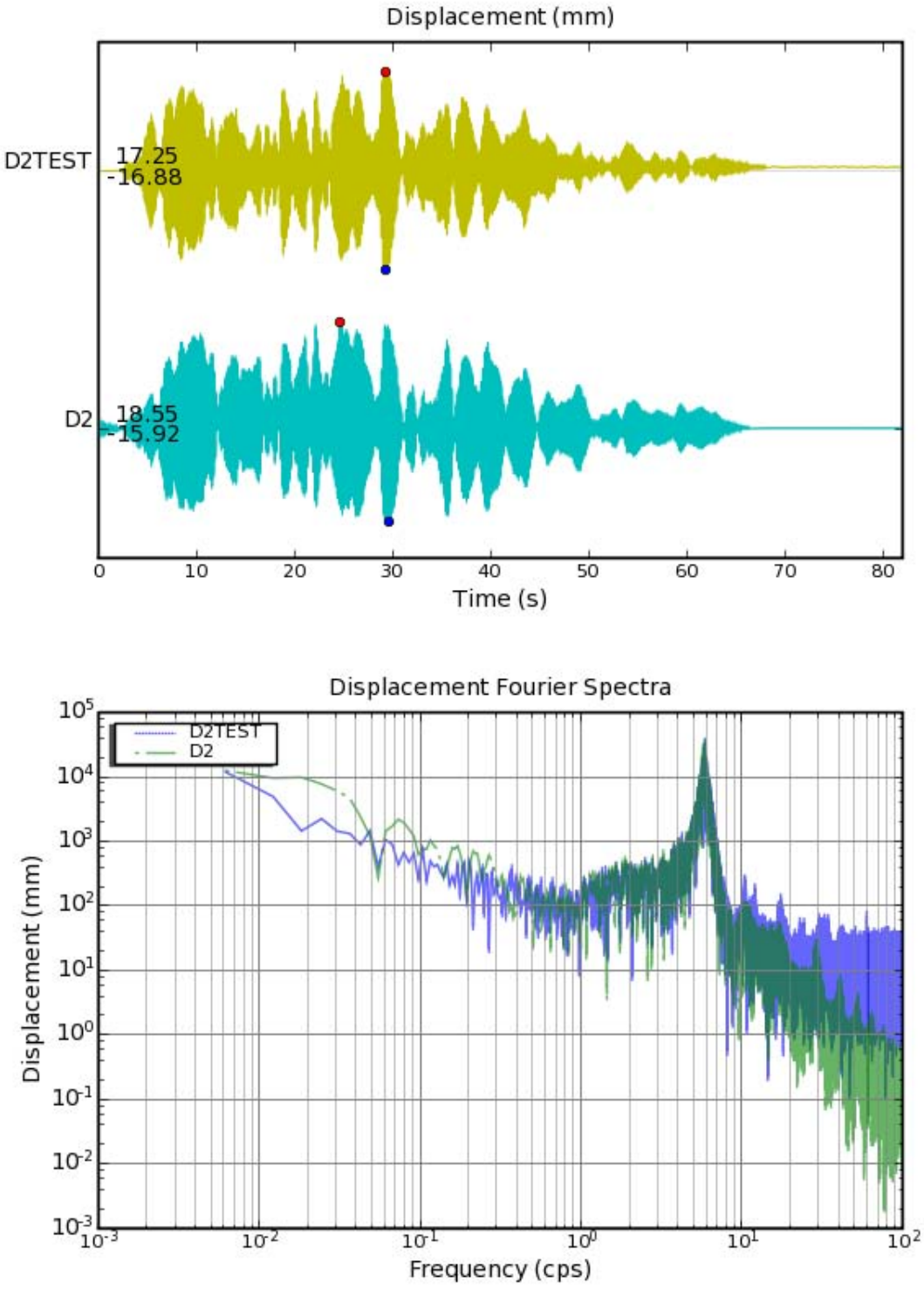

Figure 4-31 Displacement D2 Comparison for DM4-2(1) (Fresh Start)

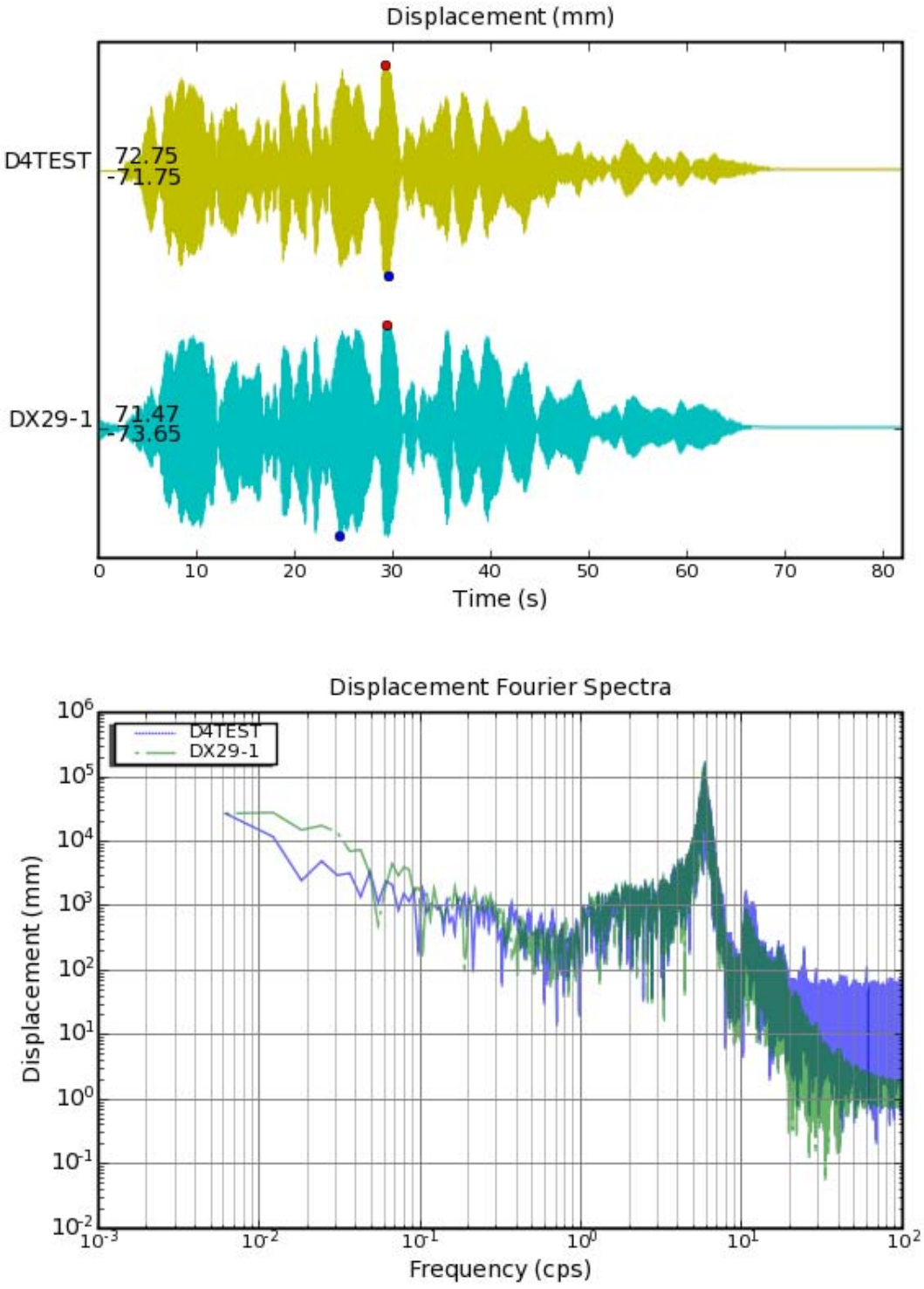

Figure 4-32 Displacement D4 Comparison for DM4-2(1) (Fresh Start)

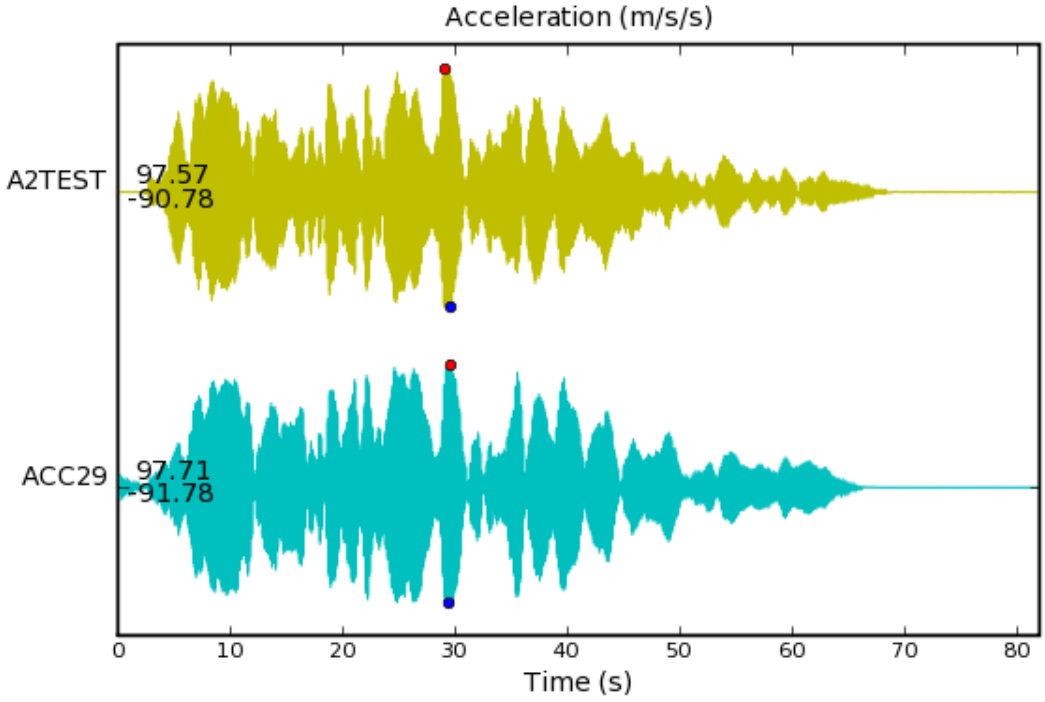

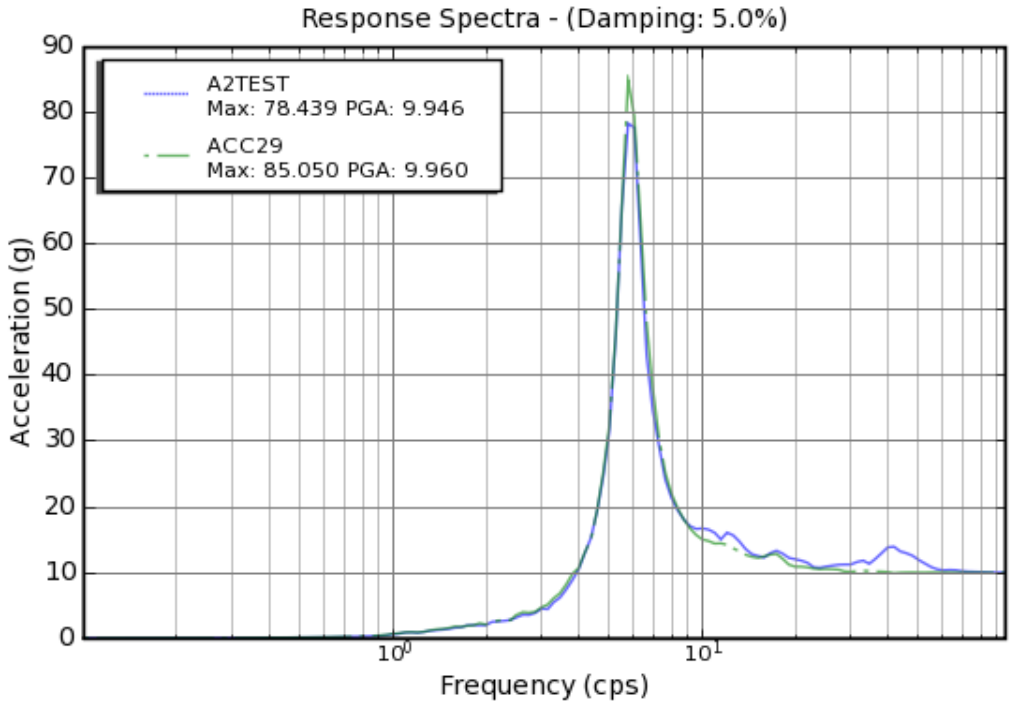

Figure 4-33 Acceleration A2 Comparison for DM4-2(1) (Fresh Start)

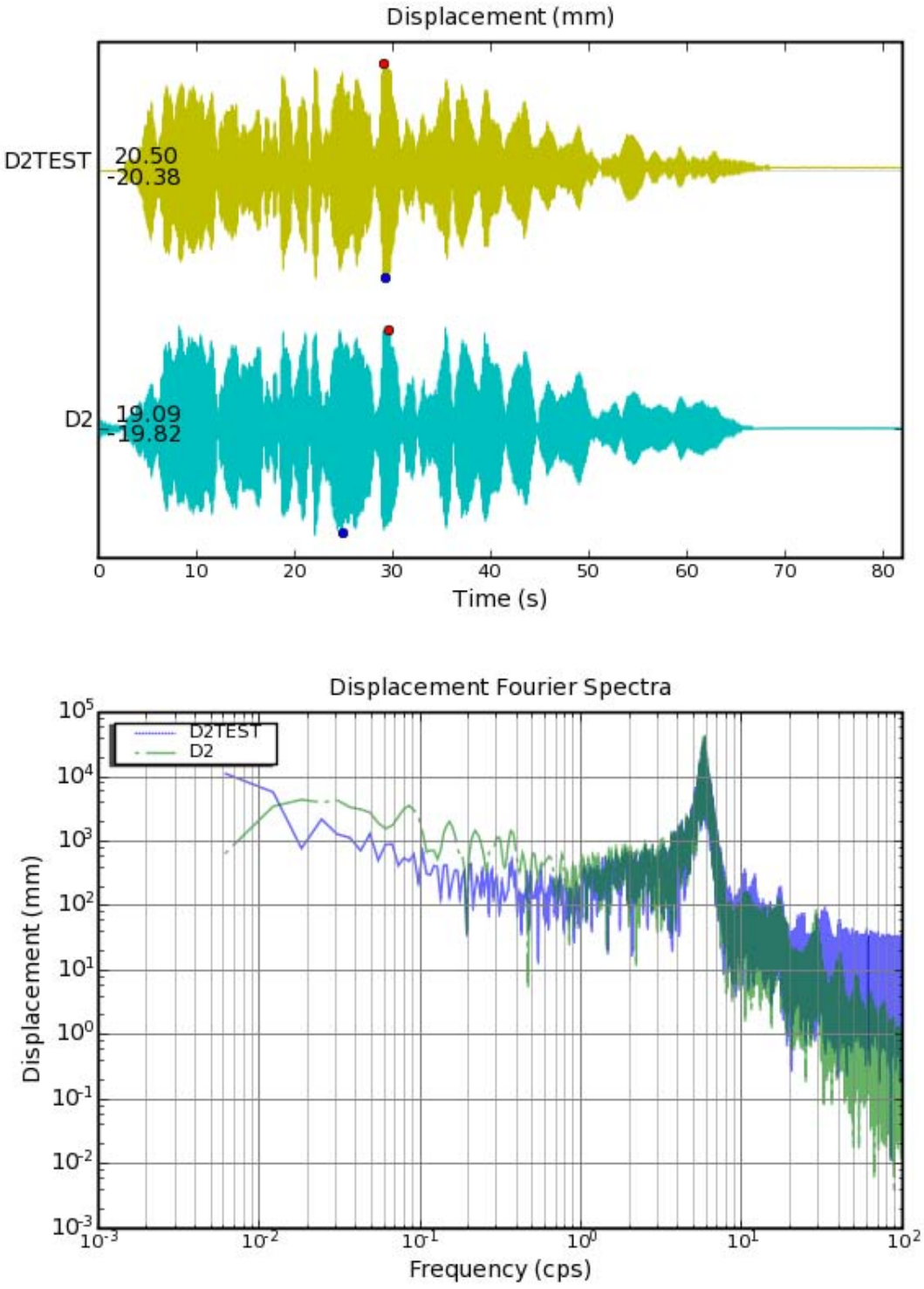

Figure 4-34 Displacement D2 Comparison for DM4-2(2) (Fresh Start)

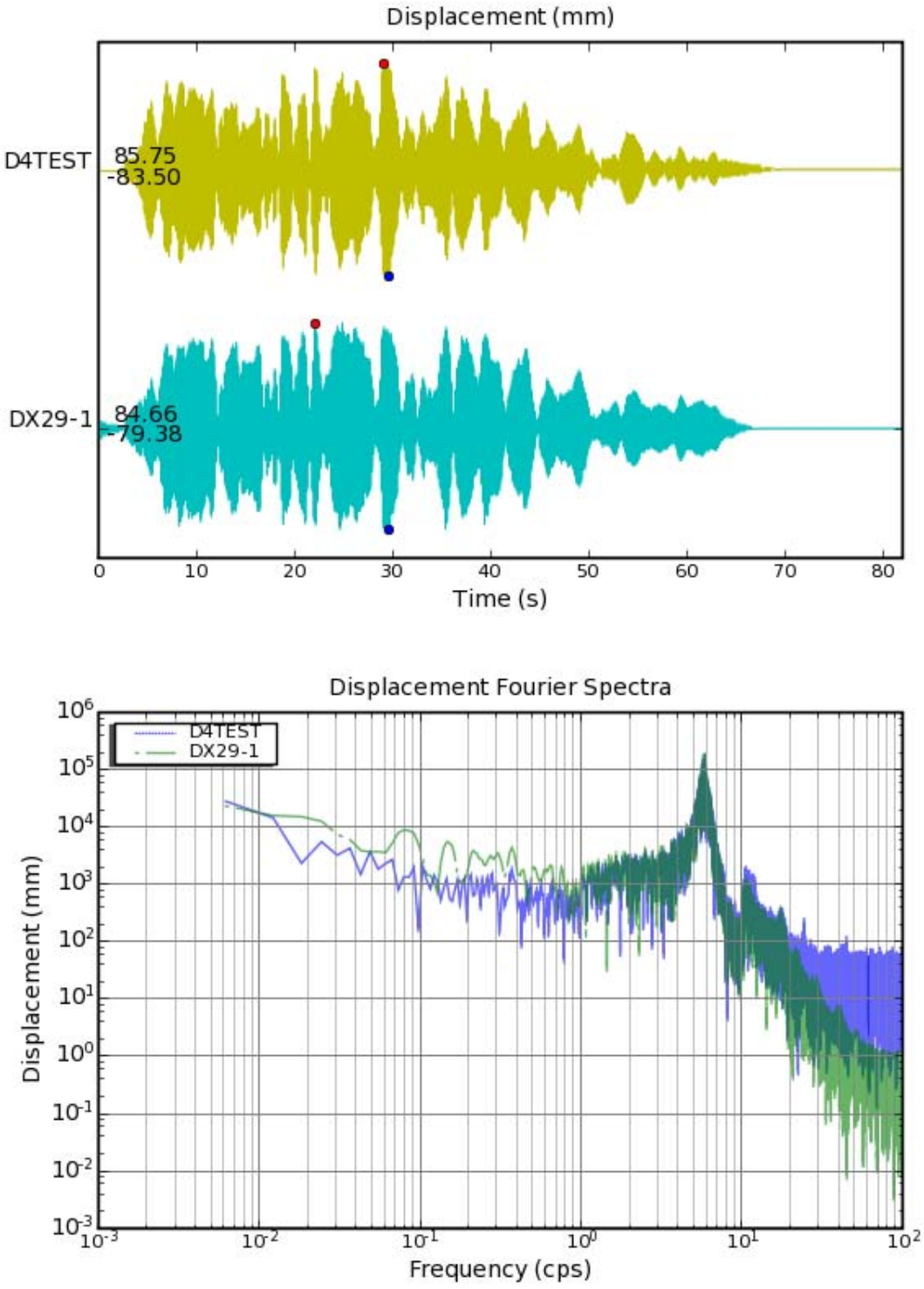

Figure 4-35 Displacement D4 Comparison for DM4-2(2) (Fresh Start)

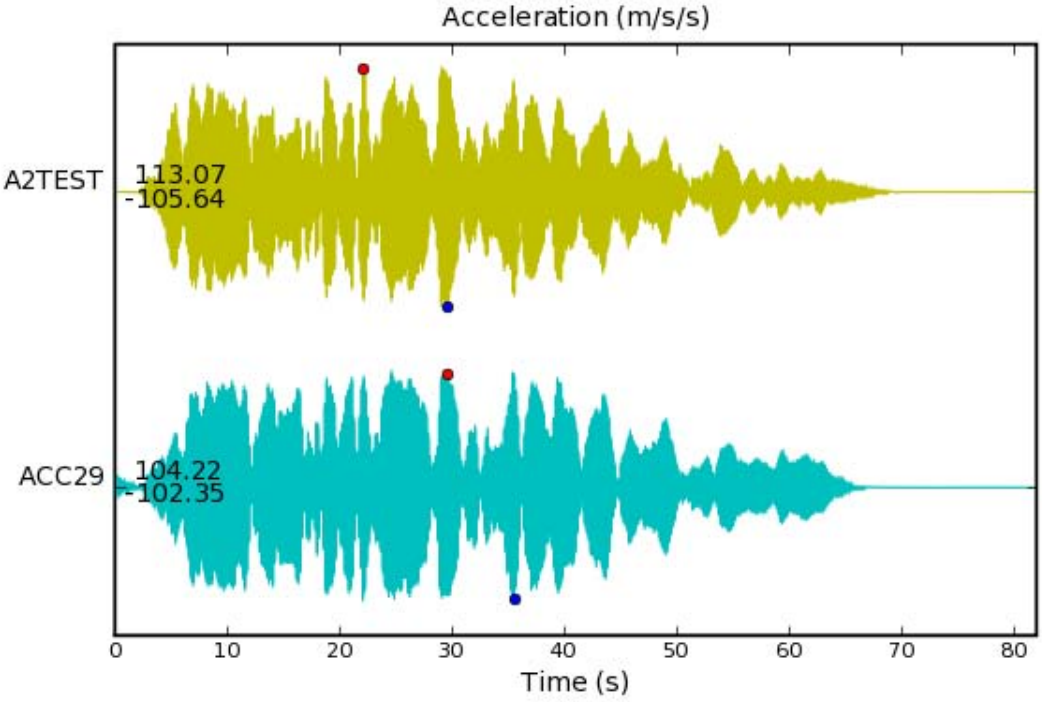

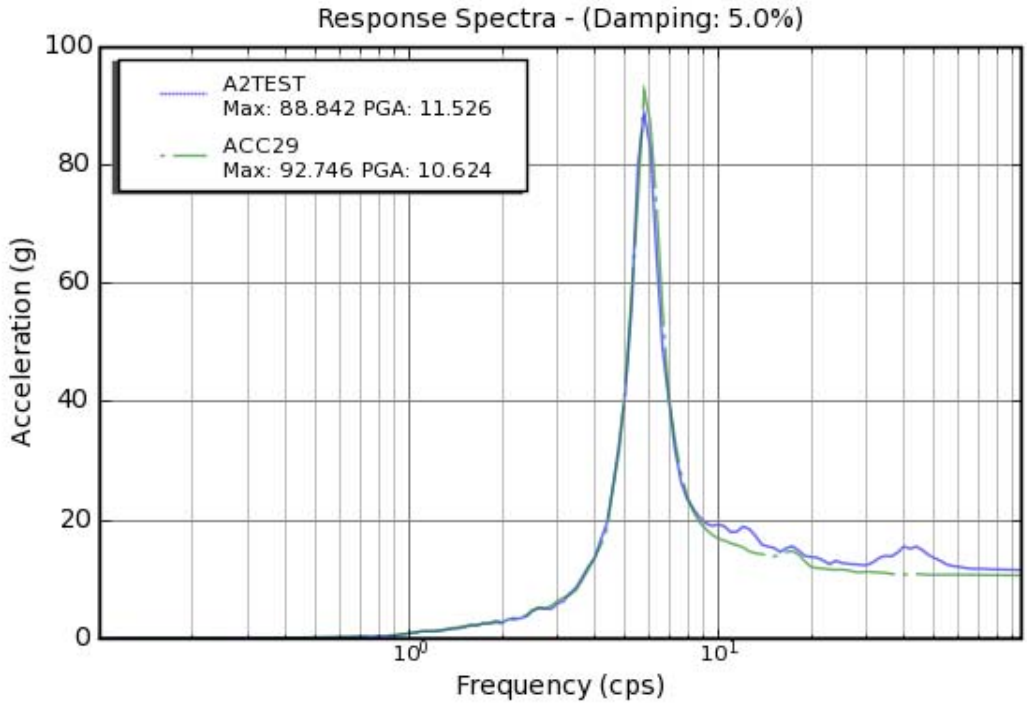

Figure 4-36 Acceleration A2 Comparison for DM4-2(2) (Fresh Start)

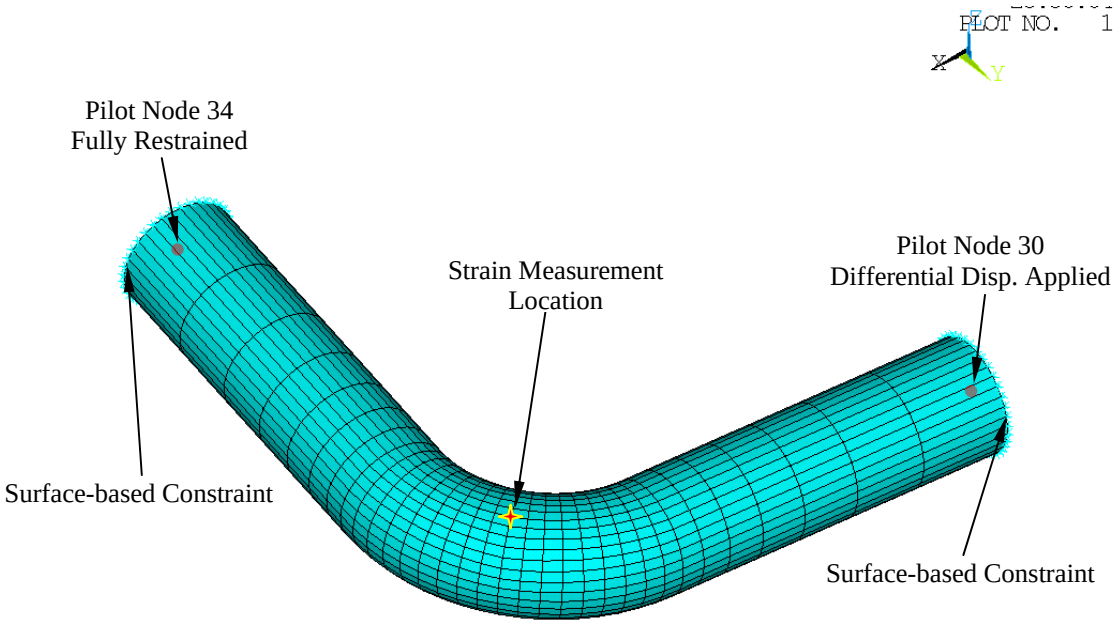

Figure 4-37 Elbow 2 Shell Model for Design Method Confirmation Tests

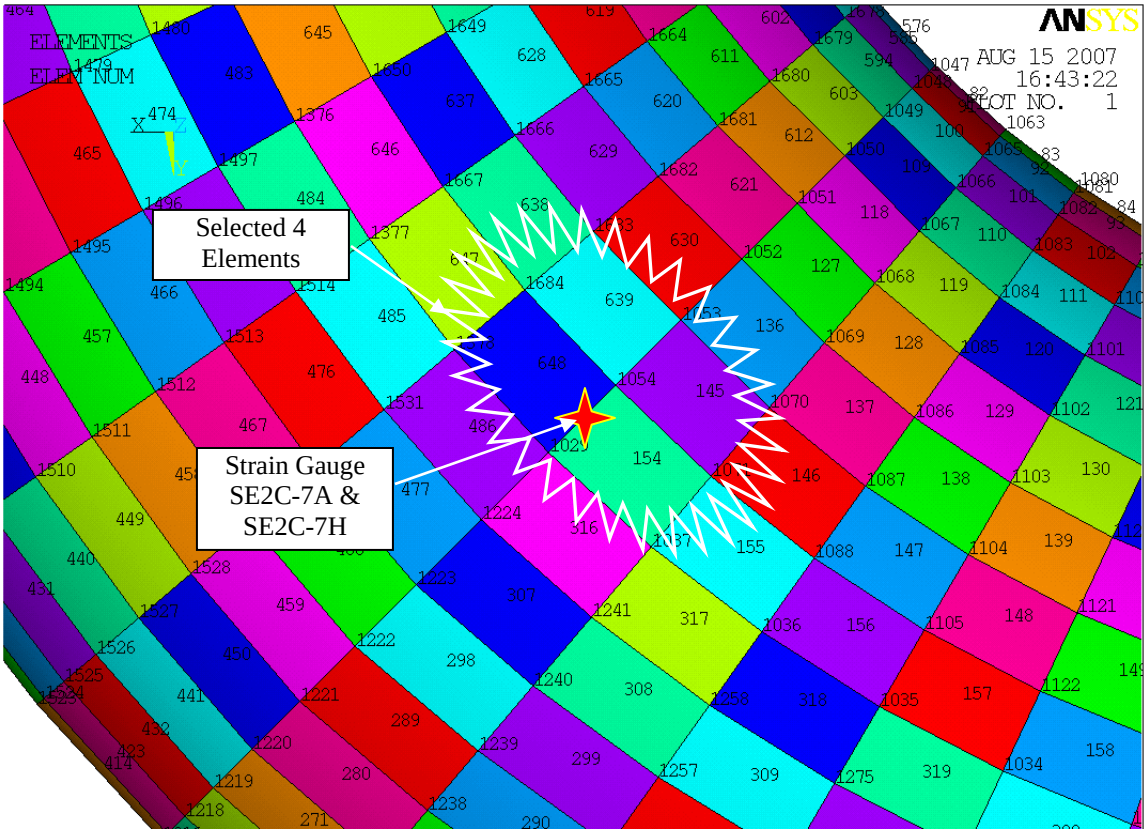

Figure 4-38 Nodes and Elements for Strain Measurements For DM Tests

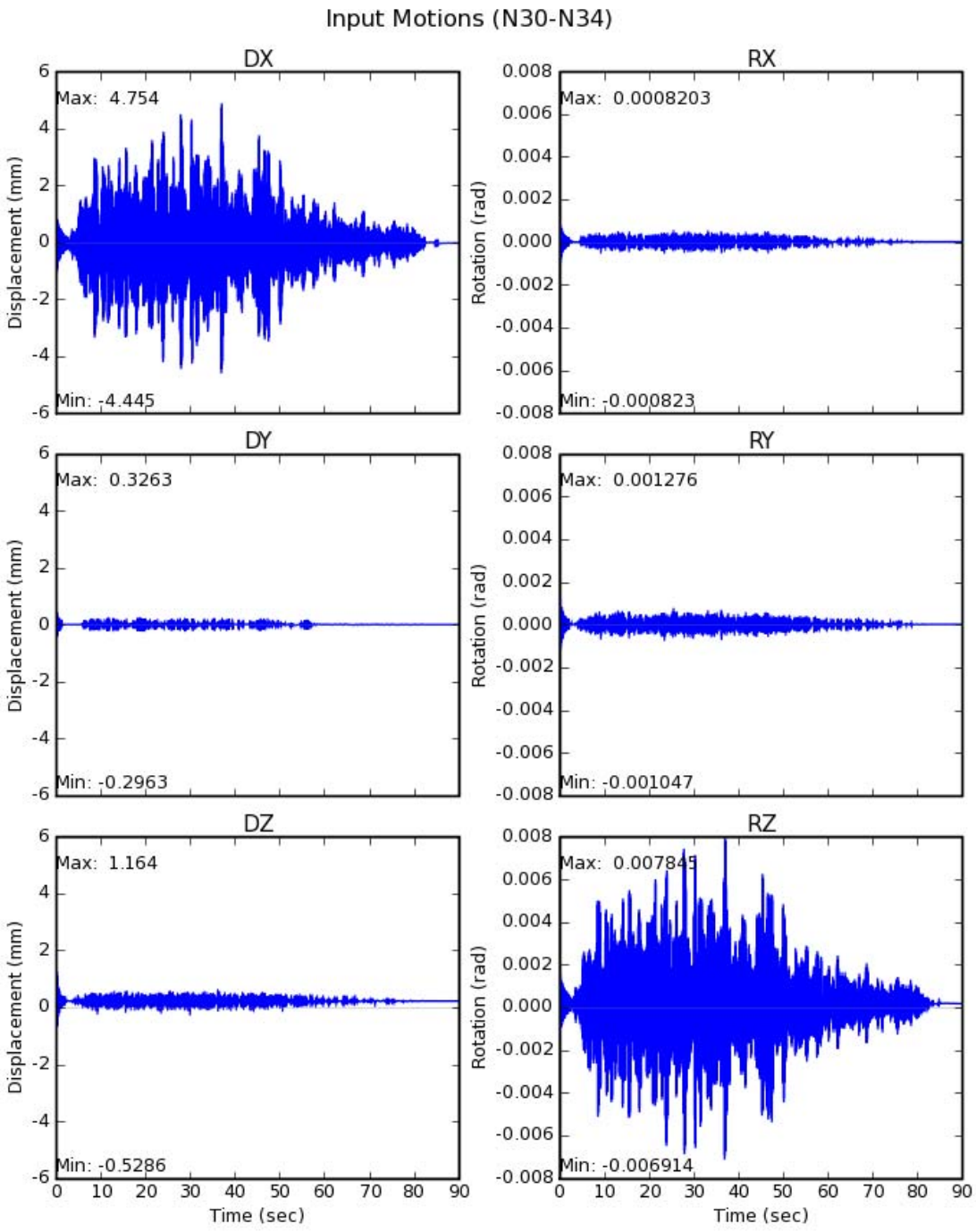

Figure 4-39 Relative Deformation Histories as Input Motions to Elbow Model for DM2-1

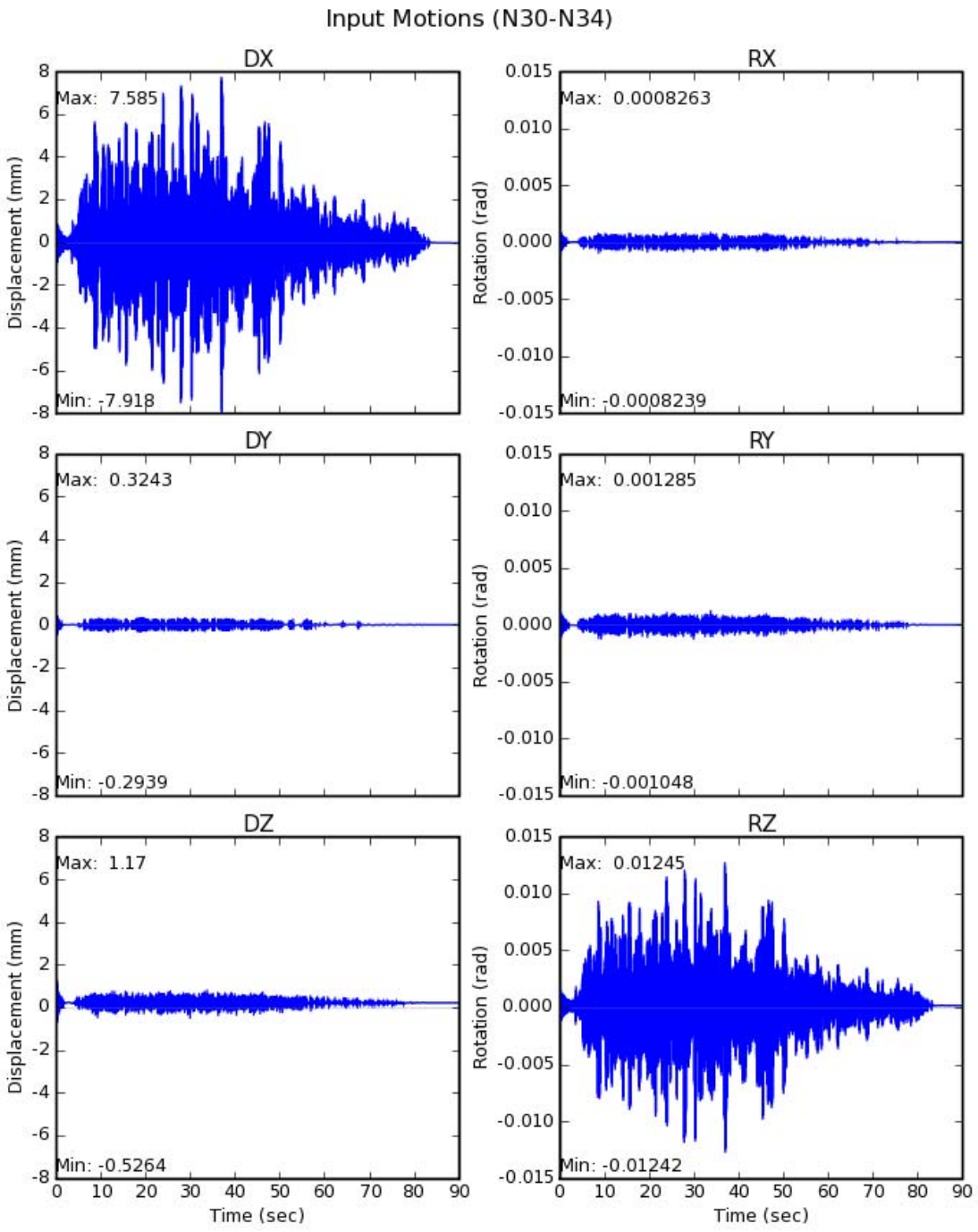

Figure 4-40 Relative Deformation Histories as Input Motions to Elbow Model for DM2-2

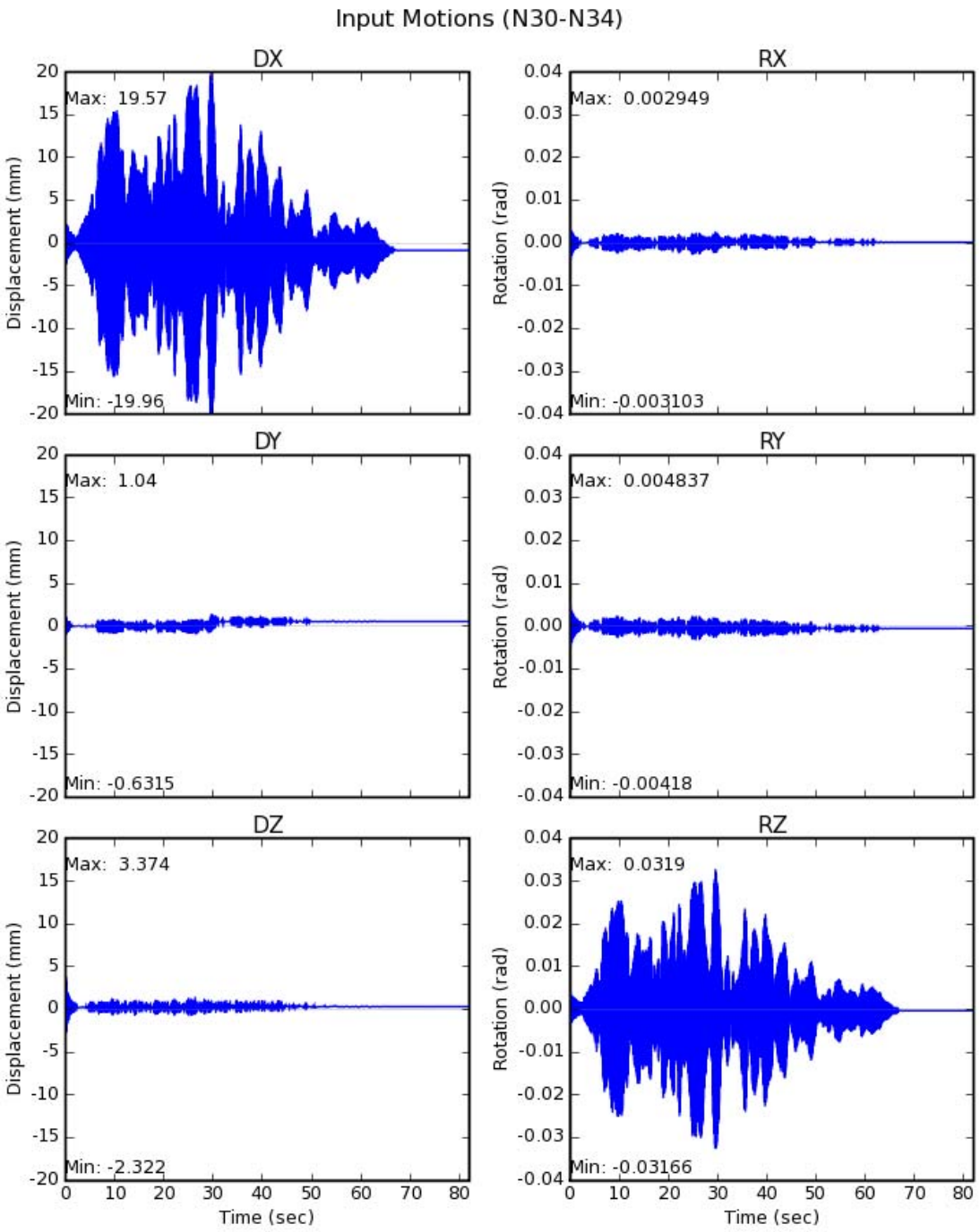

Figure 4-41 Relative Deformation Histories as Input Motions to Elbow Model for DM4-1

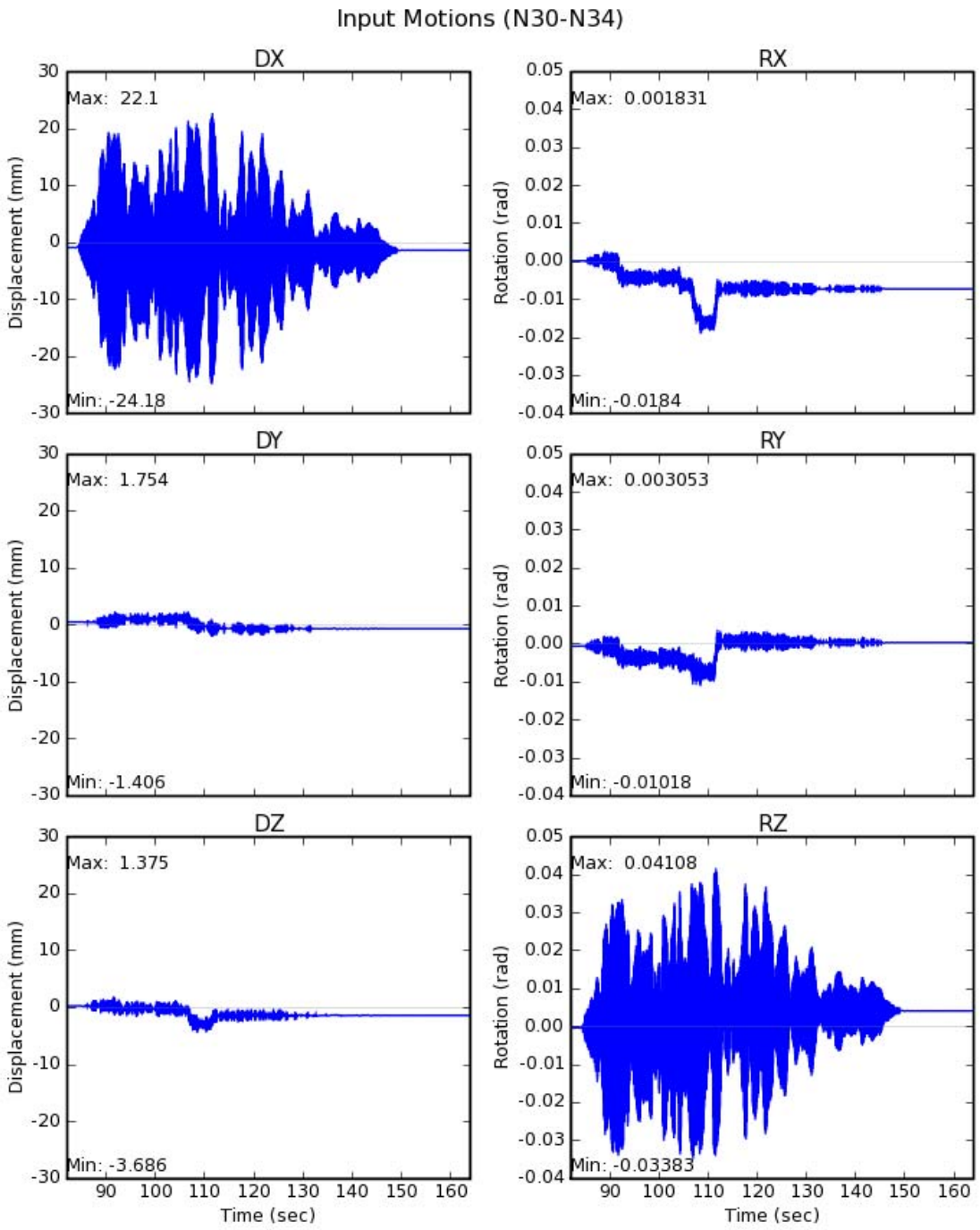

Figure 4-42 Relative Deformation Histories as Input Motions to Elbow Model for DM4-2(1) (Restart)

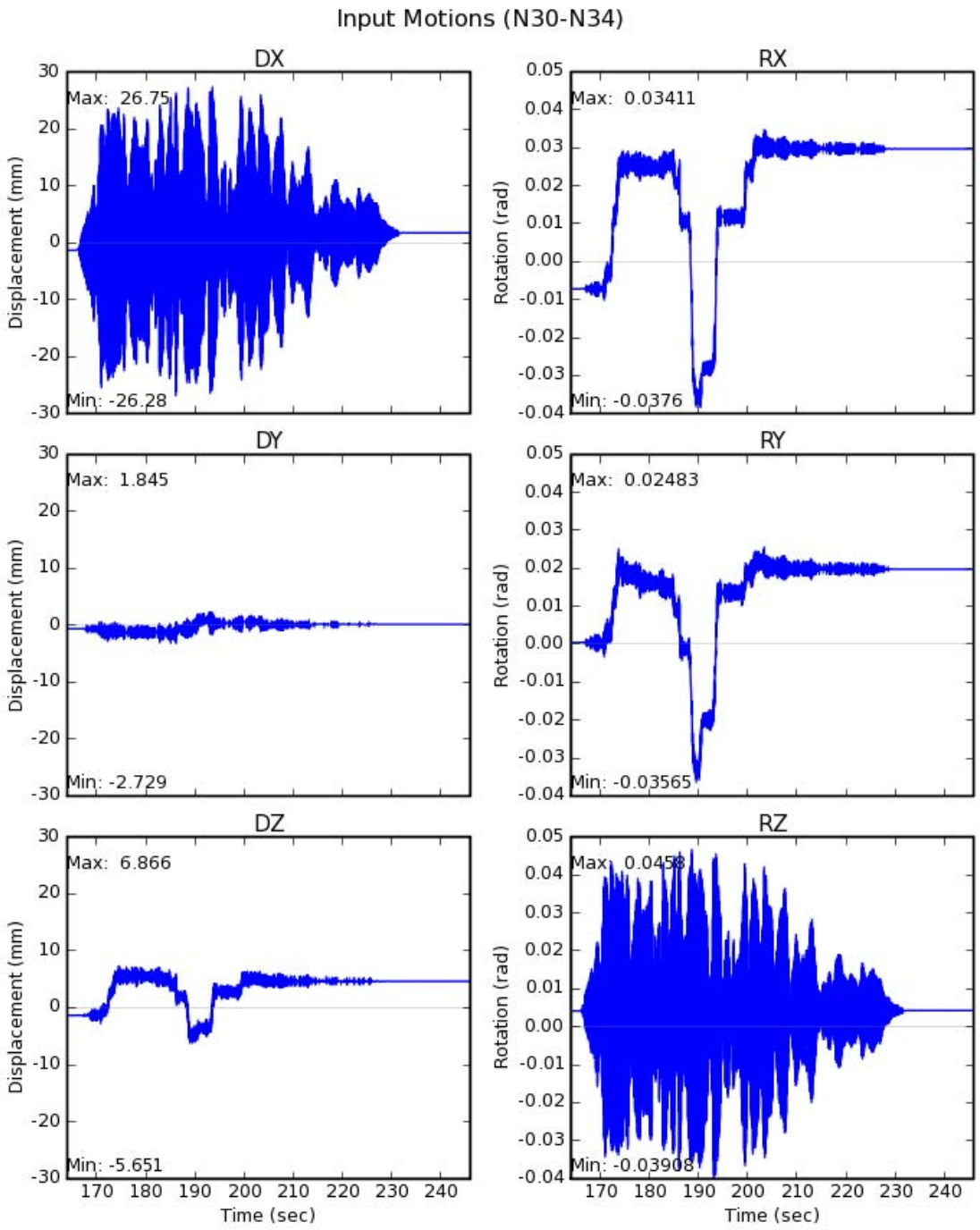

Figure 4-43 Relative Deformation Histories as Input Motions to Elbow Model for DM4-2(2) (Restart)

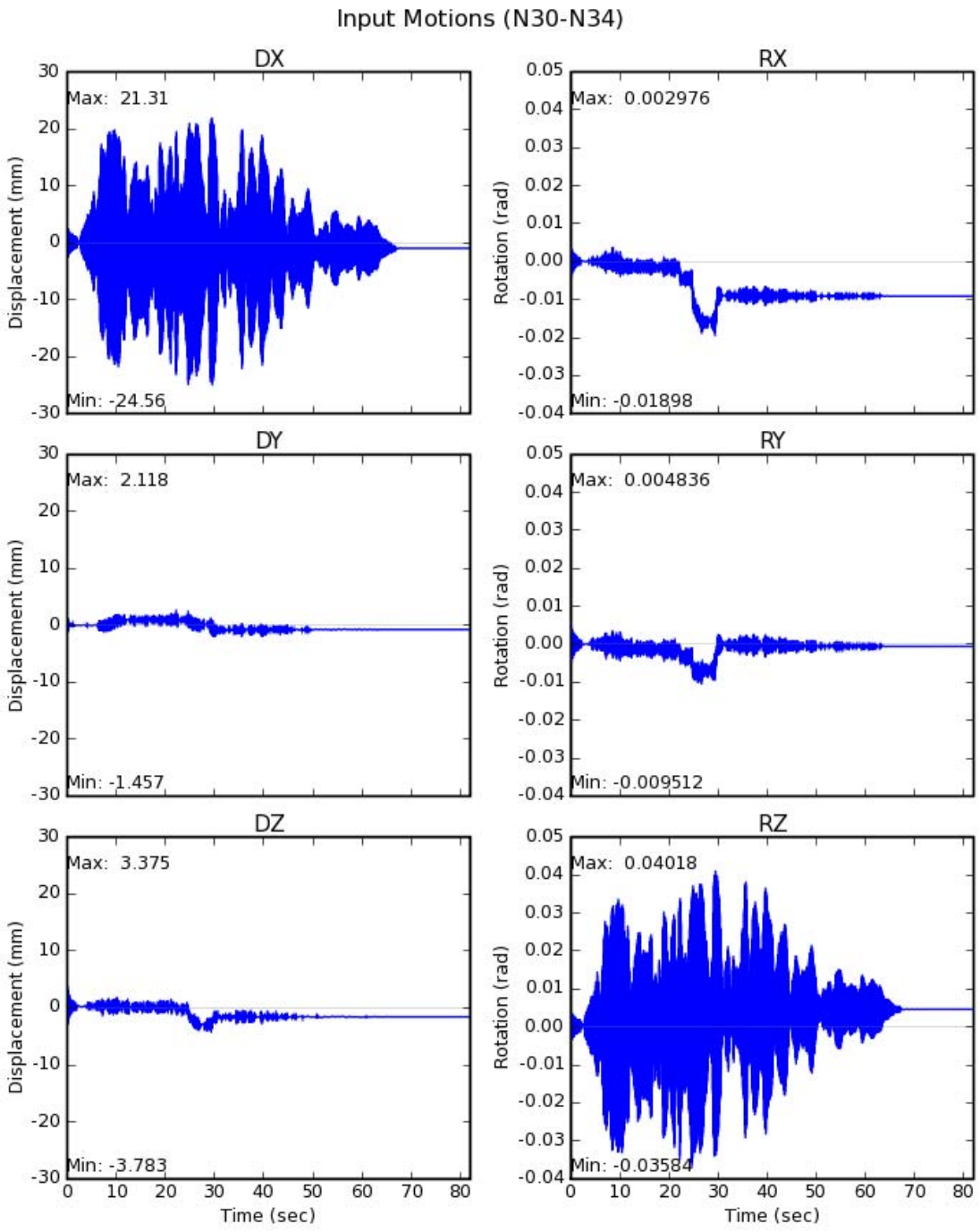

Figure 4-44 Relative Deformation Histories as Input Motions to Elbow Model for DM4-2(1) (Fresh Start)

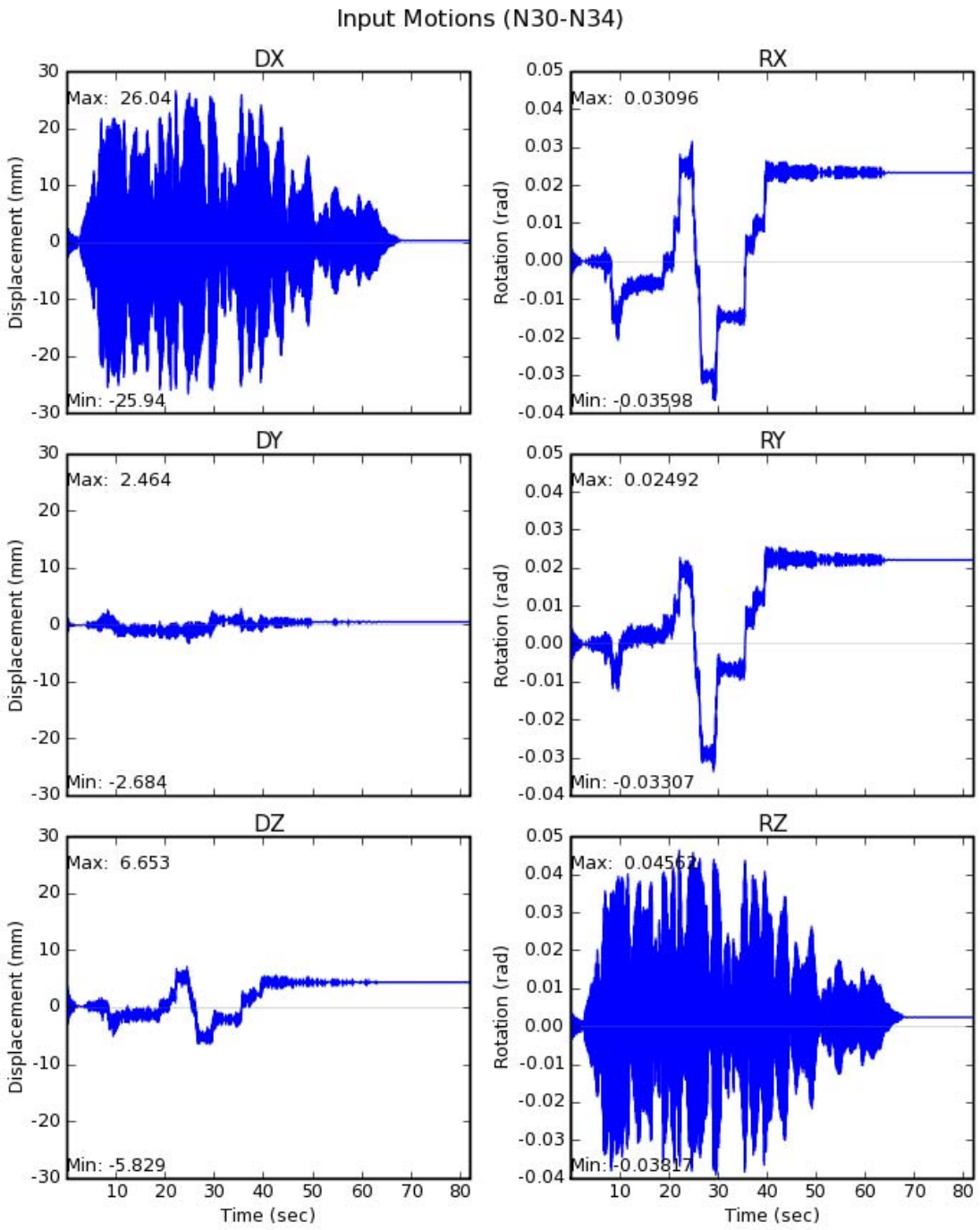

Figure 4-45 Relative Deformation Histories as Input Motions to Elbow Model for DM4-2(2) (Fresh Start)

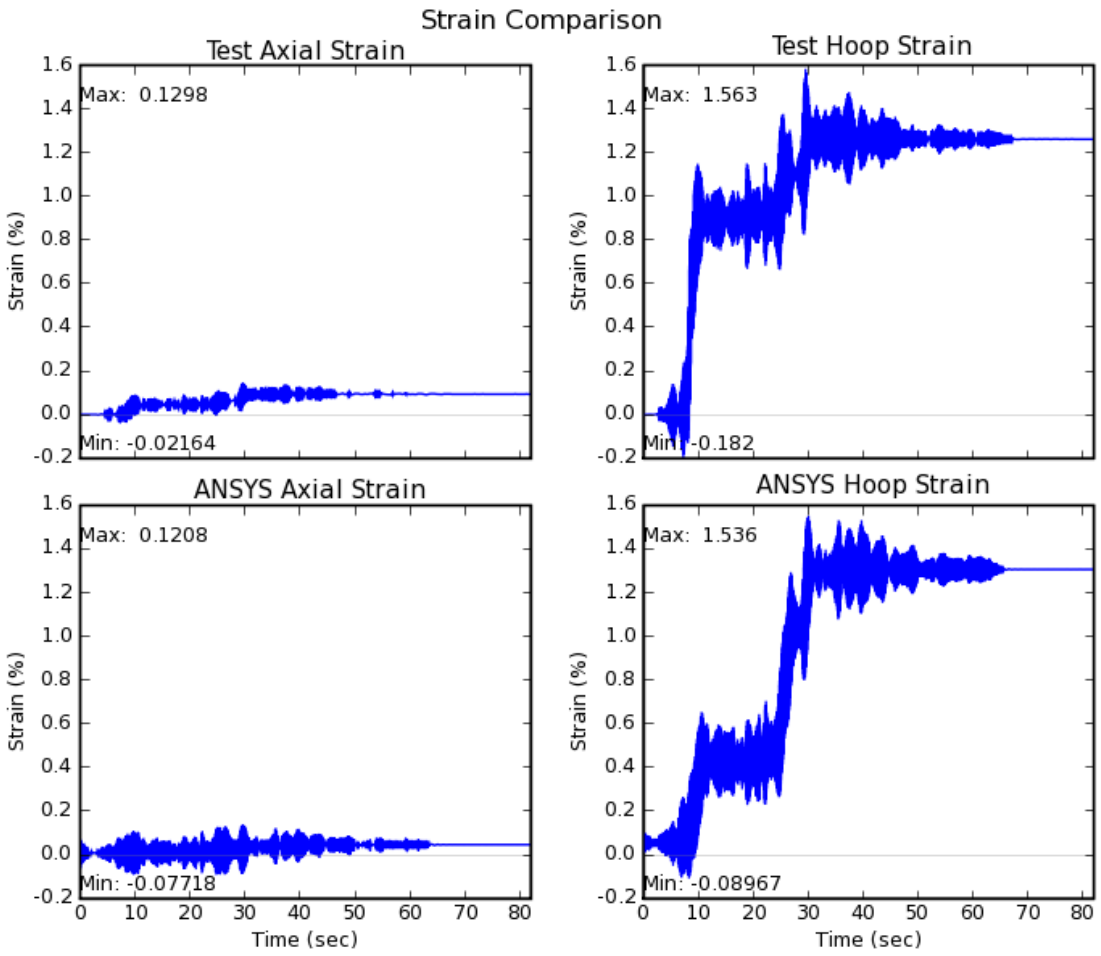

Figure 4-46 Strain Ratcheting Comparison at Element 145 for DM4-1

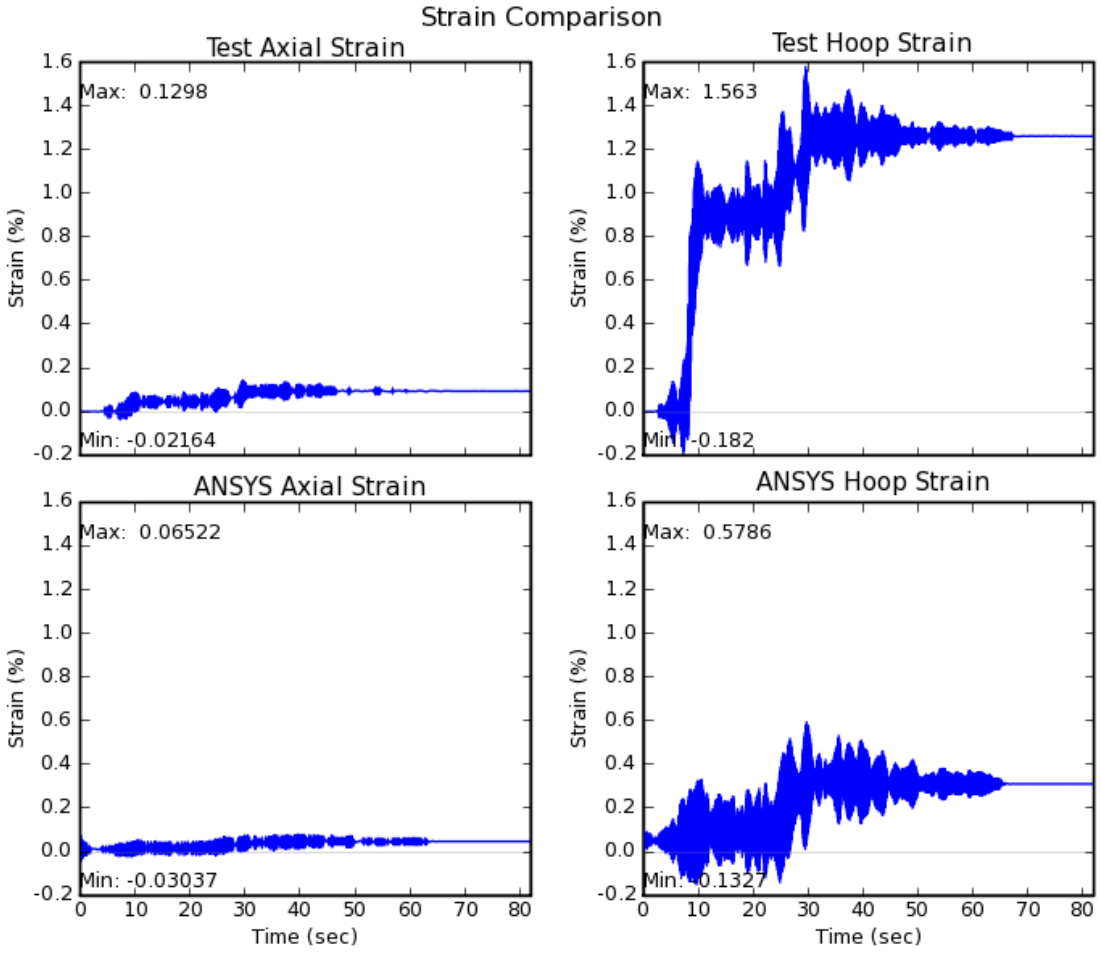

Figure 4-47 Strain Ratcheting Comparison at Element 154 for DM4-1

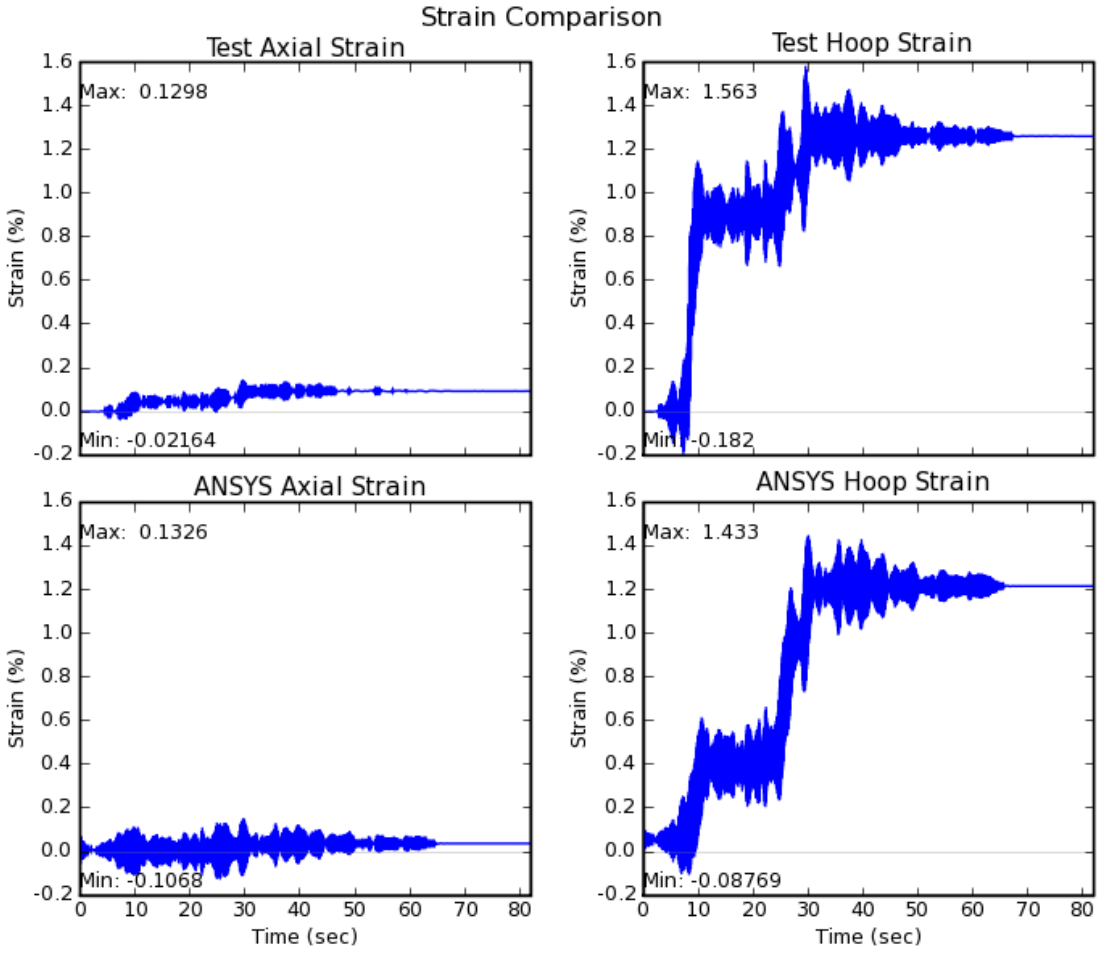

Figure 4-48 Strain Ratcheting Comparison at Element 639 for DM4-1

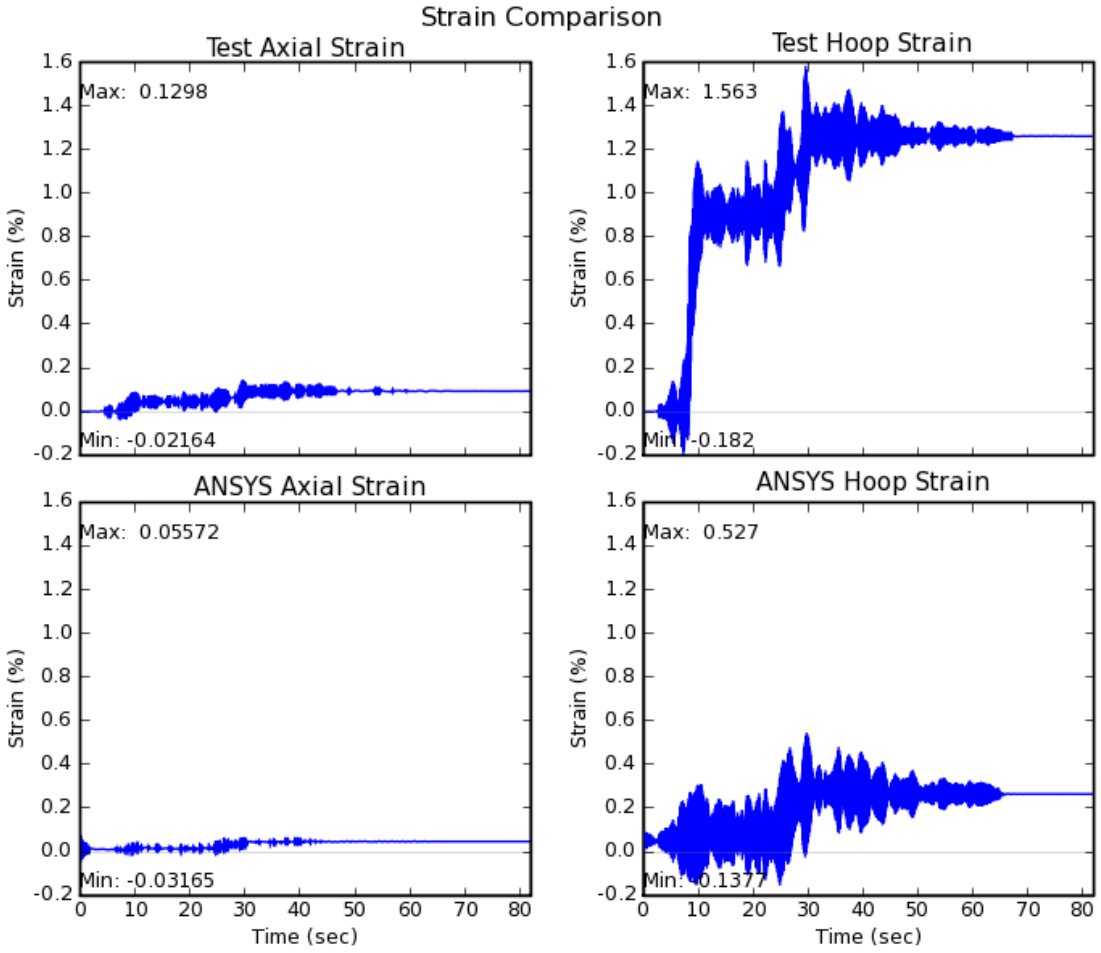

Figure 4-49 Strain Ratcheting Comparison at Element 648 for DM4-1

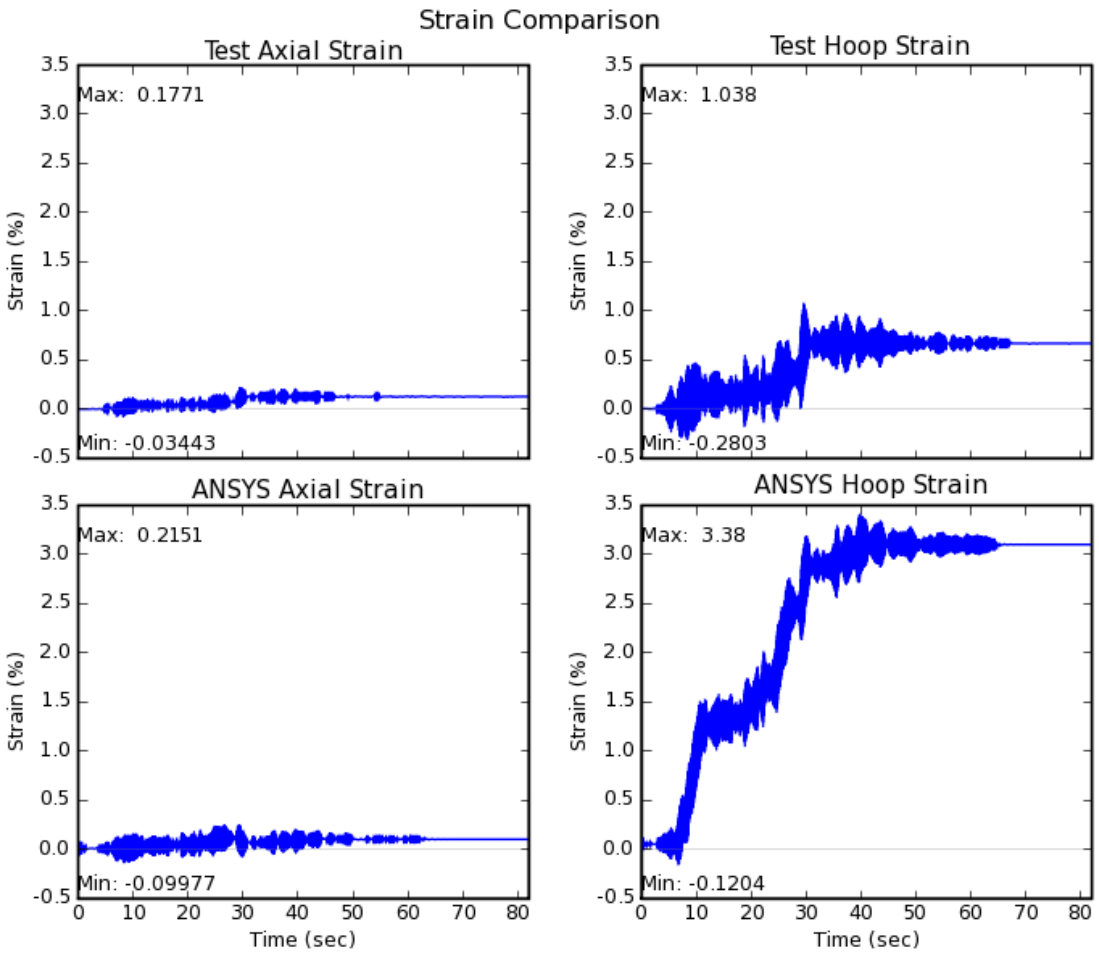

Figure 4-50 Strain Ratcheting Comparison at Element 145 for DM4-2(1) (Fresh Start)

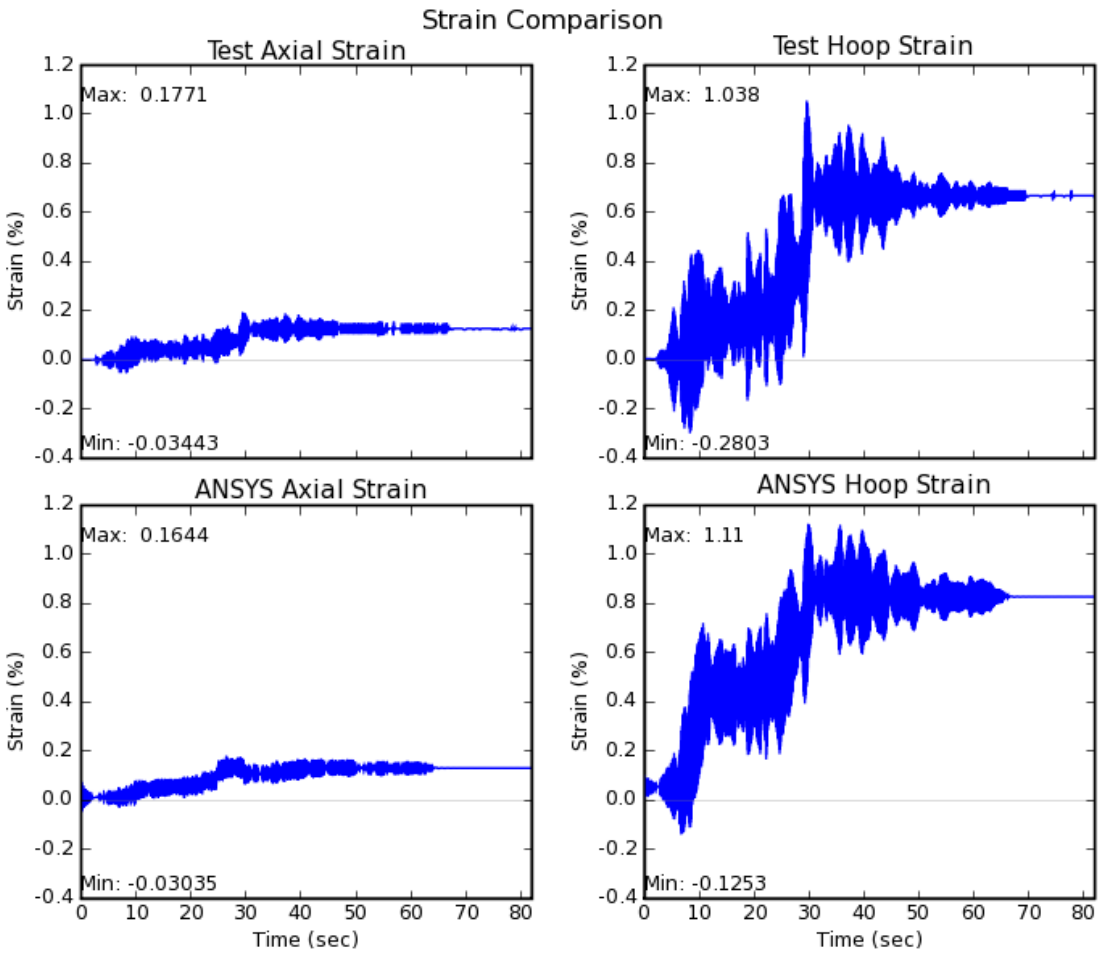

Figure 4-51 Strain Ratcheting Comparison at Element 154 for DM4-2(1) (Fresh Start)

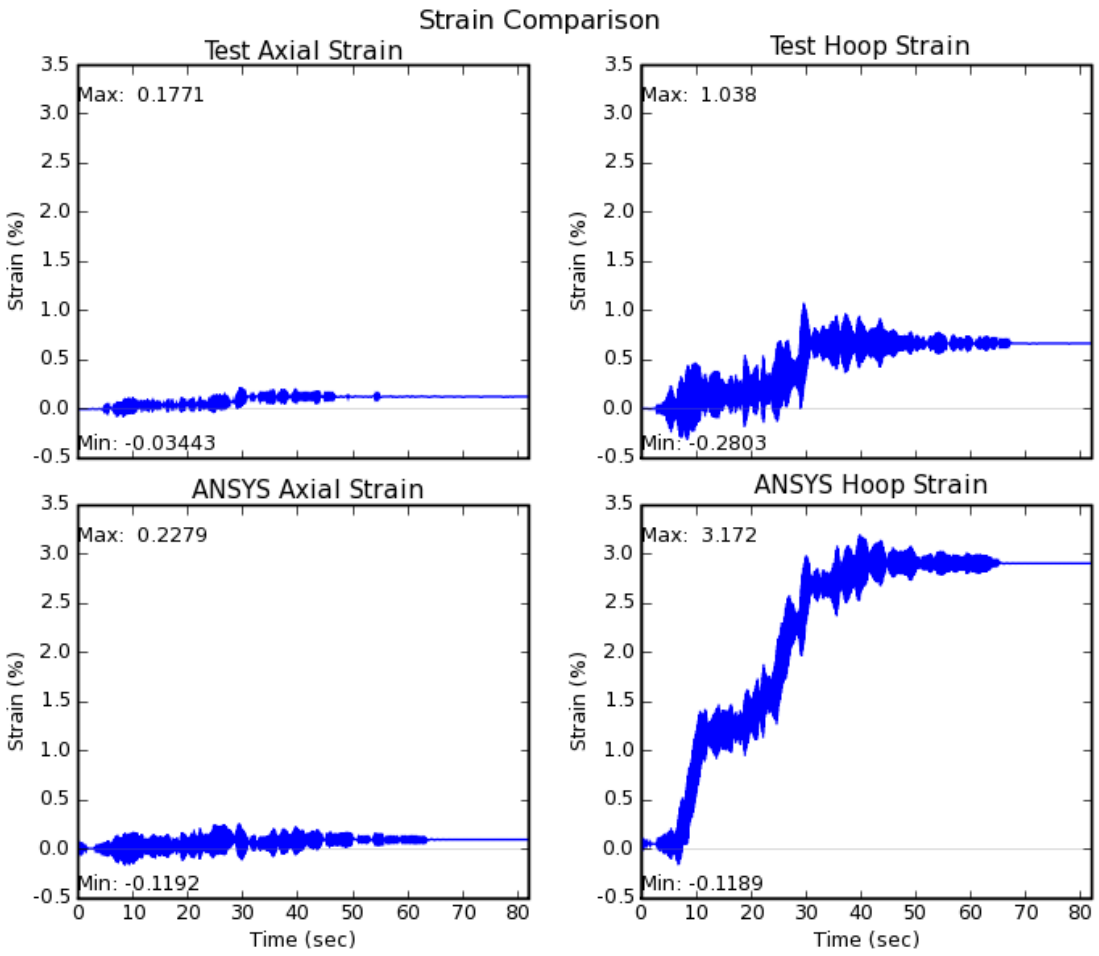

Figure 4-52 Strain Ratcheting Comparison at Element 639 for DM4-2(1) (Fresh Start)

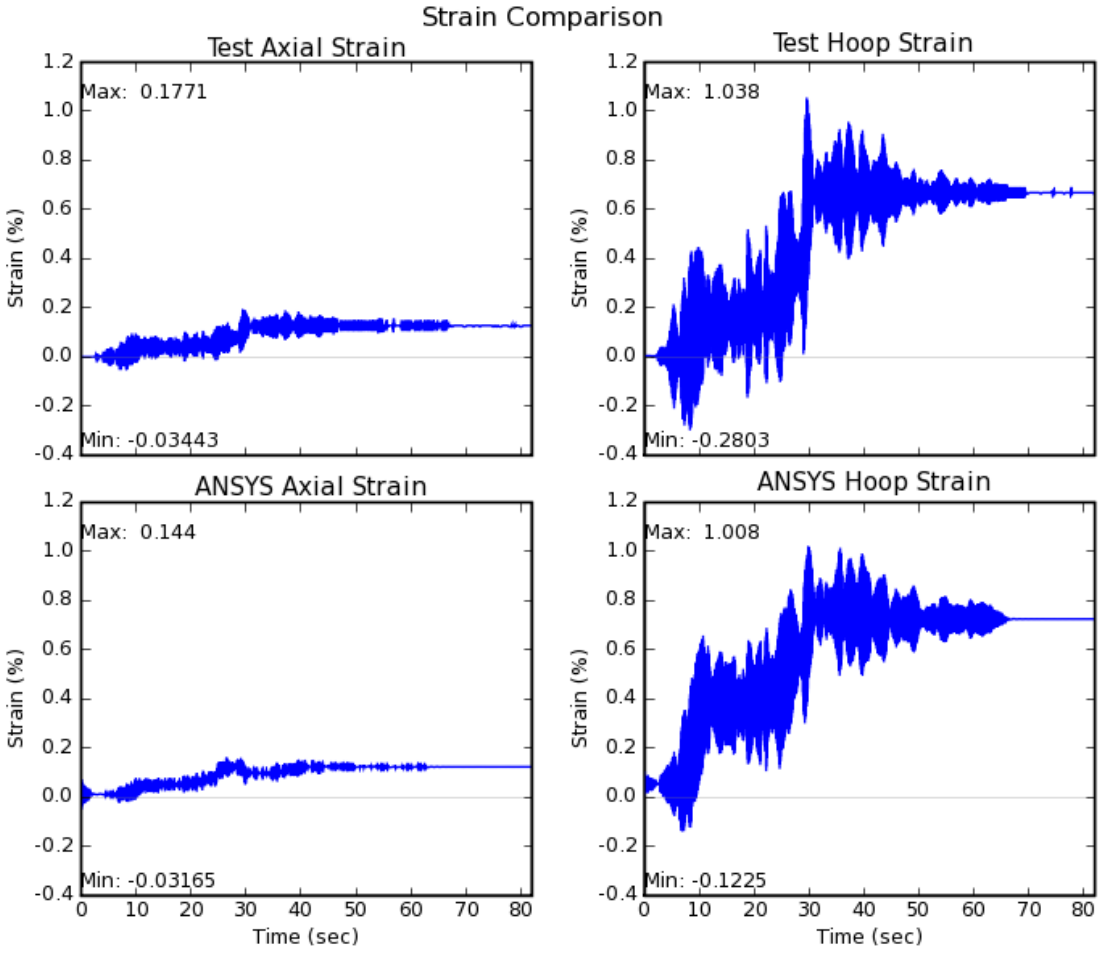

Figure 4-53 Strain Ratcheting Comparison at Element 648 for DM4-2(1) (Fresh Start)

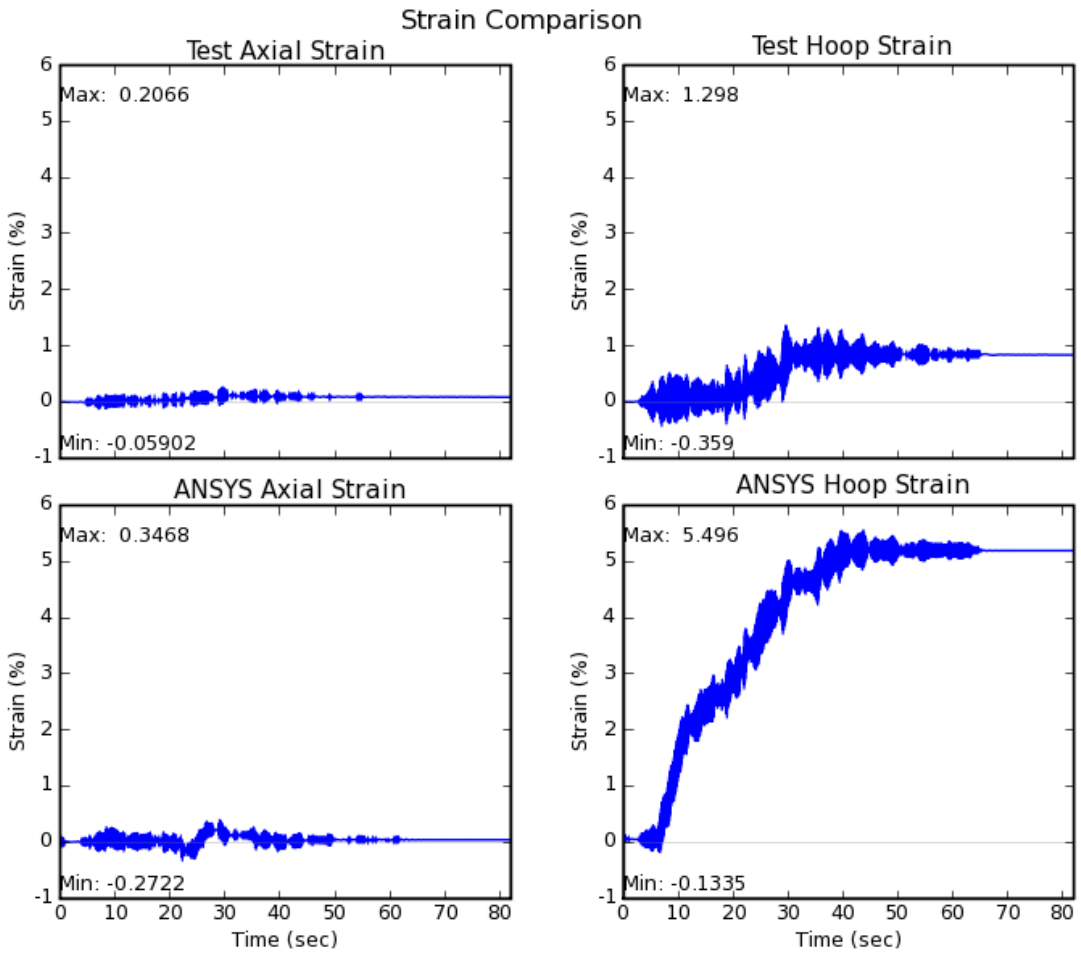

Figure 4-54 Strain Ratcheting Comparison at Element 145 for DM4-2(2) (Fresh Start)

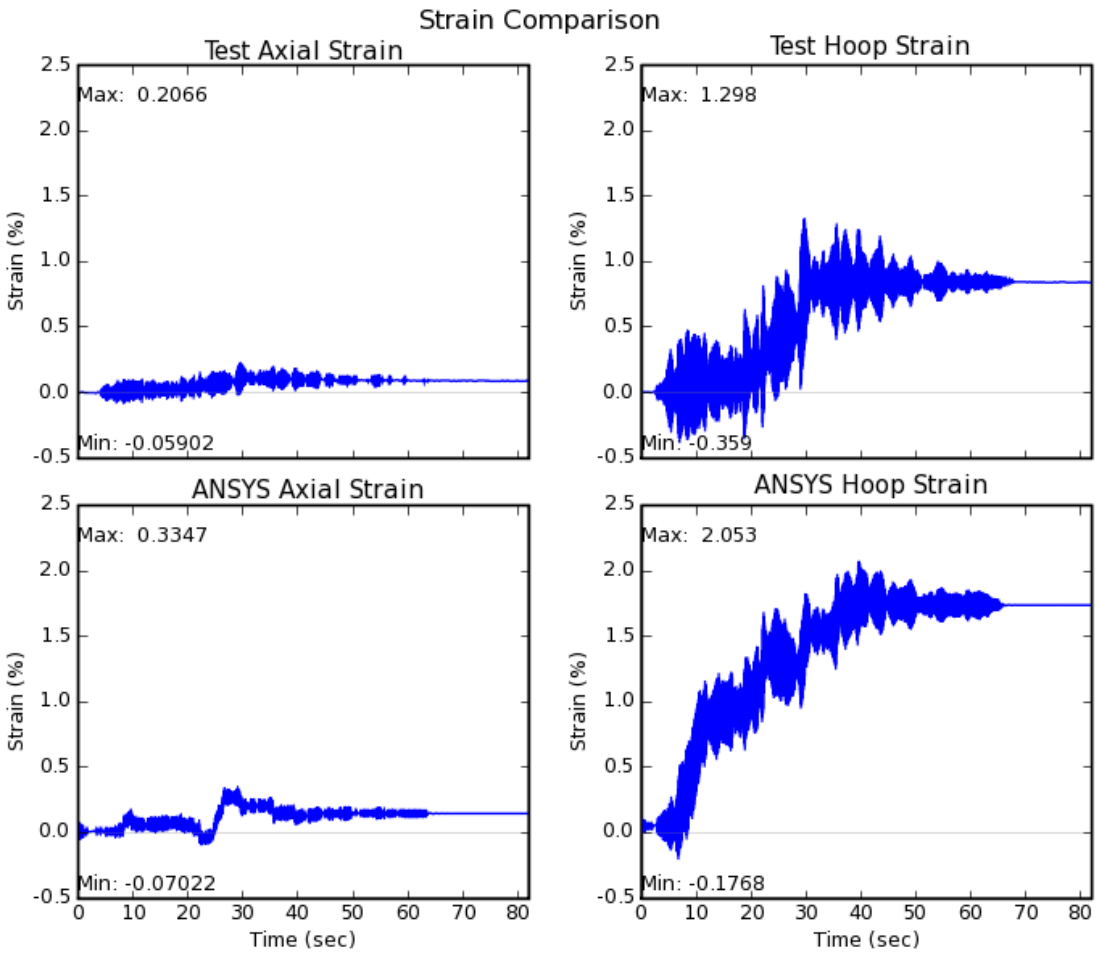

Figure 4-55 Strain Ratcheting Comparison at Element 154 for DM4-2(2) (Fresh Start)

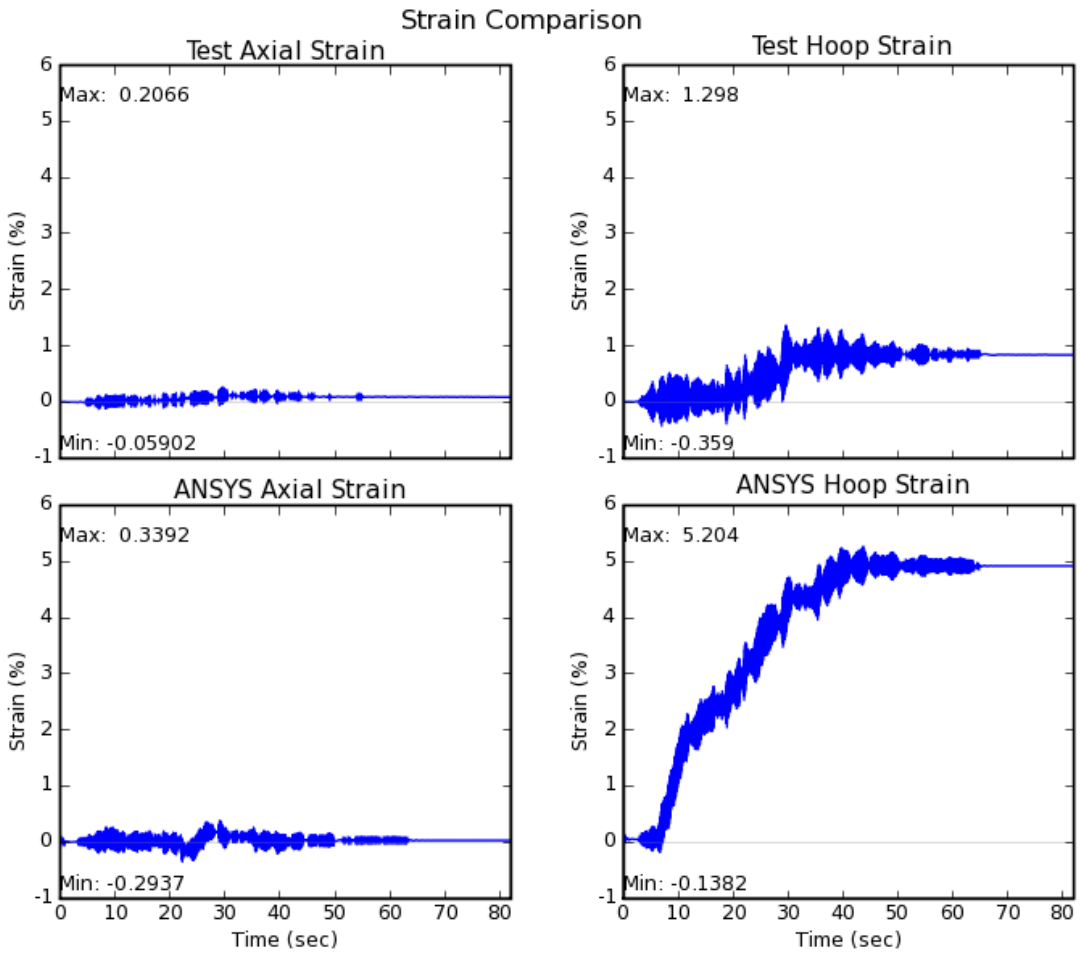

Figure 4-56 Strain Ratcheting Comparison at Element 639 for DM4-2(2) (Fresh Start)

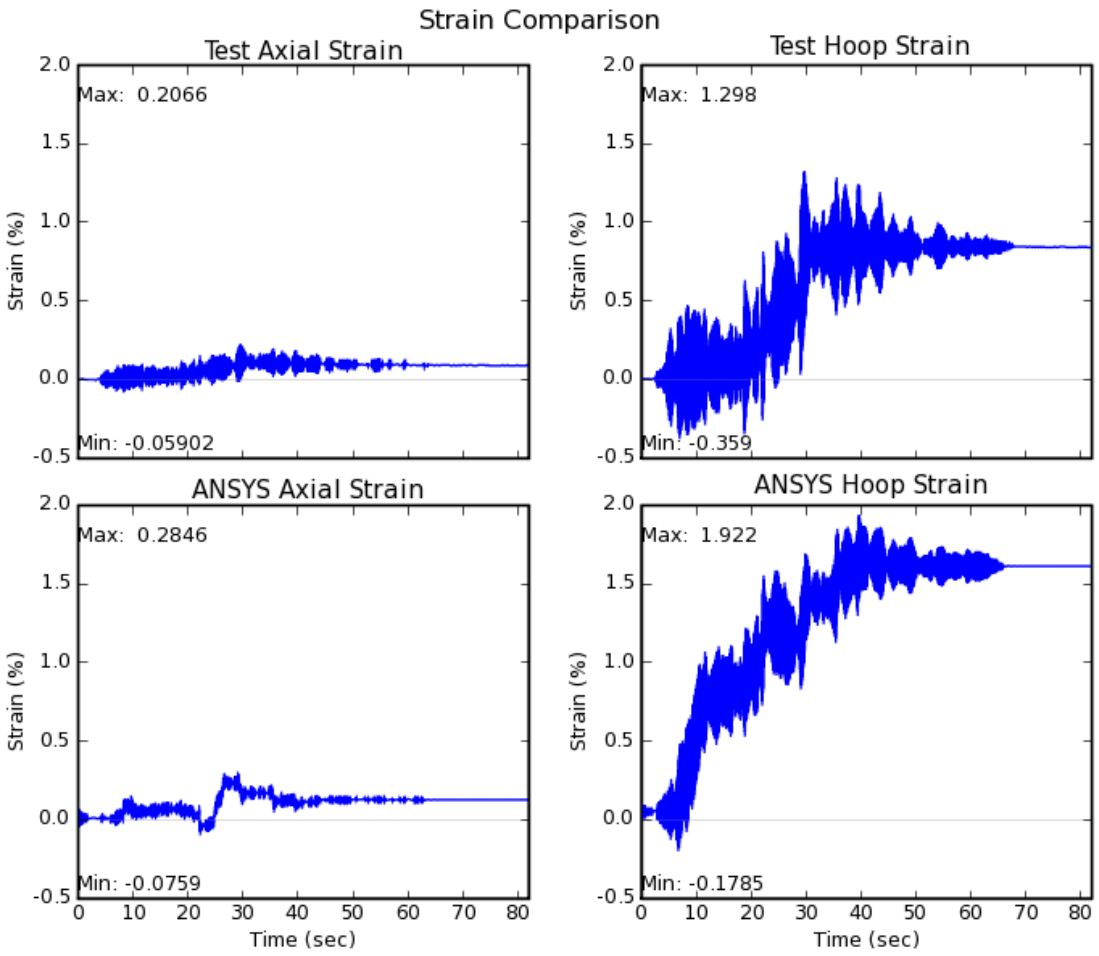

Figure 4-57 Strain Ratcheting Comparison at Element 648 for DM4-2(2) (Fresh Start)

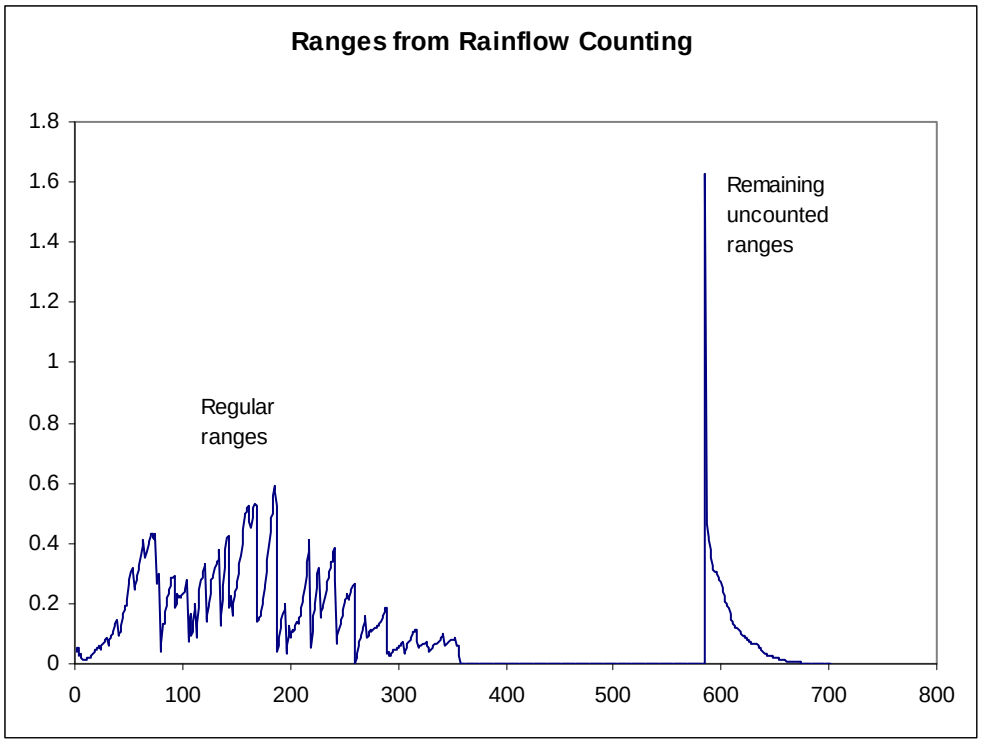

Figure 4-58 Sequence of Ranges from the Rainflow Counting Method

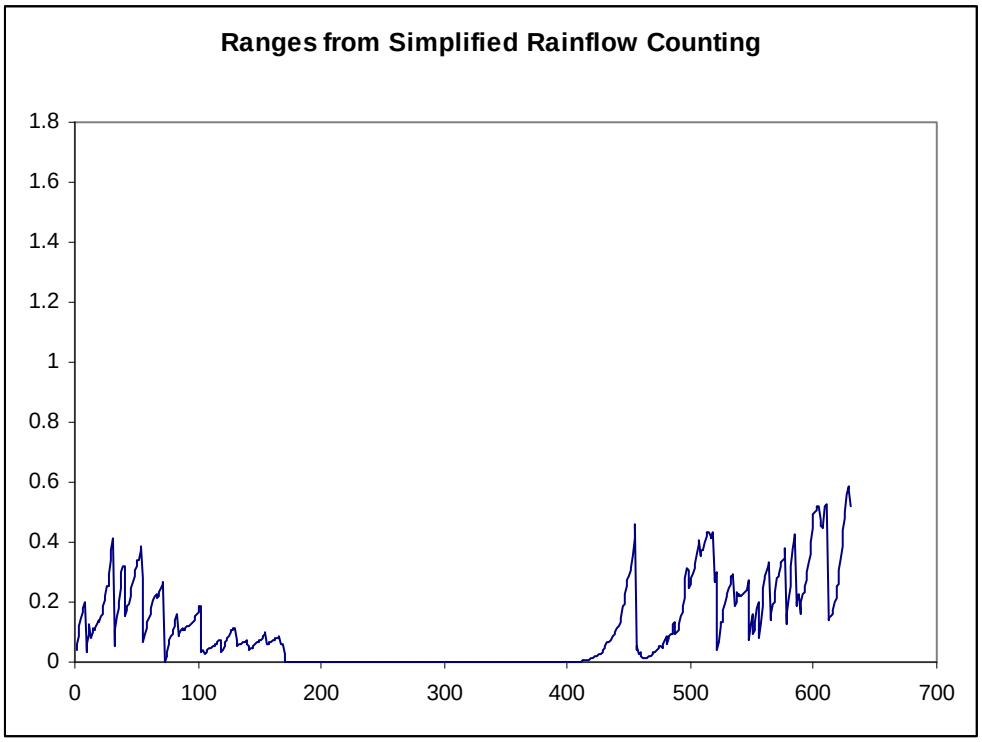

Figure 4-59 Sequence of Ranges from the Simplified Rainflow Counting Method

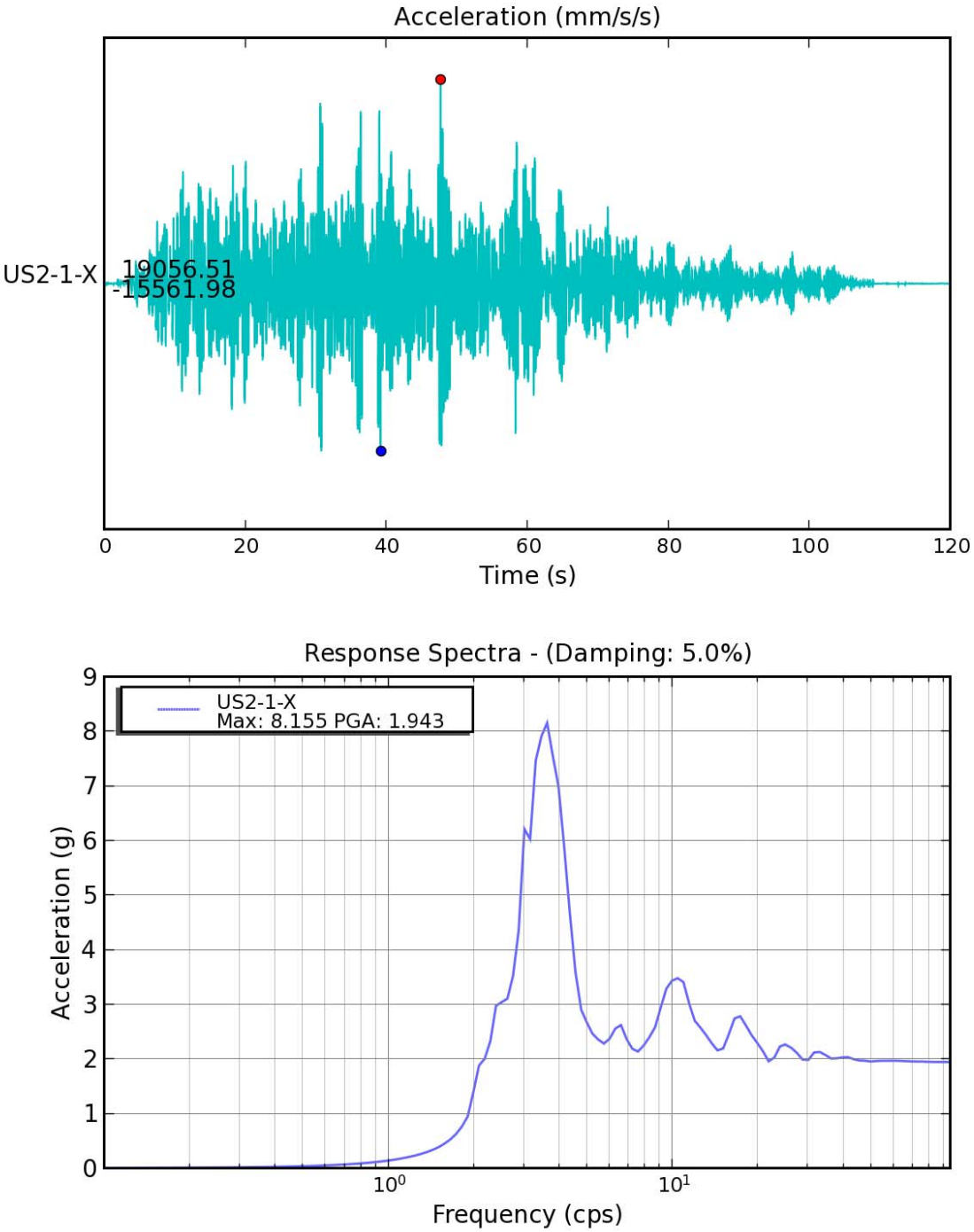

Figure 4-60 Horizontal Input Motion and its 5% Response Spectra For US2-1

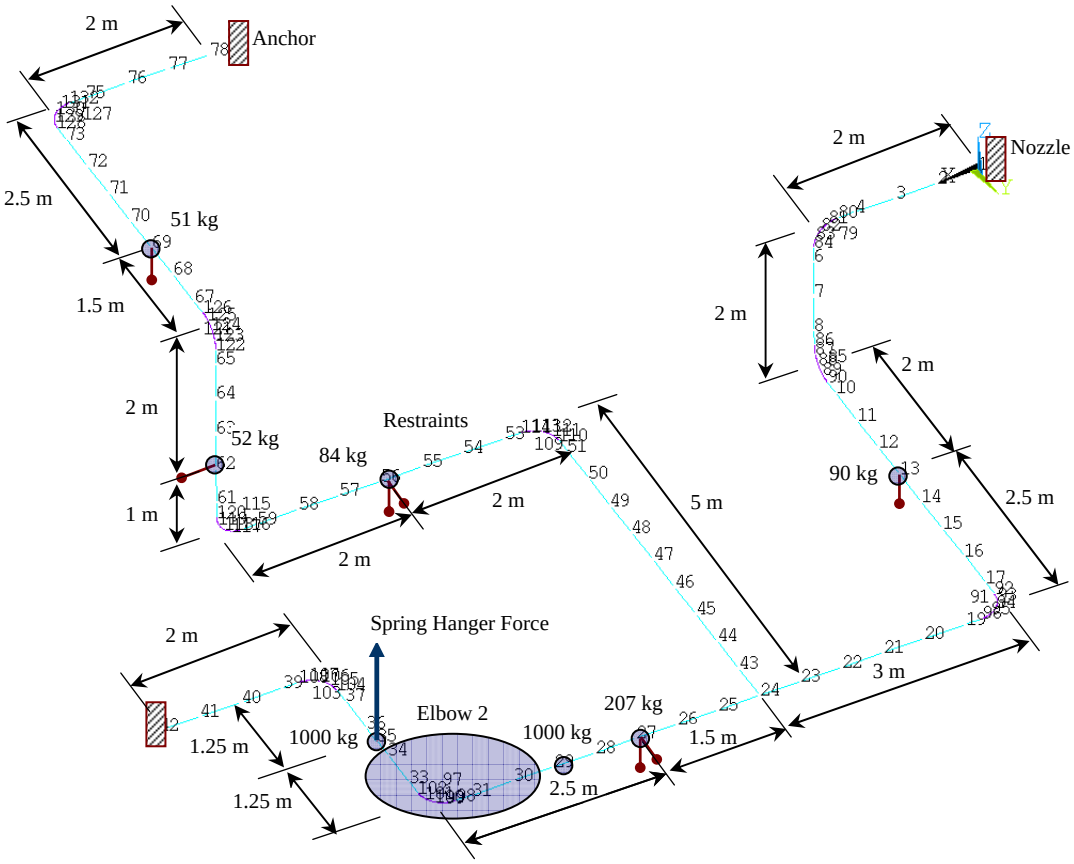

Figure 4-61 Piping System FE Model using Pipe Elements for Ultimate Strength Tests

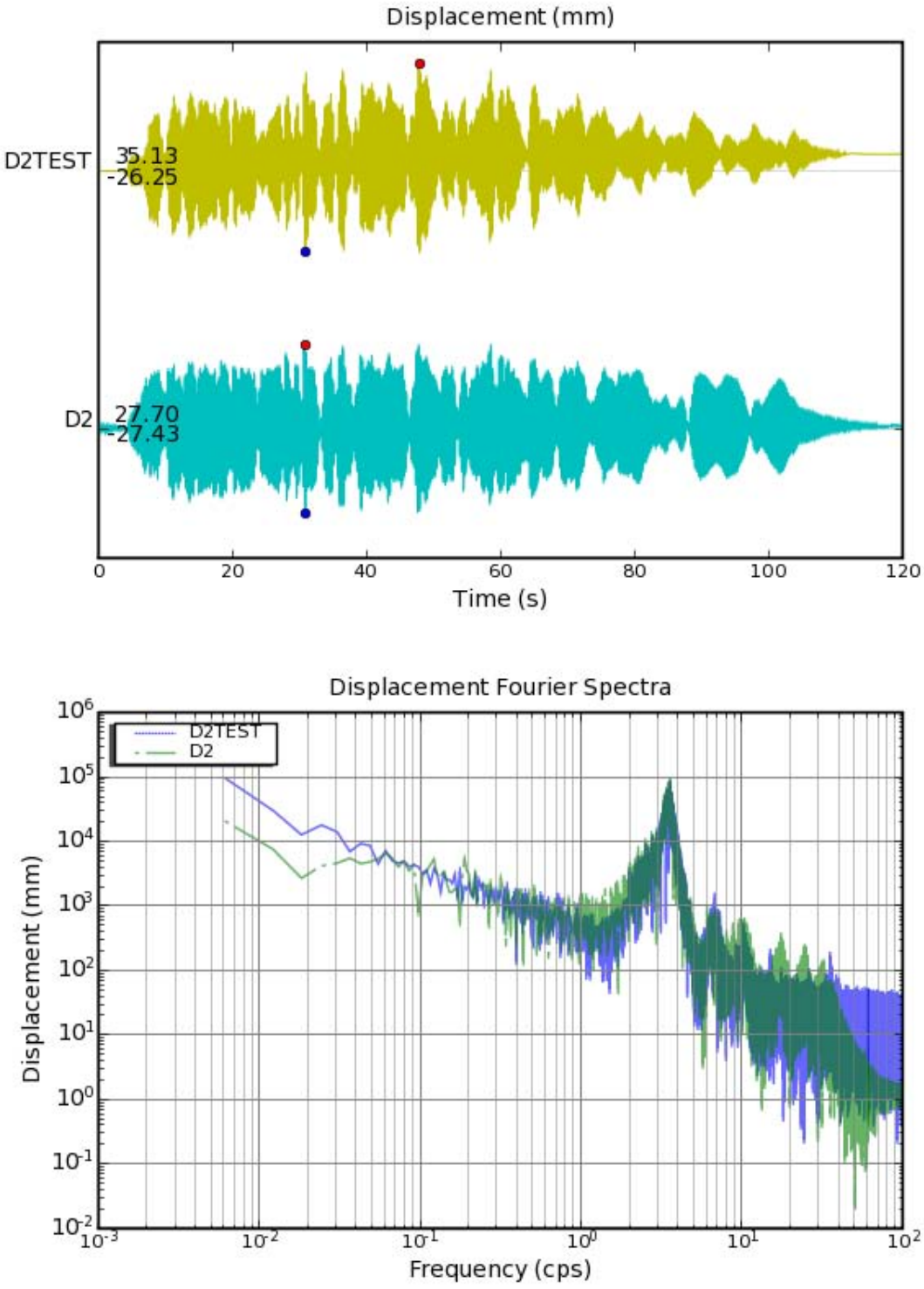

Figure 4-62 Displacement D2 Comparison for US2

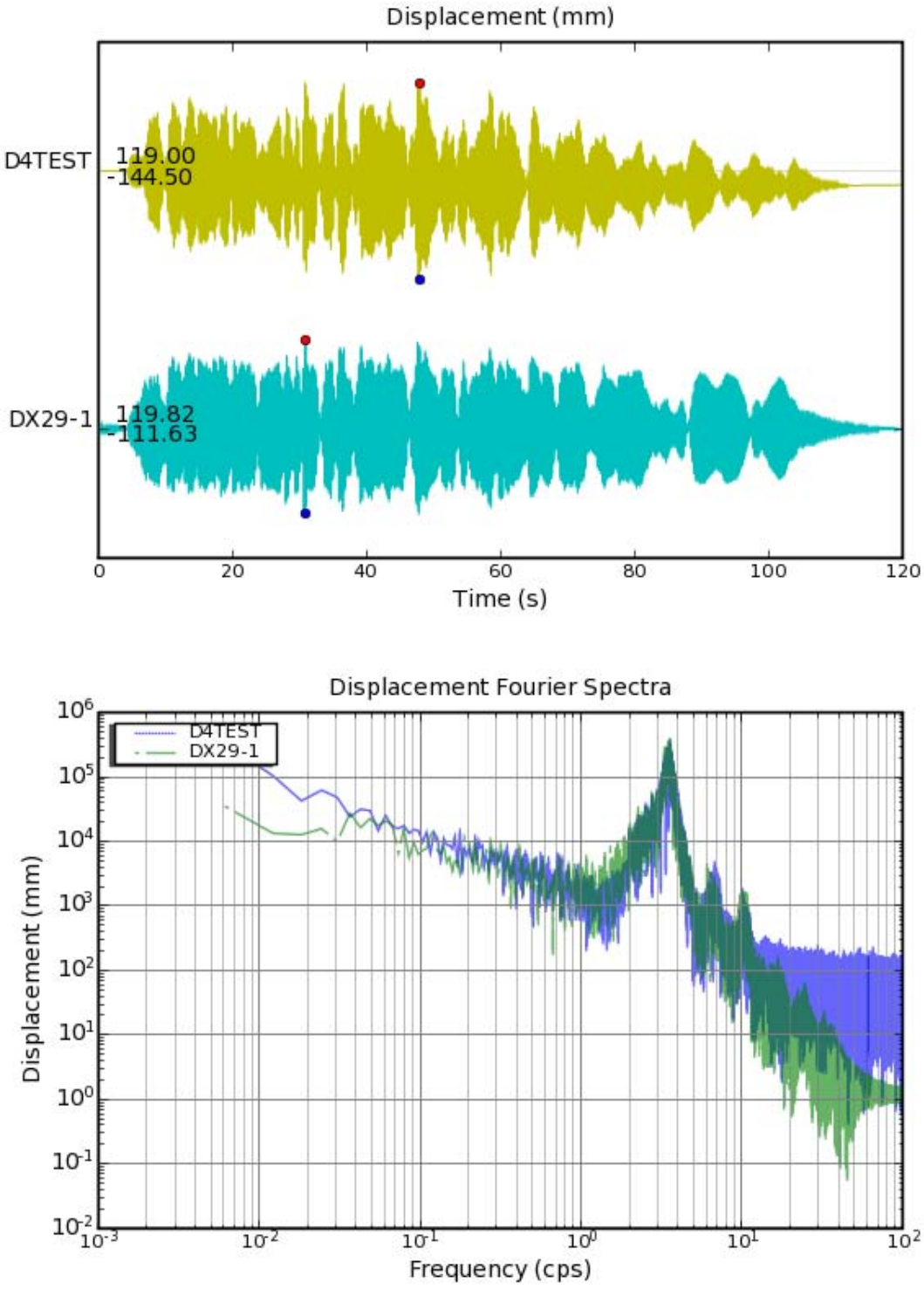

Figure 4-63 Displacement D4 Comparison for US2

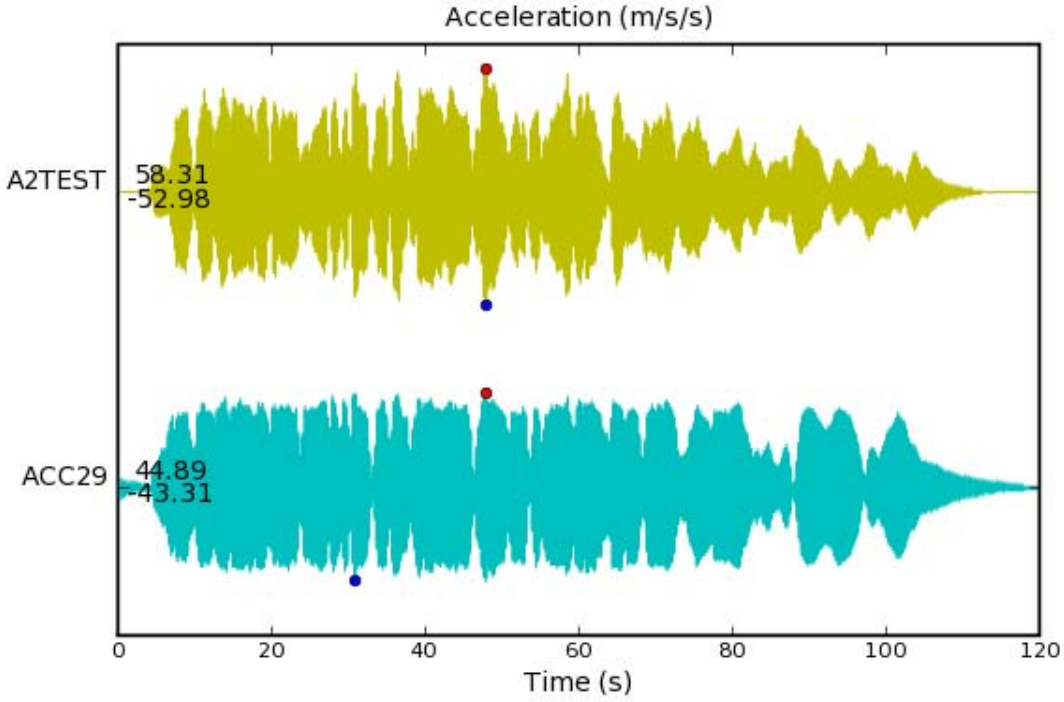

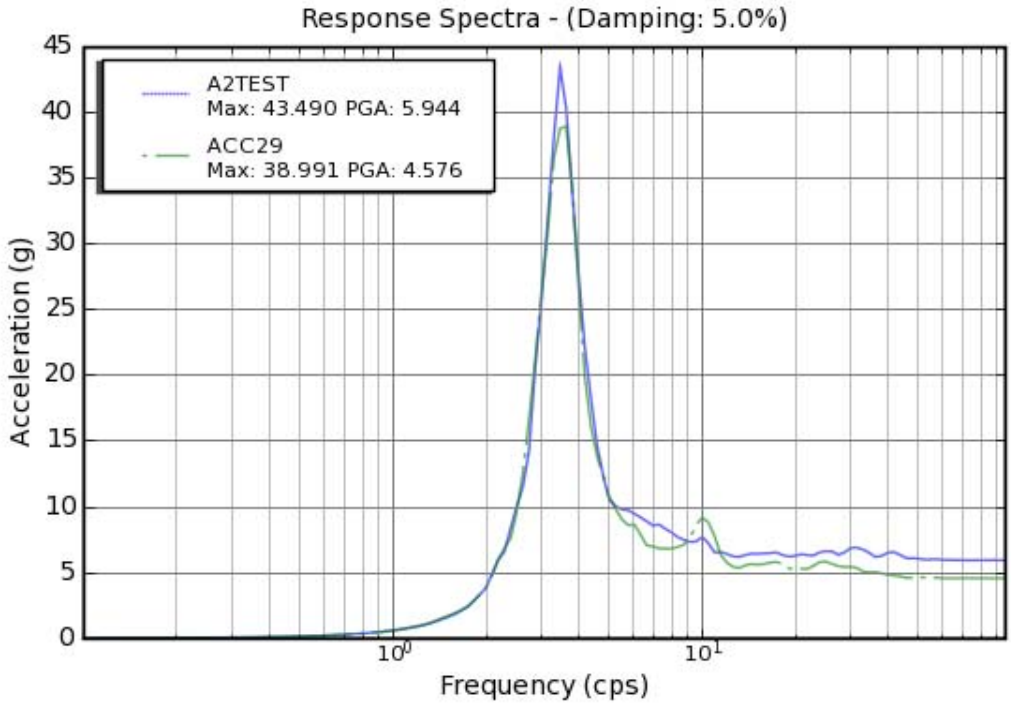

Figure 4-64 Acceleration A2 Comparison for US2

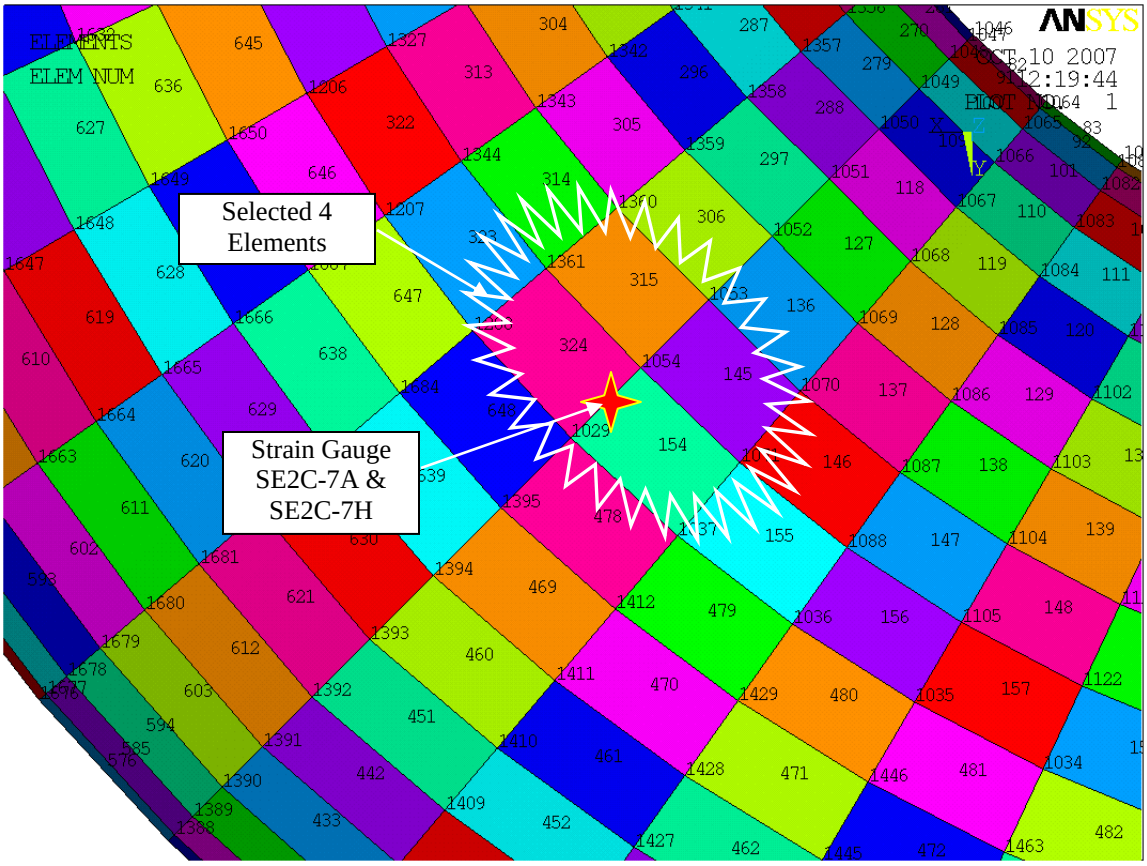

Figure 4-65 Nodes and Elements for Strain Measurements For US2-1

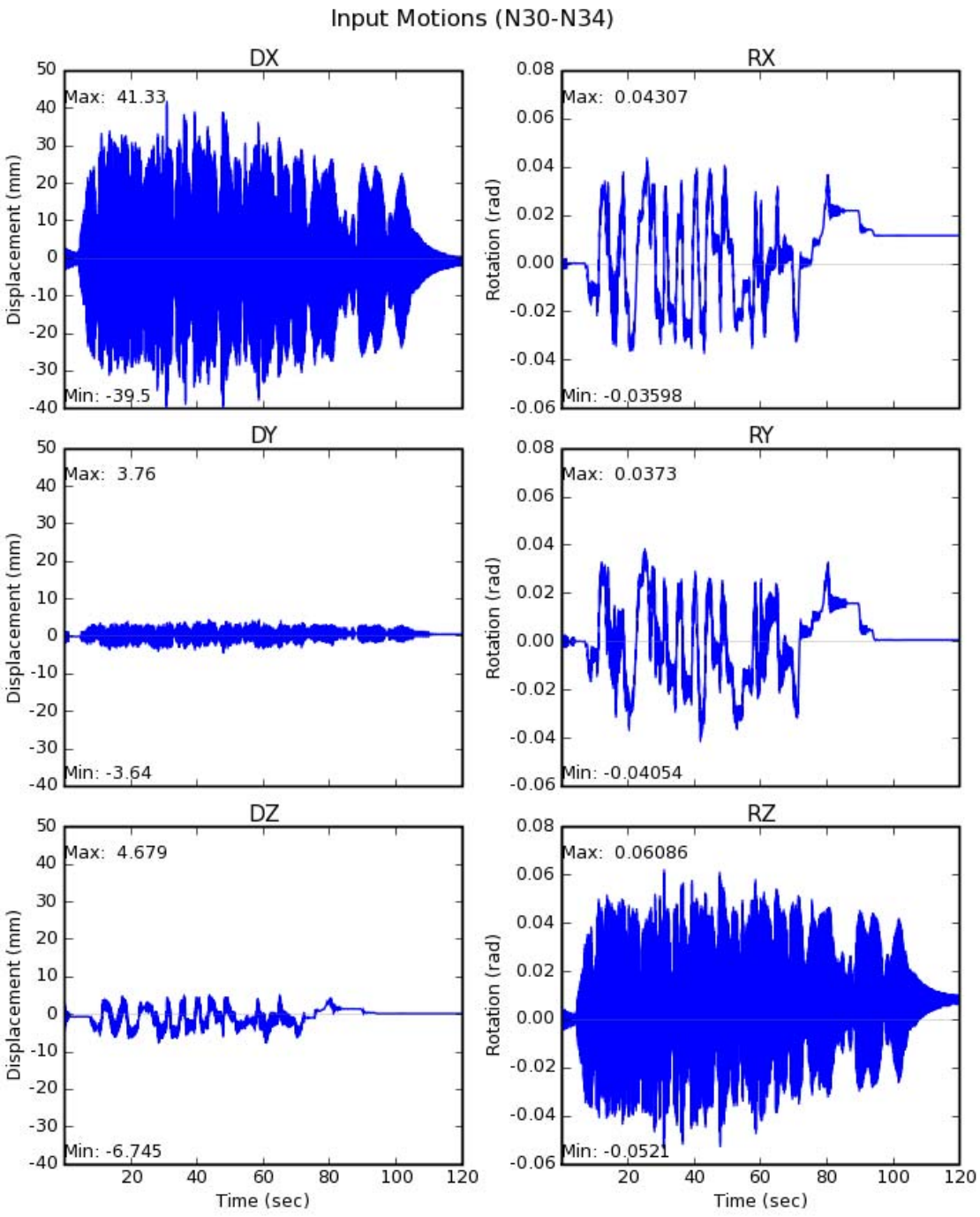

Figure 4-66 Relative Deformation Histories as Input Motions to Elbow Model for US2-1

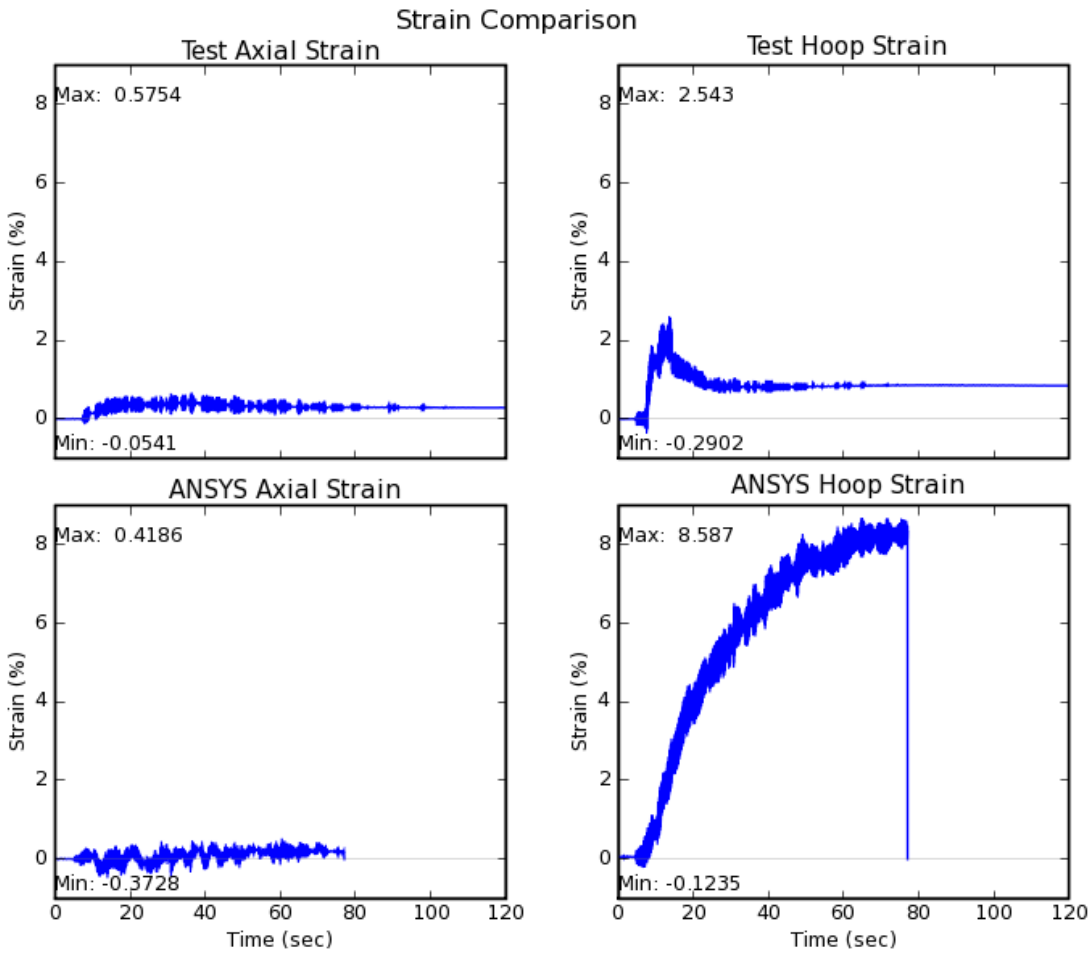

Figure 4-67 Strain Ratcheting Comparison at Element 145 for US2-1

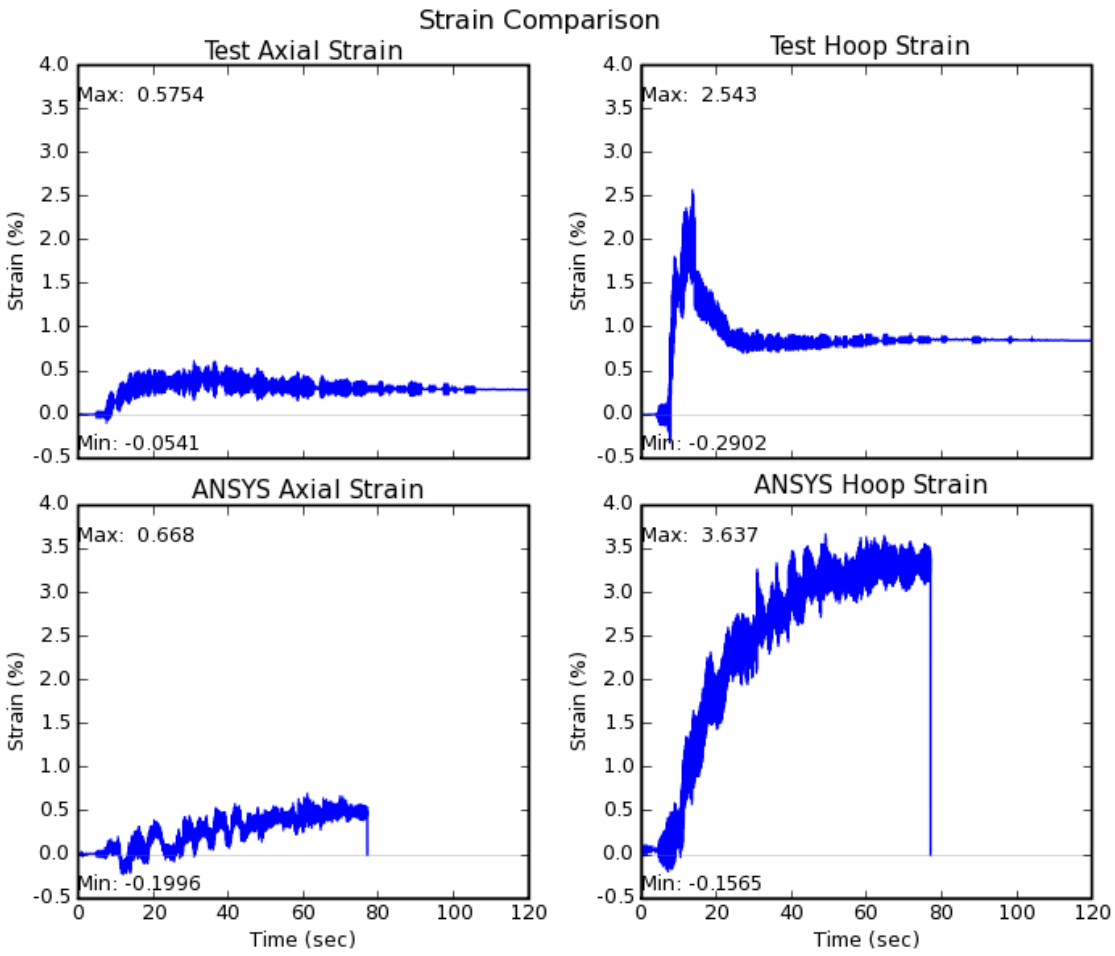

Figure 4-68 Strain Ratcheting Comparison at Element 154 for US2-1

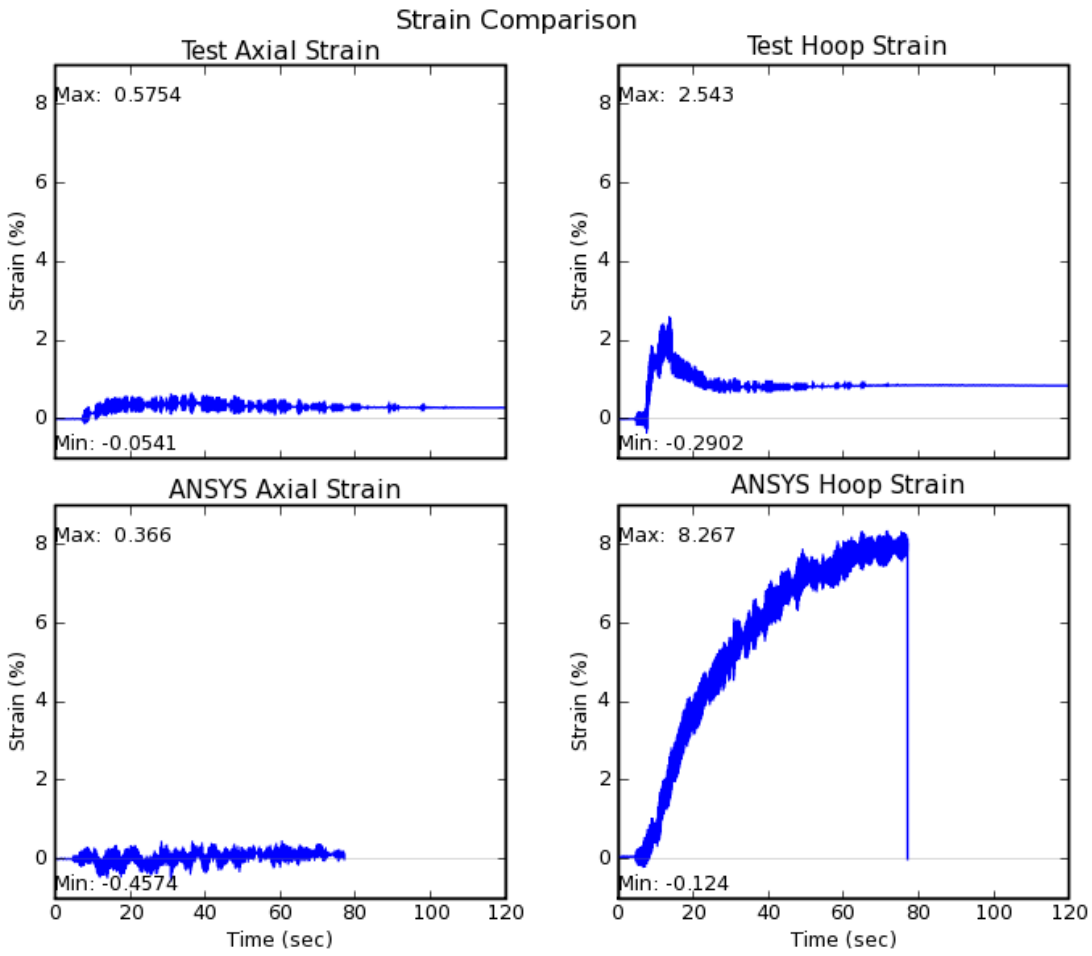

Figure 4-69 Strain Ratcheting Comparison at Element 315 for US2-1

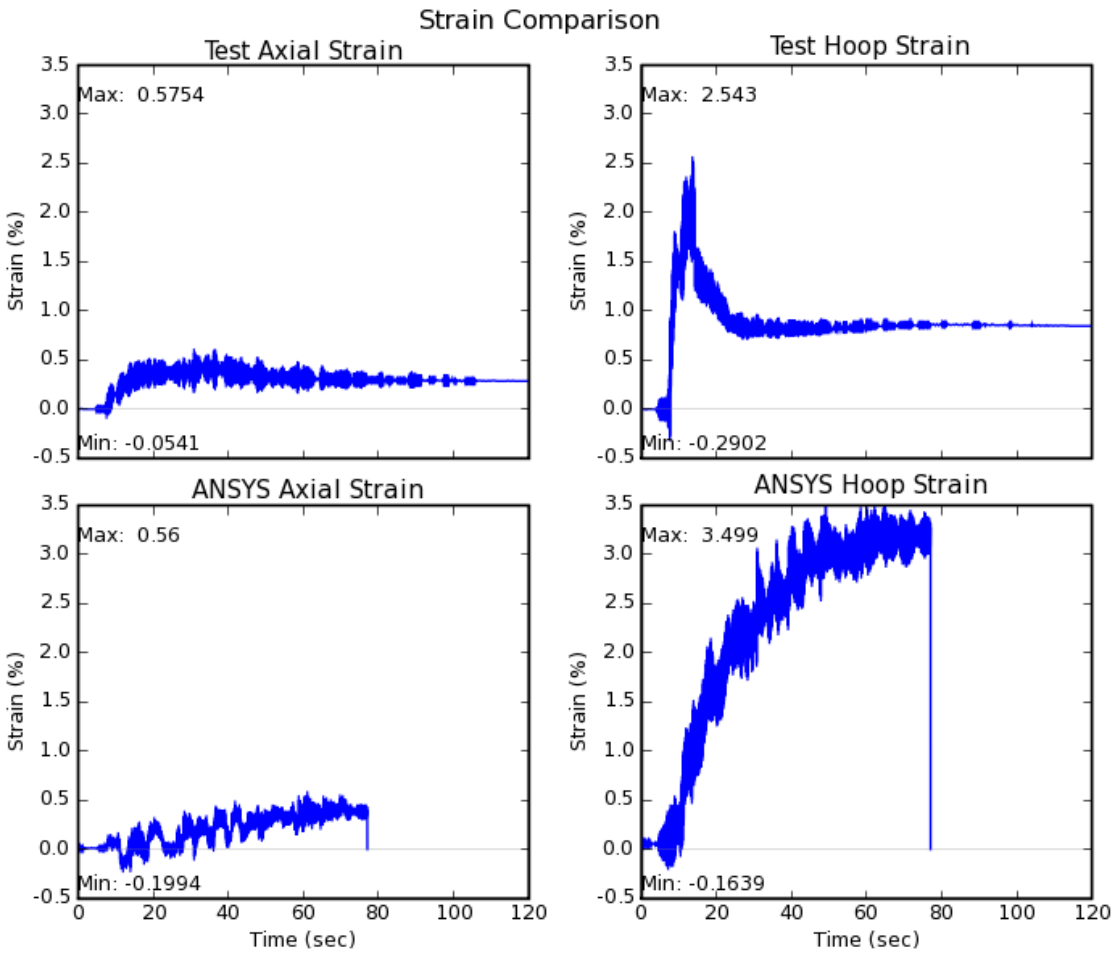

Figure 4-70 Strain Ratcheting Comparison at Element 324 for US2-1

5 CONCLUSIONS AND RECOMMENDATIONS

The JNES/NUPEC Ultimate Strength Piping Test Program has provided valuable new test data on high level seismic elasto-plastic behavior and failure modes for typical nuclear power plant piping systems. The JNES/NUPEC program was a comprehensive program, which included basic piping material tests, piping component static and dynamic tests, simplified piping system seismic tests, and shaking table seismic tests of a representative large-scale piping system to levels well above the typical design earthquake. A selected number of component and piping system tests including the large-scale piping test were carried out to failure. The test specimens were heavily instrumented to record displacements, accelerations and strains versus time at critical locations. The component and piping system tests demonstrated the strain ratcheting behavior that is expected to occur when a pressurized pipe is subjected to cyclic seismic loading. All pipe failures that were observed in this test program were characterized as through-wall cracks that occurred as a result of fatigue ratcheting.

The test data generated under this program augments the database of existing information on full-scale piping system and component seismic tests performed in the U.S. Although the JNES/NUPEC program was geared toward demonstrating margins in Japanese piping design, there are a number of similarities in materials and design requirements that make the test results applicable to U.S. piping designs. Technical justification for recent changes in the ASME Code piping design rules relied primarily on data collected under the EPRI/NRC Piping and Fitting Dynamic Reliability Program. The JNES/NUPEC data from the large-scale piping tests and from the previous simplified piping system tests [DeGrassi and Hofmayer 2005] may be evaluated in the same manner to provide additional technical justification from an independent test program.

As reported in Section 3 of this report, BNL performed linear analyses and Code evaluations for selected large-scale piping system tests. Linear analysis methods were applied in accordance with current and earlier ASME Code requirements and in accordance with NRC guidelines. The results demonstrated that the highest level JNES/NUPEC large-scale piping seismic tests subjected the piping components to stress levels well above Code allowables for the elbow. Since the as-built elbows were measured to be significantly thicker than the design dimensions, analyses were carried out using both design and as-built piping dimensions. The Code evaluation results illustrated the differences in minimum stress margins between different Code Editions and Addenda. For the ultimate strength test, which resulted in an elbow failure, the as-built piping dimension analyses showed that the 1994 and the 2004 Code analyses with 5 percent damping provided essentially identical margins of 2.63. The NRC-endorsed 1993 Code analyses using the NRC recommended damping value of 4 percent from Regulatory Guide 1.61 Revision 1 provided about 70 percent higher margins (4.50). The 1993 Code analyses using the NRC-accepted damping values from Code Case N-411 provided about 50 percent higher margins (3.94) than the 2004 Code analyses. Analyses using the Regulatory Guide 1.61 Revision 0 damping value of 2 percent provided the largest (140 percent) margins (6.35). Since a failure actually occurred at the highest stressed elbow, these margins may be interpreted as failure margins based on stress level for this specific test. However, it should be noted that since the number of cycles in these tests far exceeded the normal number of SSE cycles and the failure was characterized as a fatigue failure, some additional margin may be available. On the other hand, since the dominant seismic input frequency for the ultimate strength test was on-resonance, it is possible that a different seismic input may result in a smaller margin. As noted above, the results of these studies and of possible further evaluation of the large-scale piping test data could be useful in resolving some of the staff's technical concerns over the 2004 ASME Code alternative seismic piping design rules including damping values.

The JNES/NUPEC Ultimate Strength Piping Test Program provided substantial test data for benchmarking elasto-plastic analysis methods and computer codes. The BNL nonlinear analyses

described in Sections 4 of this report provided useful insights into the application of state-of-the-art elasto-plastic analysis methods for predicting the seismic response of a piping system. The BNL nonlinear analyses attempted to further develop and refine the earlier simplified piping system analysis methods for application to the large-scale piping analyses. This included improvements in defining the material models, input motion characterization, and finite element mesh density. Numerous complex nonlinear transient analyses were carried out. Two finite element models were created for both the design method confirmation tests and the ultimate strength tests. The first was a piping system model which used plastic pipe elements and a multi-linear material model to obtain the displacement and acceleration responses for the entire piping system. The second model was an elbow model which used finite strain shell elements and the Chaboche nonlinear material model to obtain the strain responses. The displacement responses at two nodes around one elbow, generated from the piping system model, were used as the input displacement boundary conditions for the elbow model.

The analyses showed that the piping system model can accurately predict the displacement and acceleration responses for low to moderate input motions and less accurately for high input motions. For the design method confirmation tests, it was noted that the plasticity accumulation in the piping system model affected the performance of the piping system model only during the early part of the input motion and did not change the overall response for the entire time histories. The displacement and acceleration responses appear to be restrained for large input motions which may imply that the multi-linear material model resulted in shakedown behavior. The elbow model predicted relatively accurate strain ratcheting histories compared to test data. However, it was noted that the level of accuracy for the analysis to test strain comparisons was not as good as for the piping system displacement and acceleration response. The comparison of the maximum strain ranges appeared to be more consistent among the four selected elements and generally better than comparisons using the entire strain ratcheting histories.

For potential further studies of these test results, some additional modeling and analysis improvements can be explored. These improvements may include (1) refinement of the piping system model with smaller element sizes, (2) refinement of the elbow model locally at the strain range location, (3) characterization of the strain gradient along the hoop direction, (4) a transient analysis of the elbow model to take into account the inertia and damping effect, (5) a combined model with pipe elements for straight pipe segments and shell elements for the elbows and nozzles, (6) investigation of methods to better consider the plasticity accumulation over a series of consecutive tests, and (7) examination of the fatigue ratcheting failure mechanism. Items 4 through 7 require the use of high performance computers.

Although improvements in the analytical predictions with the updated material and finite element models were observed, large variations in the test comparisons, particularly for strain and strain ratcheting were still noted. The nonlinear dynamic characteristics of a large piping system are difficult to predict with high accuracy even when state-of-the-art models and finite element codes are used. In regulatory activities related to piping systems in nuclear power plants, reviewers should be aware of such difficulties and uncertainties in any piping system seismic analysis submittals involving elasto-plastic analysis. Furthermore, continued investigation of the subject may lead to a better understanding of the analytical methods and even quantification of the uncertainties in these methods and the supporting test data.

6 REFERENCES

American Society of Mechanical Engineers (1986). "ASME boiler and pressure vessel code, code case N-411-1, alternative damping values for response spectra analysis of class 1, 2, and 3 piping," Section III, Division 1, New York, NY. Approved February 20, 1986, Annulled May 5, 2000.

American Society of Mechanical Engineers (2004). "Dynamic analysis methods," *Boiler and Pressure Vessel Code*, 2004 Edition, Section III, Division 1, Non-Mandatory Appendix N, New York, NY.

ANSYS (2007). "Release 11.0 documentation for ANSYS," Online Manual, ANSYS, Inc.

Armstrong, P.J. and Frederick, C.O. (1966). "A mathematical representation of the multiaxial bauschinger effect," CEGB Report No. RD/B/N 731.

Bari, S. and Hassan, T. (2000) "Anatomy of Coupled Constitutive Models for Ratcheting Simulations," *International Journal of Plasticity*, Vol. **16**, pp. 381-409.

Besseling, J.F. (1958). "A theory of elastic, plastic and creep deformations of an initially isotropic material," *Journal of Applied Mechanics*, Vol. **25**, pp. 529-536.

Borsoi, L. and Ricard, A. (1985). "A simple accelerogram correction method to prevent unrealistic displacement shift," *8th SMIRT*, Vol.**K**(a), Paper K2/7, Brussels.

Chaboche, J.L. (1986). "Time independent constitutive theories for cyclic plasticity," *International Journal of Plasticity*, Vol. **2**, pp. 149-188.

DeGrassi, G. and Hofmayer, C. (2005). "Seismic analysis of simplified piping systems for the NUPEC ultimate strength piping test program," *NUREG/CR-6889*, by Brookhaven National Laboratory for the US Nuclear Regulatory Commission, December, 2005.

Downing, S.D. and Socie, D.F. (1982). "Simplified rainflow counting algorithms," International Journal of Fatigue, **4** (1), pp. 31-40.

Hadjian, A.H. (1988). "Piping system damping evaluation," EPRI NP-6035, Electric Power Research Institute, Palo Alto, California.

JNES (2003). "Ultimate strength piping test program – large scale piping system tests and analysis", Status Report, June, 2003.

Matsuishi, M. and Endo, T. (1968). "Fatigue of metals subjected to varying stress," *paper presented to Japan Society of Mechanical Engineers*, Fukuoka, Japan.

Nie, J., Xu J., and Costantino, C. (2007). "P-CARES: probabilistic computer analysis for rapid evaluation of structures," *NUREG/CR-6922*, by Brookhaven National Laboratory for the US Nuclear Regulatory Commission, January, 2007.

Prager, W. (1956). "A new method of analyzing stresses and strains in work hardening plastic solids," *Journal of Applied Mechanics*, Vol. **23**, pp. 493-496.

Suzuki, K., et al. (2001). "Seismic proving test of ultimate piping strength," ICONE-9, Paper No. **155**.

Suzuki, K., et al. (2002). "Seismic proving test of ultimate piping strength," ICONE-10, Paper No. **22225**.

U.S. Nuclear Regulatory Commission, Regulatory Guide 1.61 [1973]. "Damping values for seismic design of nuclear power plants," Revision 0, NRC, Washington D.C., October, 1973.

U.S. Nuclear Regulatory Commission, Regulatory Guide 1.61 [2007]. "Damping values for seismic design of nuclear power plants," Revision 1, NRC, Washington D.C., March, 2007.

U.S. Nuclear Regulatory Commission, Regulatory Guide 1.92 [2006]. "Combining model responses and spatial components in seismic response analysis," Revision 2, NRC, Washington D.C., July, 2006.

U.S. Nuclear Regulatory Commission, Regulatory Guide 1.122 [2006]. "Development of floor design response spectra for seismic design of floor-supported equipment or components," Revision 1, NRC, Washington D.C., February, 1978.

Ware, A.G. (1991). "The history of allowable damping values for U.S. nuclear plant piping," *Transactions of the ASME*, Vol **113**, 284-290.

APPENDIX A IMPACT OF 4% AND 5% DAMPING RATIOS ON PIPING SYSTEM RESPONSES

A.1 Introduction

Damping is a generic term representing the ability of a dynamic system to dissipate the input energy such as seismic motions, and is a significant factor in appropriately determining the dynamic response of piping systems. For mathematical simplicity in an elastic dynamic analysis, damping is practically modeled by an equivalent viscous damping, which results in a damping force proportional to the velocity. Since energy dissipation in various piping systems encompasses numerous contributors, such as piping plastic deformation, support configuration, energy radiation, equipment coupling, internal fluid, and other mechanisms, the equivalent viscous damping for a piping system is very difficult to estimate. The difficulty in estimating the viscous damping value also includes many indirect factors, such as methods in identifying the damping ratio from test data and the excitation level dependency of the damping. Significant variation in damping ratio estimate is shown in a large amount of experimental data [Hadjian 1988, Ware 1991].

However, an appropriate damping ratio of the piping systems in nuclear power plants is inevitably required for codified design and regulation; unfortunately, an agreement on its value has been far from being reached among the industry design codes and regulatory guidance documents. In particular, NRC RG 1.61, Revision 1, issued in March 2007, prescribes constant damping ratios of 4% for SSE and 3% for OBE. These constant damping ratios can be used in time history analysis, response spectrum analysis, and equivalent static analysis. RG 1.61, Revision 1 also allows the use of a frequency-dependent damping model in response spectrum analysis. The ASME Boiler and Pressure Vessel Code [2004] currently recommends a frequency-independent damping ratio of 5% for both OBE and SSE in Non-Mandatory Appendix N. Constant damping ratio(s) over all frequencies and diameters is common to both the ASME code and the RG 1.61; the recommended values of the damping ratio are different.

In late 2006, industry representatives raised dissenting comments about the 4% damping ratio for seismic analysis of piping systems recommended in the draft regulatory guide DG-1157, which was formally issued as RG 1.61, Revision 1, in March 2007. Evaluation of these comments and a recent review of the EPRI NP-6035 report, which is identified as the technical basis for the 5% damping ratio recommended in ASME Boiler and Pressure Vessel Code Section III, Non-Mandatory Appendix N [2004], do not reveal sufficient technical basis to accept 5% piping damping in RG 1.61. Therefore, the difference in damping ratios for seismic analysis of piping systems remains unresolved.

An appropriate (or correct) damping ratio (or model) for the seismic analysis of piping systems may require more than just regression analysis of the damping test data. As a minimum, a calibration of any proposed damping value based on the reliability (or the traditional safety factor) of designed piping systems should be carried out to determine whether the desired level of safety can be achieved economically.

This appendix summarizes a recent study on how much impact the 4% versus 5% damping ratios can have on the dynamic response of a typical large-scale piping system. The piping system model and the associated analysis strategy are introduced before the assessment of the response differences is presented at the end.

A.2 Piping System Models and Analyses

The piping system models discussed in Section 3, including models for the design method confirmation tests (DM tests) and the ultimate strength tests (US tests), are used for the study of the differences in dynamic response due to 4% versus 5% damping ratios. Each model also has two variations; one with

nominal dimensions for the straight pipe segments and the elbows, and the other with nominal dimensions for the straight pipe segments but as-built dimensions for elbows. The configurations of the models are shown in Figure 3-1 and Figure 3-2 of this report.

Response spectrum analyses were performed on these models. The analyses presented in this appendix consider only the seismic loads in individual directions, without combination of internal pressure, gravity load, and seismic loads in different directions. For each variation of the models, the five seismic load cases described in Section 3 are used for this study, including DM2-2 horizontal and vertical seismic loads, DM4-2(2) horizontal and vertical seismic loads, and US2-1 horizontal seismic loads. The response spectra of these loads are shown in Figure 3-3 through Figure 3-7. Each of these five load cases will include the unbroadened and broadened input spectra. The spectrum-broadening algorithm was developed following the simplified approach in the RG 1.122, which allows a 15% broadening factor at each peak (see Figure A-2 and Figure A-4 for examples).

The combination of the models, loads, and two damping ratios results in a total of 40 piping analyses using the ANSYS program.

Using the response spectrum method, a complete solution is found for each of the 40 analyses using the Combination Method B in RG 1.92, Revision 2, which is a combination of the static ZPA method and the Lindley-Yow method. The complete quadratic combination (CQC) method with the Der Kiureghian correlation coefficient, designated as the CQC combination method in ANSYS, is used to combine the periodic modal responses. For a few cases where the first natural frequency is lower than the frequency of the lowest-frequency spectral acceleration peak (peak frequency), the rigid response coefficient is set to zero (conservatively) in accordance with the RG 1.92 requirement. This modification indicates that the beginning part of the input spectrum with frequencies below the peak frequency is considered to generate purely periodic response. ANSYS can only handle 20 data points for any input spectrum; therefore, data points are selected from the modified input spectra curve such that approximations occur in the high frequency range where the modal contribution to the complete solution is small. Without performing a sensitivity analysis to determine the significant modes, the frequency for zero period acceleration (ZPA) is conservatively selected as 60 Hz; any mode of a frequency less than 60 Hz is retained in the modal combination.

Figure A-1 through Figure A-4 show the original input spectra and their modified versions to remove the rigid response component in the application of Lindley-Yow method for various analysis scenarios for the US2-1 model. In these figures, the red line designates the original spectra, the blue line designates the modified spectra, and the dots on the blue curve designate the data points used for the ANSYS input. The vertical dashed lines indicate the natural frequencies selected for the modal combination. ANSYS linearly interpolates the input spectra in log-log scale; therefore, the deep valleys are not visible in ANSYS and do not affect much the accuracy anyway because they locate in the region of high frequency modes.

A.3 Result Assessment

Table 3-1 through Table 3-6 of Section 3 summarizes the maximum code stresses in elbows, tees, nozzles for different damping ratios. These stresses include the responses from internal pressure, gravity load, and seismic loads in two directions (except for US2-1 that has only one horizontal seismic component). Compared to 5% damping, the maximum stress is on average 9% higher for 4% damping. The natural frequency shift due to the use of nominal dimension or as-built dimension does affect the percentage difference in the maximum code stress between the 4% and 5% damping ratios; however, the influence of the frequency shift depends on whether it shifts toward or away from the peak frequency of the input spectra. For example, because the fundamental frequency for DM2-2 shifts away from the peak frequency by switching the nominal dimensions to the as-built dimensions, the increase of the maximum

code stress by using a damping ratio of 4% rather than 5% decreases from 8% to 2%. However, the case for the US2-1 shows just the opposite.

To evaluate the impact of the damping ratio in a slightly different way, the reactions to the piping systems are utilized in this appendix for comparison. For the DM model, there are 17 reaction forces and 9 reaction moments. For the US2-1 model, there are 16 reaction forces and 9 reaction moments. The comparison was made by either considering all reactions or considering only the significant ones, which are defined as the top half reactions when ranked by magnitude.

Figure A-5 and Figure A-6 show histograms for the ratio of the reaction forces and the ratio of the reaction moments using all data. The mean and the standard deviation of the percentage increase in these reactions (PIR) using 4% damping versus 5% damping are about 11~12% and 4~5%, respectively. If the top half significant reactions (ranked by magnitude) are used in the comparison to merit more weight on the large reactions, as shown in Figure A-7 and Figure A-8, the mean of the same percentage increase decreases slightly to 10~11% while the standard deviation remains about the same. The four comparisons shown in these figures also show that the maximum percentage increase is about 20%. The PIR appear to be somewhat larger than those for the maximum code stress, partly because the internal pressure and gravity load used in the maximum code stress calculation do not change with damping. It should be noted that the internal pressure, gravity load, and seismic load in other directions are not considered in the analyses to obtain the reactions.

The effect of spectrum broadening on the PIR is demonstrated through Figure A-9 through Figure A-16. By using broadened input spectra instead of the unbroadened input spectra, the mean of the PIR uniformly increases by 3% for all cases, the standard deviation of the PIR slightly decreases, and the maximum of the PIR increase in various degrees but remains close to 20%. Therefore, using the broadened spectra as in the current design practice is unambiguously conservative in assessing the difference in dynamic responses due to 4% damping versus 5% damping.

In summary, compared to 5% damping, the reactions of piping systems subjected to just seismic excitations can be 10~16% [mean ~ mean + standard deviation] higher using 4% damping, while the maximum increase in reactions can be 20%. These observations should be applicable to the internal forces/moments in the piping systems as the linear analyses implies. Comparing cases using 4% damping versus 5% damping, the slightly lower increase in the maximum code stress (9%) is believed to be caused by the loads other than the subject seismic load. Broadening of the input spectra can add an additional 3% percentage increase in reactions, compared to using unbroadened input spectra.

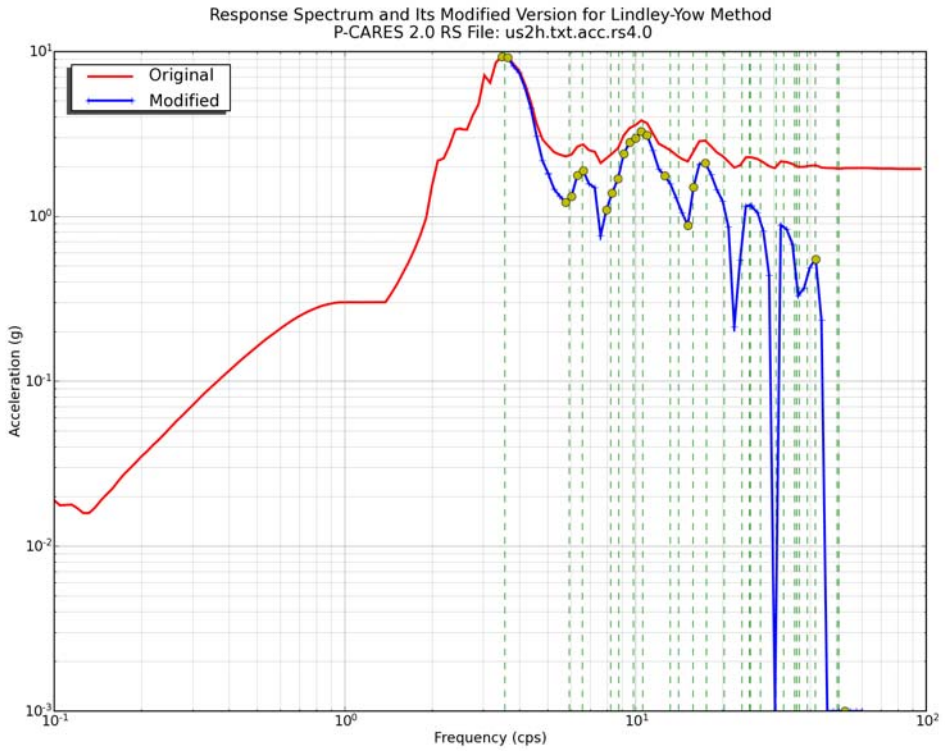

Figure A-1 Original and Modified Response Spectra for Lindley-Yow Method for US2-1 As-built Dimension and 4% Damping

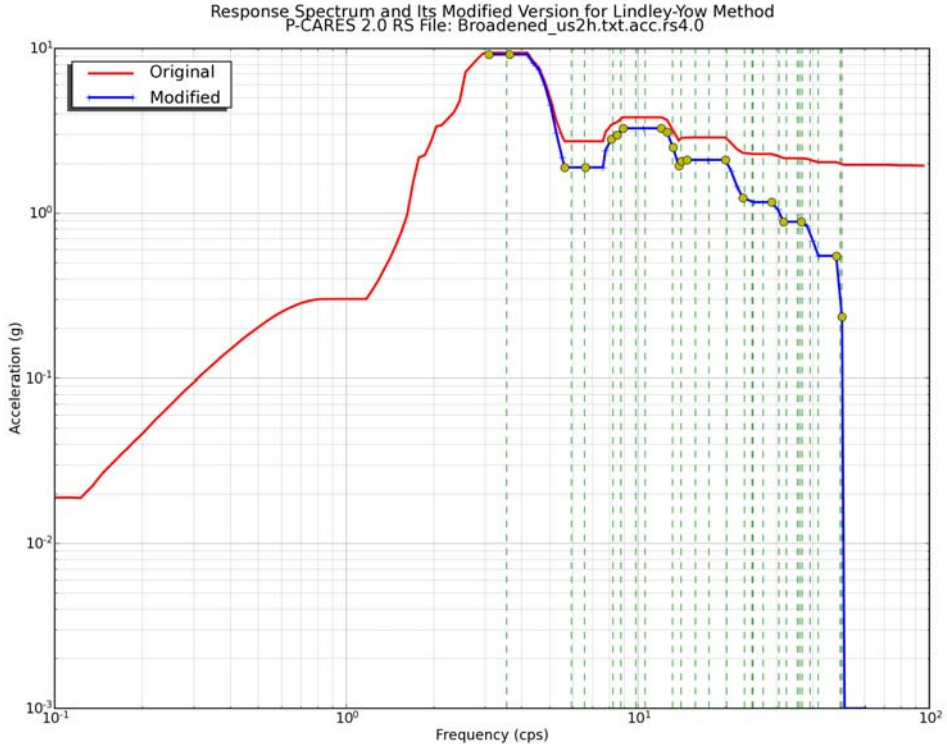

Figure A-2 Broadened Original and Modified Response Spectra for Lindley-Yow Method for US2-1 As-built Dimension and 4% Damping

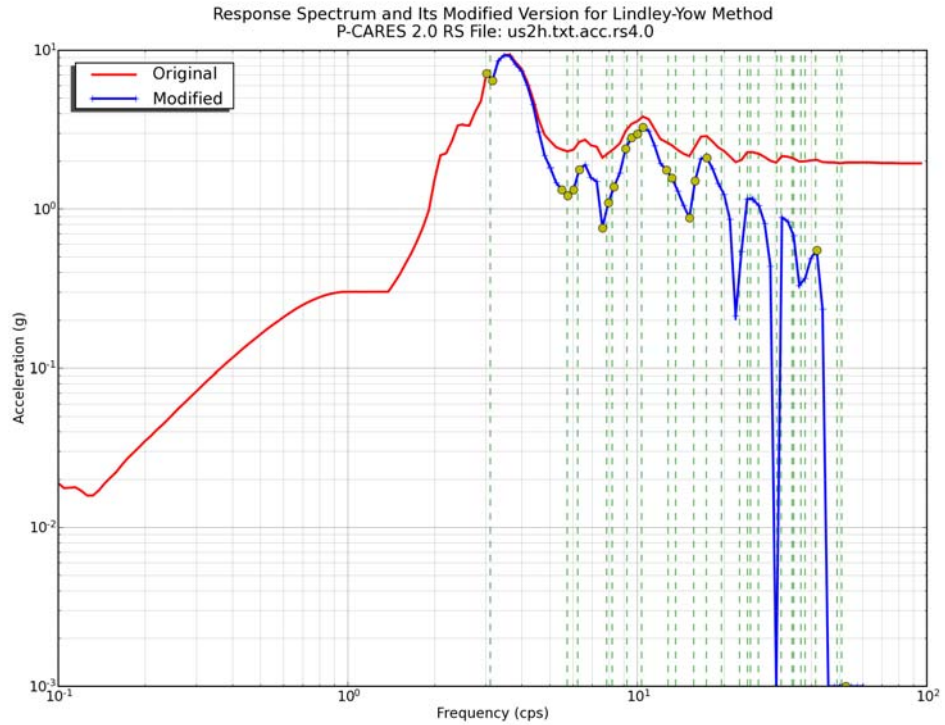

Figure A-3 Original and Modified Response Spectra for Lindley-Yow Method for US2-1 Nominal Dimension and 4% Damping

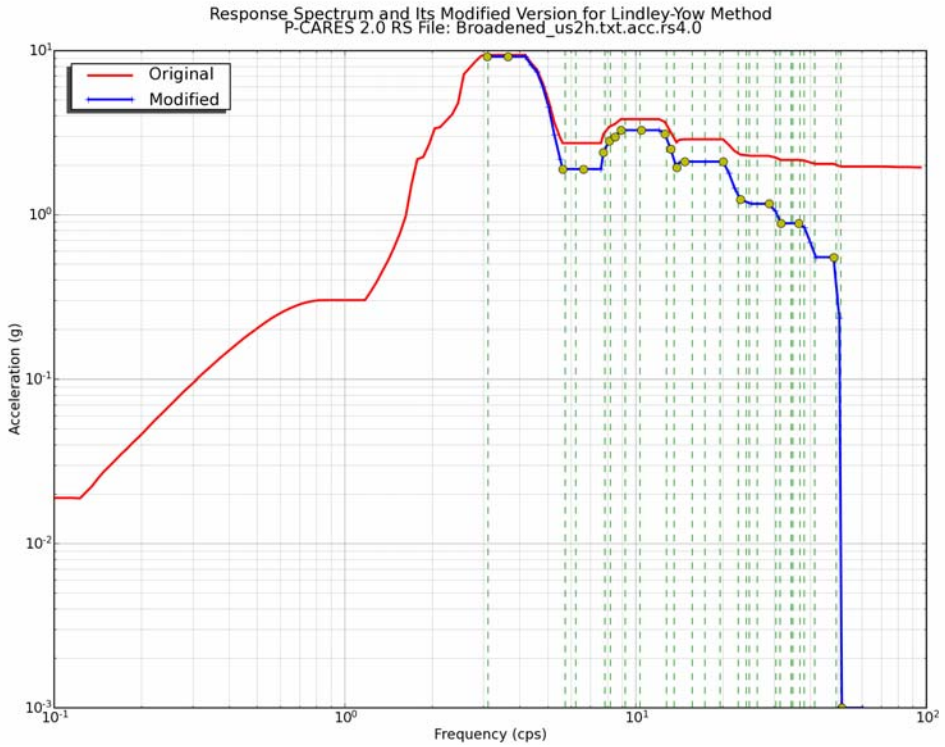

Figure A-4 Broadened Original and Modified Response Spectra for Lindley-Yow Method for US2-1 Nominal Dimension and 4% Damping

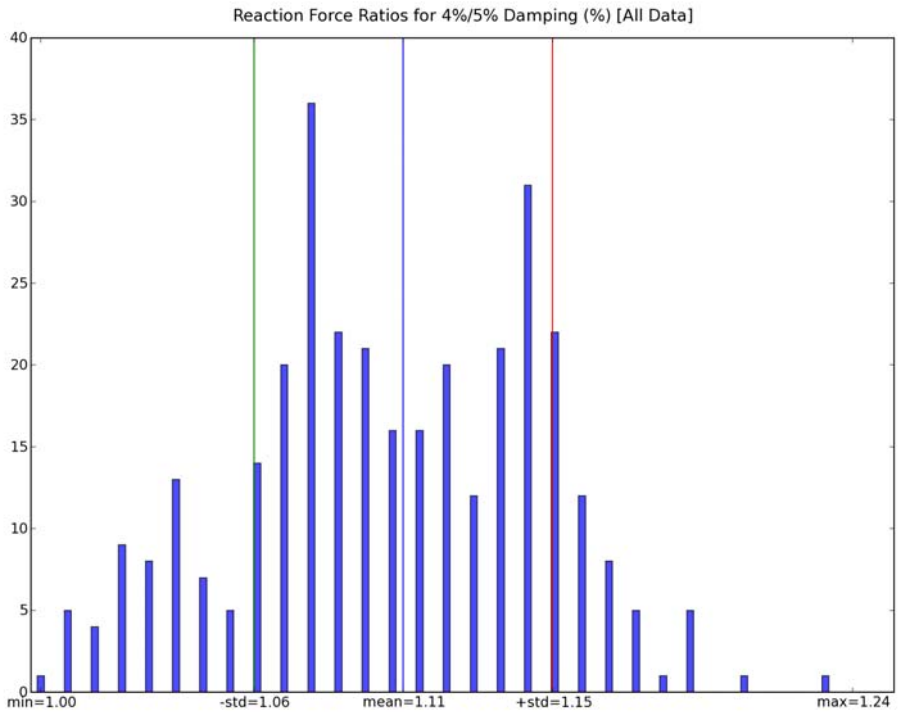

Figure A-5 Ratio of Reaction Forces using All Data

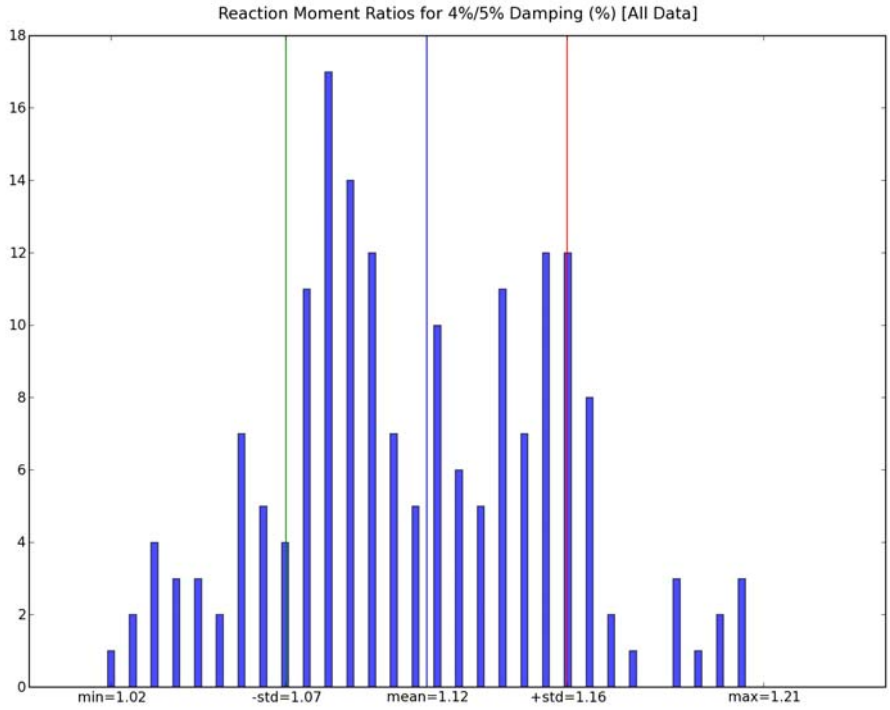

Figure A-6 Ratio of Reaction Moments using All Data

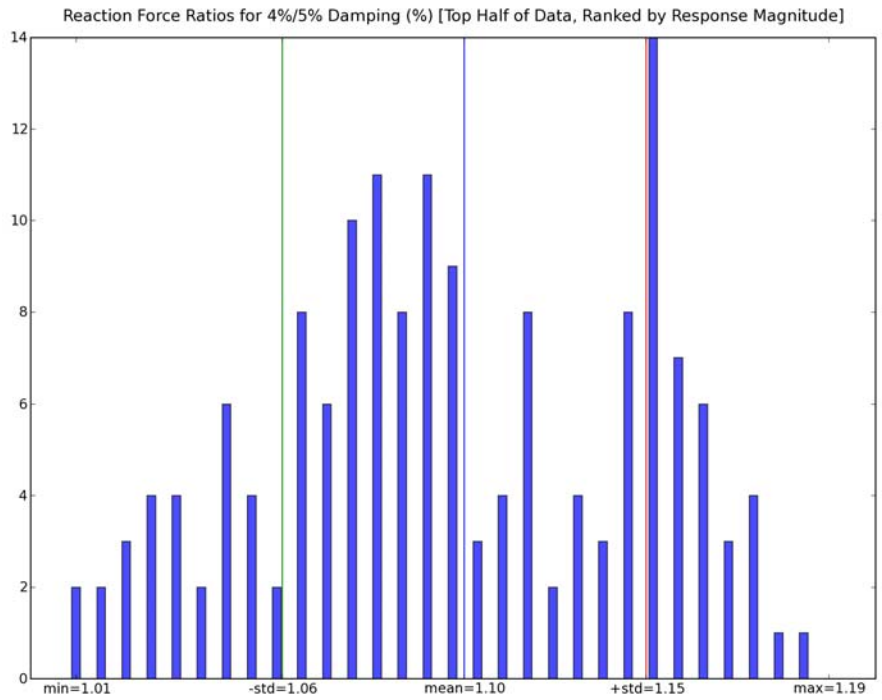

Figure A-7 Ratio of Top Half Significant Reaction Forces

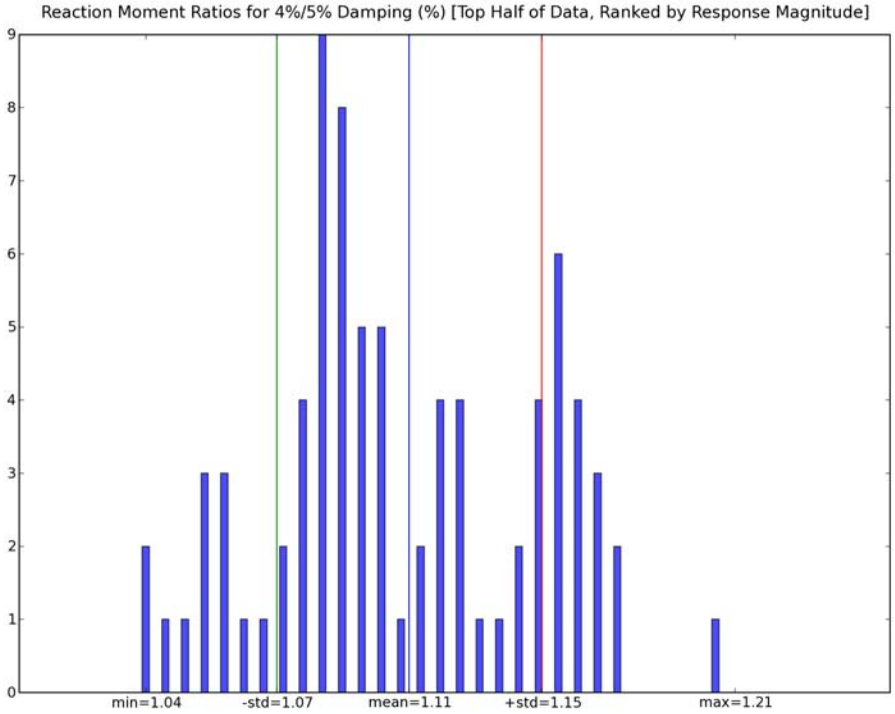

Figure A-8 Ratio of Top Half Significant Reaction Moments

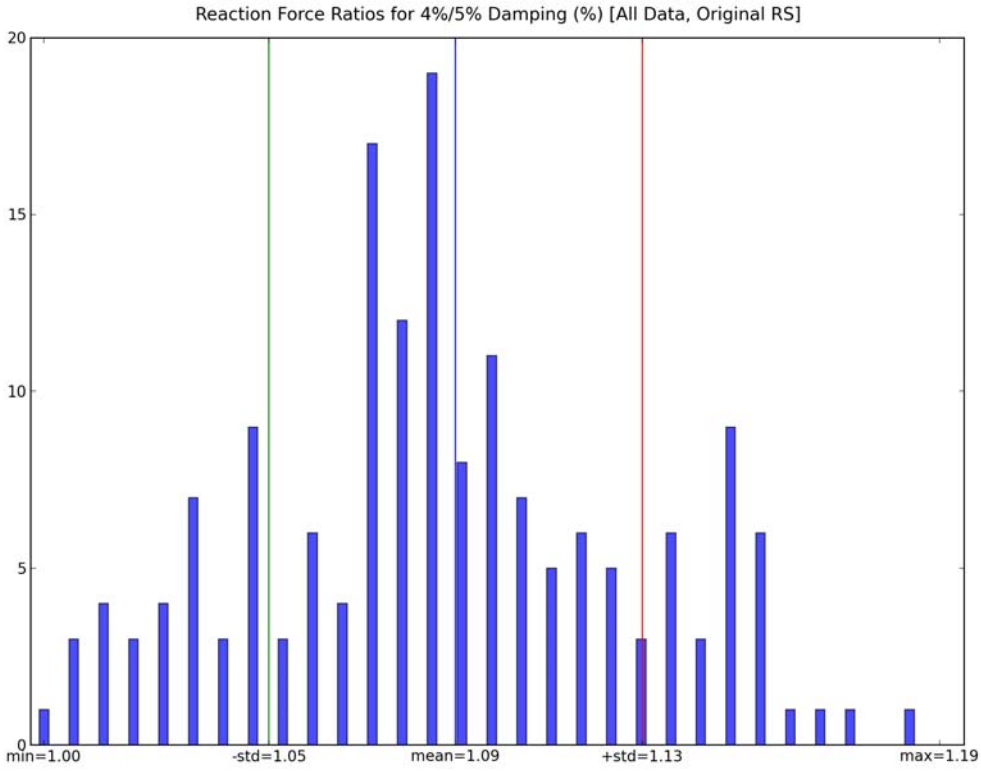

Figure A-9 Ratio of Reaction Force using All Data (Unbroadened Spectra)

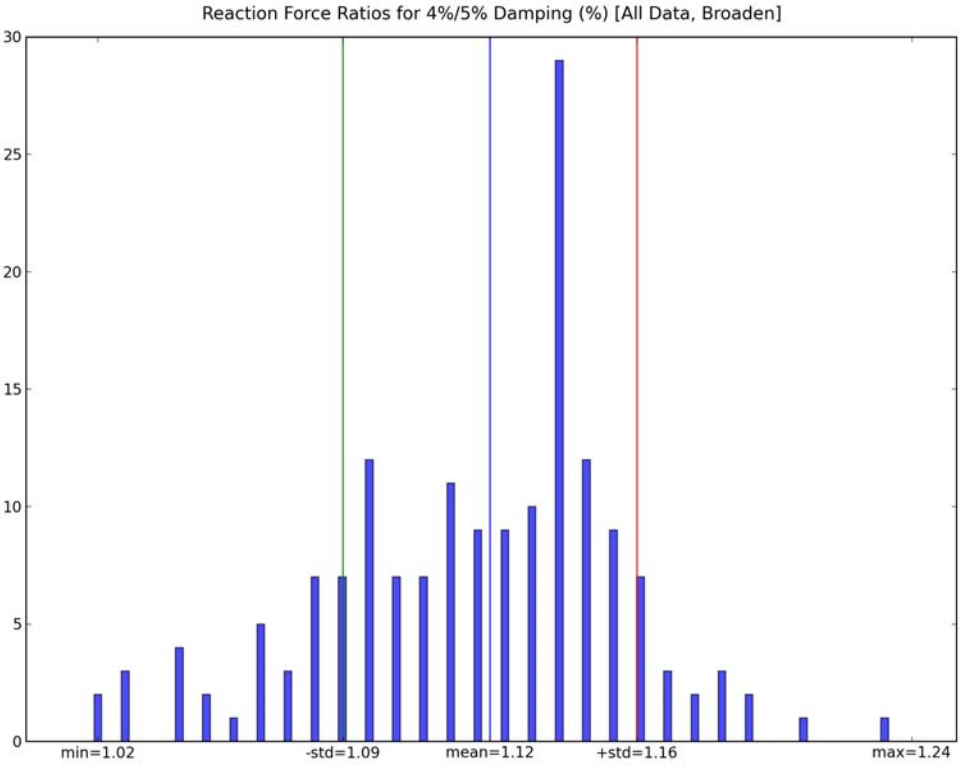

Figure A-10 Ratio of Reaction Forces using All Data (Broadened Spectra)

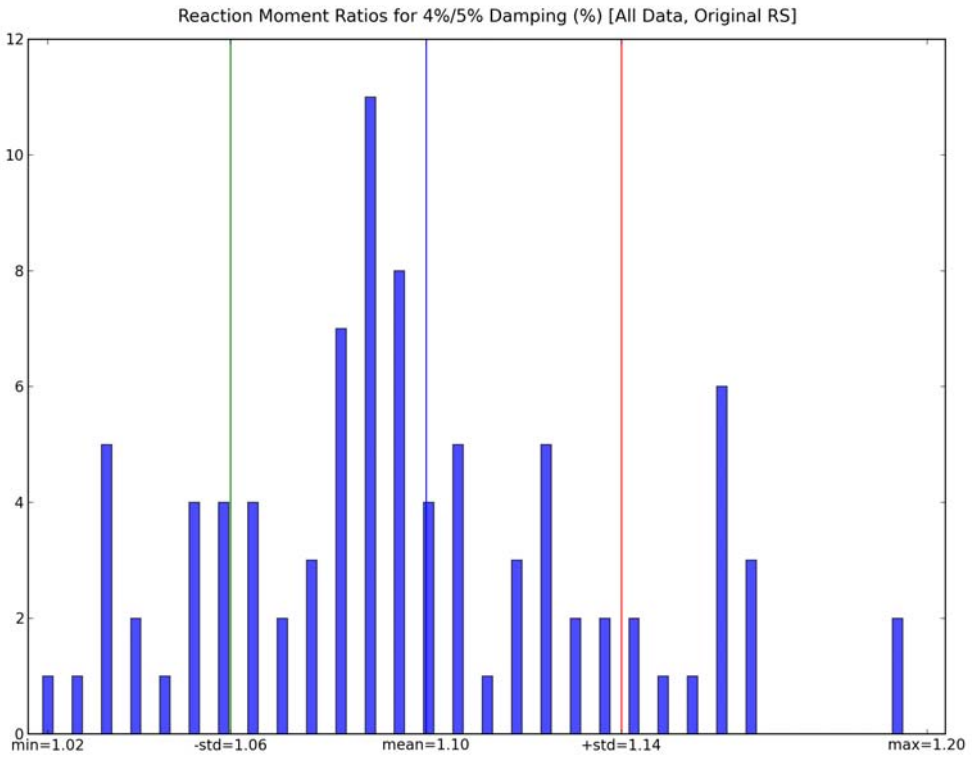

Figure A-11 Ratio of Reaction Moments using All Data (Unbroadened Spectra)

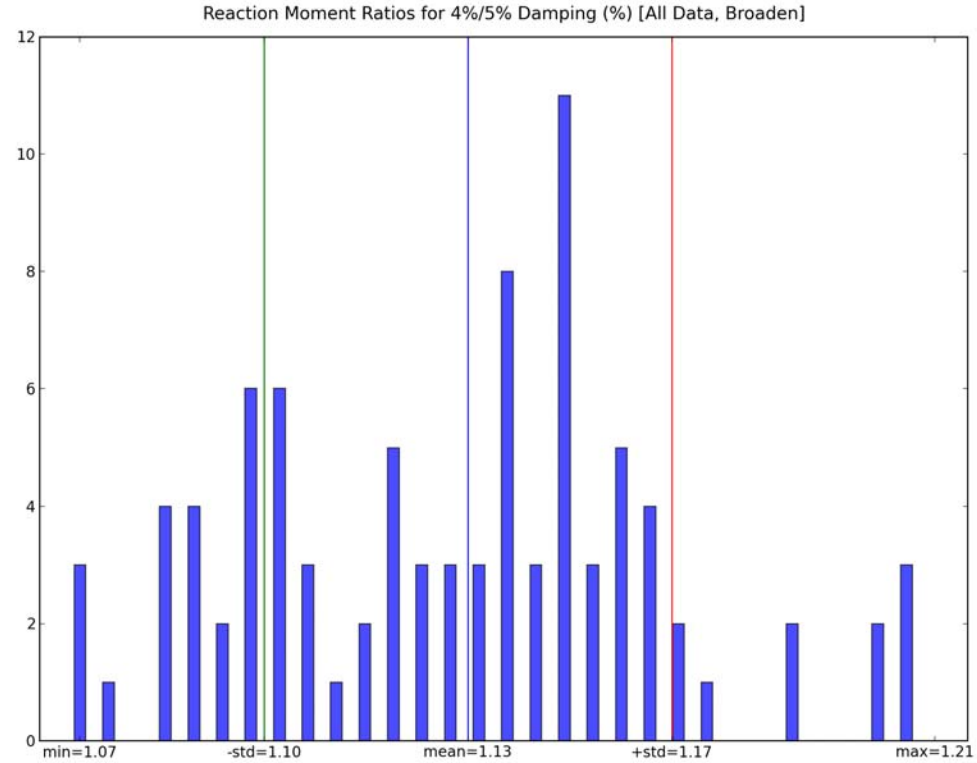

Figure A-12 Ratio of Reaction Moments using All Data (Broadened Spectra)

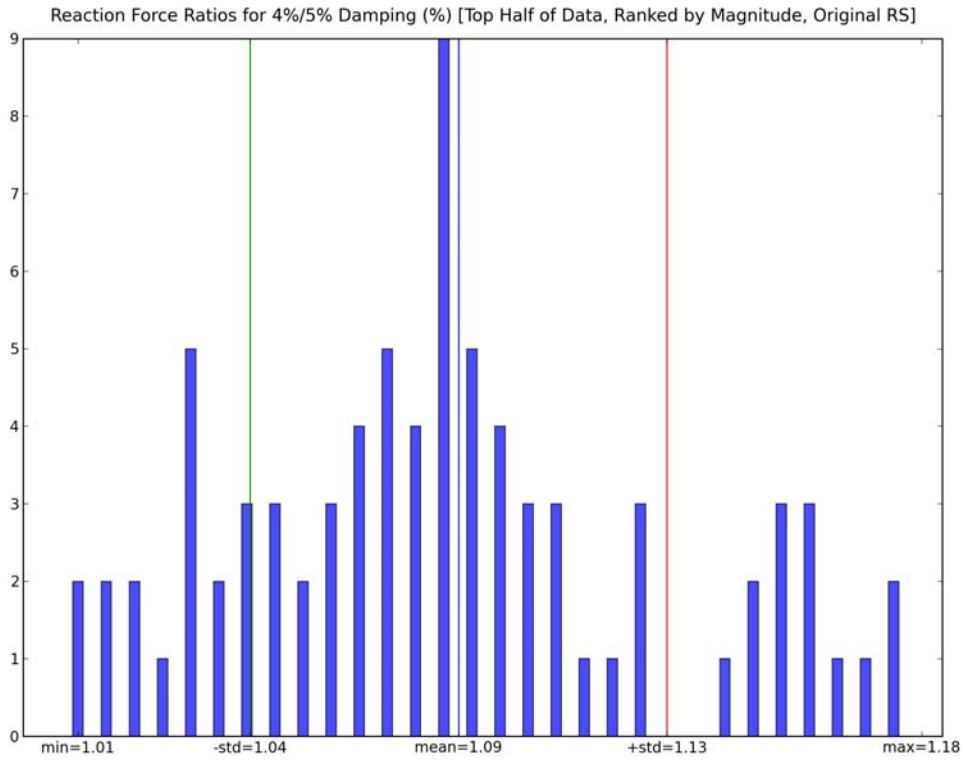

Figure A-13 Ratio of Top Half Significant Reaction Forces (Unbroadened Spectra)

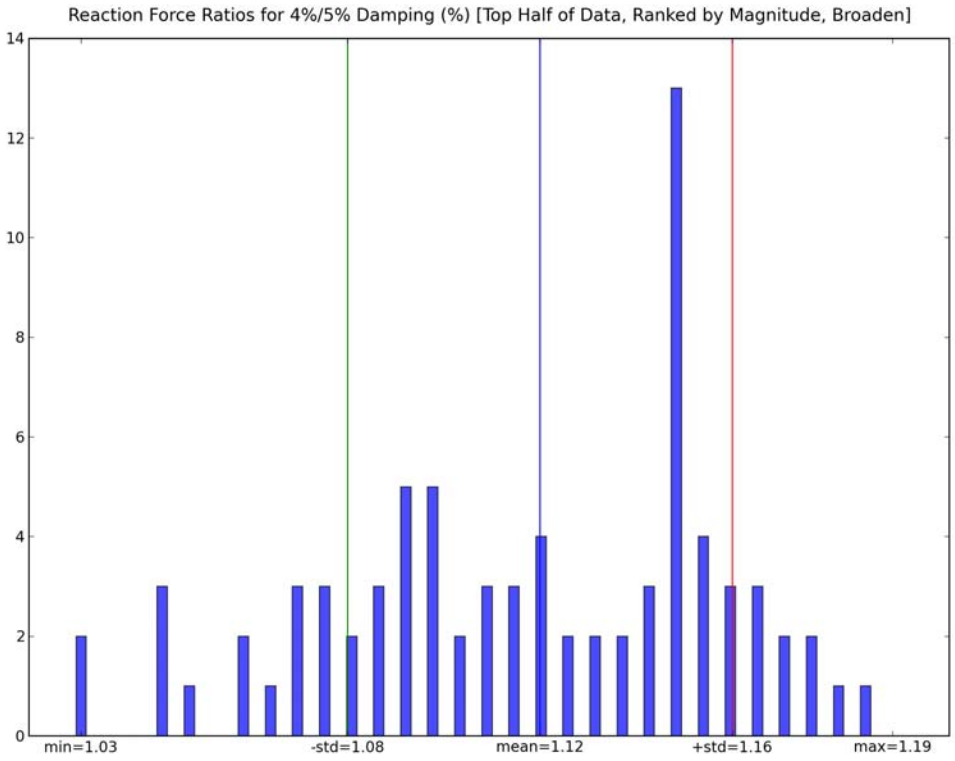

Figure A-14 Ratio of Top Half Significant Reaction Forces (Broadened Spectra)

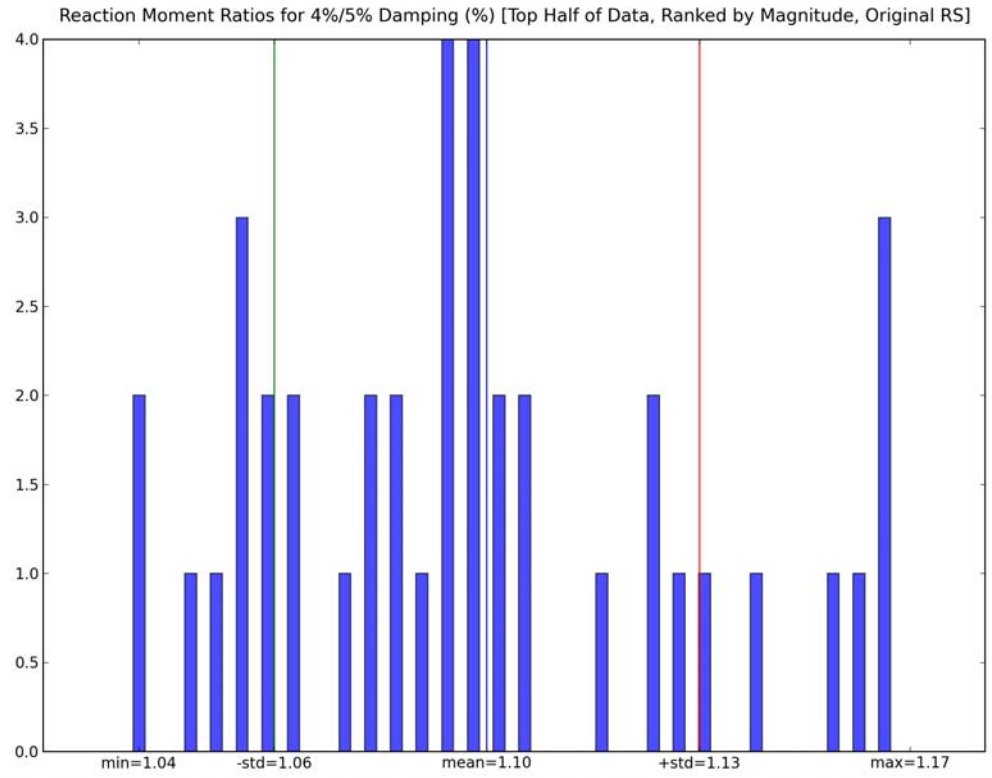

Figure A-15 Ratio of Top Half Significant Reaction Moments (Unbroadened Spectra)

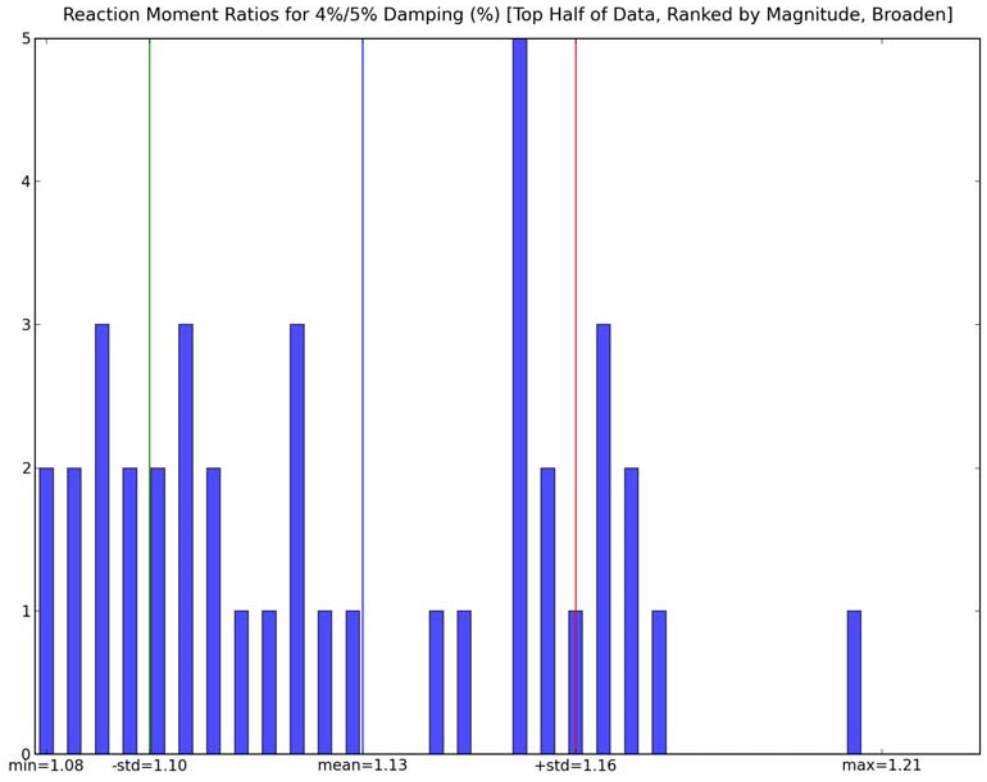

Figure A-16 Ratio of Top Half Significant Reaction Moments (Broadened Spectra)

NRC FORM 335
(2-89)
NRCM 1102,
3201, 3202

U.S. NUCLEAR REGULATORY COMMISSION

BIBLIOGRAPHIC DATA SHEET

(See instructions on the reverse)

1. REPORT NUMBER
(Assigned by NRC, Add Vol., Supp., Rev., and Addendum Numbers, if any.)

NUREG/CR-6983
BNL-NUREG- 81548-2008

2. TITLE AND SUBTITLE

Seismic Analysis of Large-Scale Piping Systems for the JNES/NUPEC Ultimate Strength Piping Test Program

3. DATE REPORT PUBLISHED

MONTH	YEAR
November	2008

4. FIN OR GRANT NUMBER

JCN: N–6076

5. AUTHOR(S)

G. DeGrassi, J. Nie, C. Hofmayer

6. TYPE OF REPORT

Technical

7. PERIOD COVERED *(Inclusive Dates)*

8. PERFORMING ORGANIZATION - NAME AND ADDRESS *(if NRC, provide Division, Office or Region, U.S. Nuclear Regulatory Commission, and mailing address; if contractor, provide name and mailing address.)*

Energy Sciences & Technology Department
Brookhaven National Laboratory
Upton, NY 11973-5000

9. SPONSORING ORGANIZATION - NAME AND ADDRESS *(if NRC, type "Same as above"; if contractor, provide NRC Division, Office or Region, U.S. Nuclear Regulatory Commission, and mailing address.)*

Division of Engineering
Office of Nuclear Regulatory Research
U.S. Nuclear Regulatory Research
Washington DC 20555-0001

10. SUPPLEMENTARY NOTES

S. Ali, NRC Project Manager.

11. ABSTRACT *(200 words or less)*

The Japan Nuclear Energy Safety Organization/Nuclear Power Engineering Corporation (JNES/NUPEC) conducted a multi-year test program for the Ministry of Economy, Trade and Industry (METI) of Japan to investigate the behavior of typical Nuclear Power Plant (NPP) piping systems under large seismic loads. The objectives of this program were to develop a better understanding of the elasto-plastic response and ultimate strength of nuclear piping systems, to ascertain the seismic safety margins in current piping design codes, and to assess new code allowable stress rules. The test program consisted of a series of static and dynamic material tests, piping component tests, simplified piping system tests, and large-scale piping tests. As part of collaborative efforts between the United States and Japan on seismic issues, the U.S. Nuclear Regulatory Commission (NRC) and Brookhaven National Laboratory (BNL) participated in this program by performing both pre-test and post-test analysis for selected tests, and by evaluation of program results. A summary of the BNL analysis of the simplified piping system tests was documented in an earlier NUREG/CR report. This report describes the BNL post-test analyses of the large-scale piping system tests and discusses the insights gained from this program.

12 KEY WORDS/DESCRIPTORS *(List words or phrases that will assist researchers in locating the report.)*

Seismic Analysis, seismic testing, piping design, ASME code evaluation, fatigue ratcheting, plasticity, kinematic hardening, fatigue failure.

13. AVAILABILITY STATEMENT

unlimited

14. SECURITY CLASSIFICATION

(This Page)
unclassified

(This Report)
unclassified

15. NUMBER OF PAGES

16. PRICE

NRC FORM 335 (2-89)